BNL-52641
Formal Report

Proceedings of RIKEN BNL Research Center Workshop Volume 34

High Energy QCD: Beyond the Pomeron

May 21- 25, 2001

Organizing Committee:

John Dainton, Wlodek Guryn, Dmitri Kharzeev, and Yuri Kovchegov

RIKEN BNL Research Center

Building 510A, Brookhaven National Laboratory, Upton, NY 11973-5000, USA

Available electronically at-

`http://www.doe.gov/bridge`

Available to U.S. Department of Energy and its contractors in paper from-

U.S. Department of Energy
Office of Scientific and Technical Information
P.O. Box 62
Oak Ridge, TN 37831
(423) 576-8401

Available to the public from-

U.S. Department of Commerce
National Technical Information Service
5285 Port Royal Road
Springfield, VA 22131
(703) 487-4650

Printed on recycled paper

Preface to the Series

The RIKEN BNL Research Center (RBRC) was established in April 1997 at Brookhaven National Laboratory. It is funded by the "Rikagaku Kenkyusho" (RIKEN, The Institute of Physical and Chemical Research) of Japan. The Center is dedicated to the study of strong interactions, including spin physics, lattice QCD, and RHIC physics through the nurturing of a new generation of young physicists.

During the first year, the Center had only a Theory Group. In the second year, an Experimental Group was also established at the Center. At present, there are seven Fellows and eight Research Associates in these two groups. During the third year, we started a new Tenure Track Strong Interaction Theory RHIC Physics Fellow Program, with six positions in the first academic year, 1999-2000. This program has increased to include ten theorists and one experimentalist in the current academic year, 2001-2002. Beginning this year there is a new RIKEN Spin Program at RBRC with four Researchers and three Research Associates.

In addition, the Center has an active workshop program on strong interaction physics with each workshop focused on a specific physics problem. Each workshop speaker is encouraged to select a few of the most important transparencies from his or her presentation, accompanied by a page of explanation. This material is collected at the end of the workshop by the organizer to form proceedings, which can therefore be available within a short time. To date there are thirty-three proceeding volumes available.

The construction of a 0.6 teraflops parallel processor, dedicated to lattice QCD, begun at the Center on February 19, 1998, was completed on August 28, 1998.

T. D. Lee
August 2, 2001

* Work performed under the auspices of U.S.D.O.E. Contract No. DE-AC02-98CH10886.

CONTENTS

QCD overtakes the Pomeron?

In (experimental) pursuit of the Structure,
and therefore Chromodynamics,
of the Hadronic Interaction

John Dainton
University of Liverpool, GB

Contents

"We dance around in a ring and suppose,
But the secret sits in the middle and knows."

Robert Frost, "The Secret Sits"

Introductory remarks at the International Workshop
"High Energy QCD – Beyond the Pomeron",
May 21 - 25, 2001, Brookhaven, Long Island, NY

1. Archaeology

- strong interaction between nucleons

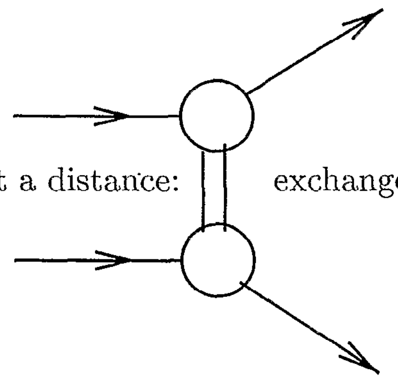

action at a distance: exchange

– uncertainty Yukawa

$$\Delta t \cdot \Delta E \sim \hbar \qquad \Delta x \cdot \Delta p \sim \hbar$$

– space–like $\equiv$ sum of time orderings

$\equiv$ emission + absorption Feynman

– range $\propto \frac{1}{\text{mass}} \sim 1$ fm scale!

– high energy?

2. History

– hadron+hadron→ X+hadron

analyticity $s \leftrightarrow t \leftrightarrow u$

leading Regge dominance

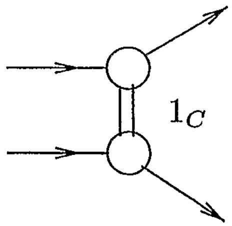

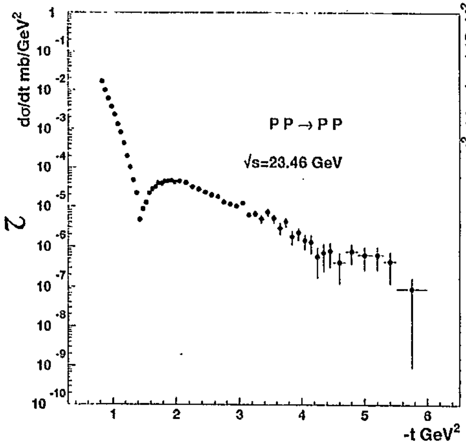

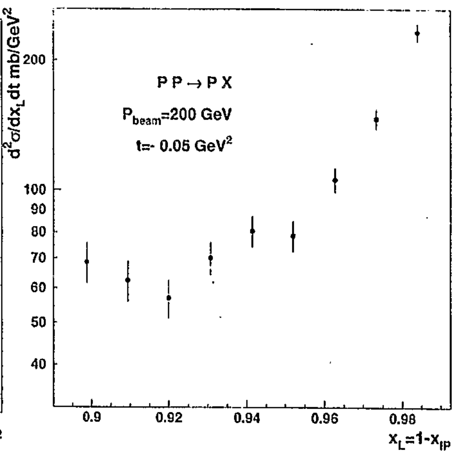

4–momentum^2 $|t|$ leading p momentum fraction

$x_L = 1 - x_{I\!P} = 1 - x_{1C/p}$

peripheral: $e^{bt} \to |t|$ small, inelasticity $x_{1C/p}$ small

diffraction dimension$\sim \frac{1}{b}$ "leading" hadron

– asymptotic $(x_{1C/p} \to 0)$ Pomeranchuk Gribov Regge Mandelstam Chew Frautschi

$$\boxed{\left(\frac{d\sigma}{dM_X^2\,dt}\right)_{M_X^2} \propto \left(\frac{1}{x_{1C/\mathrm{hadron}}}\right)^{2\alpha(t)-2} \cdot f(M_X^2, t)}$$

$$x_{1C/\mathrm{hadron}} = \frac{M_X^2 - m_1^2 - t}{W^2 - m_1^2 - m_2^2} \xrightarrow{|t|\ \mathrm{small}} \frac{M_X^2 - m_1^2}{W^2 - m_1^2 - m_2^2}$$

• universal 1_C Regge trajectories $\alpha(t)$

reggeon $I\!R$: $\rho\, a_2\, f_0$

$\alpha(t) \sim 0.5 + 0.9 \cdot t$

reggeon $I\!R$: π .....

$\alpha(t) \lesssim 0.5 + 0.9 \cdot t$?

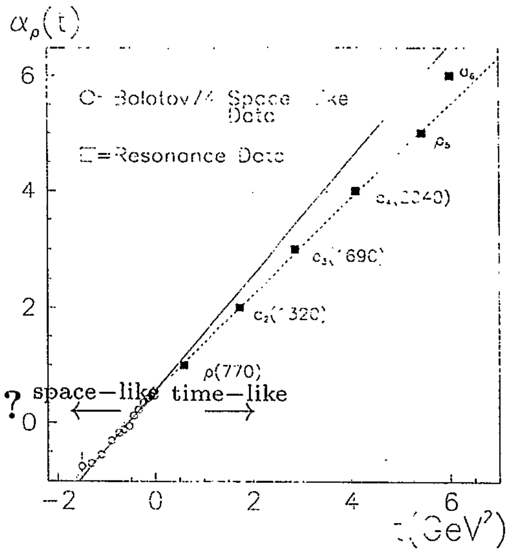

↪ Regge motivated models

exchanged Reggeons ⟷ resonances

$I\!R \to$ $I\!P \to$

↑ mesons

$\alpha_{I\!R}(t) \sim$ linear, universal

QCD $(q\bar{q})_{8_C}$+string$_{8_C}$

↑ ?

$\alpha_{I\!P}(t)$?

2 strings$_{8_C}$?

– *$I\!P$, $I\!R$ in the proton?* Feynman Ingelman+Schlein

$$\boxed{\mathcal{P}_{1C/p} \propto \left(\frac{1}{x_{1C/p}}\right)^{2\alpha(t)-1}}$$ "splitting"

— asymptotic $s \gg$ masses^2: $\sigma \propto \left(\frac{1}{x_{I\!P/p}}\right)^{1+2\lambda} \equiv \sigma \propto s^{2\lambda}$

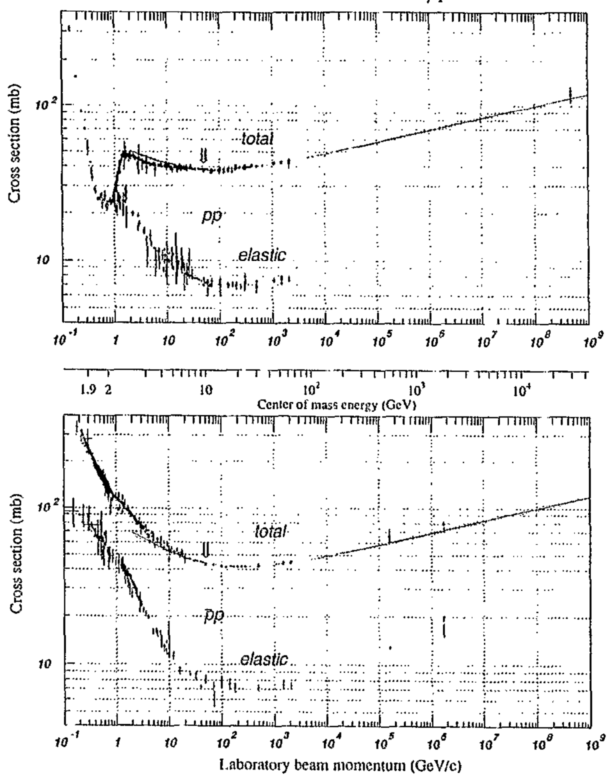

optical theorem	elastic scattering
$\sigma_{pp\,\mathrm{tot}}(s) \sim s^{\alpha_{I\!P}(0)-1}$	$\left(\frac{d\sigma_{pp\to pp}}{dt}\right)_t \sim s^{2\alpha_{I\!P}(t)-2}$

$\alpha(t)$	"splitting" $\mathcal{P}_{1C/p} \propto \left(\frac{1}{x_{1C/p}}\right)^{2\alpha(t)-1}$	energy dependence $\sigma \propto s^{2\alpha(t)-2}$
> 1	falling	rising
< 1	rising	falling
	with increasing $x_{1C/p}$	with increasing s

- **helicity dependence**

exclusive $\pi \overset{\leftrightarrow}{p} \to \pi p$ $\quad I\!R_1 + I\!R_2 + ...$ 1_C

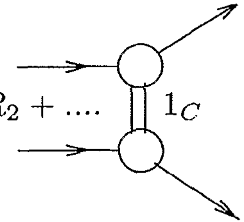

$$\frac{\frac{d\overset{\rightarrow}{\sigma}}{dt} - \frac{d\overset{\leftarrow}{\sigma}}{dt}}{\frac{d\overset{\rightarrow}{\sigma}}{dt} + \frac{d\overset{\leftarrow}{\sigma}}{dt}} \begin{cases} = 0 & 1_C = I\!R_1 \\ \neq 0 & 1_C = I\!R_1 + I\!R_2 + \ldots \\ \neq 0 & 1_C = I\!R_1 + \text{"cuts"} \end{cases}$$

diffraction $I\!R = I\!P \to T_{\Delta\lambda\neq 0} \equiv 0 \to$ forward peak

reggeon exchange $I\!R \to T_{\Delta\lambda=0}$ $\quad\to$ forward $\overset{\text{peak}}{\text{dip}}$

inclusive $\overset{\leftrightarrow\uparrow}{\gamma^*} \overset{\leftrightarrow}{p} \to \overset{\leftrightarrow\uparrow}{X}\, Y$ $\quad \overset{\leftrightarrow\uparrow}{X} \to$ hadrons

diffraction $I\!R = I\!P$ $\quad\to$ SCHC ?

proton spin structure $\quad\to$ "spin crisis"

dynamics: $s-$channel and/or $t-$channel or ?

$\hookrightarrow$ polarised beam/target $\quad$ RHIC,HERA

— $pp \to p + 2\text{–jets}$ UA8

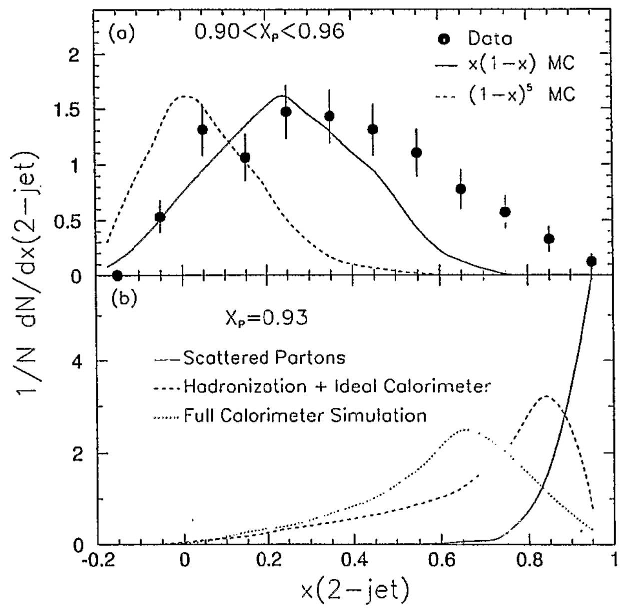

– partons exposed in diffractive exchange ($I\!P$)

– QCD partons 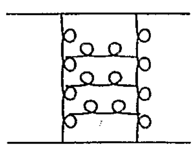 ?

$\uparrow$

elastic diffraction $= 1_C$ exchange $\neq$ LO (cf QED)

• **chromodynamic spectroscopy**

– QCD: non-abelian flux tubes $\to$ strings

– long distance "string" $V(r) = kr$+constant

$\hookrightarrow$linear meson trajectory

$$J(M^2) = \alpha(0) + \alpha' M^2$$

light quarkonia $u\bar{u}\ d\bar{d}\ s\bar{s}$

$$3_C \otimes 8_C \otimes \bar{3}_C \to 1_C$$

$\alpha' \sim 0.9\,\mathrm{GeV}^{-2}$ (tonnes!)

gluonia gg

$$8_C \otimes \bar{8}_C \to 1_C$$

$\alpha' \lesssim 0.5\,\mathrm{GeV}^{-2}$

• QCD degrees of freedom at low scale

— Russian resilience – Reggeise your gluons! BFKL

"Reggeised gluon ↔ structure ↔ angular momentum"

Lipatov

elastic diffraction $qq \to qq$

$$T_{qq\to qq} \propto .....+\int_1^{x_{I\!P}} g\frac{dx_n}{x_n}\cdot\int_1^{x_n} g\frac{dx_{n-1}}{x_{n-1}}\ldots\int_1^{x_n} g\frac{dx_1}{x_1}+.....$$

$.....+$ 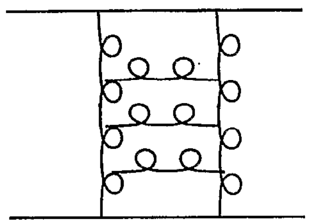 $+.....$

$$T_{qq\to qq}(x_{I\!P},t) \propto \sum_{\text{rungs}\, n}\left(\frac{g}{n!}\ln\frac{1}{x_{I\!P}}\right)^n = \left(\frac{1}{x_{I\!P}}\right)^{g(t)}$$

— Regge form Amati, Fubini, Stangellini, BFKL, Gribov
coupling g ↔ intercept → running intercept?
→ universal $I\!P$?

— $gg, gggg, \ldots\ J^{PC} = 0^{++}\ldots$. natural $I\!P$
$ggg, \ldots\ J^{PC} = 0^{--}\ldots$. unnatural odderon?

— $q\bar{q}$ $I\!R$ trajectories running intercept?
universal?

— reggeon calculus, effective field theory

• **the mystery**

phenomenology (Regge)	QCD
t−channel "meson"	glueball?
diffraction	t−channel gluons?
leading $\alpha_{I\!P}(t)$	gluon ladder(s)?
universal $\alpha_{I\!P}(t)$?	running α_S
helicity conserv$^{\underline{n}}$?	$q \to qg$ helicity conserv$^{\underline{n}}$
C +($I\!P$)/−(odderon)?	even/odd no. gluons?
meson	quarkonium?
sub-leading $\alpha_{I\!R}(t)$	t−channel quarks?
universal $\alpha_{I\!R}(t)$?	running α_S
helicity structure?	$q \to qg$ helicity structure?

Yuri Dokshitzer

Around the Pomeron.

I gave a brief overview of the concept of Pomeron (leading vacum channel complex angular momentum singularity), the prehistory of the subject ("Before the Pomeron"), and, in particular, the history of muddling through the s-channel unitarity problems ("Inside the Pomeron"). [Given a massive confusion which, as it transpired during the meeting, the Pomeron and related concepts cause to the minds of experimenters and young theorists, I wish someone gave a two-day lecture course on the subject rather than a 30 minutes talk.]

I tried to stress the relation between understanding high energy scattering and understanding confinement.

In the "Besides the Pomeron" part of the talk, I pointed out a number of apparently "anti-Pomeron" phenomena, such as "baryon stopping" (long-range quantum number correlations) and the process dependence of the relative yield of strange hadrons. Comparative studies of pA, heavy ion and pp interactions are of primary importance for understanding both the structure of hadrons and colour dynamics of multiple hadron interactions.

And in QCD?

"Pile-up" of glue = increasing Colour field →

→ Confinement = QUARKS!

How to access the issue?

Theoretically — ... Best of luck and attention to Gribov Light Quark Confinement

Experimentally —

study

- particle production
- fluctuations
- relative yields in pp / pA / AB environme
- $p_\perp$ dependences

Basic Inputs into the $I\!P$ concept:

hinted at

— $\sigma_{tot} \simeq$ Const ⇒ Glue spin = 1

— $K_\perp$ limited ⇒ $\alpha_s(k_\perp)\downarrow$ (As. Fr.)

— short-range quantum # fluctuations ... well, how about baryon stopping

Anti-ℙ dossie

1) Long-range quantum # ~~fluctuatio~~ correlations

"Baryon stopping" [which ain't any bloody stopping but a proton decay $p \to \pi^+\pi^-K^+$]

- first observed in heavy ion collisions,
- then in pA [stronger than in AB!]
- present even in pp!

As far as final state hadroproduction is concerned, COLOUR dynamics is likely to push us to revise the Basic ℙ picture

Double-scratch picture of proton scattering

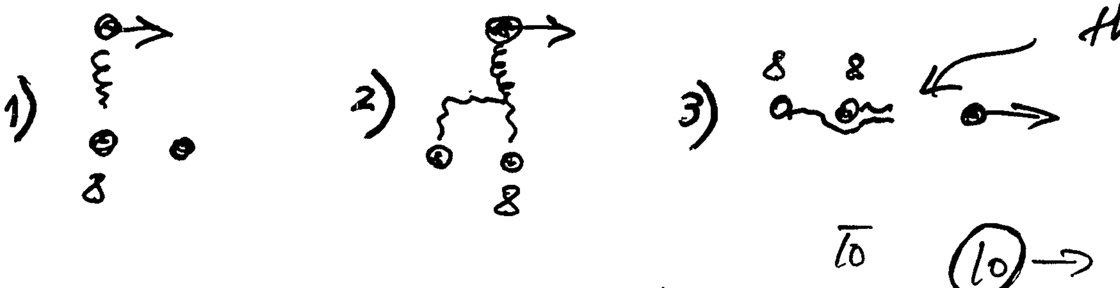

A curious PAINTING ampl.

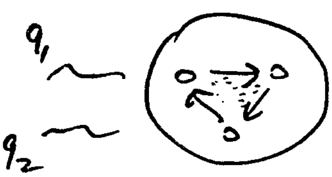

$A \propto [\vec{q}_1 \vec{q}_2]\cdot\vec{S}$

$8\times 8=\overline{10}$

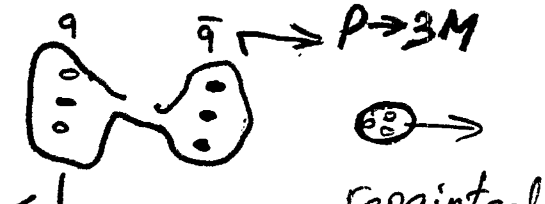

(2) Strange pattern of STRANGENESS production

$\frac{K}{\pi}$ increases with centrality in H.I.C.

plasma?

BUT pA (NA-49)

BUT pp! $\frac{\varphi}{\pi}$

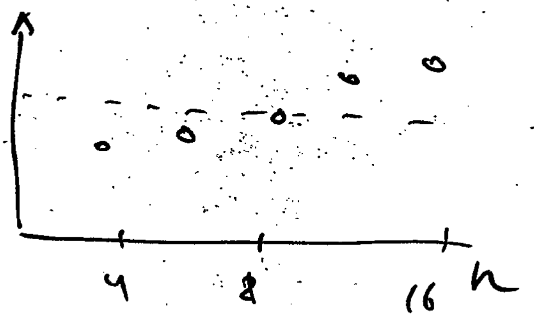

(NO) parallel non-interacting "ladders"

Stronger colour fields $\Rightarrow$ larger $p_\perp$, more strange (eventually, CHARM, ...) particles, more e^+e^- pairs, ...

How does the vacuum break up in an unusual colour environment?

e.g.

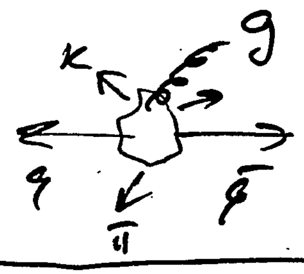

vs.

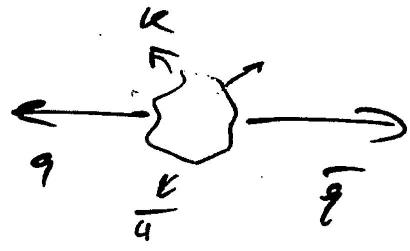

?

"Z is dead, baby. Z is dead."

B.W.

A precursor ~~to~~ the Feynman parton model:

"Interaction of γ-quanta and electrons with nuclei at high energies"

V.N. Gribov (1969)

25 years later: Lecture notes on confinement (unpub.)

1. "Confinement is older than quarks themselves"

2. "... can be checked on nuclei."

A technical motto that in the ∞-momentum frame (light-cone description)
the VACUUM DECOUPLES
ain't true for WEE,
especially in a QFT with inherently unstable InfraRed dynamics.

To understand High Energy Scattering

$=$ equals

to understand Confinement

Kovchegov-Mueller Dichotomy

$$c \, \frac{\alpha_s A}{\pi R^2} [x G(x)] = c' \alpha_s \rho [x G(x)] \cdot L$$

gluon saturation scale

in-medium multiple scattering: gluon broadening

MV McLerran-Venugopalan

Fast nucleus $\Rightarrow$ WW field
$\Rightarrow$ scattering $\Rightarrow$ saturation (?)

an alternative /complementary/ view:

Nucleus at rest $\Rightarrow$ medium-induced gluon radiation off a fast projectile, and $p_\perp$ broadening $\Rightarrow$ quenching

$$\hat{q} = \rho \int dq^2 \, q^2 \, \frac{d\sigma}{dq^2}$$

transport coefficient

THERE ARE TWO POMERONS !

A DONNACHIE + P V LANDSHOFF

SOFT POMERON CONTRIBUTES

$$F_2(x, Q^2) \sim f_1(Q^2)\, x^{-\epsilon_1}$$

$\epsilon_1 \approx 0.08$ (DL)

0.10 (CUDELL et al)

HARD POMERON :

$$f_0(Q^2)\, x^{-\epsilon_0}$$

$\epsilon_0 = 0.4$ $\pm$ 10% OR MORE

$$\sigma^{\gamma p} = \frac{4\pi^2\alpha}{Q^2} F_2 \Big|_{Q^2=0}$$

THE REAL-PHOTON DATA ARE AN IMPORTANT CONSTRAINT.

USE THEM, PLUS ZEUS + H1 DATA

WITH $x \leqslant 0.001$ $\quad 0.045 \lesssim Q^2 \lesssim 35$

HARD POM

$$X_0 \left(\frac{Q^2}{1 + Q^2/Q_0^2}\right)^{1+\epsilon_0} \left(1 + Q^2/Q_0^2\right)^{\frac{1}{2}\epsilon_0} x^{-\epsilon_0}$$

3 PARAMETERS $\quad X_0, \; \epsilon_0, \quad Q_0 \approx 3\,\text{GeV}$

SOFT POM

$$X_1 \left(\frac{Q^2}{1+Q^2/Q_1^2}\right)^{1+\epsilon_1} \quad x^{-\epsilon_1}$$

$\epsilon_1 = 0.0808$ $\quad X_1$ DETERMINED BY $\sigma^{\gamma p}$

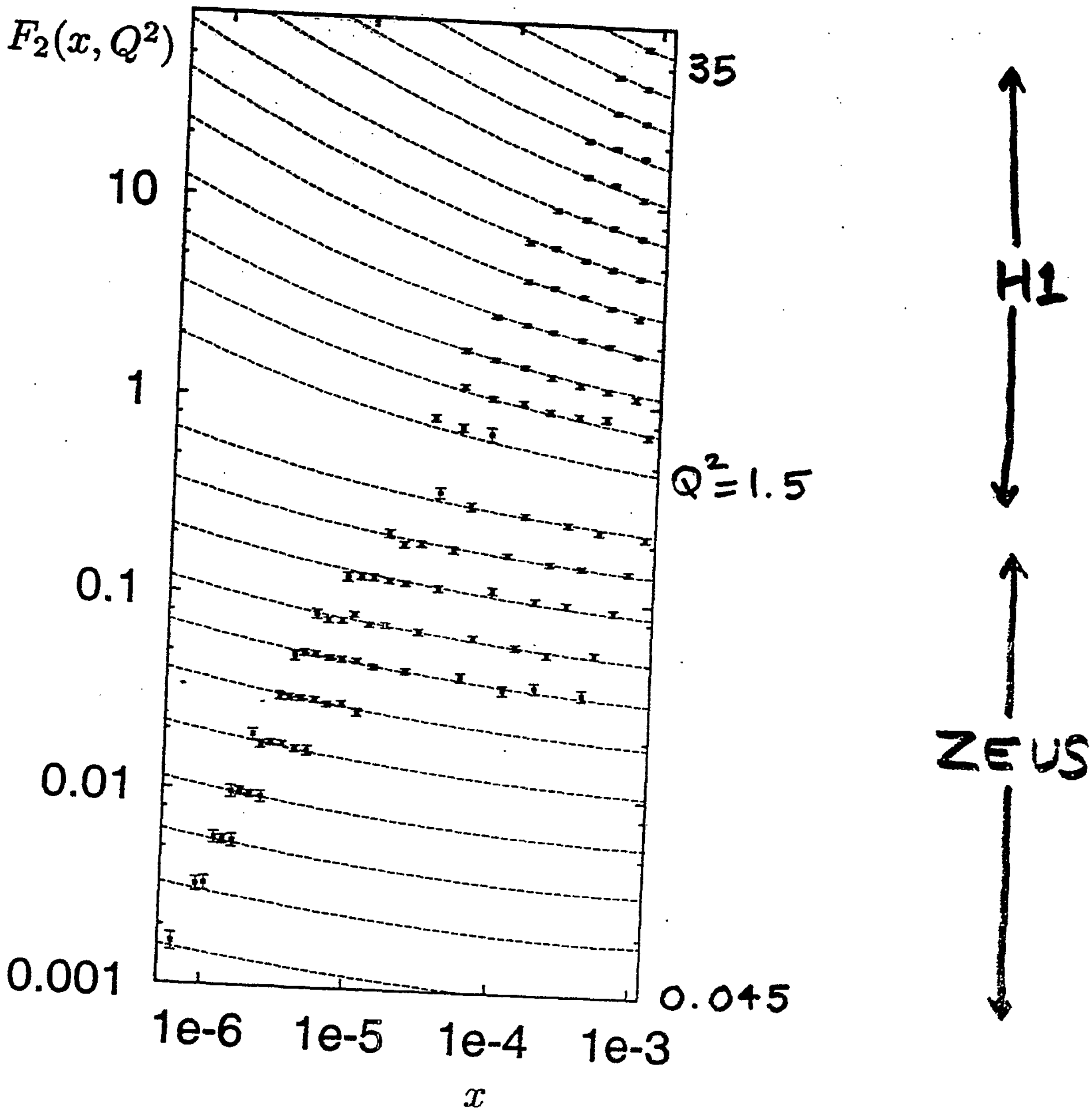

$\epsilon_0 = 0.437$

CHARM STRUCTURE FUNCTION

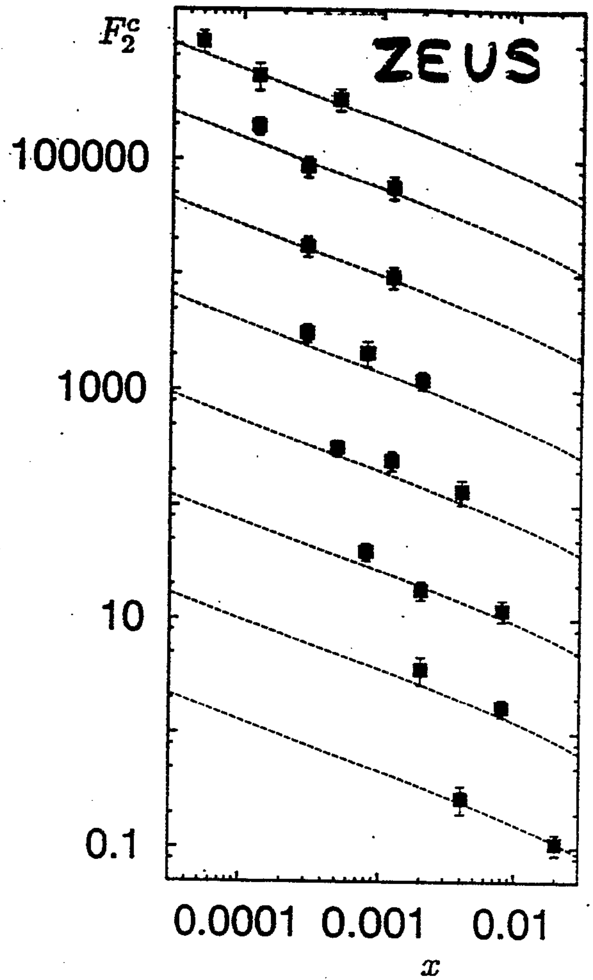

$Q^2 =$
--- 1.8 (x 10^7)
--- 17.5 (x 10^3)
--- 130

HARD POMERON ONLY!

FLAVOUR BLIND:

$\frac{2}{5}$ HARDPOM PART OF F_2

$$\frac{2}{5} = \frac{4}{9} \Big/ \left(\frac{4}{9} + \frac{1}{9} + \frac{4}{9} + \frac{1}{9} \right)$$

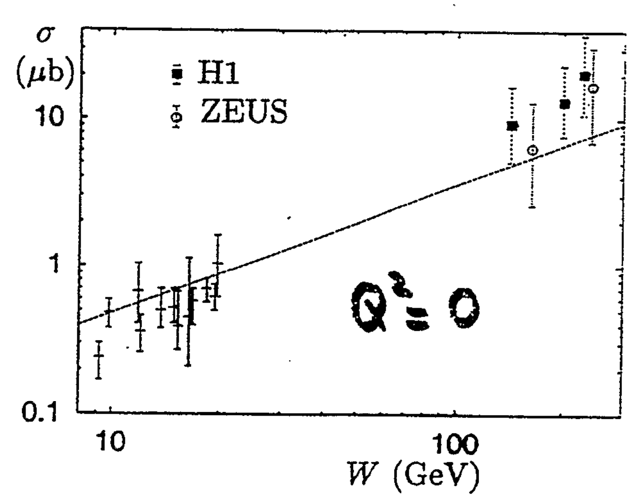

$0.064\ (2\nu)^{0.437}$

$\gamma p \rightarrow J/\psi \; p$

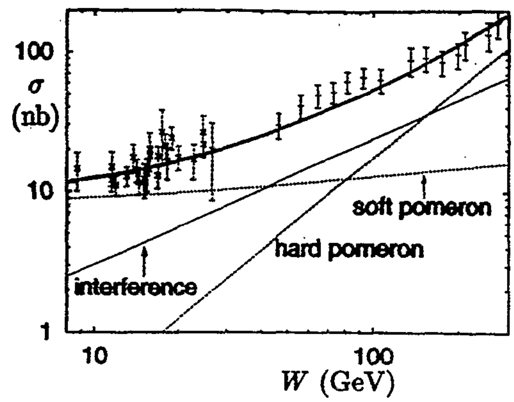

H1

$$A(s,t) = i \sum_{i=0,1} \beta_i \, F_1(t) \, (\alpha_i' s)^{\alpha_i(t)-1} \; e^{-\frac{1}{2} i\pi(\alpha_i(t)-1)}$$

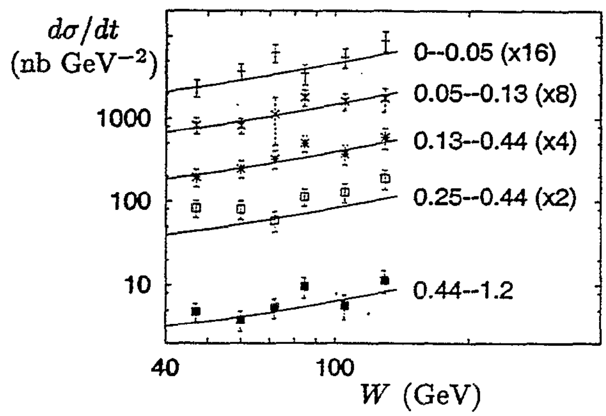

H1

STRAIGHT TRAJECTORIES

$$\left.\begin{aligned} \alpha_0' &= 0.1 \ \mathrm{GeV}^{-2} \\ \alpha_1' &= 0.25 \ \mathrm{GeV}^{-2} \end{aligned}\right\} \Rightarrow \text{NO SHRINKAGE!}$$

Key questions

- Are there really two separate pomerons?
- Are they simple poles in the N plane?
- Does the hard pomeron contribute already at $Q^2 = 0$?
- Is it really flavour-blind, even at small Q^2?
- **How do we resum pQCD?**

Hard Diffraction and the nature of the QCD Pomeron

(Robi Peschanski)

Using in an unifying framework S-Matrix and Field-Theoretical properties, we show that 3 different approaches of Hard Diffraction at HERA. can be related after some modification. The Soft Color Interaction models (à la Buchmuller-Hebecker, Ingelman et al.) can be obtained from the QCD dipole formulation with a modified form of the short-distance source of the deep-inelastic interaction. Equivalently, the partonic content of the Pomeron (à la Ingelman-Schlein and followers) is related to the QCD-dipole prescription for the Diffractive Structure function, again with a modified - semi-hard - effective BFKL formula. Consequences for the perturbative / non-perturbative QCD interface and the nature of the QCD Pomeron can be drawn leading to a complementarity of both PQCD / ~~P~~QCD aspects and a variable effective Pomeron based on an universal kernel

Hard Diffraction and the Nature of the QCD Pomeron

①

R. Peschanski, Saclay
Beyond the Pomeron 2001

1) Motivation : the perturbative / non perturbative QCD Interface

2) 3 models ≡ 3 different (?) Interfaces

3) An Unifying Picture: General S-Matrix + Field-Theory framework

20

4) Application : a "Synthetic" Diffractive Structure Function:

partonic Pomeron ↔ QCD Dipoles

Soft Color Interaction ↔ QCD Dipoles

with H. Navelet
hep-ph/0105.

5) Conclusion / Outlook

S-Matrix Relations.

②

Disc$_1$ A (3 − 3) =

Disc$_2$ A (3 − 3) =

Disc$_3$ A (3 − 3) =

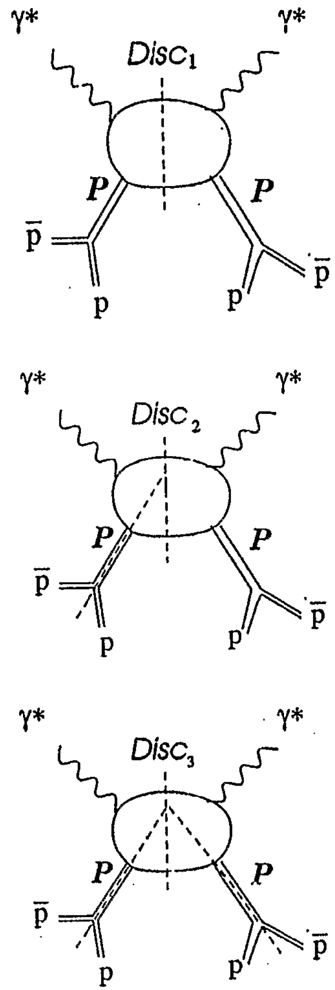

Fig. 2

"Triple Regge" ⇒ Disc$_1$ = Disc$_2$ = Disc$_3$

S-Matrix ⊕ QCD Descriptions

③

H.Navelet and R.P. ph/0805..

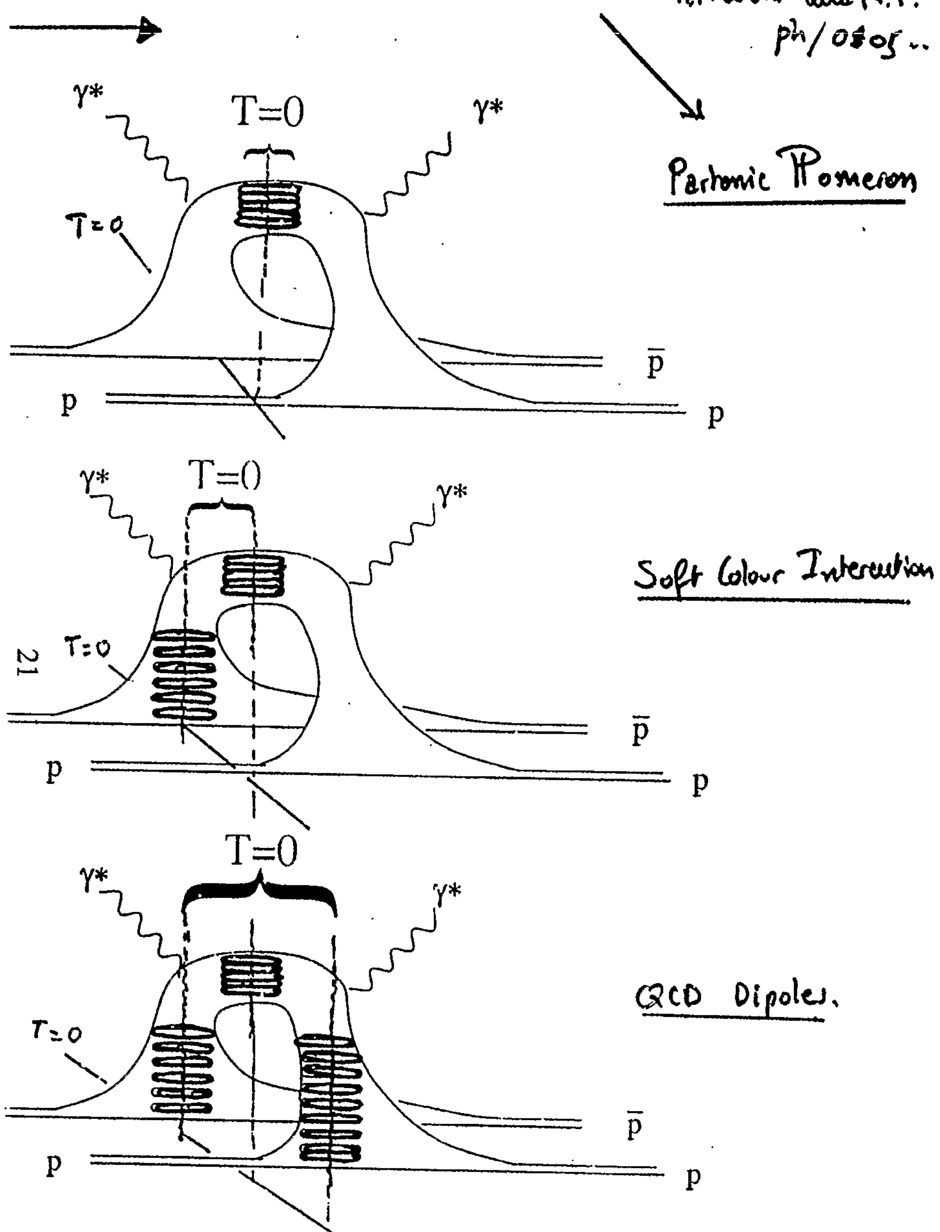

Fig. 3

④

QCD Dipoles → Soft Color Interaction

let us perform:

$$\boxed{\int_{y_{min}}^{Y} dy\, F^{Inel}_{\gamma^*_p}(y,Y;Q^2) \underset{\substack{\text{triple saddle-point}\\ \text{in } \gamma_1,\gamma_2,y}}{=} \frac{1}{\lambda}\, F^{\text{`BFKL'}}_{\gamma^*_p}(\underline{\text{fixed}}\ \gamma = \gamma^*)}$$

PQCD • γ^*: solution of $\Delta(\gamma^*) = 2\Delta\left(\frac{1-\gamma^*}{2}\right)$

($\gamma^* \simeq .185$, universal

$\cancel{P}$QCD • $\frac{1}{\lambda}$: $\Longrightarrow$ see Soft Color Interaction!

N.B. $F^{\text{`BFKL'}}_{(\text{fixed } \gamma^*)} \neq F^{BFKL}_{(\text{moving } \gamma_{s.p.})}$

$$F^{BFKL} \simeq \mathcal{N}\left(\frac{Q}{Q_0}\right)^{2\gamma_{s.p.}} \frac{\exp\left\{Y\Delta(\gamma_{s.p.})\right\}}{\sqrt{2\pi\Delta''(\gamma_c)Y}}$$

moving $\gamma_{s.p.} = \frac{1}{2}\left(1 - 4\frac{\log Q/Q_0}{\Delta''(\gamma_c)Y}\right) \neq \gamma^*_{\text{fixed, universal}}$

QCD Dipoles $\longrightarrow$ partonic Pomeron

(5)

Inel.

$$F_p(y,Y;Q^2) \underset{\substack{\text{double saddle-point}\\ \text{in } \gamma_1,\gamma_2}}{=} \exp(2\Delta(1/2)\,y)\; F^{\text{"harder"}}_{\gamma^* \mathbb{P}}(Y-y,Q^2)$$

"harder"

$$F \sim \exp\{(Y-y)\Delta_S\} \times \left(\frac{Q}{Q_0}\right)^{\gamma_S} e^{-2\frac{\log^2 Q/Q_0}{\Delta''_S (Y-y)}}$$

22

$$\Delta_S = \Delta(1/2) + \frac{\Delta''(1/2)}{8(1+2\eta)} \geq \Delta(1/2)$$

$$\gamma_S = \frac{\eta}{1+2\eta} \geq 0 \quad \text{(but less than } 1/2\text{!)}$$

$$\Delta''^{-1}_S = \Delta''^{-1}(1/2)\,\frac{1+2\eta}{\eta} \geq 2\Delta''^{-1}(1/2)$$

(less diffusion than BFKL)

"harder" "intermediate" between Soft and Hard

and depending on "external" variables Q^2, Q_0^2 and $\eta \equiv \frac{Y-y}{y}$

Unified Approach to Hard Diffraction

(6)

Consequence: low-β component determined as a "Synthesis"

$$F^{\,\text{Diff}}(y,Y,Q^2) = \frac{\mathcal{N}^{Pot}}{N_c^2}\,\frac{1}{x_p}\int \frac{d\gamma_1}{2i\pi}\frac{d\gamma_2}{2i\pi}\frac{d\gamma}{2i\pi}\,\delta(1-\gamma_1-\gamma_2-\gamma) \times \left(\frac{Q}{Q_0}\right)^{2\gamma} \exp\left\{y\left[\Delta(\gamma_1)+\Delta(\gamma_2)\right] + (Y-y)\Delta(\gamma)\right\}$$

γ

p̸QCD

$\underbrace{\text{"Triple-BFKL-Regge" formula}}_{\text{PQCD}}$

Conclusions

We don't know yet ...

→ PQCD. uncomplete

→ $\not{P}$QCD unknown

→ Interface "variable"

... but our exercise shows interesting

features → PQCD / $\not{P}$QCD Complementarity

→ Universality / Diversity of the Pomeron

→ Matching of S-Matrix / Field theoretical Properties

Disentangling Pomeron Dynamics from Vertex Function Effects

Sandy Donnachie

Application of models of the pomeron requires using the wave functions (vertex functions) of the participating particles.

These can control many aspects of the dynamics.

This is illustrated for

- $\gamma^* p \to V p$, $V = \rho, \phi, J/\psi$: small $|t| \lesssim 0.5$
  (Donnachie, Gravelis, Shaw: hep-ph/0101221)

- $\gamma p \to V X$, $V = \rho, \phi, J/\psi$: large $|t| \gtrsim 1.0$
  (Forshaw, Poludniowski: preliminary)

- F_2, F_2^c, F_L, $\sigma^{Tot}_{\gamma p}$; $\sigma^{Tot}_{\gamma\gamma}$, F_2^γ ---- : $t = 0$
  (Donnachie, Dosch: preliminary)

In each case a good simultaneous description of all relevant data is obtained, with a very small number of parameters.

$\gamma^* p \to V p$: $|t| < 0.5$ GeV^2

Two pomerons, two-gluon exchange: non perturbative (Diehl) or perturbative (Cudell & Royon or pdfs). Model fixes t-dependence, wave functions (3 parameters in all) and normalisation (2 parameters) do the rest. Energy dependence by hand as Donnachie and Landshoff. Excellent global description of all ρ, ϕ, J/ψ data.

$\gamma p \to V X$: $|t| > 1.0$ GeV^2

Hard pomeron: pdfs $(x', t) \otimes$ BFKL (LLA, $t \neq 0$)
Non-relativistic approximation ($M_V = 2m_q$) for wave functions. Two parameters: effective α_s in BFKL and scale in LLA. Excellent description of ρ, ϕ, J/ψ data.

F_2, F_2^c, F_L etc: $t = 0$

Dipole picture with two pomerons. Proton treated as a quark-diquark system ie dipole. Dipole-dipole cross section obtained from pp scattering.
Assume if both dipoles are larger than R_c only the soft pomeron couples; if at least one dipole is smaller than R_c the hard pomeron couples. Energy dependence put in by hand, as Donnachie + Landshoff. $R_c \simeq 0.22$ fm fixed from $F_2(x, Q^2)$.

The rest is prediction.

F_2^c dominated by hard pomeron, even at small Q^2
F_L more sensitive to hard pomeron than F_2
F_2^γ has comparable sensitivity to hard pomeron as F_2
$\sigma_{\gamma^*\gamma^*}$ dominated by hard pomeron
$\sigma_{\gamma p}$, $\sigma_{\gamma\gamma}$ have significant hard-pomeron component.

$\gamma p \to \rho p$

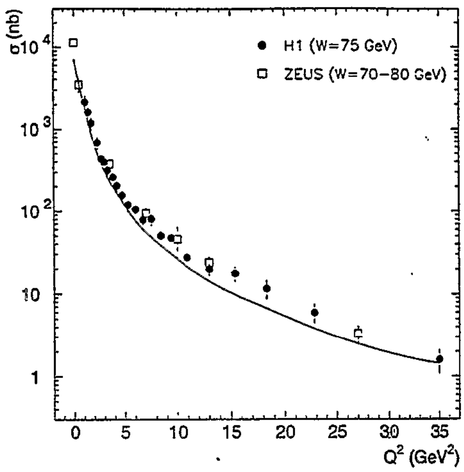

Figure 13: Q^2 dependence of the ρ-meson cross-section at $W = 75\,\text{GeV}$ in model S2. The data are from: H1 [64]; and ZEUS [51] [60] [62].

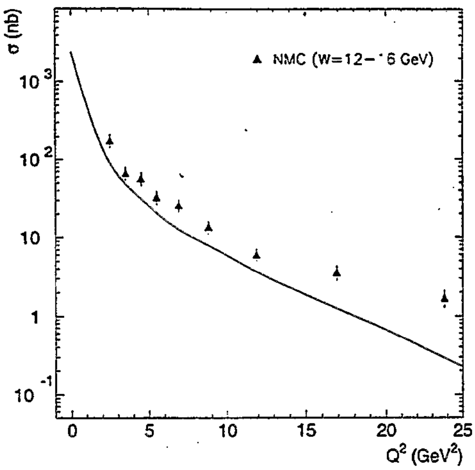

Figure 14: Q^2 dependence of the ρ-meson cross-section at $W = 15\,\text{GeV}$ in model S2. The data are from: NMC [48].

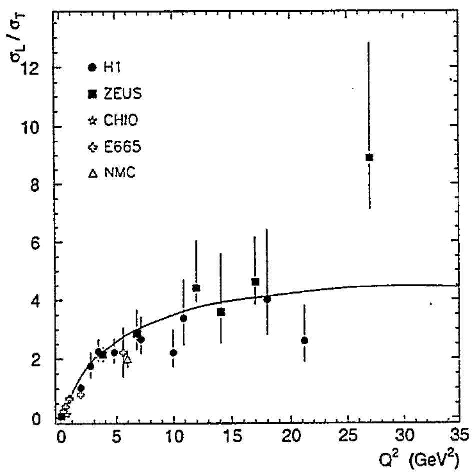

Figure 15: Q^2 dependence of the ρ-meson longtitudinal to transverse cross-section ratio at $W = 75\,\text{GeV}$ in model S2. The data are from: CHIO [42]; NMC [48]; E665 [57]; H1 [52] [53] [64]; and ZEUS [49] [51] [62].

σ_L/σ_T is very sensitive to the ρ wave function. Small changes in P_ρ produce large changes in the ratio.

The normalisation of the soft Pomeron term is essentially fixed by the ρ data, which it dominates.

$\gamma p \to J/\psi\, p$

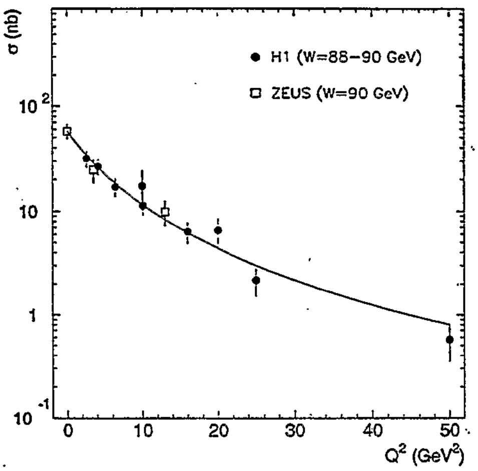

Figure 25: Q^2 dependence of the J/Ψ-meson cross-section at $W = 90$ GeV in model S2. The data are from H1 [54] [63]; and ZEUS [58] [62].

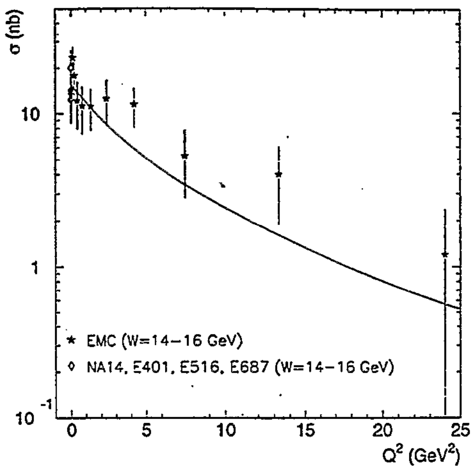

Figure 26: Q^2 dependence of the J/Ψ-meson cross-section at $W = 14$ GeV in model S2. The data are from The data are from EMC [44]; E401 [43]; E516 [45]; NA14 [46]; and E687 [47].

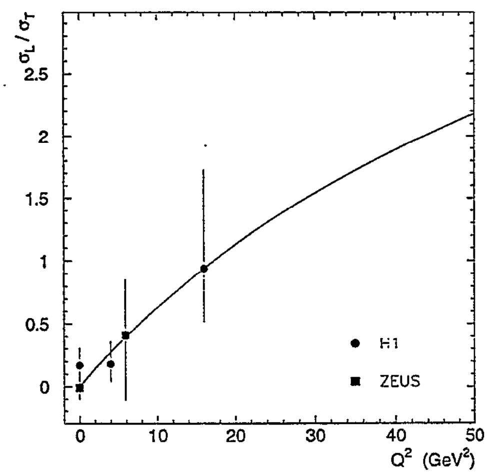

Figure 27: Q^2 dependence of the J/Ψ-meson longtitudinal to transverse cross-section ratio at $W = 90$ GeV in model S2. The data are from: H1 [54] [63]; and ZEUS [58] [62].

The J/ψ data fix the normalisation of the hard pomeron term. Interference between soft and hard is important at HERA energies. The wave function automatically selects the appropriate mix of soft and hard.

$\gamma p \to VX$ at W = 100 GeV

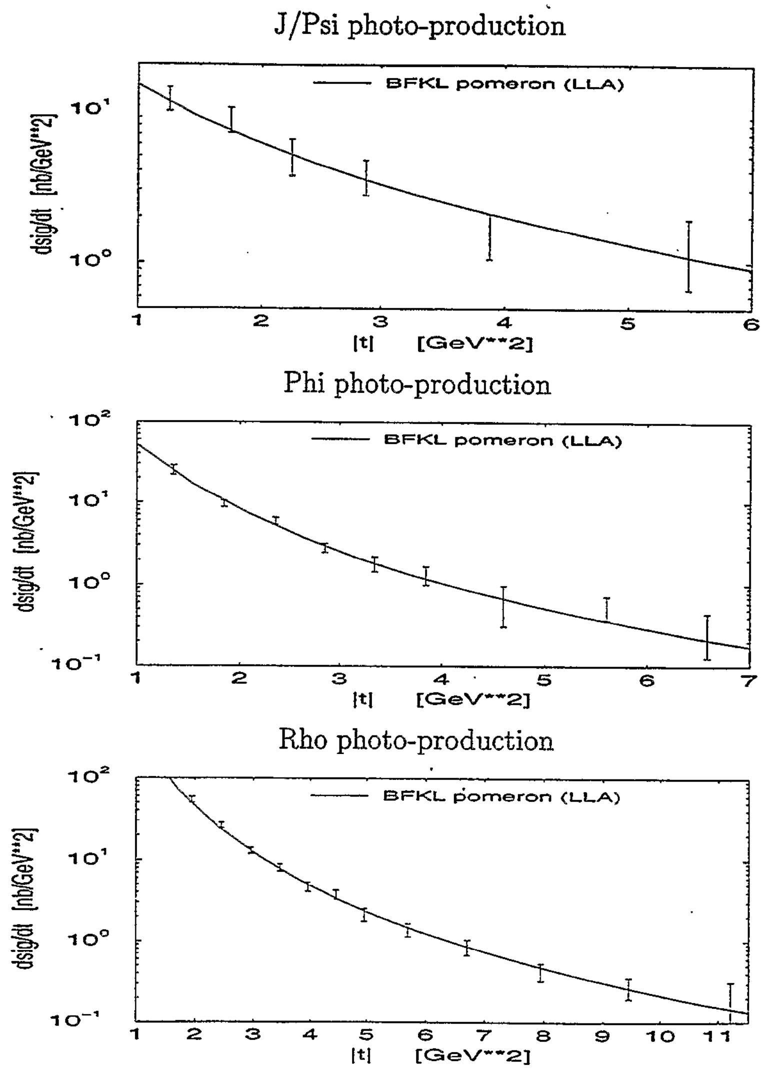

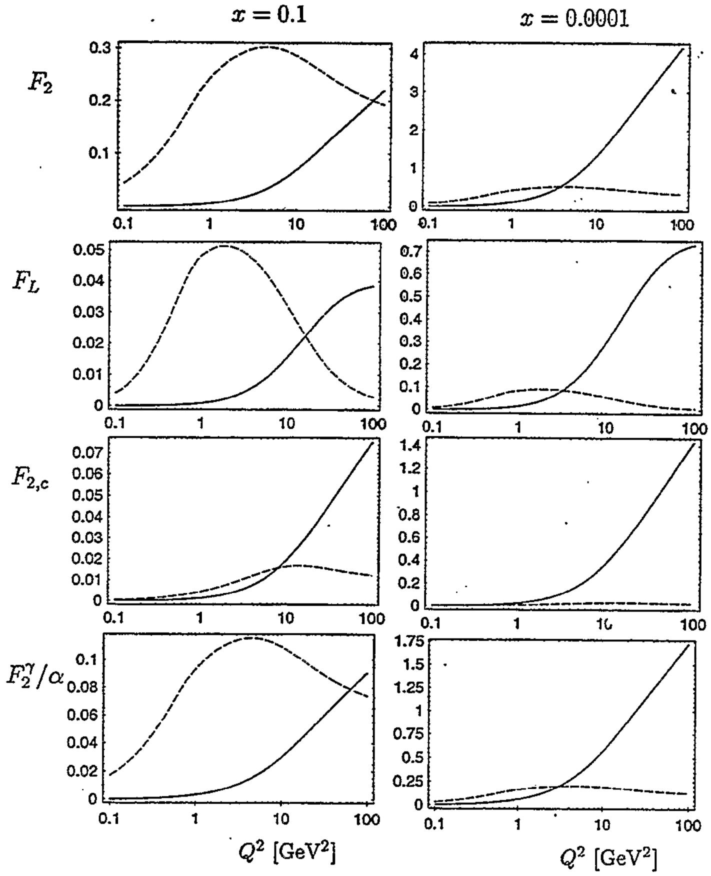

Reflects fit of Donnachie & Landshoff.

Sensitive to hard pomeron over wide (x, Q^2) range

Very comparable to F_2

Figure 2: The soft and hard contribution to structure functions at different values of x. Solid line hard contribution from the model; dashed line soft contribution from the model. First row proton structure function F_2; second row (p,L) longitudinal proton structure function F_L ; third row (p,c) charm contribution to the proton structure function F_{2c} , last row photon structure function F_2^γ/α.

QCD Instantons and the Soft Pomeron

Yuri V. Kovchegov

Department of Physics, University of Washington
Seattle, WA 98195, USA

We study the rôle of semi-classical QCD vacuum solutions in high energy scattering by considering the instanton contribution to hadronic cross sections. We propose a new type of instanton-induced interactions ("instanton ladder") that leads to the rising with energy hadronic cross section $\sigma \sim s^{\Delta}$ of Regge type (the Pomeron). We argue that this interaction may be responsible for the structure of the soft Pomeron. The intercept $\Delta > 0$ is calculated. It has a non-analytic dependence on the strong coupling constant, allowing a non-singular continuation into the non-perturbative region. To obtain the intercept we have to resum powers of the parameter $\exp\left(-\frac{4\pi}{\alpha_s}\ln s\right)$. We derive the Pomeron trajectory, which appears to be approximately linear in some range of (negative) momentum transfer t, but exhibits a curvature at small t and eventually flattens out at some larger t, similar to what is suggested by some phenomenological observations.

I would like to thank Dima Kharzeev and Genya Levin for collaboration on this project.

BFKL pomeron can be viewed as a cascade of gluons:

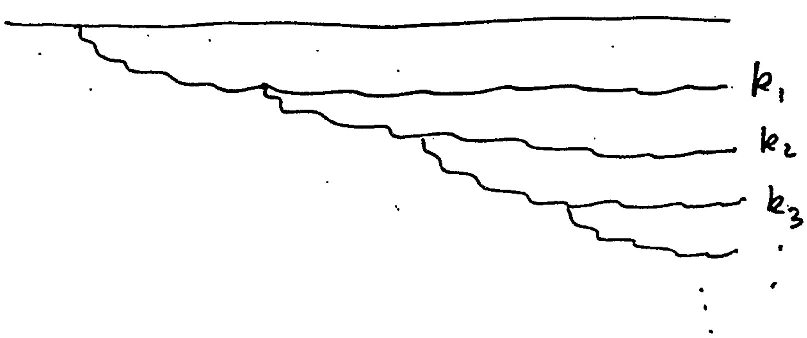

$k_{1+} >> k_{2+} >> k_{3+} >> \ldots$

$\tau_1 \sim \frac{k_{1+}}{\underline{k}_1^2}, \quad \tau_2 \sim \frac{k_{2+}}{\underline{k}_2^2}$

$\tau_1 >> \tau_2 >> \tau_3 >> \ldots$

a small-x gluon spreads over large longitudinal distances. In the rest frame of a proton $\ell \sim \frac{1}{2m_p x} \sim 100\,\text{fm}$ for $x = 10^{-3}$.

Even in the dilute instanton gas model it can interact with several instantons (typical size $\rho_0 \simeq .3\,\text{fm}$, typical separation $d \sim 1\,\text{fm}$)

OUR PICTURE:

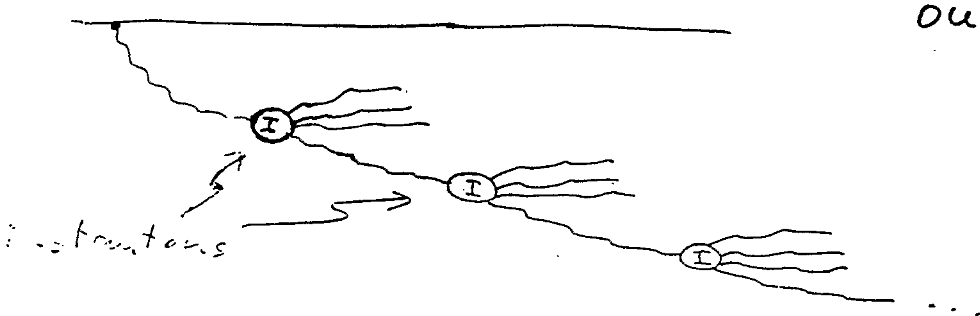

assume that $\alpha_s = \alpha_s(\rho_0) << 1$ and gluonic degrees of freedom still make sense

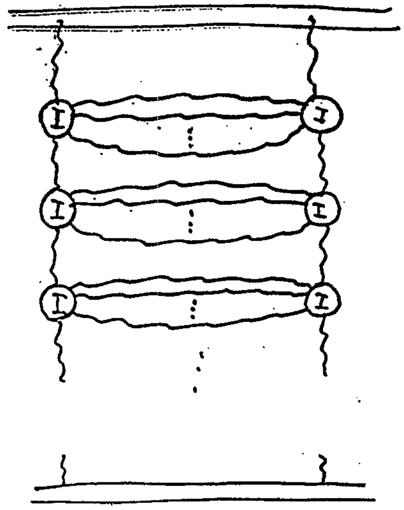

$\Rightarrow$ Consider a ladder diagram with instanton - induced vertices

$\Rightarrow$ each vertex gives a factor of $e^{-\frac{2\pi}{\alpha}}$, which is a small parameter for $\alpha \ll 1$.

$\Rightarrow$ we are resumming leading log's of energy:

$$e^{-\frac{4\pi}{\alpha}} \ll 1 \quad , \quad \ln s \gg 1$$

we are resumming powers of

$$\left(e^{-\frac{4\pi}{\alpha}} \ln s\right)^{\cdots} \sim 1$$

$\Rightarrow$ since the coherence length of a small-x gluon $l \sim 100\,fm$ is $\gg$ the typical instanton size $\rho_0 \sim .3\,fm$, we will use point-like instanton vertices

$\Rightarrow$ We will discard usual perturbative vertices as $\alpha \ll 1$.

D. Kharzeev, Yu.K., E. Levin,
cf. E. Shuryak & I. Zahed, '0(

We can plot Δ_P as a function of α_s:

$$\Delta_{soft} = \frac{.014\, d^2 \bar{\pi}}{(N_c^2-1)^2} \left(\frac{2\bar{\pi}}{\alpha}\right)^{4N_c} e^{-\frac{4\bar{\pi}}{\alpha}} \frac{(4\pi)^6}{\alpha^3} \frac{E_{sph}^2 \rho_0^2}{6e^2} \cdot \frac{1}{81} \cdot$$

$$\cdot \left[{}_2F_4\left(\frac{9}{2}, \frac{9}{2}; 1, 1, \frac{11}{2}, \frac{11}{2}; -\frac{\pi E_{sph}^4 \rho_0^4}{6\alpha e^2}\right) - 1 \right]$$

$$\Delta_P = \delta \left[\prod_{q=u,d,s} 1.3 \left(m_q \rho_0 - \frac{2\bar{\pi}^2}{3} (0|q\bar{q}|0) \rho_0^3 \right) \right]^2 \cdot \Delta_{soft}$$

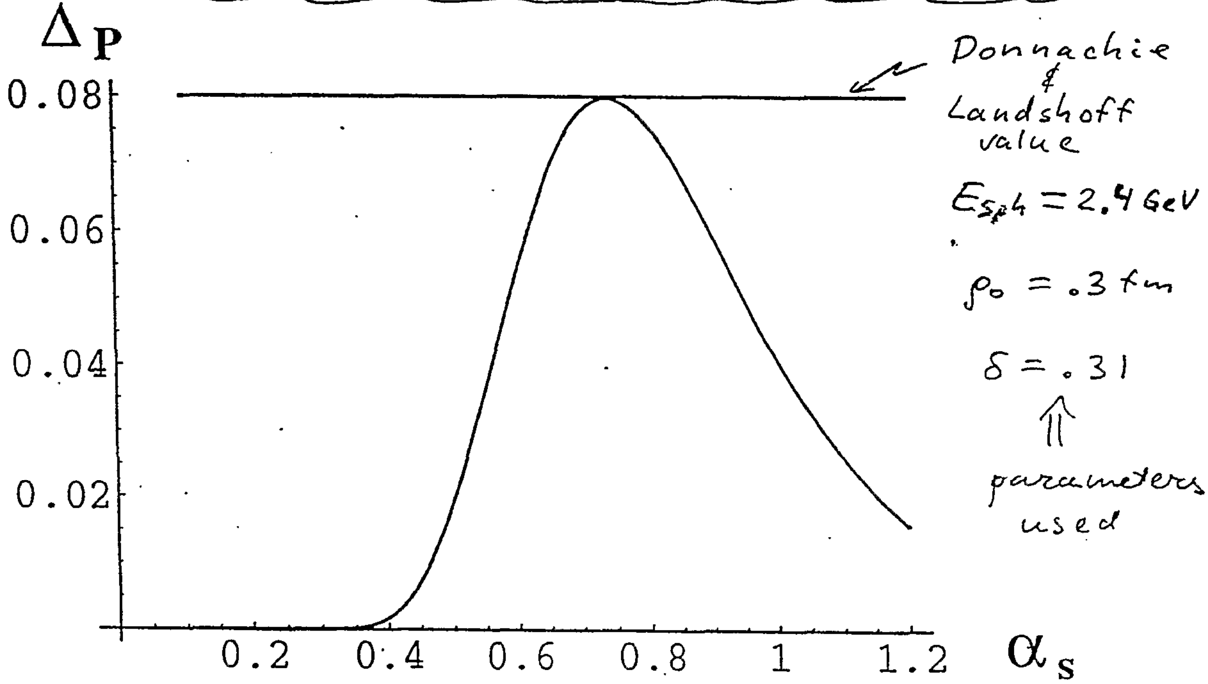

δ ~ factor taking into account virtual corrections

$\left[\prod 1.3 \left(m_q \rho_0 - \frac{2\bar{\pi}^2}{3} (0|q\bar{q}|0) \rho_0^3 \right) \right]^2$ ~ to include quark lines

Shifman, Vainshtein, Zakharov

$\Longrightarrow$ Even if $\alpha_s \to \infty$ at large distances our pomeron's intercept is finite, $\Delta_P \to 0$ as $\alpha_s \to \infty$

Pomeron's trajectory:

$$\Delta_{soft}(t) = \frac{\pi\, d^2}{(N_c^2-1)^2}\left(\frac{2\pi}{\alpha}\right)^{4N_c} e^{-\frac{4\pi}{\alpha}}\, \frac{(4\pi)^6}{\alpha^3}\,\frac{1}{81}\,\frac{E_{sph}^2\rho_0^2}{6\,e^2}\left[{}_2F_4\left(\frac{9}{2},\frac{9}{2};1,2,\frac{11}{2},\frac{11}{2};\frac{\pi E_{sph}^4\rho_0^4}{6\,\alpha e^2}\right)-1\right]$$

$$\times\frac{\pi}{256}\left\{2e^{t\rho_0^2/2}-e^{t\rho_0^2/4}-\frac{t\rho_0^2}{2}\left[2\,Ei\left(\frac{t\rho_0^2}{2}\right)-Ei\left(\frac{t\rho_0^2}{4}\right)\right]\right\}. \quad (58)$$

After taking into consideration the virtual corrections and the quark contributions the answer for the pomeron's trajectory becomes

$$\Delta_P(t) = \delta\left[\prod_{q=u,d,s,\ldots} 1.3\left(m_q\,\rho_0-\frac{2\pi^2}{3}\langle 0|\bar{q}q|0\rangle\,\rho_0^3\right)\right]^2 \Delta_{soft}(t), \quad (59)$$

where $\Delta_{soft}(t)$ is given by Eq. (58)

The soft pomeron's trajectory of Eq. (59) is depicted in Fig. 8. It is plotted for $\rho_0 = 0.3fm$, $E_{sph} = 2.4GeV$, $\delta = 0.31$ and $\alpha \approx 0.75$, i.e., the same values as were used for the estimates of the pomeron's intercept in Sect. IIIC.

$t = -q^2$

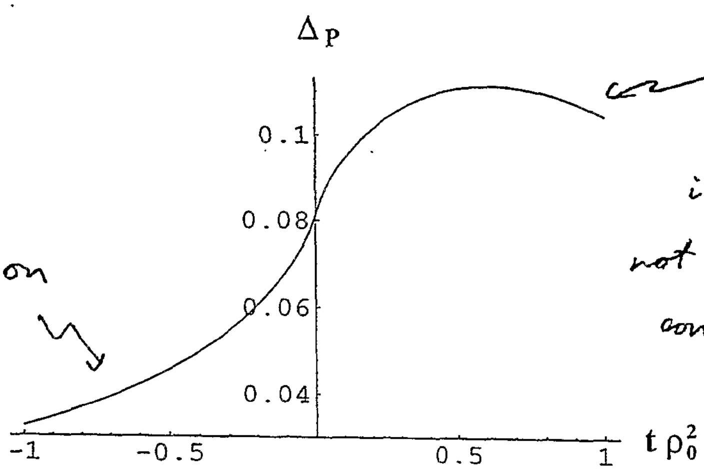

physical region $t<0$

not a straight line

instantons can not account for confinement

FIG. 8. Soft pomeron's trajectory. t is measured in the units of ρ_0^2.

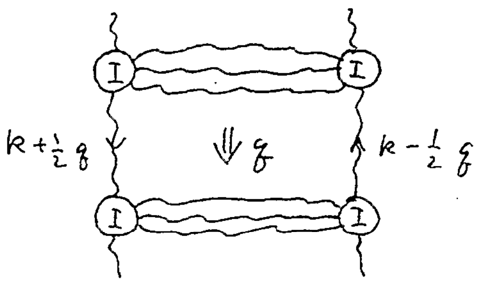

We can calculate the trajectory of our pomeron by considering non-zero momentum transfer.

$\sim s^{\Delta(t)}$, $\Delta(t)$ is the trajectory

Pomeron's slope: $\Delta(t) \simeq \Delta_{soft} + \alpha' t$ for small t.

$$\alpha' \simeq \Delta_{soft}\cdot\frac{\pi\rho_0^2}{256\, I_0}\ln\frac{1}{q\rho_0} \simeq \Delta_{soft}\cdot\rho_0^2\cdot\ln\frac{1}{q\rho_0} \simeq .2\ GeV^{-2}$$

which is consistent with experimental $\alpha'_{exp} = .25\ GeV^{-2}$

CONCLUSIONS

I. We have constructed a qualitative model of a pomeron, generated by a strong classical vacuum field.

II. We have quantified our model using the instanton field. The resulting pomeron's intercept has some non-analytic dependence on α_s. For reasonably small $\alpha_s \simeq .2-.3$ the intercept is $\Delta_{soft} \simeq .1$ The intercept goes to a finite limit for diverging α_s.

III. The slope of the obtained pomeron is $\alpha'/\Delta \simeq 2.0\ GeV^{-2}$, i.e. $\alpha' \simeq .20\ GeV^{-2}$, which is in agreement with the experimental $\alpha'_{exp} = .25\ GeV^{-2}$. We have also plotted the pomeron's trajectory, which is non-linear.

Pomeron at Strong Coupling

Chung-I Tan, Brown U.

21/5/2001

Key Idea:

4d YM Theories at weak coupling is **dual** to higher dim String Theories with AdS Background

R. C. Brower, S. Mathur, C-I Tan,
hep-ph/0102127; hep-th/0003115;
hep-th/9908196

Outline

- Goal: Non-pert. QCD at HE
- Why Strong Coupling?
- Ancient Lore of QCD at HE and Strings
- Mass Generation and Higher Dimensions
- Maldecena/Witten duality
- Full J^{PC} Glueball Spectrum at Strong Coupling
- Pomeron and Pomeron Intercept
- Future Directions

It has been a long held belief that QCD in a non-perturbative setting can be described by a string theory. This thirty-year search for the QCD strings has recently led to a remarkable conjecture: 4-dim QCD is exactly dual to a critical string theory in a non-trivial gravitational background at higher dimensions. In such a framework, Pomeron should emerge as a closed string excitation. We provide here a brief review for the Maldecena duality conjecture, and summarize results for the glueball spectrum and the Pomeron intercept in the strong coupling limit.

We first recall that in the early days of string theory, (or the "dual resonance model" to use the nomenclature that predates both string theory and QCD), one observed that it was reasonable to represent the hadronic spectrum beginning with zero width "resonances" on exactly linear Regge trajectories. With the advent of QCD this approach was reformulated as the $1/N$ expansion at fixed 't Hooft coupling, $g_{YM}^2 N$. States with vacuum quantum numbers could be assigned to closed-strings, including a massive 2^{++} tensor glueball on the leading Pomeron trajectory, $\alpha_P(t) = \alpha_P(0) + \alpha'_P\, t$. Soon a three-fold crisis appeared: *zero-mass states, extra dimensions, supersymmetries.* A careful study of negative norm states (i.e ghosts), tachyon cancellation and the consistency of the perturbative expansion at the one loop level led to supersymmetric string theories in 10 space-time dimensions. At the one-loop level unitarity requires that pair creation of two open strings, each contains "zero-mass" spin-1 states, is dual to a vacuum exchange with an intercept $\alpha_P(0) = 2$. This leads to a massless 2^{++} state, the **graviton.** In fact the low energy, perturbative string theory was clearly not QCD but rather **supergravity in 10 dimensions**!

What is the mechanism which allows our 4-d space/time and yet is able to generate a non-zero mass gap for tensor glueballs? How can one "lower" the Pomeron intercept so that $\alpha_P(0)$ takes on its phenomenological value of $1.1 \sim 1.2$? The key ingredient turns out to be **duality**, which allows a dual description of QCD involving extra dimensions and a nontrivial background metric which breaks supersymmetries.

This recent development has led to the rebirth of active QCD string studies. A rich glueball spectrum can be computed at strong coupling. In particular, ond finds:

$$\alpha_P(0) \simeq 2 - 0.66\,(\frac{4\pi}{g^2 N}) + 0(\frac{1}{g^4 N^2})\,. \qquad (1)$$

With $N = 3$ and $g^2/4\pi \simeq 0.25$ at a characteristic confinement scale, Λ_{QCD},this leads to a value for $\alpha_P(0) \simeq 1.12$.

Pomeron in Strong Coupling

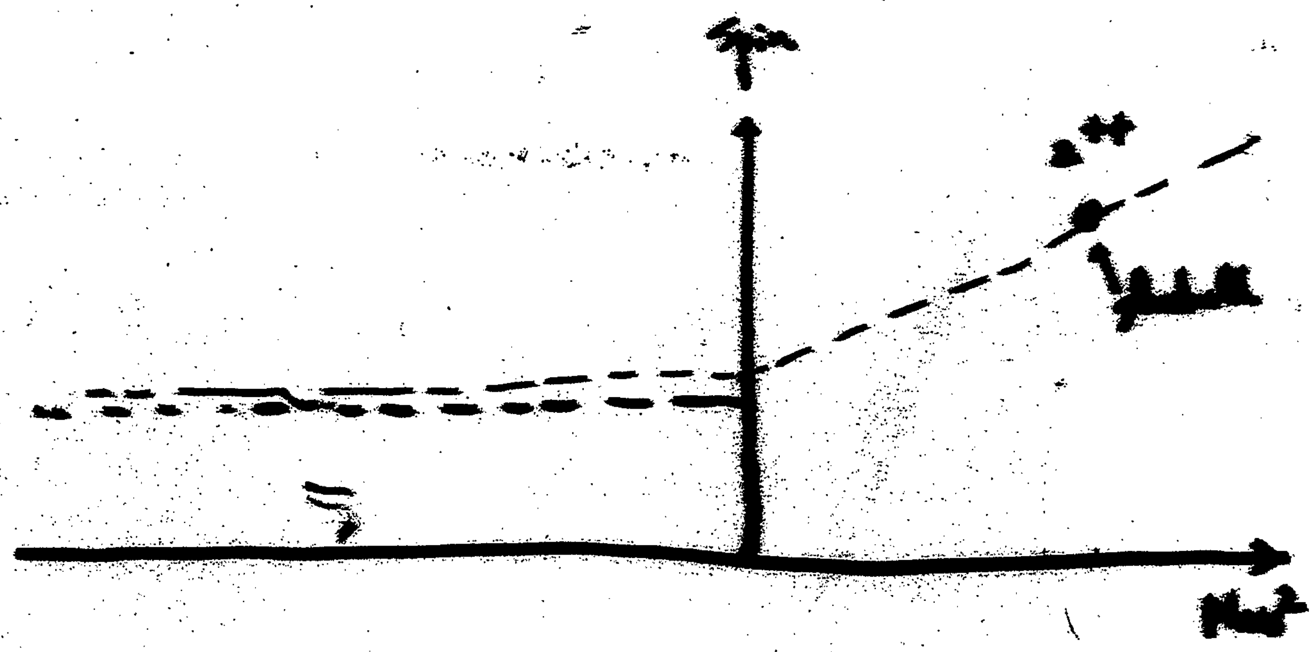

- $\alpha_P(0) \approx 1.1 \sim 1.4 \to \frac{g^2}{4\pi} \approx 0.2 \sim 0.3$ for $N=3$

  "cross over" region ?

- $\alpha_P(0)$: "lowered" from 2 for finite $\frac{g^2N}{4\pi}$

- "Bounded" from below by 1 ??

Pomeron Intercept in Strong Coupling:

$$\alpha_P(t) \simeq \alpha_P(0) + \alpha'_P\, t$$

$$\alpha_P(t) = 2 + \alpha'_P\,(t - m_T^2)$$

$$m_T^2 \simeq \left[(9.86)^2 + O\left(\frac{1}{g^2 N}\right)\right] \beta^{-2}$$

$$\alpha'_{P} \simeq \left(\frac{27}{32\pi^2}\right)\left(\frac{1}{g^2 N}\right)\left[1 + O\left(\frac{1}{g^2 N}\right)\right] \beta^2$$

$$\boxed{\alpha_P(0) = 2 - 0.66\left(\frac{4\pi}{g^2 N}\right) + O\left(\frac{1}{g^4 N^2}\right)}$$

V. QCD After Brane-Revolution

"New Chapter for Non-perturbative QCD"

* Weak Coupling → Perturbative QCD

unchanged

* Non-perturbative QCD: (Dual description)
  - Effective degrees of freedom ... massless fields of Type IIA String th.
  - AdS/BH Background
  - Glueball Spectrum in Strong Coupling Limit

* Pomeron as Massive Graviton

  - Pomeron Intercept in strong coupling

$$\alpha_{\mathbb{P}}(0) = 2 - 0.66\left(\frac{4\pi}{g^2N}\right) + O\left(\frac{1}{g^4N^2}\right)$$

Universal Pomeron from High Energy Relativistic Quantum Field Theory

Jacques SOFFER[1]
Centre de Physique Théorique
CNRS Luminy Case 907
13288 Marseille Cedex 09 France

From the very high energy behavior of Relatistic Quantum Field Theory, it is possible to deduce some essential features of high energy hadron elastic scattering. This was first realized thirty years ago by Cheng and Wu, who investigated massive Quantum Electrodynamics. They were the first to predict the rise of total cross sections, resulting from the existence of the so-called *tower diagrams*, which generate a term $S(s) = s^c/(lns)^{c'}$. This is the basic ingredient to built up our Universal Pomeron. In the framework of the impact-picture approach, we assume a factorization property to construct the Born term of the hadron elastic scattering amplitude, as a product of $S(s)$ and a function $F(b)$ of the impact parameter b, related to the internal hadronic matter distribution. The eikonalization is done in order to insure unitarity. These considerations have led us to the so-called, Bourrely-Soffer-Wu (BSW) model, which was proposed twenty years ago. It allowed a good description of pp and $\bar{p}p$ elastic scattering up to ISR energies and was able to give very accurate predictions up to CERN SPS collider and Tevatron energies.

Here we present an update version of the BSW model for pp and $\bar{p}p$, including new data and some predictions which can be tested at RHIC-BNL, in the near future by the *pp2pp* experiment. We have also extended our approach to describe $\pi^{\pm}p$ and $K^{\pm}p$ elastic scattering up to the highest available energy, with the same Pomeron. We make predictions in the TeV energy range in view of a possible fixed target physics programme at LHC. Some predictions for $\gamma\gamma$ and γp total cross sections are presented and we compare them some with latest LEP and HERA data.

[1]E-mail: soffer@cpt.univ-mrs.fr

UNIVERSAL POMERON FROM HIGH ENERGY RELATIVISTIC QUANTUM FIELD THEORY

(J. SOFFER RIKEN-BNL
MAY 21, 2001)

1. THEORETICAL FRAMEWORK
   HADRON SCATTERING IS COMPLICATED
   1^{st} SIMPLIFICATION : ELASTIC SCATTERING
   2^{nd} SIMPLIFICATION : HIGH ENERGY
   FROISSART-MARTIN BOUND $\sigma_{tot} < \text{const} (\ln s)^2$
   THE INSIGHTS FROM HIGH ENERGY BEHAVIOUR OF RQF

2. DESCRIPTION OF pp ($\bar{p}p$) ELASTIC SCATT. AND NUMERICAL RESULTS

3. πp ELASTIC SCATT.

4. Kp ELASTIC SCATT.

5. γp AND $\gamma\gamma$ TOTAL CROSS SECTIONS

6. CONCLUDING REMARKS

RESULTS FROM RQFT (1970)

PICTURE THREE DECADES AGO

$\sigma_{tot} \to$ FINITE LIMIT (GEOMETRICAL SIZE)

CHENG AND WU UNDERTAKE PROGRAMME TO STUDY BEHAVIOR OF RQFT AT VERY HIGH ENERGIES USING MASSIVE QED

COMPTON $V + f \to V + f$

2nd ORDER  $\cdot\ g^2 s^0$

4th ORDER 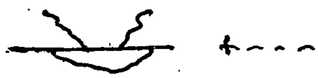 $:\ g^4 s^0$

6th ORDER 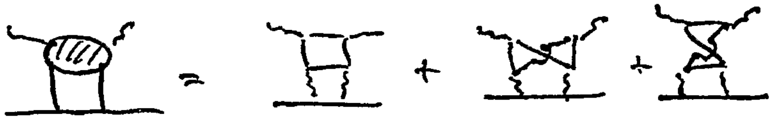 $i g^6 s$

SO 6th ORDER MORE IMPORTANT THAN 2nd AND 4th BECAUSE PAIR PROD. PEAKS FORWARD

8th ORDER 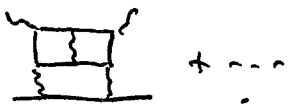 $i g^8 s$

BUT 10th ORDER 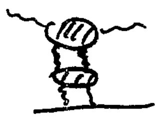 $i g^{10} s \ln s$

14th ORDER 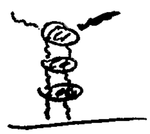 $i g^{14} s \ln^2 s$

MØLLER $f + f \to f + f$

8th ORDER 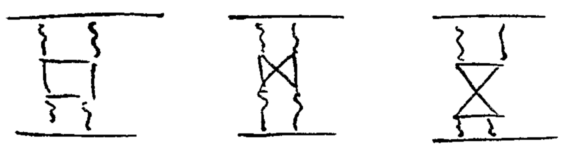 $s \ln s$

AFTER SUMMATION OF TOWER DIAGRAMS GET

$i\, s^{c} / (\ln s)^{c'} \Rightarrow$ RISING σ_{tot}

C. Bourrely et al. / Physics Letters B 339 (1994) 322–324

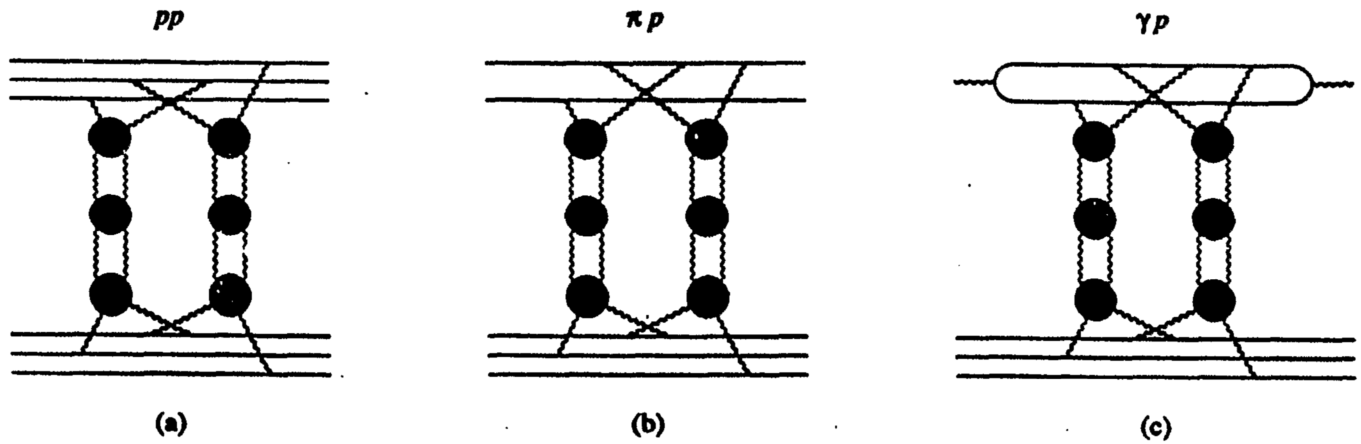

Fig. 1. Multi-tower diagrams for (a) pp and $\bar{p}p$, (b) $\pi^{\pm}p$ and (c) γp scattering.

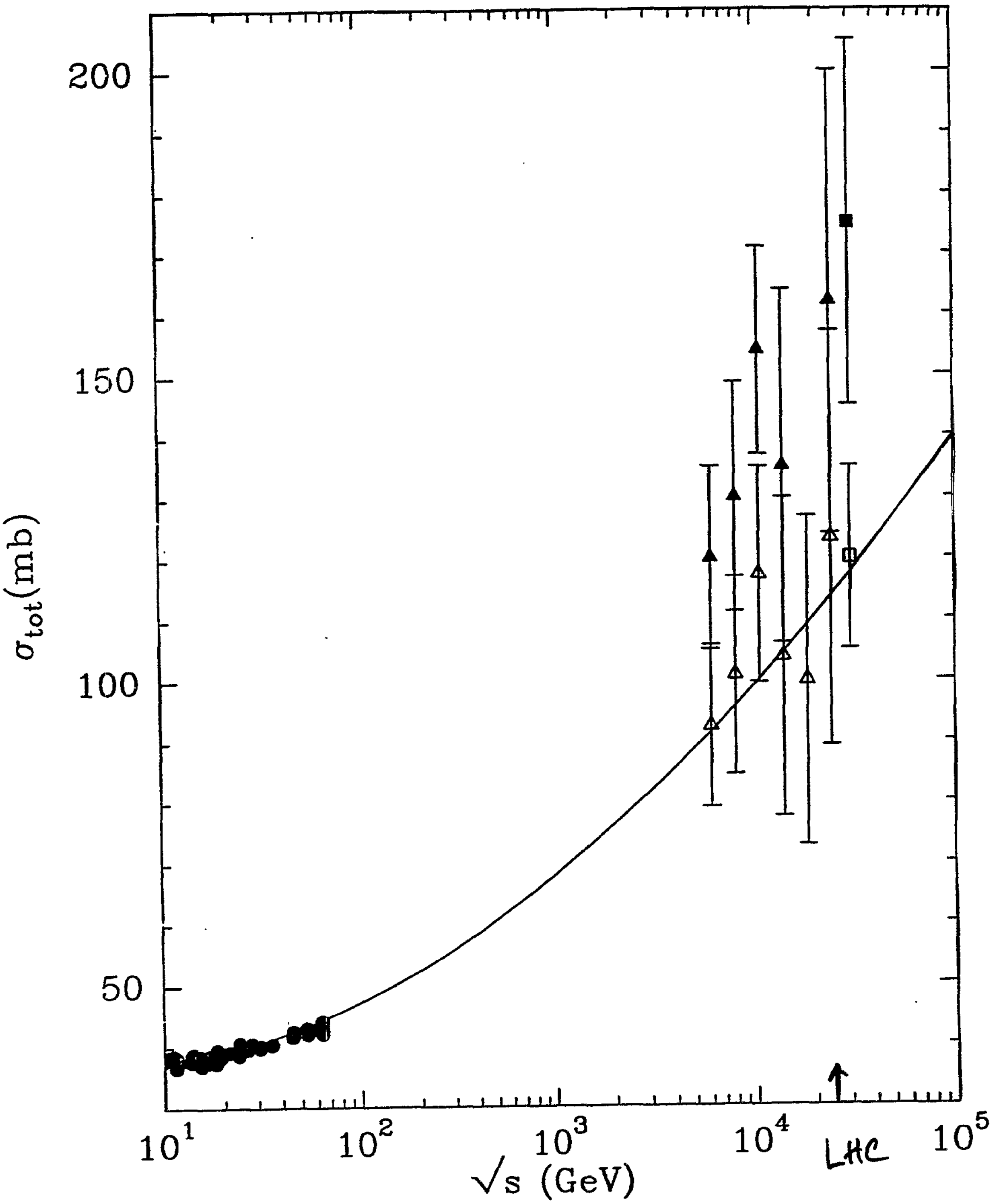

$\sigma_{tot}(14\,\text{TeV}) = 104.56$ mb

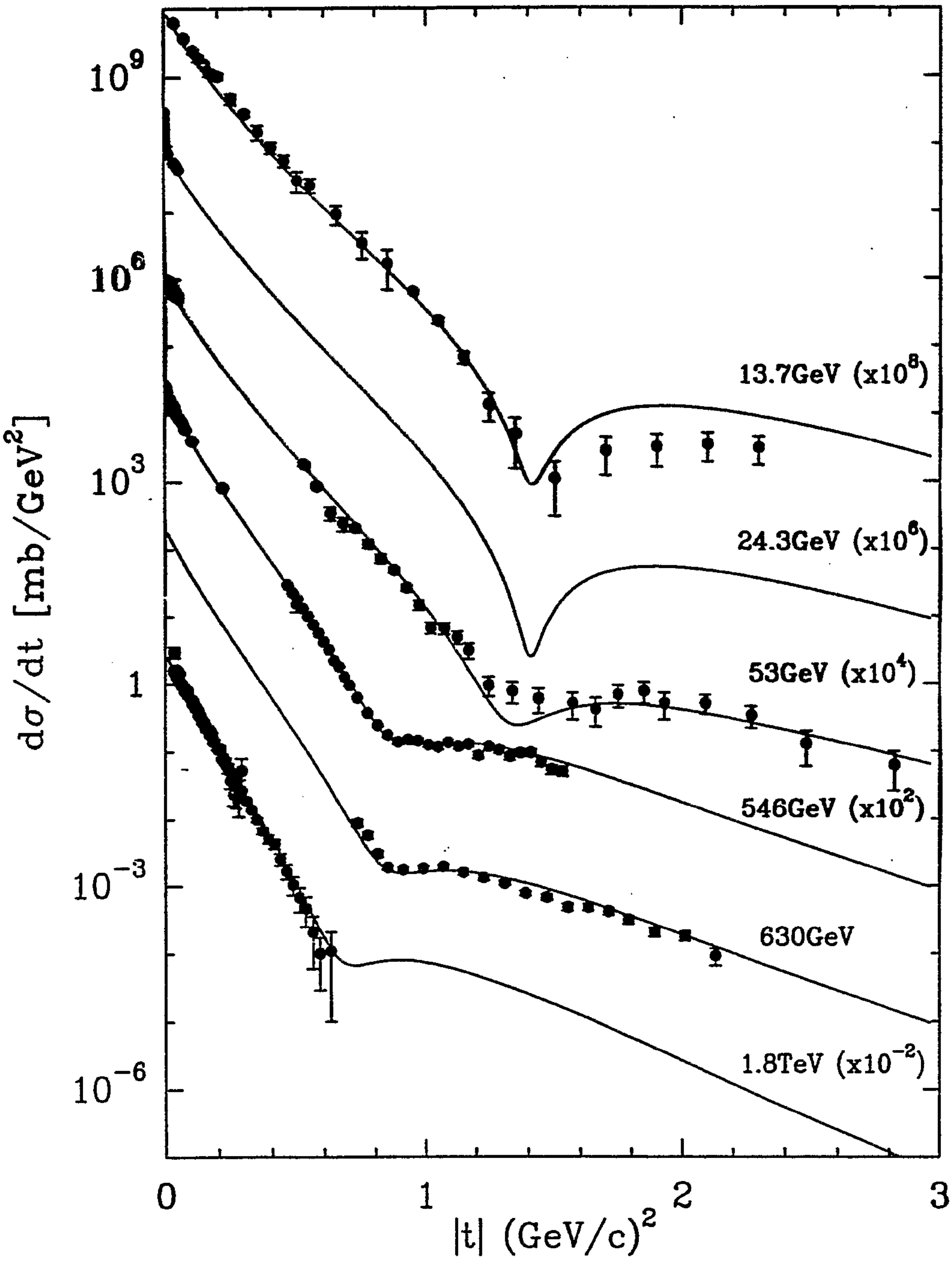

Figure 4: $d\sigma/dt$ for $\bar{p}p$ as a function of $|t|$ for $\sqrt{s} = 13.7, 24.3, 53, 546, 630, 1800$GeV. Experiments [25, 24, 26, 28, 29, 30, 31].

PREDICT THAT
ISR DIP TURNS
INTO A SHOULDER
AT $p\bar{p}$ COLLIDER

6. CONCLUDING REMARKS

- THE HIGH ENERGY BEHAVIOUR OF A RQFT HAS GENERATED A <u>UNIVERSAL</u> POMERON FOR THE DESCRIPTION OF pp, $\bar{p}p$, $\pi^{\pm}p$, $K^{\pm}p$, γp AND $\gamma\gamma$ SCATTERING

- THIS IMPACT PICTURE IS VERY SUCCESSFUL
  IT WOULD BE DESIRABLE TO DERIVE FROM QCD THE FEW PARAMETERS WHICH WERE INTRODUCED, NAMELY c, c' FOR s DEPENDENC

- OPEN PROBLEMS FOR THE FUTURE
  - POLARIZATION
  - INELASTIC DIFFRACTIVE SCATTERING
  - ----

$$\sigma_{tot}^{\gamma p}(\sqrt{s}) = A\alpha\left[\sigma_{tot}^{\pi^+ p}(\sqrt{s}) + \sigma_{tot}^{\pi^- p}(\sqrt{s})\right]$$

$$A = 0.33437$$

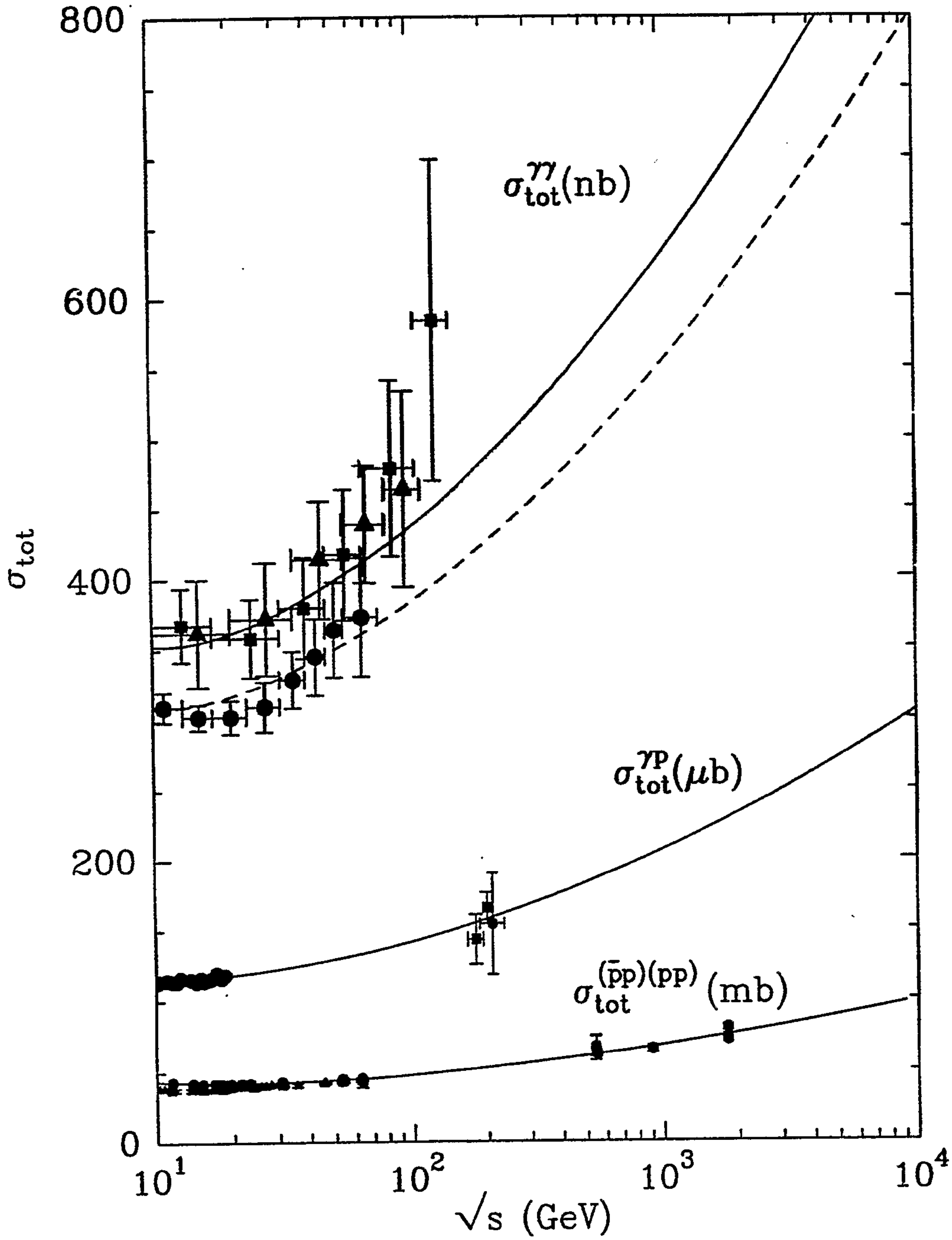

Figure 16: A plot of total cross sections, $\bar{p}p$, γp $\gamma\gamma$ as a function of $\sqrt{s}$(GeV). For $\sigma_{\gamma\gamma}$ two different LEP energies are drawn [42], [43]. Model predictions, solid curve $A = 9.23\ 10^{-6}$, dashed curve $A = 8.1\ 10^{-6}$.

$$\sigma_{tot}^{\gamma\gamma}(W_{\gamma\gamma}) = A\,\sigma_{tot}^{pp}(\sqrt{s})$$

Coherence in Nuclear Interactions at RHIC

Joakim Nystrand

Department of Physics,
Lund University, Lund, Sweden

In very peripheral collisions (b>2R), nuclei may interact through their electromagnetic and nuclear fields. The exchange particles of the fields couple coherently to the entire nucleus for small momentum transfers. The coherence requiremnt limits the mass and transeverse momentum of the final state to $\sim 2\gamma\hbar c/R$ and $\sim \sqrt{2}\hbar c/R$, respectively. At RHIC, the maximum center of mass is about 6 GeV for a heavy system such as Au+Au. Two-photon, photon-Pomeron, and Pomeron-Pomeron interactions are possible.

The cross sections for coherent vector meson production in heavy-ion interactions at RHIC are large[1]. This is because of the high flux of equivalent photons from the electromagnetic fields of the nuclei and vector meson dominance. The cross sections have been calculated in [1] using the Weizsäcker-Williams method to estimate the equivalent flux of photons. The photonuclear cross sections $\sigma(\gamma + A \rightarrow V + A)$ have been obtained from a Glauber model calculation with data on $\sigma(\gamma+p \rightarrow V+p)$ as input. Because of the strong fields, the cross sections for multiple vector meson production, $A + A \rightarrow A + A + V + V$, are appreciable at RHIC.

It is generally not possible to determine which nucleus emitted the photon and which emitted the Pomeron in a photon-Pomeron interaction. The median impact parameters for producing a vector meson in Au+Au interactions at RHIC range from about 20 to 40 fm. For vector meson transverse momenta $p_T < \hbar c / < b >$ interference will occur[2]. The cross section is calculated as an integral over the impact parameter

$$\frac{d\sigma}{dy dp_T} = \int_{b>2R} |A_1 + A_2|^2 db^2 \qquad (1)$$

where A_1 and A_2 are the amplitudes for production off a single nucleus. Since the electric field is antisymmetric and the nuclear density symmetric under spatial inversion, the interference will be destructive. The interference does not affect the overall vector meson production cross sections significantly, but does change the transverse momentum distribution. The change in the transverse momentum distribution should be experimentally observable.

The separation between the nuclei is generally much larger than the $c\tau$ of the vector mesons ($< b > \approx 40$ fm and $c\tau = 1.3$ fm for the ρ^0). This means that the vector meson will have decayed before the amplitudes from the two sources can overlap. The system thus works as a two-source interferometer for unstable particles.

The photon from the emitting nucleus may interact incoherently with the target nucleus resulting in break-up of that nucleus. The dominating process is photonuclear excitation of the target into a Giant Dipole Resonance[3]. Coherent vector meson production can occur in coincidence with Coulomb excitation of one or both nuclei. If the photonuclear excitation and the vector meson production are uncorrelated, a vector meson is accompanied by mutual break-up of both nuclei in about 10% of the interactions. Requiring production in coincidence with nuclear break-up reduces the median impact parameters in the interacions by roughly a factor of 2. This should affect the interference discussed above.

Acknowledgements

I would like to acknowledge Spencer Klein, LBNL, Berkeley, my collaborator in the studies of vector mesons and interference. I would like to thank Tony Baltz and Sebastian White, BNL, Brookhaven, for providing the Coulomb interaction probabilities from their paper[3] and for useful discussion.

References

[1] S.R. Klein, J. Nystrand Phys. Rev. **C60**, 014903 (1999).

[2] S.R. Klein, J. Nystrand Phys. Rev. Lett. **84**, 2330 (2000).

[3] A.J. Baltz, C. Chasman, S.N. White Nucl. Inst. Meth. **417**, 1 (1998).

Peripheral Collisions at RHIC

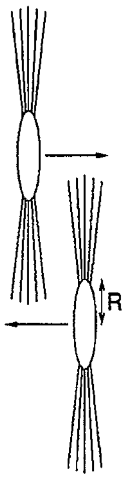

What happens when the nuclei miss each other, b> 2R?

Interaction between the electromagnetic and nuclear fields

EM field:	long range
Nuclear field:	short range

For small mometum transfers (Q<1/R), the fields couple coherently to all nucleons.

Enhances cross section: Z^2 , A^2 ($A^{4/3}$)

Truly coherenct interactions: coherent coupling to both nuclei: $\gamma\gamma$, γ-Pomeron(meson), Pomeron-Pomeron

Max CM energies at heavy-ion accelerators:

$$W \approx 2\,\gamma_{CM}\,(hc/R)$$

For heavy nuclei (Au/Pb):

	γ_{CM}	W [GeV]
BNL AGS	3	0.1
CERN SPS	9	0.5
RHIC	100	6
LHC	2,940	160

Experimental consequences of coherence

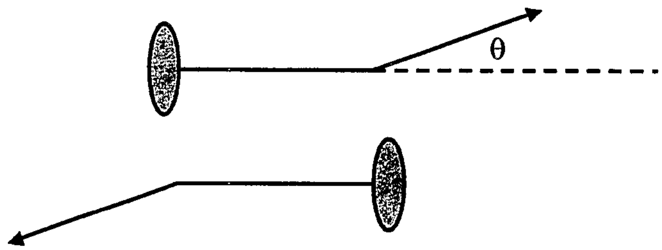

The coherence requirement limits the angular deflection to

$$\theta \sim 0.175 / (\gamma \cdot A^{4/3})$$

At RHIC

Au	A=197	$\theta \sim$ 1 μrad
I	A=127	$\theta \sim$ 3 μrad
Si	A=28	$\theta \sim$ 17 μrad

$\Rightarrow$Not possible to tag the outgoing nuclei.

Experimental method: Reconstruct the entire event, signal of coherence from low p_T.

Coherent Vector Meson Production

The electromagnetic field of one nucleus corresponds to a stream of photons impinging upon the other nucleus (Weizsäcker-Williams).

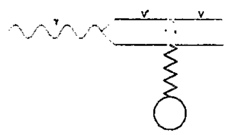

The photon may fluctuate into a vector meson (qq-pair) which scatters elastically off the target nucleus.

$$\gamma\text{+Pomeron} \rightarrow V$$

The cross section can be calculated as the convolution of the WW photon spectrum with the γA photonuclear cross section.

$$\sigma(A+A \rightarrow A+A+V) = \int n(\omega)\, \sigma_{\gamma A}(\omega)\, d\omega$$

Note: This assumes that one can determine which nucleus emitted the photon or the Pomeron.

NOT possible in general $\Rightarrow$

Some interesting quantum mechanical effects.

Experimental signal of coherence – p_T spectrum

Convolution of p_T distributions

$f_{1,2}(p_T) = \int f_1(p_T') f_2(p_T - p_T') dp_T'$

$f_1(p_T) = | F(\omega^2/\gamma^2 + p_T^2) |^2 (p_T/(\omega^2/\gamma^2 + p_T^2))^2$ γ

$f_2(p_T) = | F(E^2/\gamma^2 + p_T^2) |^2$ P

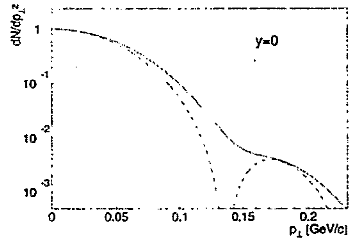

Production off two nuclei

$$\frac{d\sigma}{dY dP_T^2} = \int \underbrace{k_1 \frac{dn}{dk_1 db^2}}_{\text{Photon flux } |\int E(b,t) e^{ikt} dt|^2} \sigma(\gamma A_2 \rightarrow VA_2) f_{1,2}(p_T) + k_2 \frac{dn}{dk_2 db^2} \sigma(\gamma A_1 \rightarrow VA_1) f_{2,1}(p_T) \, db^2$$

Impact parameter, b, measurable in principle (but not in practice)

Integration over b only valid if $p_T >> 1/b$.

$\Rightarrow$ Add amplitudes

$$d\sigma/dy \, dp_T = \int | A_1 + A_2 |^2 db^2$$

Quantum mechanical aspects of the interference

-The production is localized to the two nuclei because of the short range of the nuclear force.

- $c\tau << \langle b \rangle$, $c\tau \sim 1\text{fm}$ $\langle b \rangle \sim 40$ fm

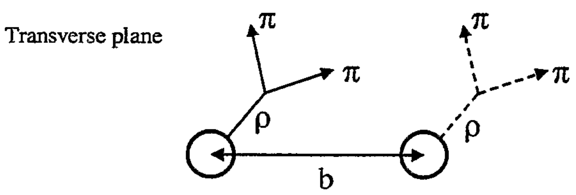

- The ρ will have decayed before the amplitudes from the two sources can overlap.
- For interference, the wave function of the pions must retain information about their origin long after the decay.
- A two-source interferometer for unstable particles!

Electromagnetic dissociation

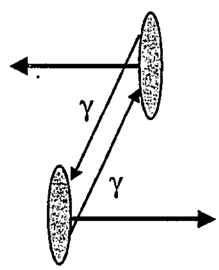

The "target" nucleus is excited by a photon from the EM field of the other nucleus and breaks up.

The cross sections are large (Baltz,Chasman,White NIM A417(1998)1)

single dissociation (1 nucleus) : $\sigma = 95$ b

double dissociation (both nuclei) : $\sigma = 3.7$b

In a grazing collision (b=2R), P(double dissociation) ≈ 35%

Vector meson production in coincidence with Coulomb disscociation

If Coulomb excitation and V.M. production independent:

$$\sigma = \int (1 - P_{HAD}(b))\, P_C(b)\, P_V(b)\, 2\pi b \, db$$

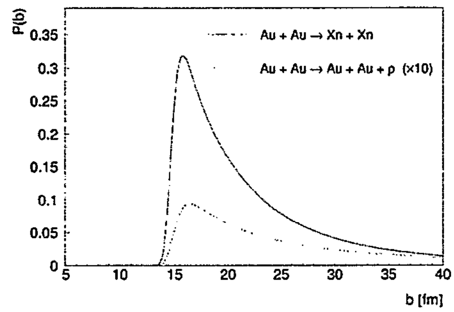

Vector Meson	Au + Au → Au + Au + V	Au + Au → Au* + Au* + V
ρ	σ = 590 mb	σ = 42 mb
ω	σ = 59 mb	σ = 4 mb
φ	σ = 39 mb	σ = 3 mb
J/ψ	σ =0.29 mb	σ = 0.04 mb

• Easier to trigger on experimentally (at least in experiments primarily designed for central AA collisions, ZDC Calorimeters).

• Dissociation cross sections for emission of 1neutron vs. any number of neutrons (Au+Au at 200 A GeV)

$\sigma(Xn,Xn) = 3.7$ b $\quad \sigma(1n,Xn) = 1.4$ b $\quad \sigma(1n,1n) = 0.45$ b

In coincidence with ρ production

$\sigma(Xn,Xn,\rho) = 42$ mb $\quad \sigma(1n,Xn,\rho) = 13$ mb $\quad \sigma(1n,1n,\rho) = 3.4$ mb

Ratios different, e.g.

$\sigma(1n,1n)/\sigma(1n,Xn)$	=	0.329	(Exp. 0.34±0.01)
$\sigma(1n,1n,\rho)/\sigma(1n,Xn,\rho)$	=	0.268	

• Requiring coincidence gives a measure of the impact parameter

ρ	<b> = 46 fm	1n,Xn,ρ	<b> = 18 fm
1n,1n, ρ	<b> = 20 fm	Xn,Xn,ρ	<b> = 18 fm

Photon-Pomeron Interactions at RHIC

Falk Meissner * *for the STAR Collaboration*

In ultra-peripheral heavy ion collisions the two nuclei interact via their long range fields at impact parameters $b > 2R_A$, where neither nucleus is disrupted. In exclusive ρ^0 production $AuAu \rightarrow AuAu\rho^0$, a virtual photon emitted by one nucleus fluctuates to a $q\bar{q}$ pair, which then scatters diffractively from the other nucleus. Both, the photon and the Pomeron couple coherently to the nuclei with a coupling strength proportional to Z^2 for the photon and between $A^{4/3}$ ($\propto$ surface) and A^2 ($\propto$ volume) for the Pomeron. It follows, that the cross section for this process is expected to be large: 380 mb or 5% of the hadronic cross section at $\sqrt{S_{NN}} = 130$ GeV[1]. Coherent coupling yields the condition that the interaction takes place only at small transverse momenta $p_T < 2\hbar/R_A \sim 100$ MeV.

Besides photo-nuclear interactions, ultra-peripheral collisions can also involve purely electromagnetic photon-photon processes like e^+e^- pair production; these may be sensitive to non-perturbative QED since the coupling constant $Z\alpha \approx 0.6$ is large. Purely hadronic double diffractive interactions may produce exotica as glue balls. Nevertheless, the cross section for Pomeron-Pomeron processes is expected to be small due to the short range of the strong force.

Exclusive ρ^0 meson production at low p_T has a specific experimental signature: the $\pi^+\pi^-$ decay products of the ρ^0 meson are observed in an otherwise 'empty' spectrometer; the pion tracks are back-to-back in the transverse plane. The two nuclei remain in their ground state, therefore no signal is detected in the zero degree calorimeters.

To detect ultra-peripheral collisions with the STAR detector a low-multiplicity topology trigger was implemented, suppressing background from cosmic rays, beam gas events, and debris from upstream interactions. The central trigger barrel was divided into quadrants. A hit was required in both a South and a North quadrant, while the Top an Bottom quadrants acted as a veto to suppress possible cosmic rays. A fast online reconstruction eliminated events with more than 15 tracks and events with tracks not emerging from the the collision region. Using this trigger, the STAR collaboration collected 7 hours of data in 2000. The level 0 trigger rate varied from 20 to 40 Hz and was reduced to about 1-2 Hz by the level 3 trigger[2].

The ρ^0 analysis selected events with exactly two tracks that formed a primary vertex. The transverse momentum distribution (c.f. slides) for the ρ^0 candidates is peaked around $p_t <$ 100MeV, showing the coherent coupling to both nuclei. For pairs within the peak at $p_T < 100$ MeV a clear signal of about 300 ρ^0 is observed in the $M_{\pi\pi}$ invariant mass spectrum. For comparison, combinatorial background (modeled by like-sign pairs and shown as the shaded histograms in the plots) shows neither the coherent peak, nor a ρ^0 mass peak.

In parallel to the production of a ρ^0 meson, the two nuclei can be excited by the exchange of one or more photons yielding the emission of neutrons which are detected in the zero degree calorimeters (ZDC). About $800,000$ events with coincident neutron signals in both ZDC's (minimum bias trigger) have been recorded in 2000. About 300 coherent ρ^0 events at the characteristic low p_T have been found in this data sample.

In summary, the first observation of coherent ρ^0 production in ultra-peripheral heavy ion collisions is reported. The two processes $AuAu \rightarrow AuAu\rho^0$ and $AuAu \rightarrow Au^*Au^*\rho^0$, i.e. exclusive ρ^0 production with and without nuclear excitation, have been observed.

[1] S. Klein and J. Nystrand, Phys. Rev. **C60**, 014903 (1999).

[2] F. Meissner, *Ultra-Peripheral Collisions*, poster presented at Quark Matter 2001.

*Lawrence Berkeley National Laboratory

Photon-Pomeron Interactions at RHIC

Exclusive production of ρ^0 mesons Au+Au --> Au+Au + ρ^0

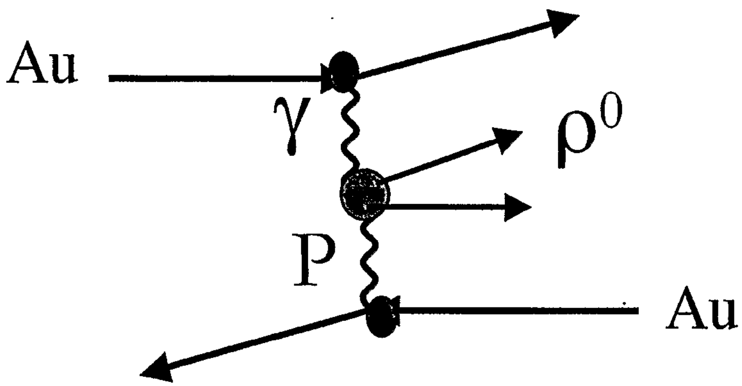

- **Interaction via long range fields**
- **Large cross section:**

  380 mb for Au at 130 GeV/nucleon

  5% of hadronic cross section
- **Coherent coupling to both nuclei**

  => Small transverse momentum:
  $p_T < 2/R_A \sim 60$ MeV

  => Longitudinal component
  $P_L < 2\gamma/R_A \sim 6$ GeV/c $<<P_{\text{nuclei}}$
- **Nuclei may be mutually excited**

Coupling Strength

•Photon $\propto Z^2$ (only $\propto$ Z for incoherent coupling to single nucleon)

•Pomeron $\propto A^{4/3}$ to A^2 ($A^{4/3} \propto$ surface, in the limit $\sigma^{\rho N} \rightarrow \infty$;
$A^2 \propto$ volume, in the weak limit)

First Goal - Proof of Principle

Observe exclusive ρ^0 production Au Au Collisions

Experimental Signature/ Trigger

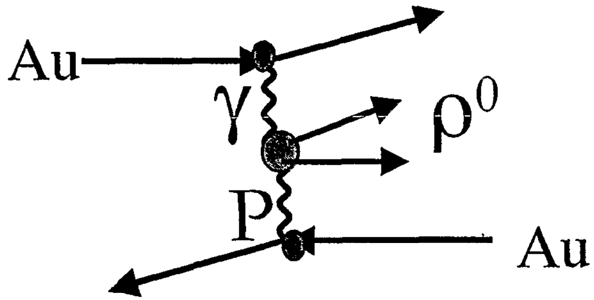

Typical Event :

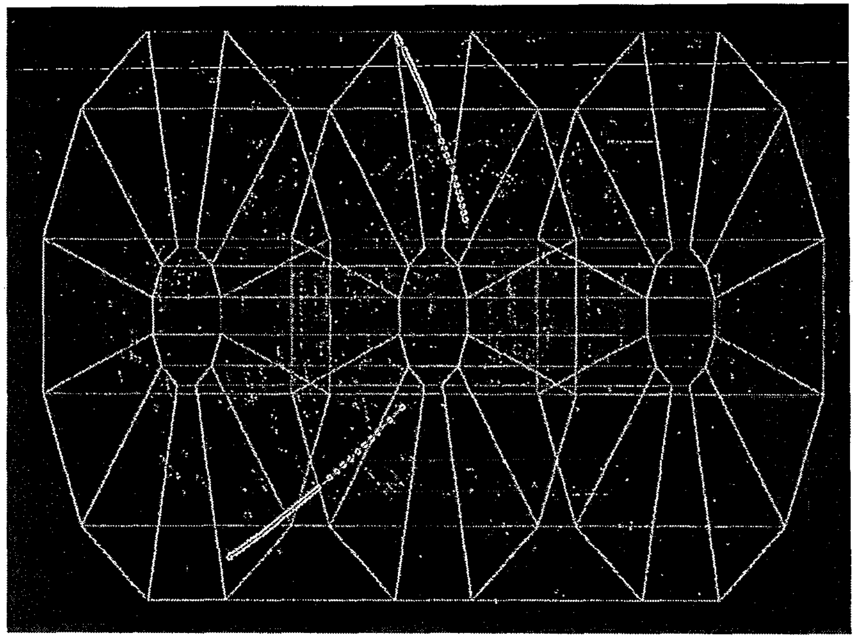

Only two oppositely charged tracks

- **Low total p_T**
- **Back-to-back in transverse plane**

Trigger Backgrounds:

- **Cosmic rays**
- **Beam-gas Events**
- **Debris from upstream events**

Topology Trigger:

- **~ 7 hours of dedicated data collection**
- **30,000 triggers in 2000**

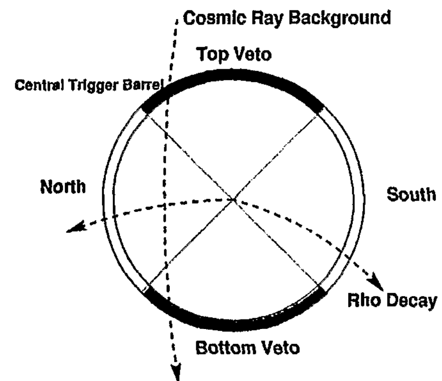

59

First Results: Invariant Mass & Transverse Momentum Spectra

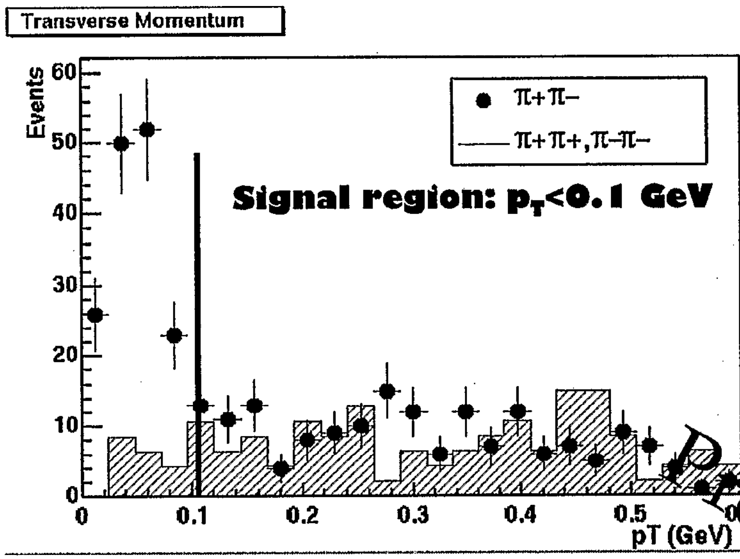

Peripheral Trigger:

Au+Au -> Au +Au +ρ^0

Peak at low p_T => signature for coherent interaction

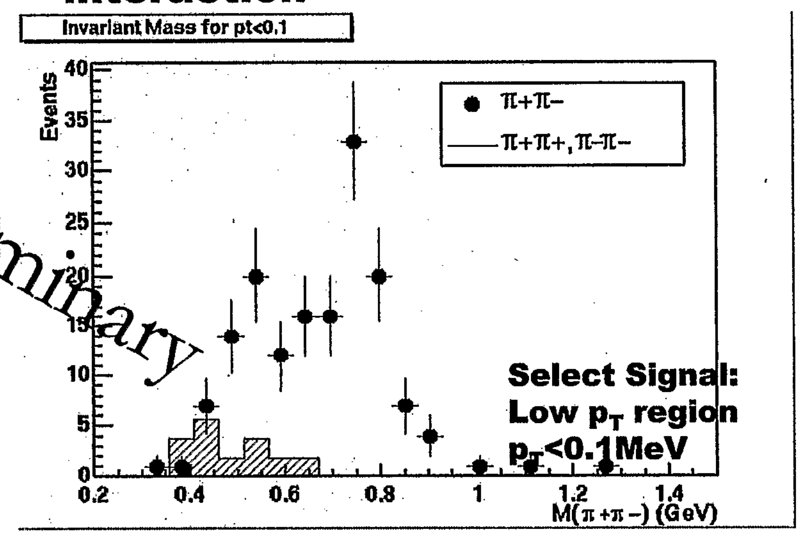

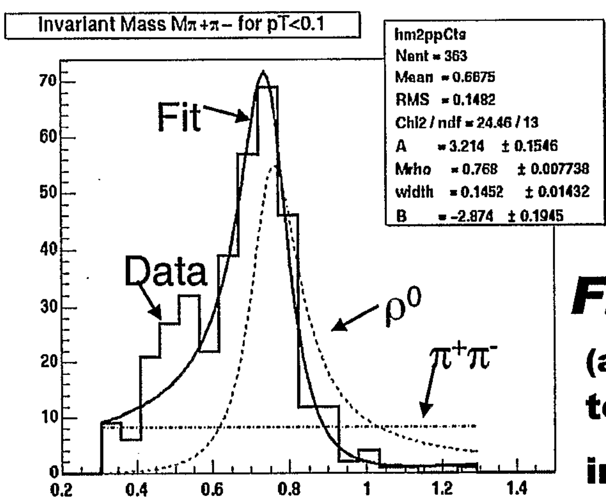

Fit of ρ^0 Lineshape

(all data: peripherally triggered+minimum bias; c.f next slide)
to ρ^0 + non resonant $\pi^+\pi^-$ production

interference is significant

Nuclear Excitation

In addition to ρ^0production, nuclei can exchange one or more separate photons and become mutually excited.

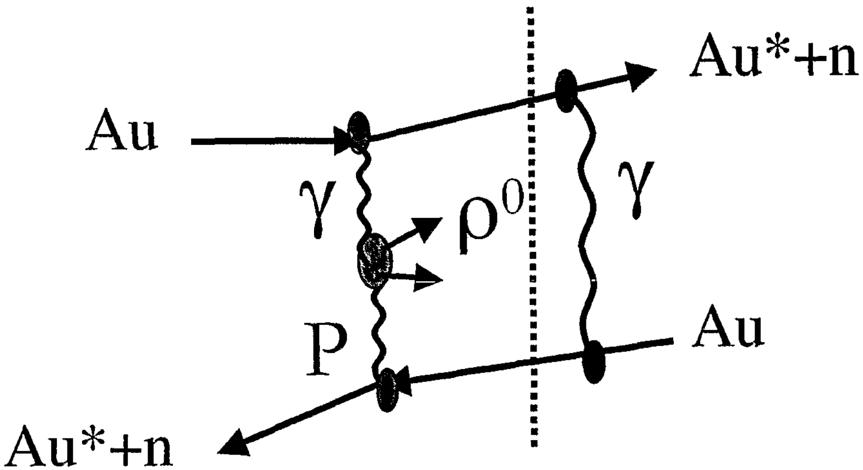

- **Believed to factorize as function of impact parameter**
- **Decay yields neutrons in Zero Degree Calorimeter (ZDC) -> minimum bias trigger**
- **Data set: ~800,000 events with minimum bias trigger**

Au+Au -> Au*+Au* + ρ^0

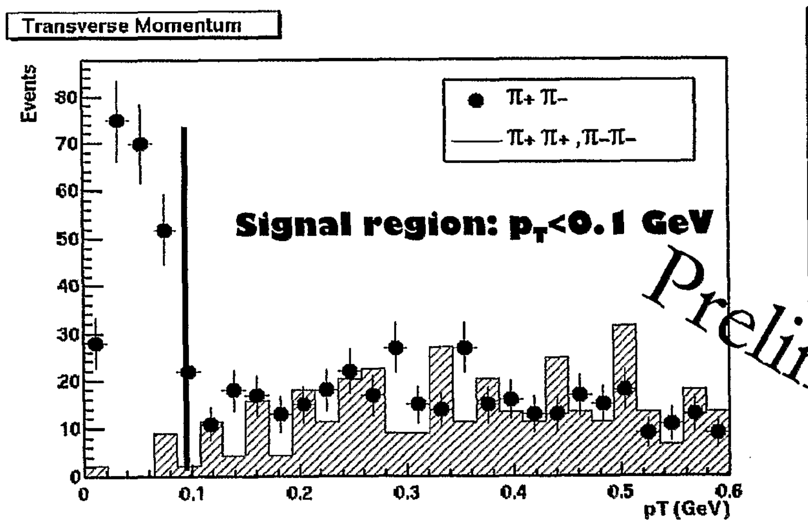

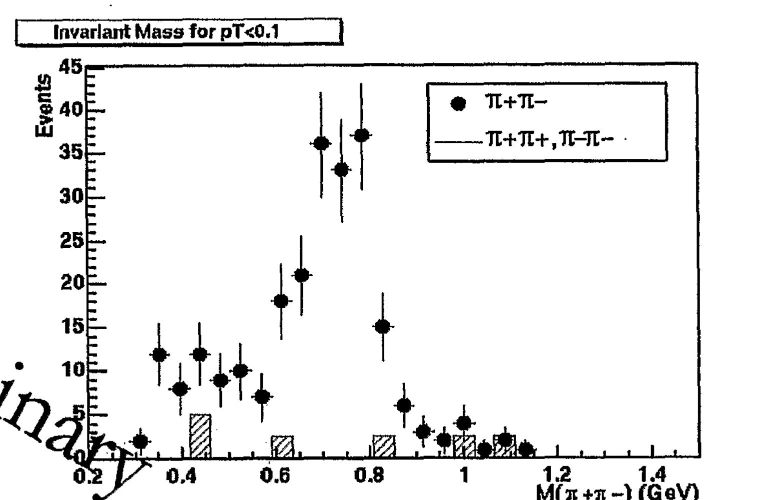

Compare ZDC Signals

(for two track events)

Ultra Peripheral Trigger

- Pedestal peak at ADC sum = 4
- Higher ADC values usually in east or west only (beam gas events)

Au+Au -> Au+Au + ρ^0

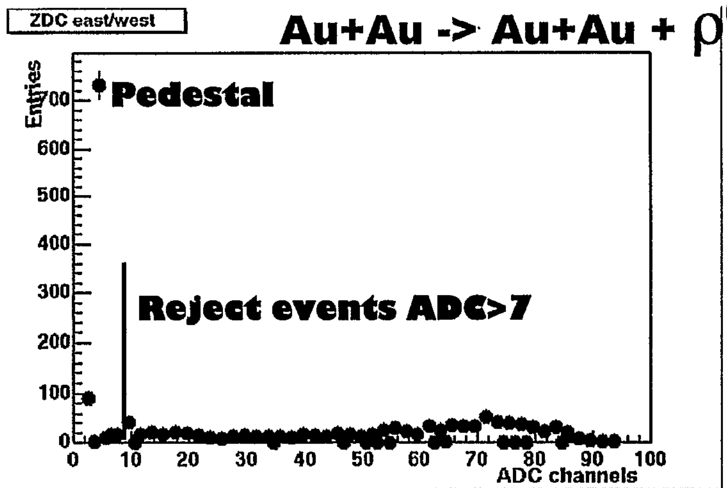

Minimum Bias Trigger

- Single neutron peak around ADC =9 coincident in east and west
- Higher ADC values from hadronic peripheral events

Au+Au -> Au*+Au* + ρ^0

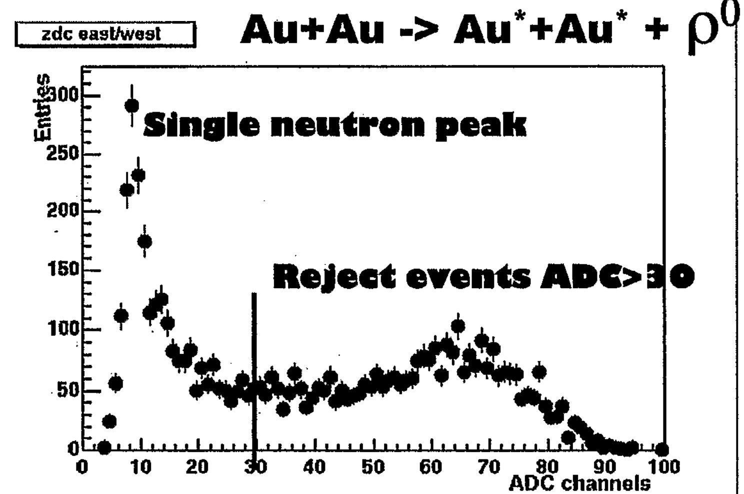

Summary:

Observe two different processes !

Au+Au -> Au+Au + ρ^0 and Au+Au -> Au*+Au* + ρ^0

First observation of Ultra-Peripheral Collisions in heavy ion interactions

RHIC is a good place to study diffractive processes in heavy ion and polarised (!) proton-proton collisions

The PP2PP Experiment at RHIC

S. Bültmann (Brookhaven National Laboratory)
E-Mail: bueltmann@bnl.gov

Summary

The PP2PP experiment at RHIC is going to measure elastic and total cross-sections in (un-)polarized proton-proton scattering. The experiment is located at the 2 o'clock interaction region of the RHIC complex. Elastic scattering at the RHIC energies, $\sqrt{s} =$ 200 GeV/c and possibly 500 GeV/c during the first year, requires detection of the scattered protons at very small angles. At a few loactions along the beam line, the scattering angle is directly proportional to the measured distance between the scattered proton and the beam axis, $\Theta = y_{Det}/L_{eff}$. One of these locations, suitable for measurements at the four-momentum transferred, $-t$, in the range 0.003 to 0.100 (GeV/c)^2, is at $L_{eff} = 20$ m.

Elastic scattering requires the detection of the two collinearly scattered protons in coincidence. We are planning to use four planes of silicon microstrip detectors, two of each measuring the position of the scattered proton along one direction perpendicular to the beam momentum, together with one trigger scintillator, per detector package. The detector packages will be mounted inside Roman Pots above and below the beam line. The two pots will allow to move the detector packages vertically to positions about 15 mm above and below the beam centre. The setup will feature additional scintillator counters close to the interaction region to tag non-elastic scattering events. These veto counters can also be used to detect single- and double-diffractive scattering events. They cover a pseudo-rapidity range of $2.6 < \eta < 5.6$.

During the Year-2001 engineering run of PP2PP the main focus of the measurements will be on the total cross-section difference between the two transverse helicity states of the beam, $\Delta\sigma_T$, the single and double transverse spin asymmetries, A_N and A_{NN}, and the energy dependence of the nuclear slope, b. Running for about two days at a reduced luminosity of about 10^{28} cm^{-2} sec^{-1}, would enable us to measure A_N and A_{NN} to about 5% relative accuracy and $\Delta\sigma_T$ to about 0.3 mb. This should allow to distinguish between different exchange models brought forward for example in[1].

We will also measure the total cross section, σ_{tot}, providing data at $\sqrt{s} = 200$ GeV/c, a region between the existing data measured at ISR on the lower energy side and Fermilab at higher energies. A measurement at $\sqrt{s} = 500$ GeV/c would add a data point to the region of Fermilabs measurements and could enable us to distinguish between models calling for saturation of the cross-section at higher energies and Pomeron exchange models[2]. A measurement at $\sqrt{s} = 500$ GeV/c would also allow us to measure the elastic differential cross-section, $d\sigma/dt$, up to a $-t$ of 1.0 GeV^2/c^2. A dip in $d\sigma/dt$ around a $-t$ of 0.8 GeV^2/c^2 is expected. This region is very sensitive to spin exchange. On the lower $-t$-side of the dip region the C-parity is positive (+1), while on the higher $-t$-side it is negative (-1).

In case of longitudinal beam polarization being available at our interaction point, also the longitudinal spin asymmetry, A_{LL}, together with the cross-section difference, $\Delta\sigma_L$, could be measured. Including the above mentioned measurements, the s-channel helicity amplitudes could be extracted.

[1] N. Buttimore et al, PRD 59:114010 (1999) and E. Leader and T. Trueman, PRD 61:077504 (2000)

[2] A. Donnachie and P. V. Landshoff, Phys. Lett. B296, 227 (1992)

pp2pp Physics Programme

Study of total and elastic cross-sections in proton-proton scattering over a large kinematic range

$$50 \leq \sqrt{s} \leq 500 \text{ GeV}/c$$

$$4 \cdot 10^{-4} \leq |t| \leq 1.5 \ (\text{GeV}/c)^2$$

- Measurments with transverse and longitudinally polarized protons to determine
  - the s-channel helicity amplitudes Φ_I

    $\Phi_1 \sim \langle ++| M |++\rangle$
    $\Phi_2 \sim \langle --| M |++\rangle$
    $\Phi_3 \sim \langle +-| M |+-\rangle$
    $\Phi_4 \sim \langle +-| M |-+\rangle$
    $\Phi_5 \sim \langle ++| M |+-\rangle$

  - determine the nature of the mediator of the elastic interaction
- Measurements with unpolarized protons
- Measurements with (un-)polarized deuterons and helium
- Diffractive Scattering

Experimental Setup

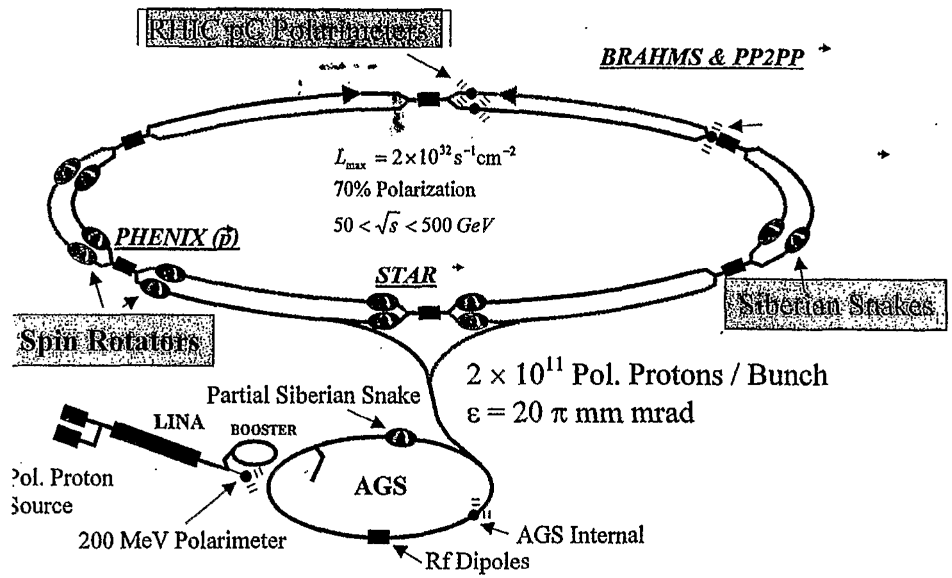

Principle of Measurement

For small scattering angles the position of the protons at the detection point are directly proportional to the angle via the beam transport matrix:

$$y_{det} = a_{11}\, y^* + L_{eff}\, \Theta_{sc}$$

Parallel to point focusing: $a_{11} = 0$ and L_{eff} large

65 Dependence of t on beam parameters:

$$t_{min} \propto \frac{k^2 \varepsilon p^2}{\beta^*}$$

$\Rightarrow$ need **large β^* and small ε**

For Coulomb region special tune is required:

$\beta^* = 195$ m and low emittance **$\varepsilon = 5\pi$ mm mrad**

Elastic Detectors

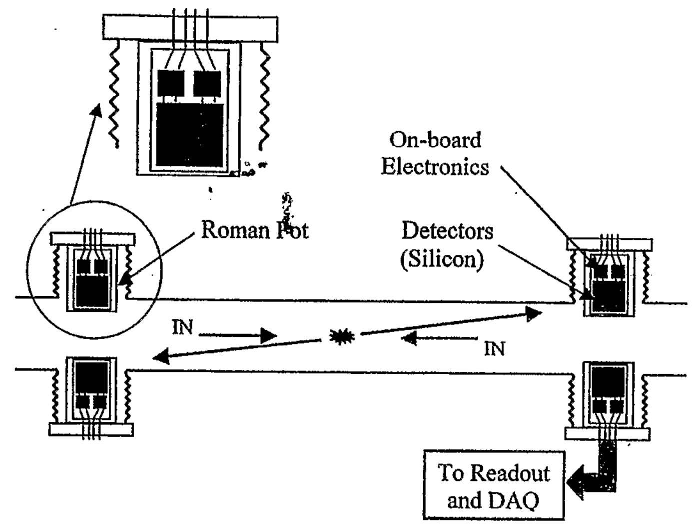

RHIC Intersection Region with PP2PP Basic CB Setup

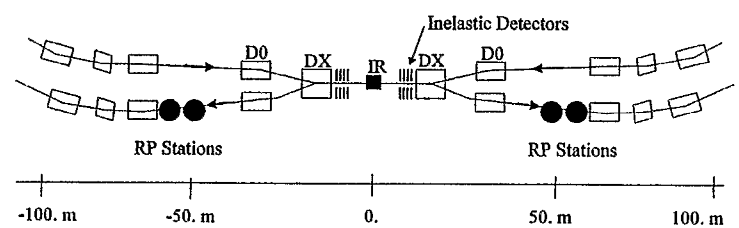

Silicon Detector Package in Roman Pot

- 400 micron thick silicon microstrips covering 5 x 8 cm
- 70 micron wide strips with 100 micron pitch (good track resolution and limited occupancy)
- 2 X-detectors (768 strips of 45 mm length)
- 2 Y-detectors (512 strips of 75 mm length)
- High and uniform efficiency
- Close proximity of detector to beam (14 mm)

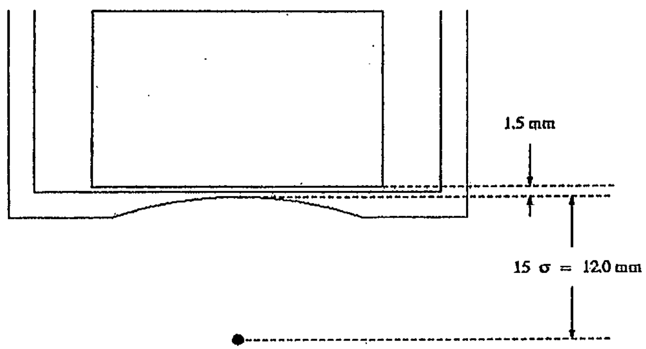

- 8 mm thick trigger scintillator behind silicon planes

RHIC Run 2001

No special conditions required:

L_{eff}= 20 m, Roman Pot position at 57 m from IP

Minimum experimental setup:

- One Roman Pot station in each outgoing beam pipe
- Veto counter system around IP

Kinematic coverage:

- at 100 GeV/c: $0.003 < -t < 0.015\ (\mathrm{GeV}/c)^2$
- at 250 GeV/c: $0.006 < -t < 0.100\ (\mathrm{GeV}/c)^2$

  (if running at this energy takes place)

Measurements in 2001

- Study CNI region, $\sigma_{tot}, A_N, A_{NN}$
- s dependence of the nuclear slope, b
- Measurement of A_N over large $-t$ range to find suitable kinematic region for polarimetry

Expected Run Plan

- Total Proton Intensity = $5 \cdot 10^{10}$ - 10^{11}
  $\Rightarrow L \approx 1.2 \cdot 10^{28}$ cm^{-2} sec^{-1}
- 100 events / sec for ~10 mb elastic cross-section
- 1.4 million events for 10 hour ring filling (assume 40% efficiency)
- One or two days of special running most practical for us
- Accuracy $\delta A_N \approx 0.002 - 0.003$
- Accuracy $\delta \Delta \sigma_{tot} \approx 0.3$ mb

Outlook

2003

- Extend measurements to **$0.1 < -t < 1.3$ (GeV/c)^2**

Beyond 2003

- Measure in CNI region, requiring special tune
  $0.0004 < -t < 0.12$ (GeV/c)^2
- Measure in large -t region
  $1.3 < -t < 5$ (GeV/c)^2
- Elastic scattering of proton-deuteron, deuteron-deuteron, and proton-^{4}He also possible

DØ Hard Diffraction in Run I and Prospects for Run II

Andrew Brandt

University of Texas at Arlington

One of the most interesting new results from Tevatron Run I was the existence of large rapidity gaps in events with a hard scattering (Slide 1). DØ published several papers on events with a central rapidity gap between jets [1] and have several more papers submitted or in preparation on related topics, including diffractive production of jets [2], diffractive production of W and Z bosons, and hard double pomeron exchange. Slides 2 and 3 summarize some of the recent results. Improved understanding of the new field of hard diffraction, which probes otherwise inaccessible details of the strong force and vacuum excitation, requires new detectors for tagging and measuring scattered protons.

To improve its capabilities for hard diffraction studies, DØ is adding a Forward Proton Detector (FPD) [3] for Run II as shown in Slide 4. The FPD consists of momentum spectrometers that make use of accelerator magnets along with points measured on the track of the scattered proton to calculate the proton's momentum and scattering angle. Tracks are measured using scintillating fiber detectors located in vacuum chambers positioned in the Tevatron tunnel 20–60 meters upstream and downstream of the central DØ detector. The vacuum chambers were built by Brazilian and Dutch collaborators and have been installed in the Tevatron. The scintillating fiber detectors are being assembled at the University of Texas at Arlington. Most of the FPD electronics has been installed and commissioned and data taking will begin soon (see Slide 5).

The FPD has acceptance for a large range of proton (anti-proton) momenta and angles. The combination of spectrometers maximizes the acceptance for protons and anti-protons given the available space for locating the detectors. Particles traverse thin steel windows at the entrance and exit of each Roman pot (the stainless steel vessel that houses the detector). The pots are remotely controlled and can be moved close to the beam (within a few mm) during stable beam conditions and retracted otherwise. The scintillating fiber detectors are read out by multi-anode photomultiplier tubes and are incorporated into the standard DØ triggering and data acquisition system.

The FPD will allow new insight into an intriguing class of events that are not currently understood within the Standard Model. It allows triggering directly on events with a scattered proton, anti-proton, or both, along with activity in the DØ detector. In addition to improved studies of recently discovered hard diffractive processes, the new detector will allow a search for glueballs and exotic phenomena. The FPD will also provide improved luminosity measurements, which are an important component to all DØ analyses.

Bibliography of Literature

[1] S. Abachi *et al.* (DØ Collaboration), Phys. Rev. Lett. **72**, 2332 (1994);
Phys. Rev. Lett. **76**, 734 (1996);
B. Abbott *et al.* (DØ Collaboration), Phys. Lett. B **440** 189 (1998).

[2] B. Abbott *et al.* (DØ Collaboration), Hep-ex 9912061, Submitted to Phys. Lett. B.

[3] DØ Collaboration, "Proposal for a Forward Proton Detector at DØ" (presented by A. Brandt), Proposal P-900 submitted to the Fermilab PAC (1997); A. Brandt *et al.* Fermilab PUB–97-377.

DØ Hard Diffraction in Run I and Prospects for Run II

Andrew Brandt
DØ / University of Texas, Arlington

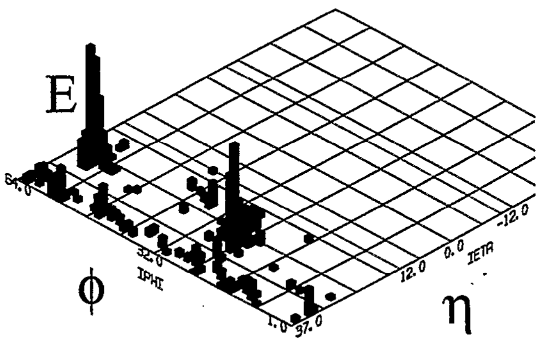

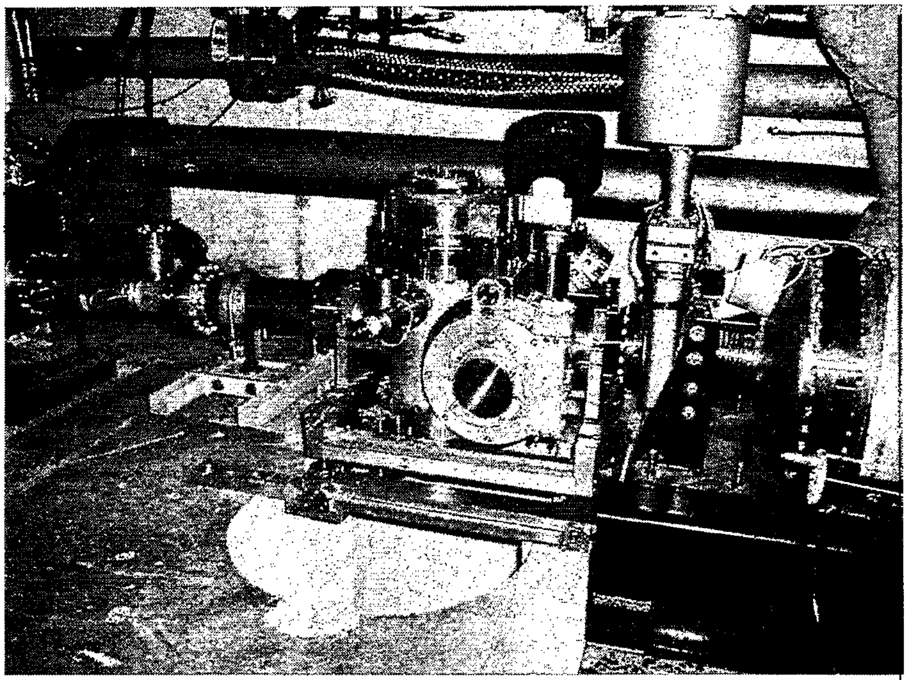

- Intro and Run I Hard Diffraction Results
- **Forward Proton Detector**

Beyond the Pomeron
May 22, 2001
Brookhaven National Lab

D∅ Single Diffractive Results

D∅ Preliminary

Sample	Data	Hard Gluon	Flat Gluon	Soft Gluon	Quark
	Gap Fraction (%)				
($s(\beta) \propto$)		$\beta(1-\beta)$	const.	$(1-\beta)^5$	$\beta(1-\beta)$
1800 Fwd	0.65 ± 0.04	2.2 ± 0.3	2.2 ± 0.3	1.4 ± 0.2	0.79 ± 0.12
1800 Cent	0.22 ± 0.05	2.5 ± 0.4	3.5 ± 0.5	0.05 ± 0.01	0.49 ± 0.06
630 Fwd	1.19 ± 0.08	3.9 ± 0.9	3.1 ± 0.8	1.9 ± 0.4	2.2 ± 0.5
630 Cent	0.90 ± 0.06	5.2 ± 0.7	6.3 ± 0.9	0.14 ± 0.04	1.6 ± 0.2
	Ratio of Gap Fraction				
630/1800 Fwd	1.8 ± 0.2	1.7 ± 0.4	1.4 ± 0.3	1.4 ± 0.3	2.7 ± 0.6
630/1800 Cent	4.1 ± 0.9	2.1 ± 0.4	1.8 ± 0.3	3.1 ± 1.1	3.2 ± 0.5
1800 Fwd/Cent	3.0 ± 0.7	0.88 ± 0.18	0.64 ± 0.12	$30. \pm 8.$	1.6 ± 0.3
630 Fwd/Cent	1.3 ± 0.1	0.75 ± 0.16	0.48 ± 0.12	$13. \pm 4.$	1.4 ± 0.3

Within the *Ingelman-Schlein* model, D∅ data can be reasonably described by a pomeron composed dominantly of quarks.

For the model to describe D∅ data as well as other measurements, a *reduced flux* factor convoluted with a gluonic pomeron containing significant soft and hard components is required.

hep-ex/9912061

FPD Layout

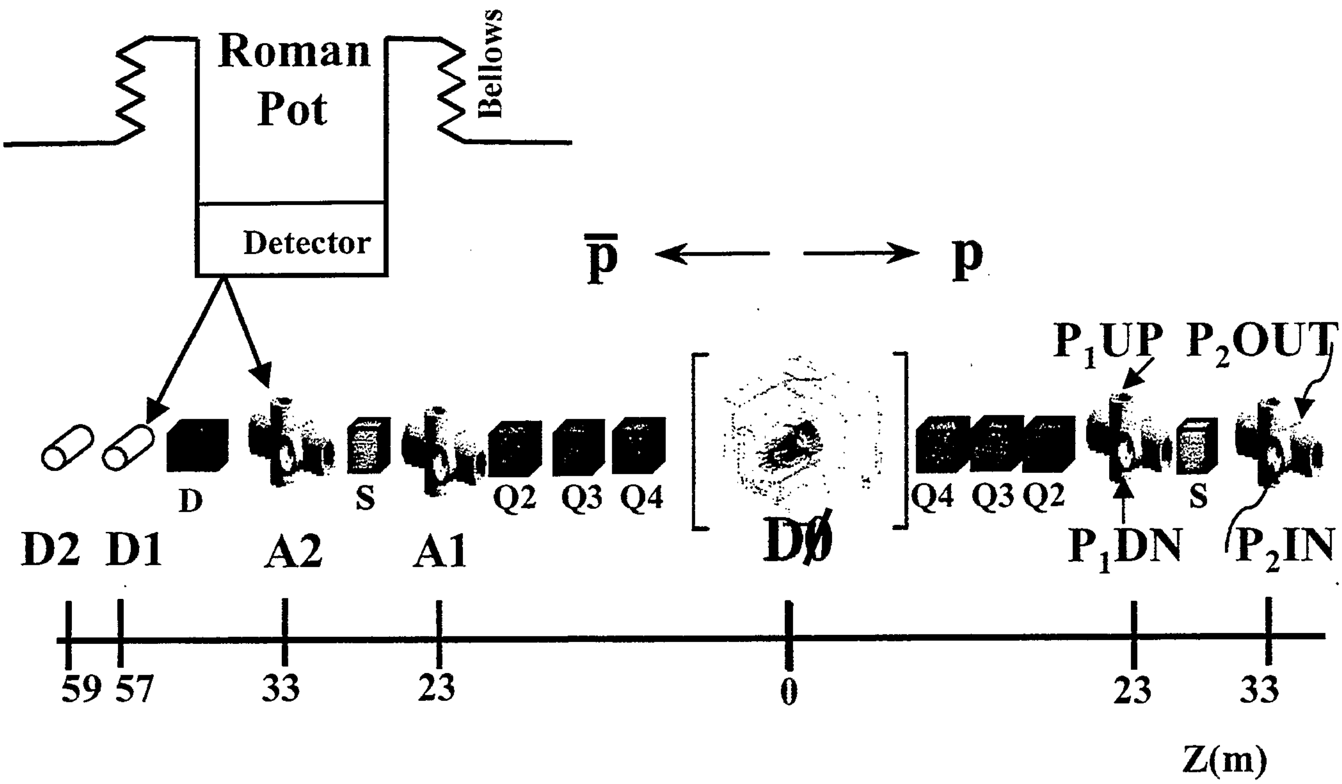

Series of 18 Roman Pots forms 9 independent momentum spectrometers allowing measurement of proton momentum and angle.

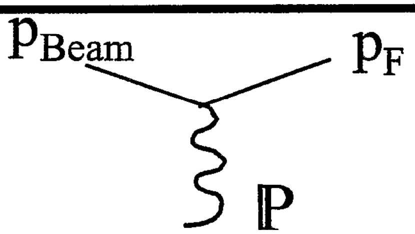

$$\xi = 1 - x_p = \frac{\Delta P}{P} \qquad t = (P_{Beam} - P_F)^2$$

1 Dipole Spectrometer ($\bar{p}$) $\xi > \xi_{min}$

8 Quadrupole Spectrometers (p or $\bar{p}$, up or down, left or right) $t > t_{min}$

Hard Color-Singlet Exchange

Count tracks and EM Calorimeter Towers in $|\eta| < 1.0$

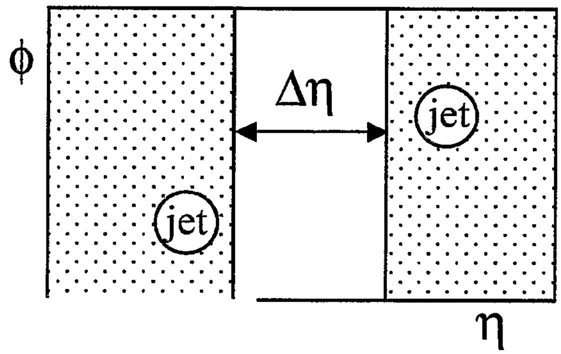

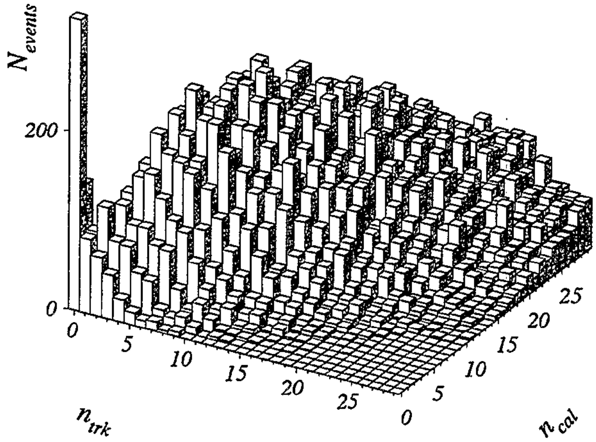

Measure fraction of events due to color-singlet exchange

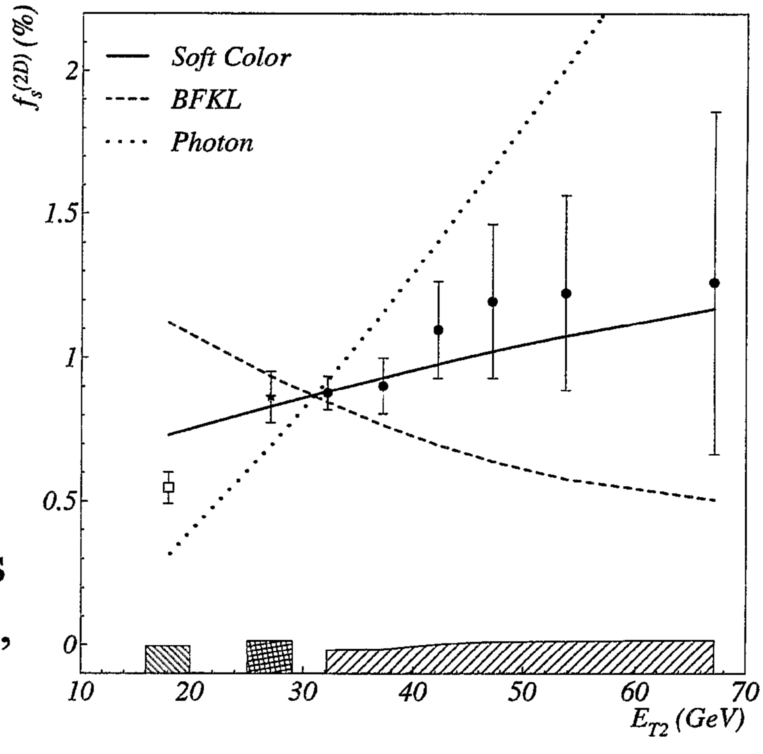

Measured fraction (~1%) rises with initial quark content :
Consistent with a soft color rearrangement model preferring initial quark states
Inconsistent with two-gluon, photon, or U(1) models

Phys. Lett. B 440 189 (1998)

Long Range Plan

- Install 8 more detectors (total of 10) during September shutdown
- Begin data taking with full DØ detector and trigger list in October
- Demonstrate working system, usefulness of horizontal plane, and secure funding for remaining MAPMT in 2002
- Early papers:
  NIM
  Elastic t-distribution
  Single diffraction distributions
  Diffractive jet production
  Double tagged double pomeron exchange

Hard Diffraction at CDF

Anwar Ahmad Bhatti
The Rockefeller University
CDF Collaboration

SOFT DIFFRACTION

1)Soft single diffraction	PRD 50 (1994) 5550
2)Soft double diffraction	NEW RESULT

RAPIDITY GAP RESULTS

3) Diffractive W	PRL 78 (1997) 2698
4) Diffractive Dijets	PRL 79 (1997) 2636
5) Diffractive Beauty	PRL 84 (2000) 232
6) Diffractive J/ψ	NEW RESULT
7) Jet-Gap-Jet 1800	PRL 74 (1995) 855
8) Jet-Gap-Jet 1800	PRL 80 (1998) 1156
9) Jet-Gap-Jet 630	PRL 81 (1998) 5278

ROMAN POT RESULTS

10) Diffractive Dijets 1800	PRL 84 (2000) 5043
11) Diffractive Dijets 630	COMING SOON!
12) Double Pomeron Dijets	PRL 85 (2000) 4215

Gluon Fraction and Factorization

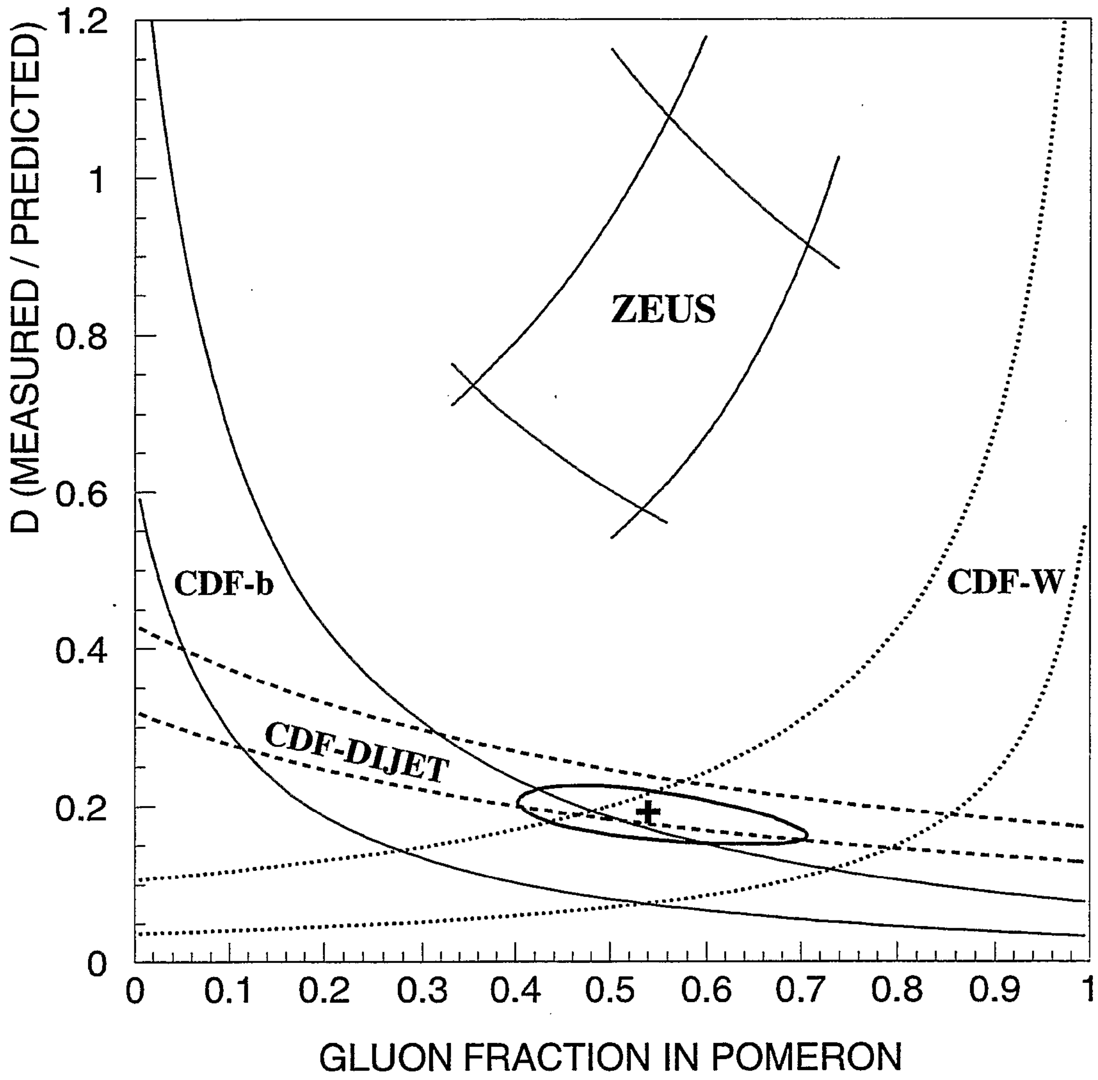

$$D = 0.19 \pm 0.04$$

$$f_g = 0.54^{+0.16}_{-0.14}$$

Measurement of diffractive structure function
Comparison with expectations from H1 results

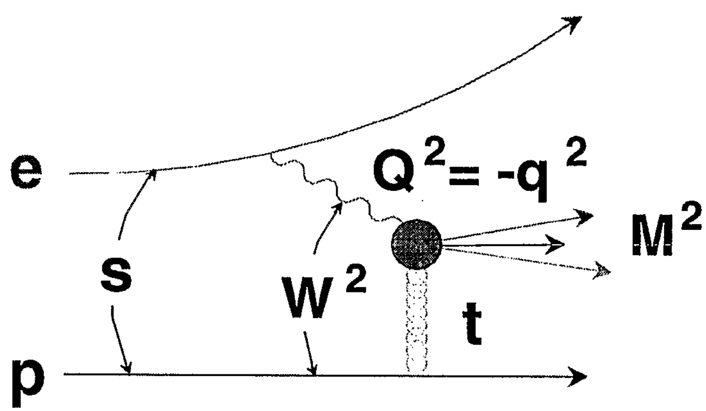

$$D = \frac{\int_{\log\beta=-1.4}^{\log\beta=0} F_{jj}^{D}(\beta; CDF)\,d\beta}{\int_{\log\beta=-1.4}^{\log\beta=0} F_{jj}^{D}(\beta; H1)\,d\beta}$$

$$= \begin{cases} 0.06 \pm 0.02 & \text{for fit-2} \\ 0.05 \pm 0.02 & \text{for fit-3} \end{cases}$$

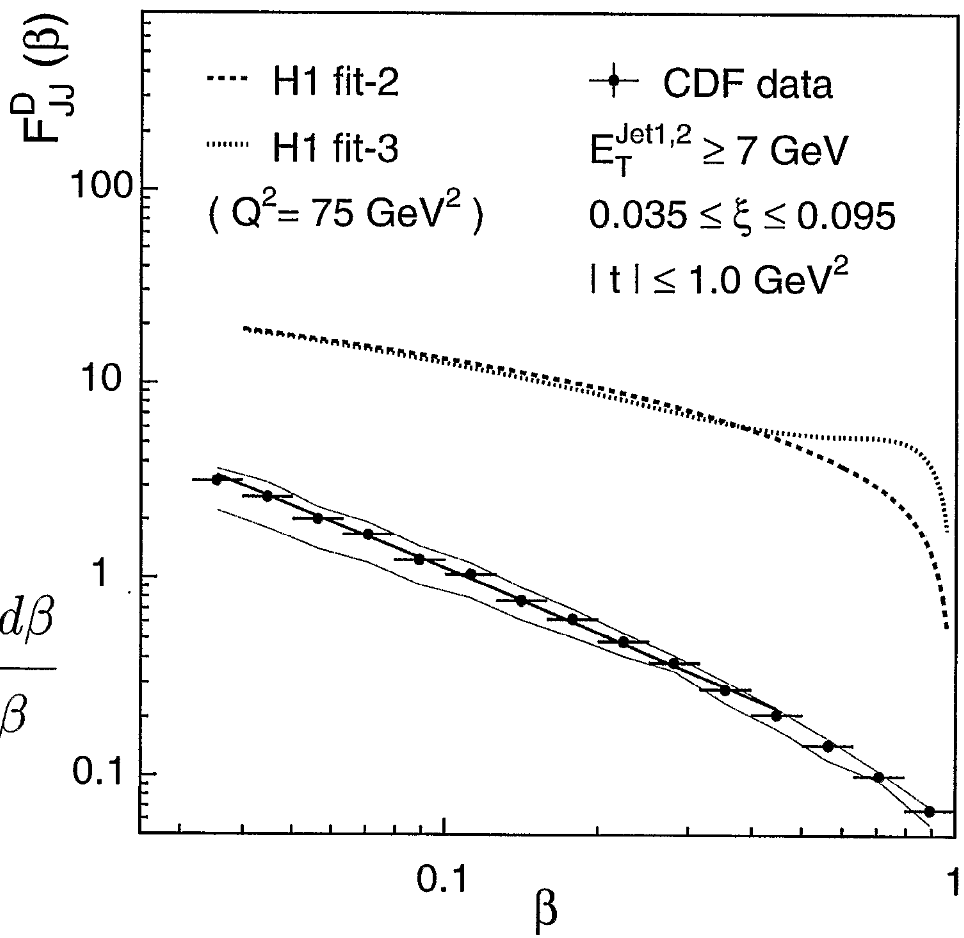

CDF normalization uncertainty $= \pm 26$ %

Diffractive J/ψ Production

Ratio of SD to ND cross sections versus x_{bj}

$$x_{bj}^{\pm} = \frac{1}{\sqrt{s}} \times p_T^{J/\psi} \left(e^{\pm\eta^{J/\psi}} + e^{\pm\eta^{jet}} \right)$$

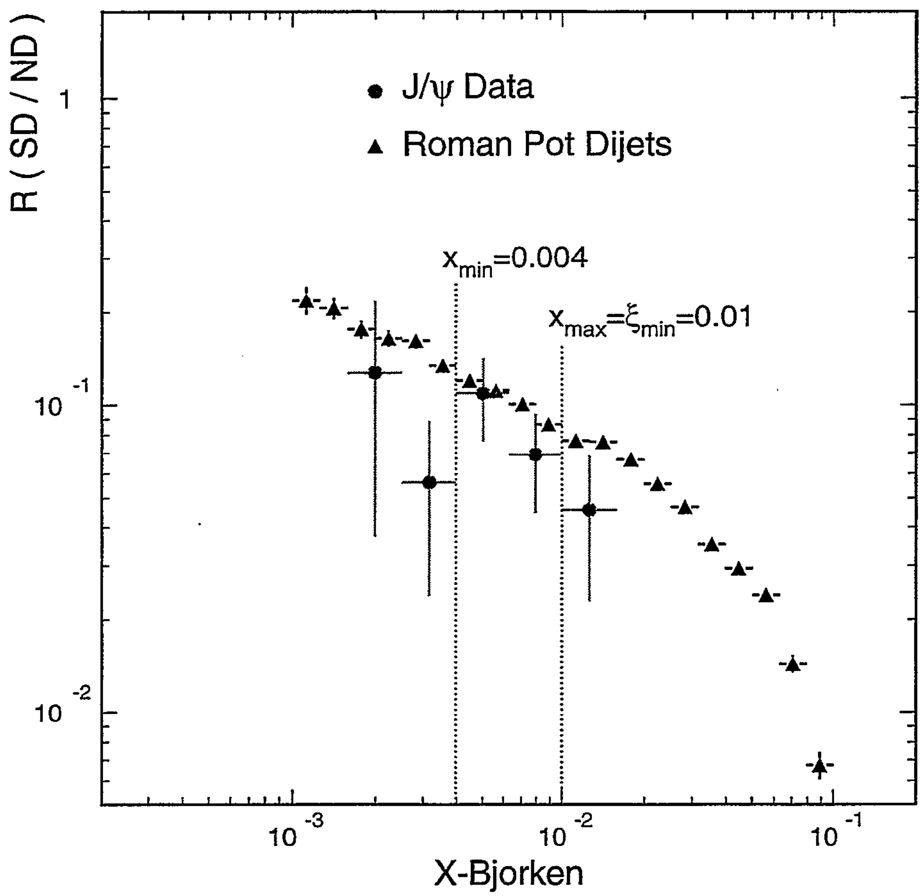

$$\left(\frac{R_{JJ}}{R_{J/\psi}} \right)_{exp} = \frac{g^D + \frac{4}{9} q^D}{g^{ND} + \frac{4}{9} q^{ND}} / \frac{g^D}{g^{ND}} = 1.17 \pm 0.27\,(\text{stat})$$

Gluon fraction : $f_g^D = 0.59 \pm 0.15\,(\text{stat} \oplus \text{syst})$

Double Pomeron Exchange : Test of Factorization

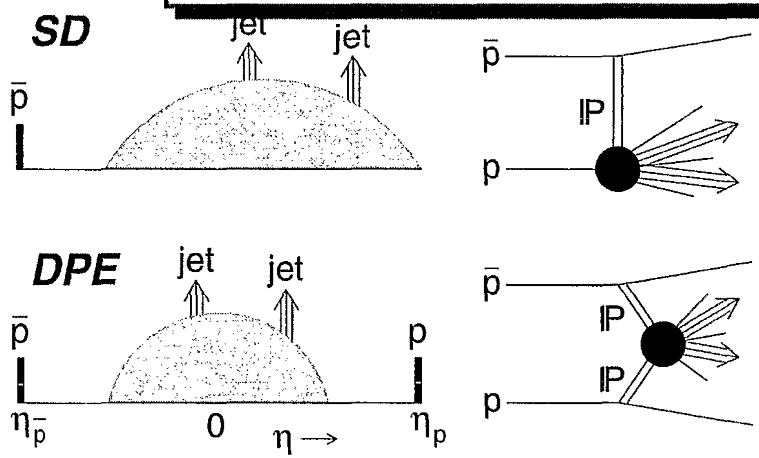

$$\sigma_{ND} = \sigma_0 F(x, Q^2)\, F(x, Q^2)$$

$$\sigma_{SD} = \sigma_0 F(x, Q^2)\, F^D(x, \xi, Q^2)$$

$$\sigma_{DP} = \sigma_0 F^D(x, \xi, Q^2)\, F^D(x, \xi, Q^2)$$

$$\overline{R_{\frac{SD}{ND}}} = 0.15 \pm 0.02(\mathrm{stat}) \pm 0.03(\mathrm{norm})$$

$$\overline{R_{\frac{DPE}{SD}}} = 0.80 \pm 0.26(\mathrm{stat})$$

$$(10^{-2.8} < x < 10^{-2})$$

Breakdown of Factorization

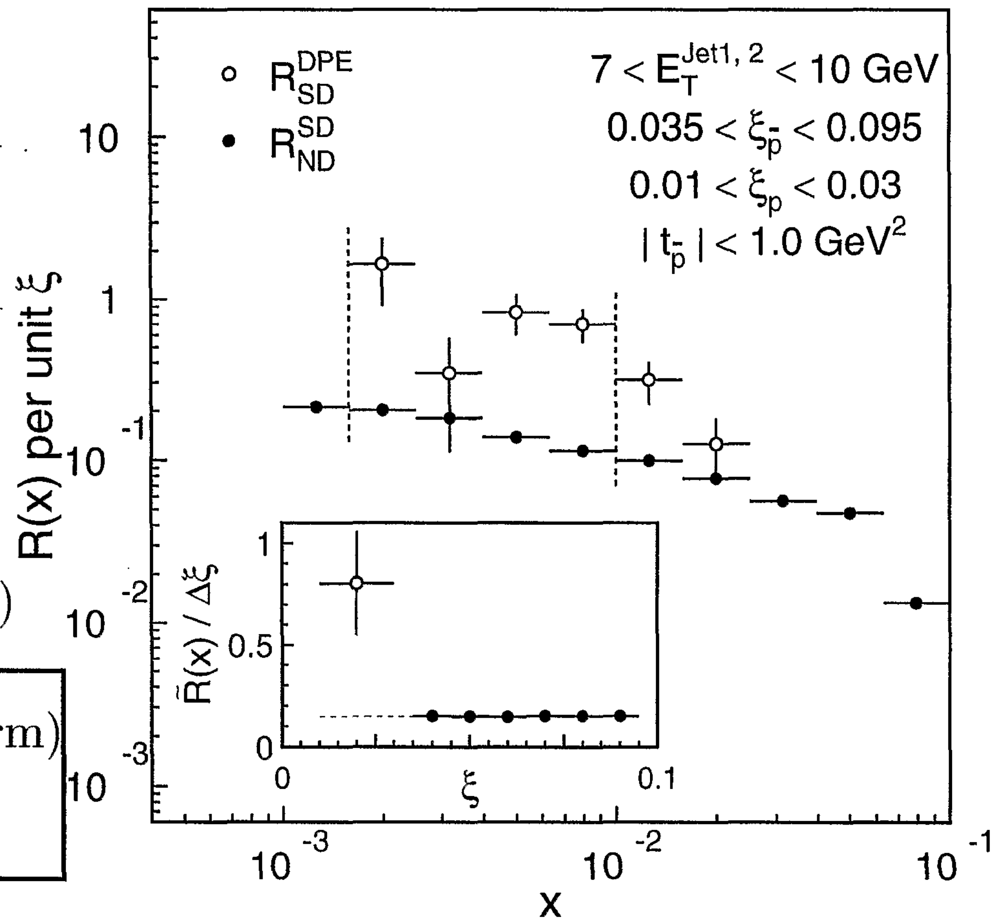

DD Cross Sections at $\sqrt{s} = 630$ and 1800 GeV

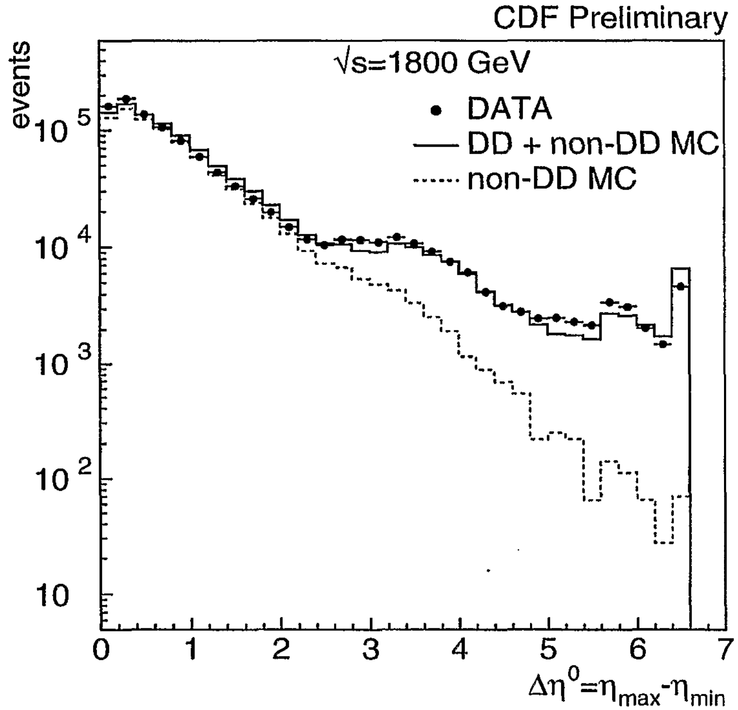

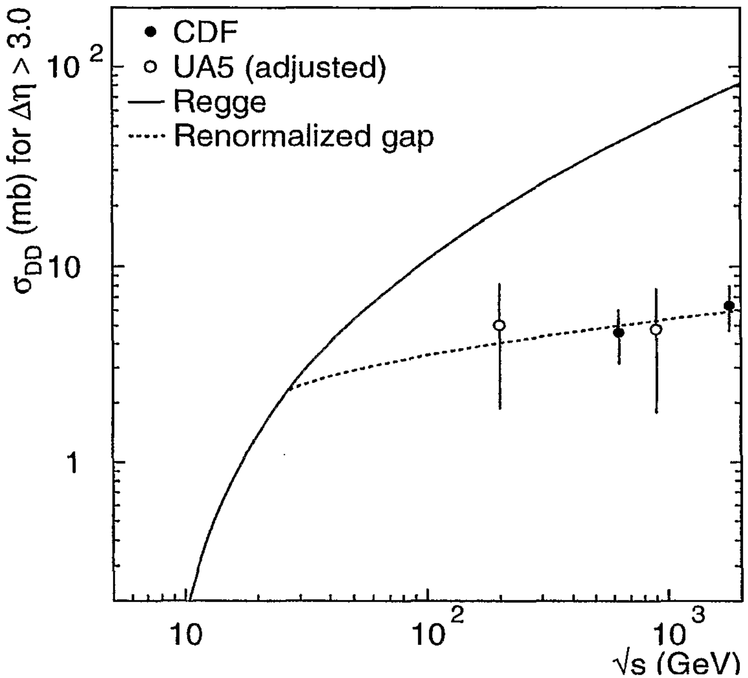

$\underline{\sqrt{s} = 1800 \text{ GeV}}$ $\quad \sigma_{DD}(\Delta\eta > 3) = 6.32 \pm 0.03(\text{stat}) \pm 1.7(\text{syst})\text{mb}$

$\underline{\sqrt{s} = 630 \text{ GeV}}$ $\quad \sigma_{DD}(\Delta\eta > 3) = 4.58 \pm 0.02(\text{stat}) \pm 1.5(\text{syst})\text{mb}$

The effective $\mathcal{P}$omeron trajectory and Double–Pomeron–Exchange Reaction in UA8

Samim Erhan[1]

University of California[2], Los Angeles, California 90095, USA.

In this talk, UA8 final results from the analysis of a double-$\mathcal{P}$omeron-exchange data sample were presented. Results were also summarized from our earlier work [S. Erhan et.al. (UA8 Collaboration), Nucl. Phys. B 514 (1998) 3, and S. Erhan & P. Schlein, Phys. Lett. B 481 (2000) 177], where we have shown that the Triple-Regge parametrization fits all available single-diffractive data at ISR, SPS and Tevetron, provided that the effective $\mathcal{P}$omeron trajectory intercept, $\alpha(0)$, is s–dependent and decreases with increasing s, as expected from unitarization (multi-$\mathcal{P}$omeron–exchange) calculations. $\alpha(0) = 1.10$ at the lowest ISR energy, 1.03 at the SPS–Collider and perhaps smaller at the Tevatron.

Despite the complications of multi-$\mathcal{P}$omeronexchange, factorization of $\mathcal{P}$omeron emission and interaction seems to be valid to a high degree. The UA8 parametrization of single-diffraction as the product of a "Flux Factor" of the $\mathcal{P}$omeron in the proton, $F_{\mathcal{P}/p}(t,\xi)$, and a proton-$\mathcal{P}$omeron total cross section ($\sigma_{p\mathcal{P}}^{total}$) has the form:

$$\frac{d^2\sigma_{sd}}{d\xi dt} = [0.72\, F_1(t)^2\, e^{1.1t}\, \xi^{1-2\alpha(t)}] \cdot [(s')^{0.1} + 4.0\, (s')^{-0.32}]. \tag{1}$$

where: $s' = \xi s$ and $\xi = 1 - x_p$. The constant, 0.72, is the product of $F_{\mathcal{P}/p}(t,\xi)$ and $\sigma_{p\mathcal{P}}^{total}$ normalizations.

The effective $\mathcal{P}$omeron trajectory, $\alpha(t)$, has a linear form, with a quadratic term added to allow for a flattening of the trajectory at high–$|t|$, as required by the data:

$$\alpha(t) = 1 + \epsilon + \alpha' t + \alpha'' t^2 \tag{2}$$

A further analysis of inelastic diffraction data at the ISR and SPS-Collider confirms the relatively flat s–independent $\mathcal{P}$omeron trajectory in the high–$|t|$ domain, $1 < |t| < 2$ GeV^2, reported earlier by Erhan et al. At $|t| = 1.5$ GeV^2, $\alpha = 0.92 \pm 0.03$ is in agreement with the trajectories found in diffractive photoproduction of vector mesons at HERA. This suggests a universal fixed $\mathcal{P}$omeron trajectory at high–$|t|$.

We have isolated double-$\mathcal{P}$omeron-exchange interactions in events which one or both of the final state p and/or $\bar{p}$ are detected in Roman-pot spectrometers. The central system is detected in the calorimeter system of the UA2 experiment, and is separated from p and $\bar{p}$ by pseudo-rapidity gaps, $2.3 < |\eta| < 4.1$. Assuming the validity of factorization in double-$\mathcal{P}$omeron-exchange interactions, we have extracted the $\mathcal{P}$omeron-$\mathcal{P}$omeron total cross section, $\sigma_{\mathcal{P}\mathcal{P}}^{total}$(M), using the above parametrization of the $F_{\mathcal{P}/p}(t,\xi)$ factor and the effective $\mathcal{P}$omeron Regge trajectory. For masses above 10 GeV, $\sigma_{\mathcal{P}\mathcal{P}}^{total}$(M) agrees with the factorization prediction of ≈ 0.1 mb. However, for smaller masses, it exhibits an intriguing enhancement, $\sigma_{\mathcal{P}\mathcal{P}}^{total}(M) \approx 1.0$ mb, which is much larger than expected from a breakdown of factorization. The low-mass enhancement of the invariant mass distribution of the central system may be an evidence for resonant $\mathcal{P}$omeron-$\mathcal{P}$omeron interactions (e.g. glueball production) in the few-GeV mass region, although the invariant mass resolution is inadequate to observe any structure.

[1]samim.erhan@cern.ch

[2]Supported by U.S. National Science Foundation Grant PHY94-23142

α(t) Summary

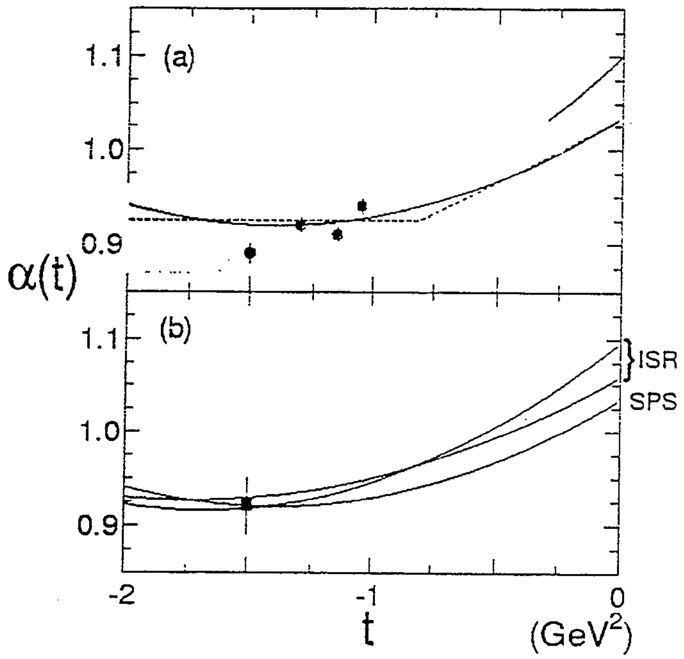

Key Results:

- No s-dependence of trajectory at high-t
- Intercept and slope exhibit s-dependence

High-t flattening of trajectory

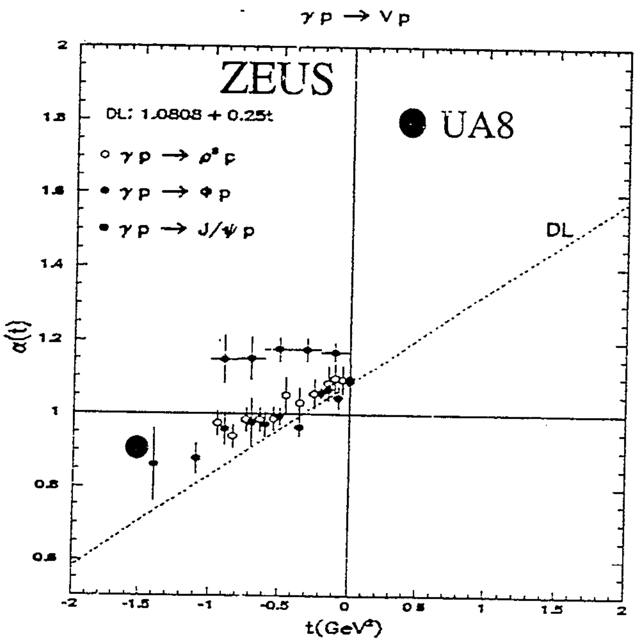

Agreement between:

HERA ρ^0, ϕ^0 photo-production

pp/p$\bar{p}$ inelastic diffraction

s-dependent ε from fits to dσ/dt

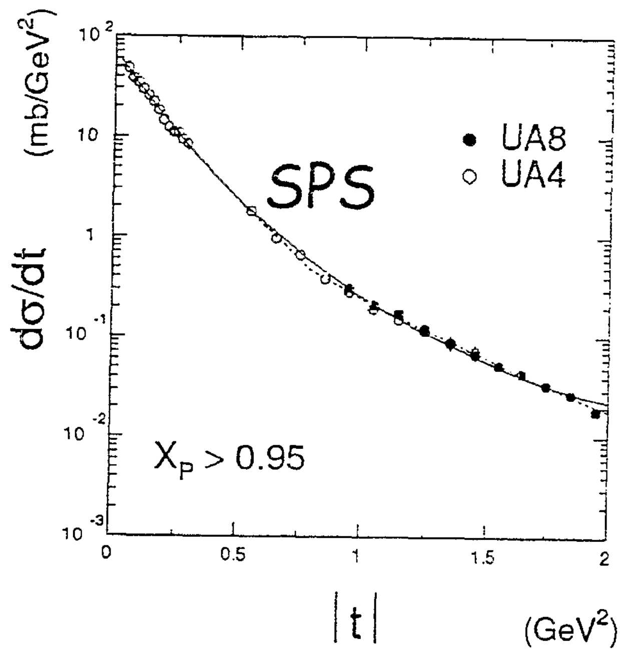

$\alpha(t) = 1.035 + 0.165\ t + 0.06\ t^2$

$\chi^2/DF = 4.2$

Integral is total σ_{dif}.

➔ The data require a smaller intercept and slope.

➔ Trajectory at high-t agrees with UA8 results.

s-dependent ε from fits to dσ/dt

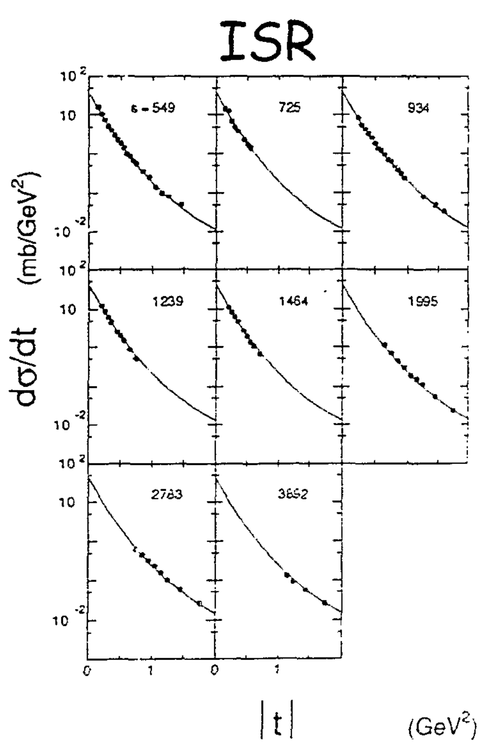

$\alpha(t) = \varepsilon + \alpha'\ t + \alpha'\ t^2$

6-parameter fit:

ε = 0.10 - 0.02 log(s/549)

α' = 0.22 - 0.03 log(s/549)

α'' = 0.06 - 0.01 log(s/549)

Similar s-dependent ε (starts within ISR range) and flattening at high-t.

DPE "AND" - "OR": $d\sigma/dM_X$

— MC σ_{PP} = 1 mb

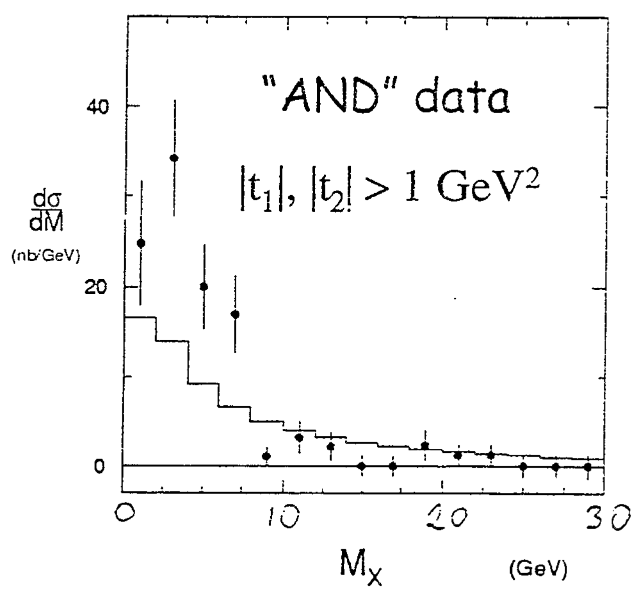

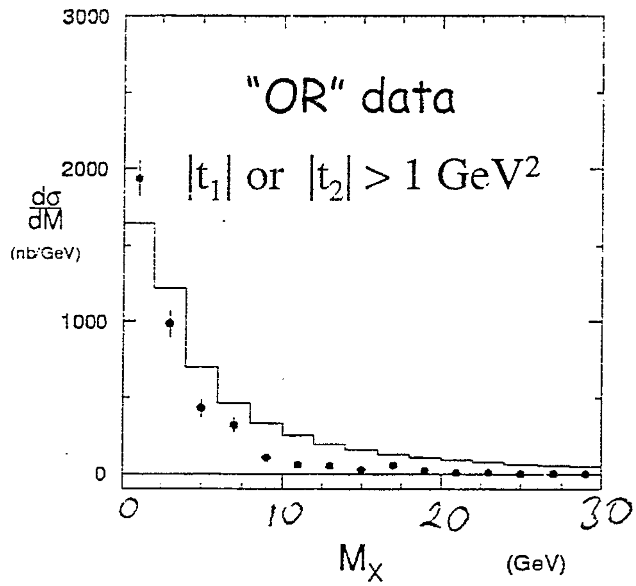

Pomeron-Pomeron Total Sigma

Red line is factorization prediction: about 0.1 mb.

→ High mass points appear to agree with prediction

→ σ_{PP} low mass enhancements in both data sets.

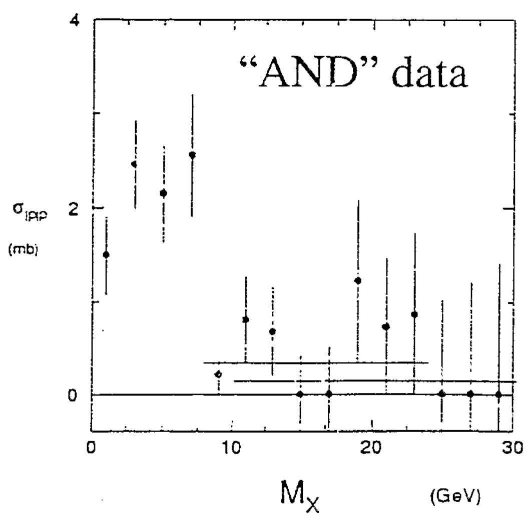

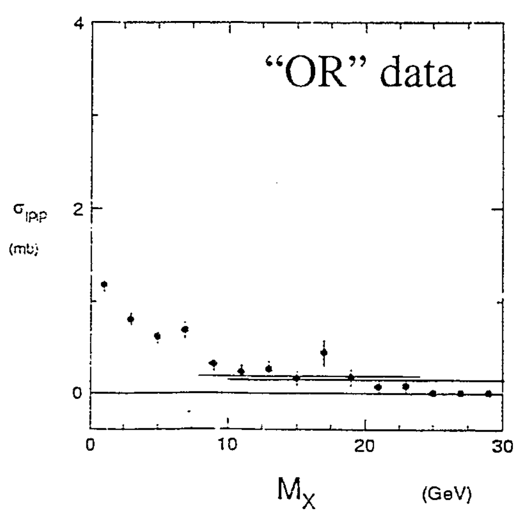

DPE "AND": Event Selection

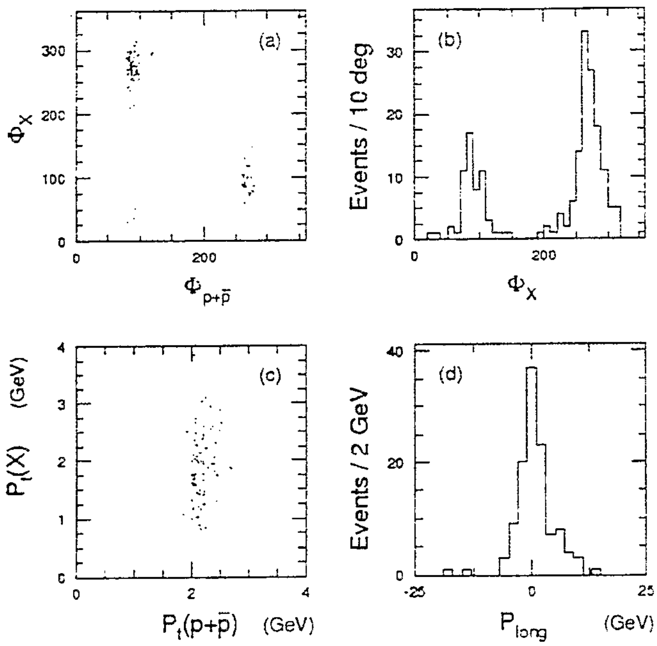

p and $\overline{p}$ Topology

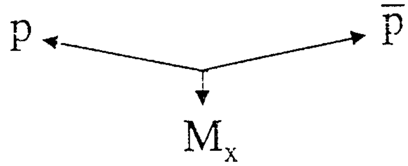

p, $\overline{p}$ UP: $\phi = 90^o$

Minimum P_t acceptance is 1 GeV/c.

DPE "OR" Calorimeter $\Sigma P_{longitudinal}$

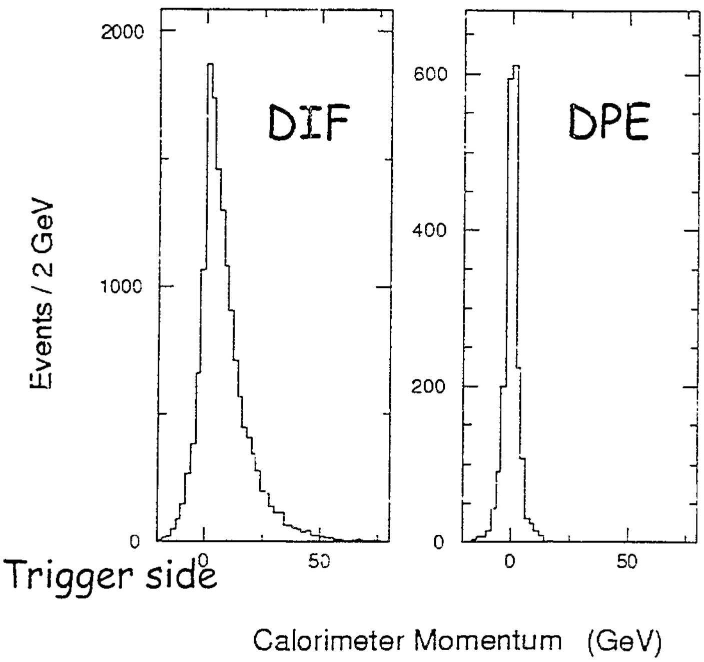

DPE "OR" Extracted from Diffractive trigger

Rapidity gaps, 2.3 - 4.1

$\overline{\text{DIF}}$ ✗

DPE ✓

➔ Rap. gaps produce symmetry in calorim.

EM/Total Energy in Calorimeter

DPE "AND" data

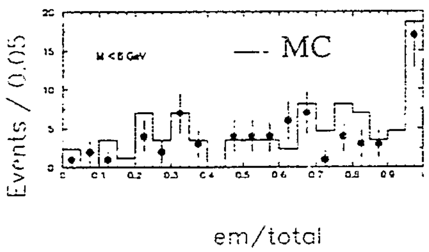

- $N\pi^0 = 0.5\, N\pi^\pm$

→No anomalous behavior

DPE "AND" Longitudinal Structure

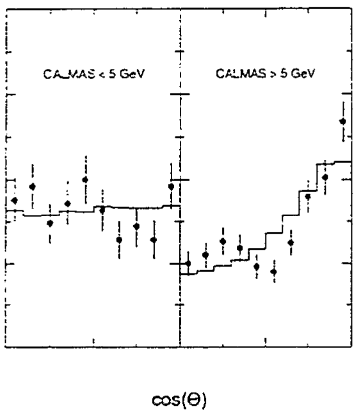

cos θ for hit calorimeter cells in c.m. of M_x

- Mx < 5 GeV: isotropic
- Mx > 5 GeV: polar peaked

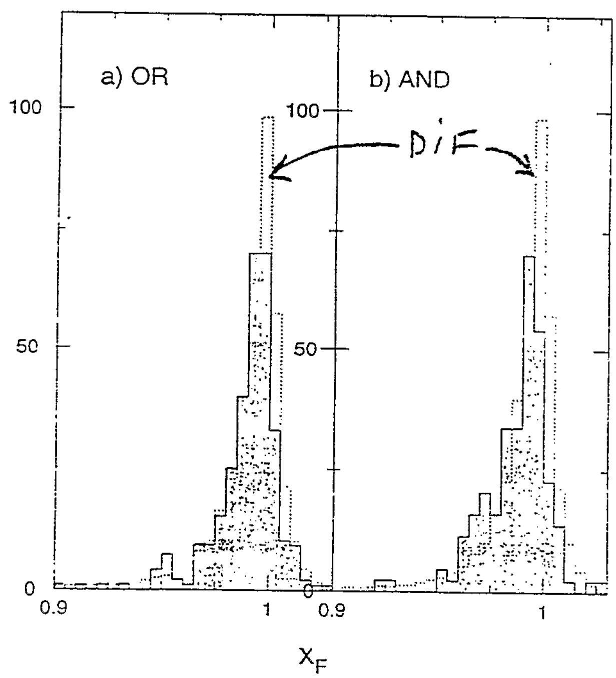

Soft

Diffractive Scattering

and

QCD Instantons

BNL 01'

(Nowak + Shuryak + Zahed)

● Set up

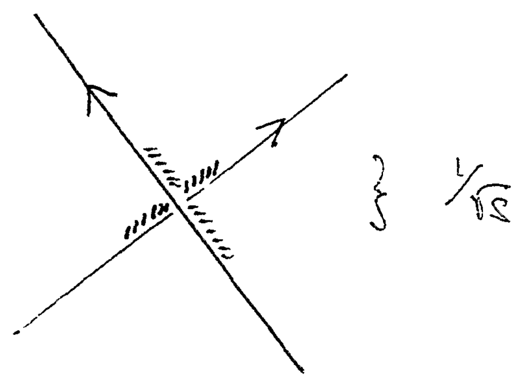

Abelian : WW

Non-Abelian : SYM, strings, Instantons, ...

Scales

SVM : $\langle \frac{\alpha_s}{\pi} G^2 \rangle \simeq 1\,\mathrm{GeV}/\mathrm{fm}^3$

S-String : $\sigma = \frac{1}{2\pi\alpha'} \simeq 1\,\mathrm{GeV}/\mathrm{fm}$

Instanton : $\kappa_0 = \underbrace{n_0}_{1\,\mathrm{fm}^{-4}} \underbrace{\rho_0^4}_{1/3\,\mathrm{fm}.} \simeq 10^{-2}$

- Trick

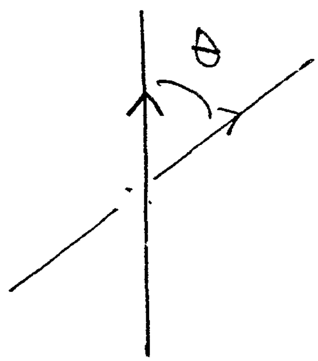

$\theta \to -iy$

$T_E \to +iT$

$$\cos\theta \to \operatorname{ch} y = \frac{1}{\sqrt{1-v^2}} = \frac{s}{2m^2} - 1$$

$$T(\theta, b_\perp) \to T(y, b_\perp)$$

Meggiolaro 98'

● Instantons

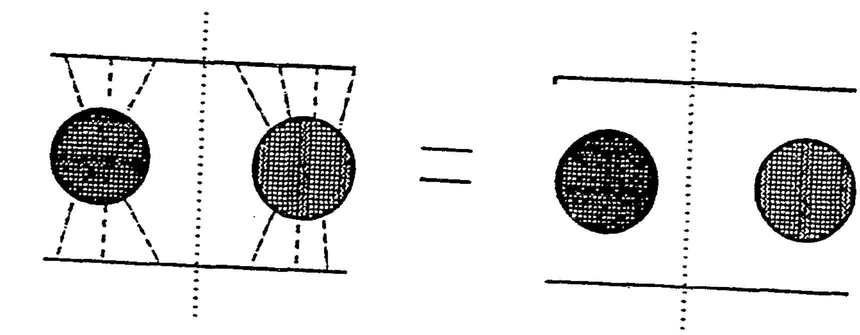

quasi-elastic

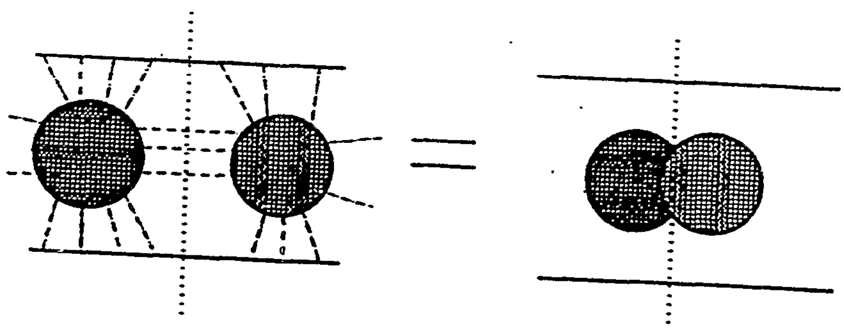

inelastic

~

Shuryak + Z. 00'

Nowak + Shuryak + Z. 00'

Results

$\frac{1}{s^2}\Big|$  $\Big|^2 \simeq \left(\frac{\pi}{-t}\right)\left(\frac{\alpha_s}{\pi}\right)^2$

$\frac{1}{s^2}\Big|$  $\Big|^2 \simeq \pi \rho_s^2 \kappa_0^2$

$\frac{1}{s^2}\Big|$  $\Big|^2 \simeq \pi \rho_s^2 \kappa_0 \ln s$ *

$$\sigma_{QE}/\sigma_{OGE} \simeq \left(\frac{\pi \kappa_0}{\alpha_s}\right)^2 \simeq \left(\frac{\pi 10^{-2}}{1/3}\right) \simeq 10^{-2}$$

~

$$\sigma_{BKFL} \simeq \pi \rho_*^2 \left(\frac{\alpha_s}{\pi}\right)^{2n+1} \ln s^n$$

String Fluctuations, AdS/CFT and the Soft Pomeron

Romuald A. Janik

In this talk we summarize the results obtained in [1,2] on the application of the AdS/CFT correspondence as a tool for studying nonperturbative high energy scattering in gauge theories.

The AdS/CFT correspondence provides an exact equivalence between certain types of gauge theories and appropriate 'dual' string theories on a curved ('Anti-de-Sitter'-like) background. In particular strong coupling properties of gauge theories get mapped to (semi-)classical properties of the relevant string theory.

Scattering amplitudes in the eikonal approximation can be expressed as correlation functions of Wilson lines (resp. loops) following classical straight line quark trajectories (resp. trajectories of a quark-antiquark pair). We perform the calculation of these correlation functions in *Euclidean* space, express them as a function of the relative euclidean angle θ, and then we perform an analytical continuation into Minkowski space. We use the AdS/CFT correspondence in the first 'Euclidean' step.

In order to study the interplay of confinement and reggeization we use a version of the AdS/CFT correspondence which exhibits confinement — Witten's black hole background. The prescriptions for calculating the expectation values of Wilson loop/loops is to find a minimal surface in the curved geometry which is spanned on the loop/loops. For large impact parameters (w.r.t the confinement scale) the minimal surface is well aproximated by the *helicoid* [1]. The resulting Euclidean formula has a branch cut structure, which, through the analytic continuation to Minkowski space gives rise to (i) inelastic amplitudes and (ii) linear Regge trajectories. The intercept in this case is 1.

In [2] we studied quadratic fluctuations of the string worldsheet around the helicoid. The resulting Euclidean expression was again continued to Minkowski space and through the branch cut structure gave rise to a shift of the intercept proportional the number of effective transverse dimensions $n_\perp$ of the dual string theory (the intercept becomes equal to $1 + n_\perp/96$).

The main result is that a (numerically small) shift of the intercept arises naturally through analytical continuation of a Lüscher-like term for the helicoid, it is independent of variations of the string tension and gives a surprisingly similar trajectory to the experimental soft pomeron for $n_\perp = 7, 8$.

[1] R.A. Janik and R. Peschanski, *Nucl. Phys.* **B586** (2000) 163.
[2] R.A. Janik, *Phys. Lett.* **B500** (2001) 118.

MOTIVATION

- GAUGE THEORY SCATTERING $\quad s \to \infty$, t FIXED/SMALL

- QUESTIONS:

$$\text{Amplitudes} \sim s^{\#} \qquad \text{AT STRONG COUPLING}$$

  - BEHAVIOUR WITH t (REGGEIZATION / TRAJECTORIES)
  - INTERPLAY WITH CONFINEMENT

- USE AdS/CFT CORRESPONDENCE

(S)YM GAUGE THEORY $\equiv$ SUPERSTRINGS ON A '$AdS_5 \times S^5$' BACKGROUND

PROPERTIES AT STRONG COUPLING $\longleftrightarrow$ 'EASY' PROBLEMS

- THERE EXIST VARIANTS FOR CONFINING THEORIES.

• ANALYTICAL CONTINUATION EUCLIDEAN $\longleftrightarrow$ MINKOWSKI

// MEGGIOLARO

• CALCULATE

$A^E(\theta_E, L) = \Big\langle$  $\Big\rangle_{\text{EUCLIDEAN}}$

ANALYTICALLY CONTINUE

$$\theta_E \longrightarrow -i\chi = -i \log \frac{s}{2m^2}$$

$$A(s, L) = A^E\left(-i \log \frac{s}{2m^2}, L\right)$$

① USING THE AdS/CFT CORRESPONDENCE CALCULATE EUCLIDEAN CORRELATOR $A^E(\theta, L)$

② WITHIN GAUGE THEORY PERFORM ANALYTICAL CONTINUATION $\theta \to -i \log s$

CALCULATION FROM AdS/CFT

- CONFINING THEORY

$\rightsquigarrow$

WITTEN'S BH GEOMETRY

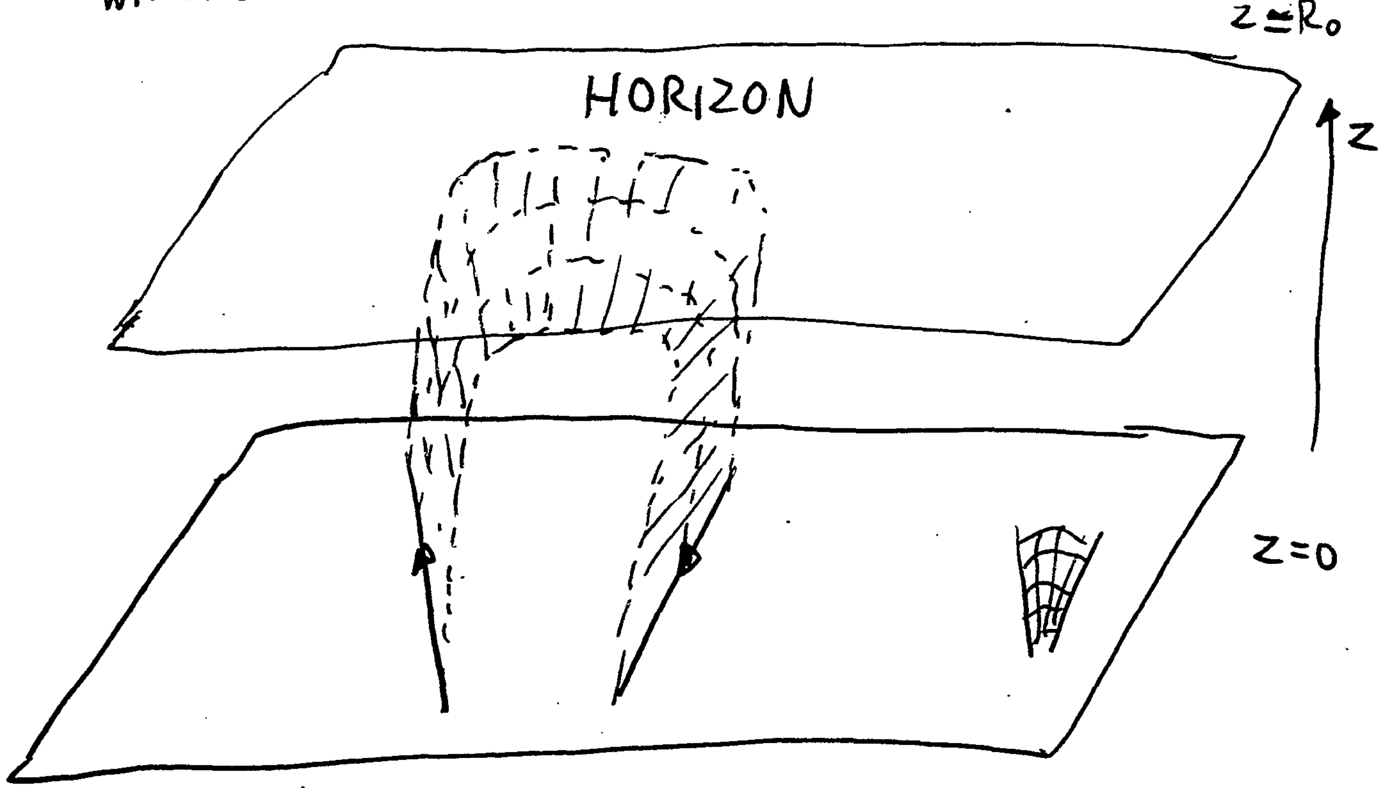

- LARGE IMPACT PARAMETERS

$\rightsquigarrow$

EVERYTHING HAPPENS NEAR THE HORIZON

- METRIC NEAR THE HORIZON FLAT

- FIND MINIMAL SURFACE IN FLAT SPACE

$$\frac{L^2}{\theta}\log[\ldots.] \longrightarrow \frac{L^2}{-i\log s}\, 2\pi \cancel{i}$$

$$\text{Amplitude} = i\, s\, e^{-\frac{1}{\alpha'_{EP}}\frac{L^2}{\log s}}$$

FOURIER TRANSFORM

$$\int d^2q \; e^{iLq} \qquad q^2 = -t$$

$$\text{Amplitude} = i\,(\log s)\; s^{1+\frac{\alpha'_{EF}}{4}t}$$

- INTERCEPT $= 1$
- LINEAR TRAJECTORY

– SMALL IMPACT PARAMETERS

$\downarrow$

DIFFERENT GEOMETRY

$\downarrow$

DIFFERENT BEHAVIOUR

'SOFT – HARD' TRANSITION

RESULT:

$$(\text{PREFACTOR})\ s^{1+\underset{\uparrow}{n/96}+\frac{\alpha'_{EFF}}{4}\cdot t}$$

STRING FLUCTUATIONS

Logs ...

$$n=7 \rightsquigarrow s^{1.073}$$

$$n=8 \rightsquigarrow s^{1.0833\ldots}$$

SOFT POMERON ?

$$s^{1.08+0.25t}$$

- α'_{EFF} IS NOT PREDICTED BUT IS DEFINED THROUGH STATIC $q\bar{q}$ POTENTIAL

  PHENOMENOLOGICAL VALUE $\alpha'_{EFF} \sim 0.8\ldots\ GeV^{-2}$

  $\Downarrow$

  SLOPE $\sim 0.2\ GeV^{-2}$

- NATURAL COUPLING TO SINGLE QUARKS
- INDEPENDENCE OF α'_{EFF}

CAUTION

$\rightsquigarrow$ PREFACTOR

$\rightsquigarrow$ FERMIONS (SHOULD BE MASSIVE)

$\rightsquigarrow$ CUT-OFF

Hard Diffraction at HERA: Results from H1

Frank-Peter Schilling / DESY
H1 Collaboration

High Energy QCD – Beyond the Pomeron
BNL, Brookhaven, May 2001

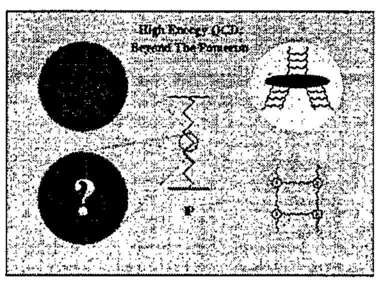

- Inclusive diffraction: F_2^D and the partonic interpretation
- A closer look:
  - Energy flow and thrust
- Diffractive final states in DIS:
  - Dijet and 3-jet production, open charm
- ... and in hadron-hadron(like) interactions:
  - Dijets in diffr. photoproduction [and at the Tevatron]

Summary and Conclusions

Diffractive dijet production (and F_2^D):

- Diffr. Dijets tightly constrain diffractive gluon distribution g^D (shape and norm.), in contrast to $F_2^{D(3)}$ measurements

- Data favour diffr. PDF's, evolving with DGLAP, strongly dominated by gluons with momentum distribution rel. flat in z ("H1 fit 2")

- Consistent picture from $F_2^{D(3)}$ and jet measurements: Concept of factorizing diffr. PDF's in DIS [Collins] works.

- Consistent with factorizing $x_{I\!P}$ dependence with $\alpha_{I\!P}(0) = 1.17$ ("Regge factorization")

- SCI and Semiclassical models not yet able to simultaneously give correct shape and normalizations of jet cross sections

- Improved models calculations based on 2-gluon exchangecan describe part of dijet cross section

Indications for breakdown of Factorization ?

- Suppression of open charm (D^*)

- Suppression of $x_\gamma < 1$ dijets for $Q^2 \approx 0$

Diffractive Dijet Production in DIS [hep-ex/0012051]

Motivation:

- Direct sensitivity to g^D through $\mathcal{O}(\alpha_s)$ process (boson gluon fusion):
- Jet P_T provides second hard scale

Kinematics (in partonic picture):

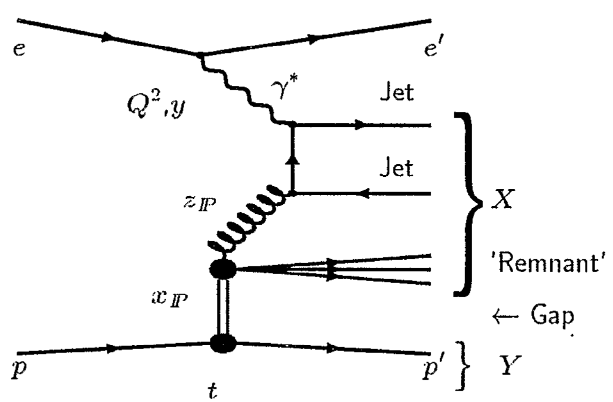

M_{12}

– Invariant mass of two leading jets

$$z_{I\!P}^{(jets)} \approx \frac{Q^2+M_{12}^2}{Q^2+M_X^2}$$

– Momentum fraction of exch. entering hard scattering

Diffractive Gluon Distribution

Dijets directly constrain shape and normalization of g^D:

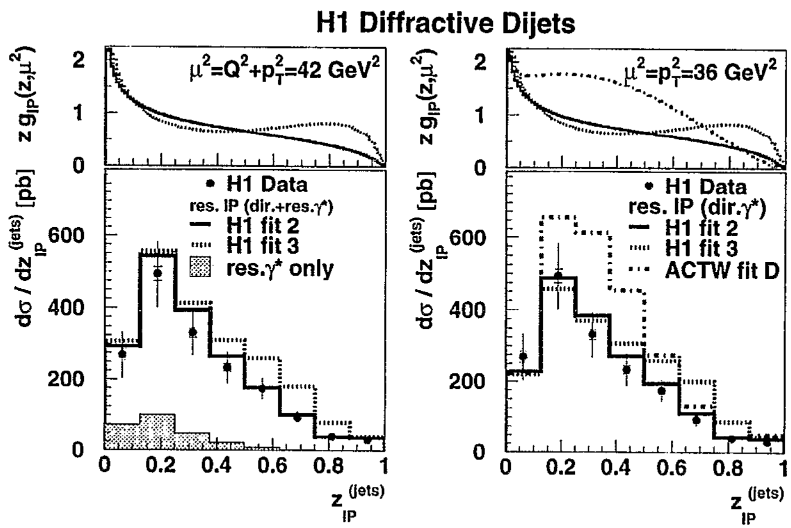

[res. γ^*, $I\!R$ and quark contributions small]

- H1 fit 2: very good agreement with data
- H1 fit 3: overshoots at high $z_{I\!P}$
- ACTW-D: too high

⇒ Support for factorizable diffr. PDF's in DIS which are gluon-dominated and rather flat in z

Proton rest frame picture: $q\bar{q}g \gg q\bar{q}$ states

Soft Colour Neutralization

- Soft Colour Interactions SCI (Edin, Ingelman, Rathsman) original version and "generalized area law" (Rathsman)
- Semiclassical Model (Buchmüller, Gehrmann, Hebecker)

H1 Diffractive Dijets

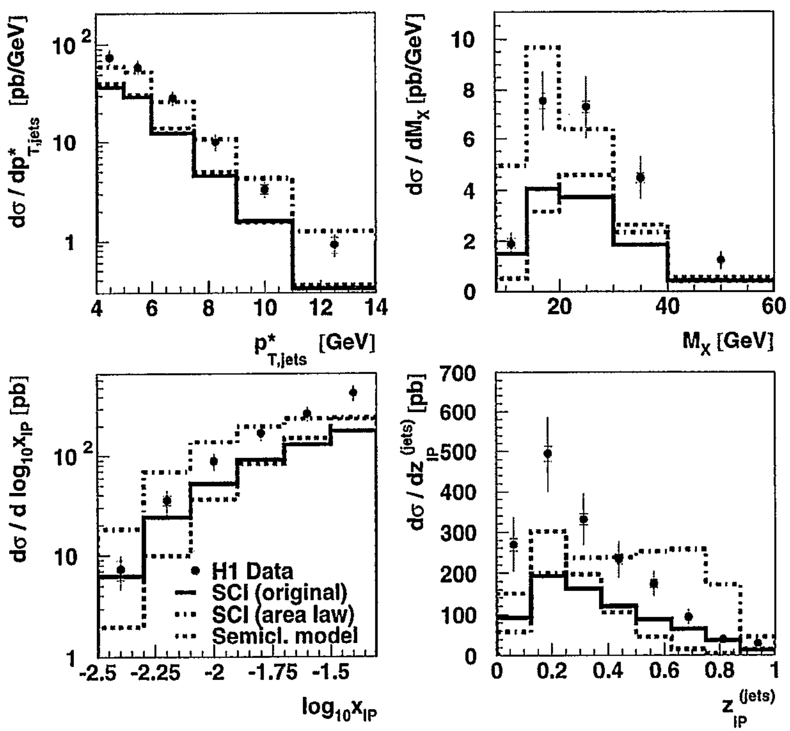

⇒ Sensitivity to differences between models which all (have been tuned to) describe $F_2^{D(3)}$!

Colour Dipole / 2-Gluon Exchange Models

$\boxed{x_{I\!P} < 0.01}$ ⇒ avoid $I\!R$ exch.; P PDF's g-dominated

H1 Diffractive Dijets - $x_{IP} < 0.01$

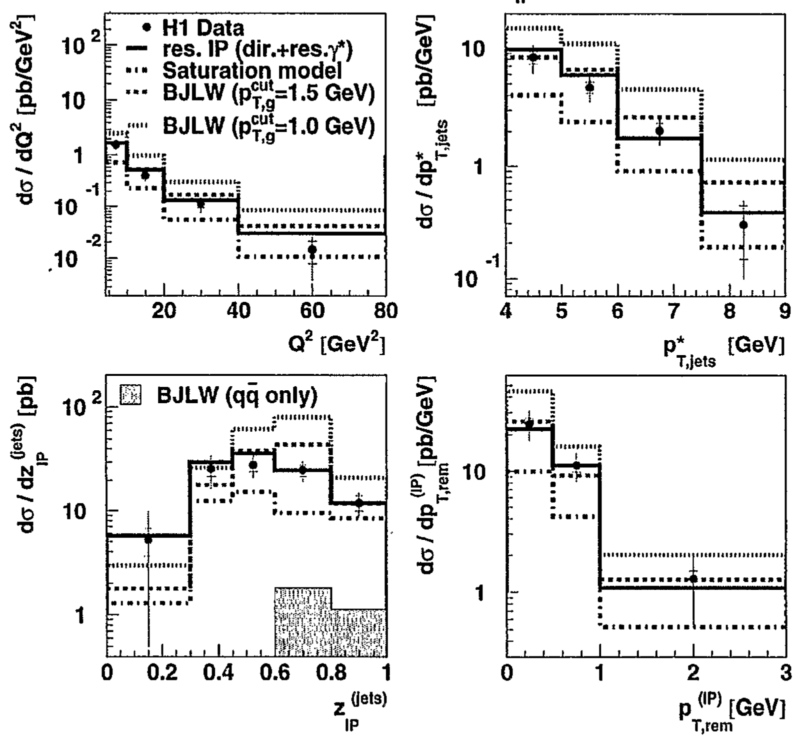

p_T of "$I\!P$ remnant"

- tiny $q\bar{q}$ contribution
- BJLW ~ OK if $p_{T,g} > 1.5$ GeV
- Saturation Model too low
- $p_{T,rem}^{(I\!P)}$ not able to discriminate ;-(

Diffractive D^* Production

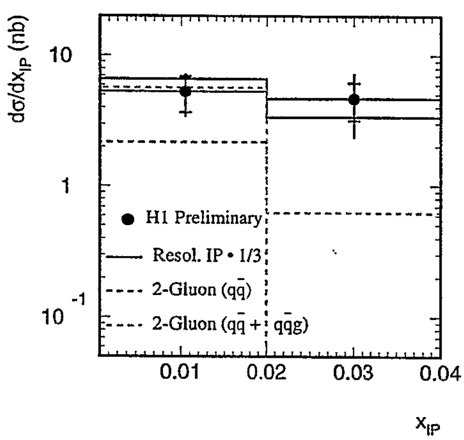

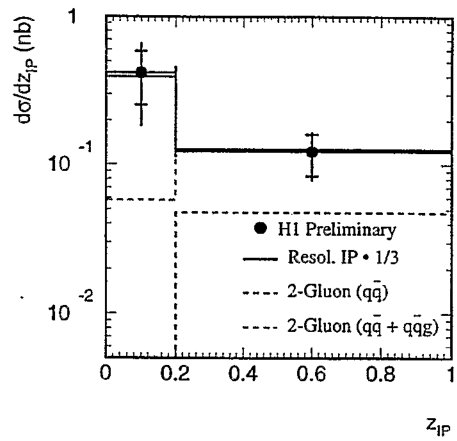

⇒ H1 fit predicts three times higher cross section !
⇒ Broken factorization (Errors still large)?
⇒ 2-gluon, $q\bar{q} + q\bar{q}g$ calculation (Bartels et al.) OK at small $x_{I\!P}$, high $z_{I\!P}$!

Dijets in Diffr. Photoproduction ($Q^2 \approx 0$)

x_γ dependence of cross section:

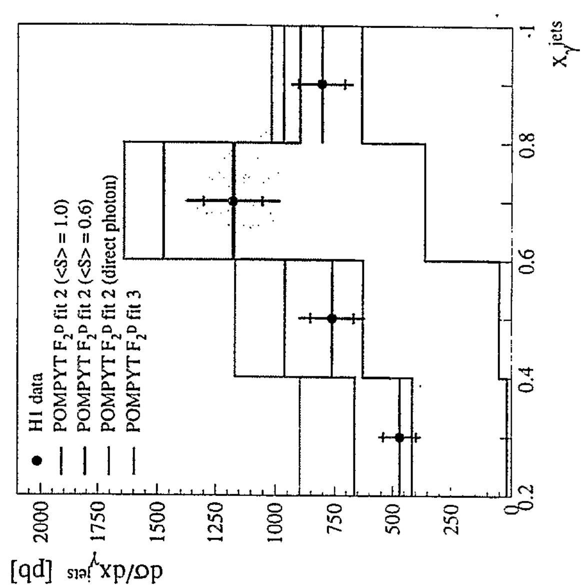

- Resolved γ similar to hadron-hadron
- Suppression factor $S = 0.6$ at small x_γ necessary !

⇒ Factorization broken ? (Large errors...)

[New measurement in progress...]

POMERON PHYSICS STUDIED WITH THE ZEUS DETECTOR

M. Derrick
Argonne National Laboratory

This talk covers four areas of HERA physics studied with the ZEUS detector:

a) The Q^2 and x dependence of the proton structure function F2 is presented, emphasizing the transition that occurs at about $Q^2 = 1$ GeV^2 from pQCD behaviour, described by DGLAP evolution in Q^2, to a Regge-type behaviour parametrized by a simple vector dominance model at the lowest Q^2 values. The cross sections extrapolation to photoproduction agrees reasonably well with those directly measured.

b) About 10% of the DIS events are diffractive. The general properties can be understood either in terms of the exchange of a pomeron in the t-channel or by the interaction of $q\bar{q}$ and $q\bar{q}g$ dipoles in the proton rest system. The data are consistent with factorizing into a pomeron flux times a pomeron structure function. The scaling violations show that the pomeron is gluon dominated. However, the resulting parton distributions are not universal, failing to account for hadronic diffraction at the Tevatron collider. The cross section data indicate a larger pomeron intercept than seen in soft hadronic diffraction. New data with diffractive masses above 20GeV show a clear three-jet structure as expected from the $q\bar{q}g$ partonic state that dominates this region.

c) Vector meson production dominates the low mass region. Both the light, ρ, ω and ϕ, as well as the heavy, J/ϕ and upsilon, mesons have been observed. The energy dependence of the light mesons in photoproduction is similar to hadronic reaction, but the t dependence, as a function of W, is different. The J/ϕ in photoproduction and the ρ in electroproduction have a much steeper W dependence leading to different pomeron trajectories. The t slope of the data shows a change from a large to a small dipole size with increase of the hard scale. Production ratios approach the SU(4) photon wave function value at high Q^2.

d) The data are compared to the saturation model of Golec-Biernat and Wuesthoff.

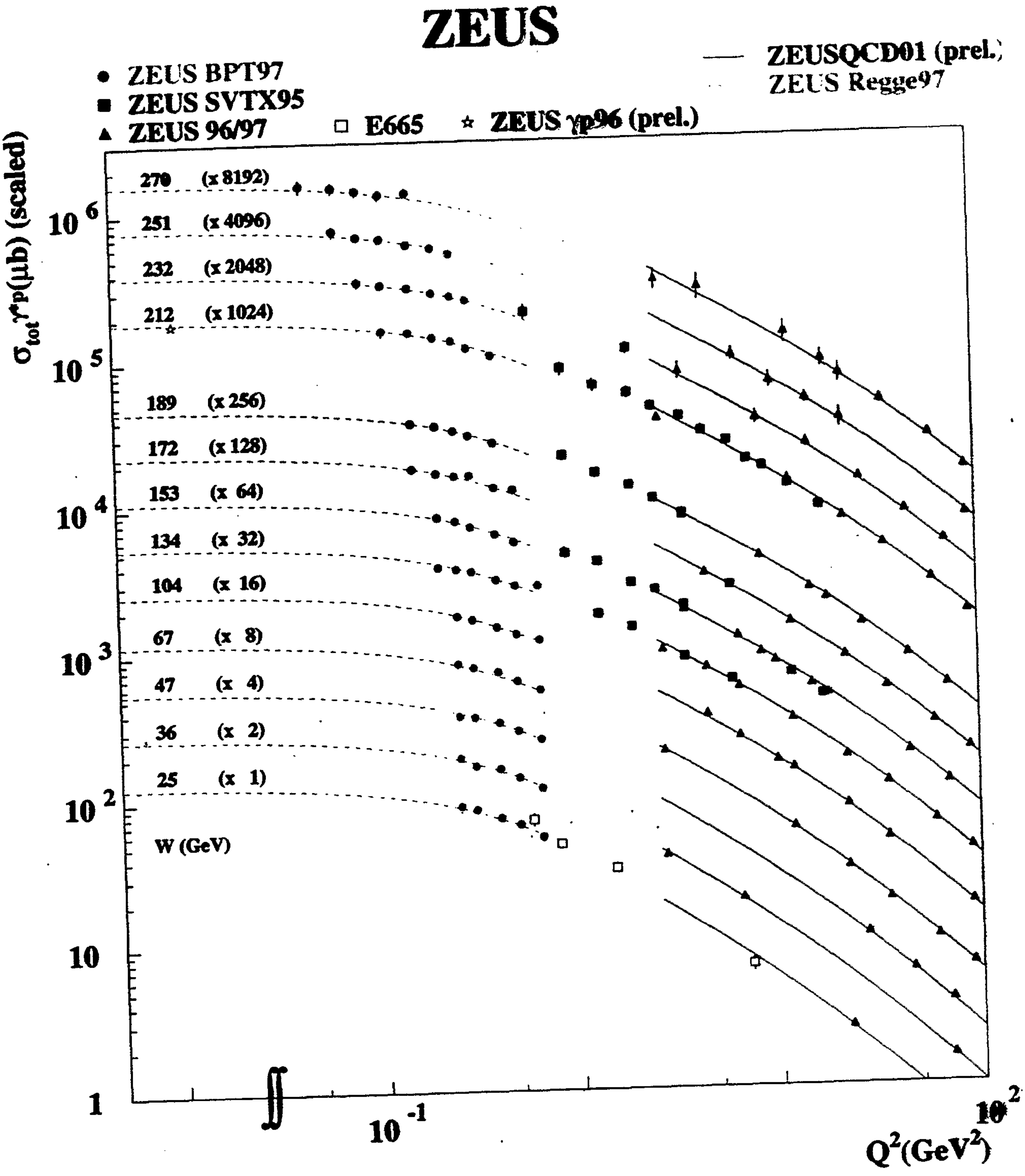

- ZEUS QCD01 & REGGE97 shown in fitted Q^2 range
- Is the slope changing?
- Quantify this from the slope $dF_2/dlog(Q^2)$

• Ingelman-Schlein factorisable model → Pomeron with partonic structure (quark and gluon densities)

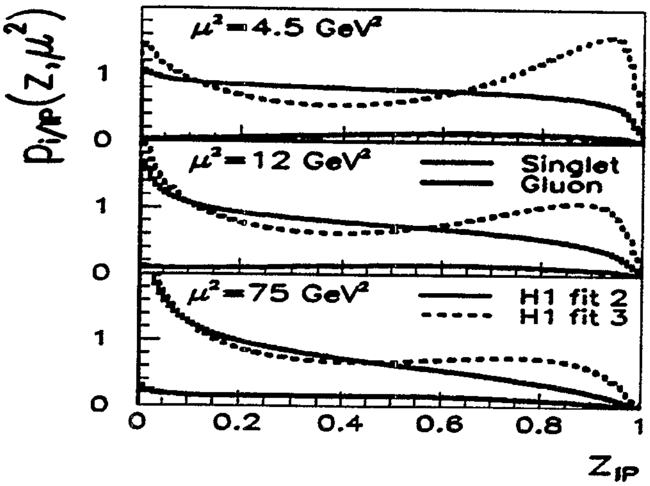

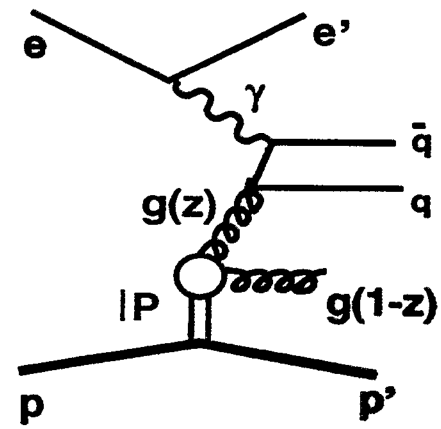

HERA data ⇒ Pomeron dominated by gluons.

• pQCD inspired models (γ-dissociation picture) → Pomeron described as two-gluons exchange

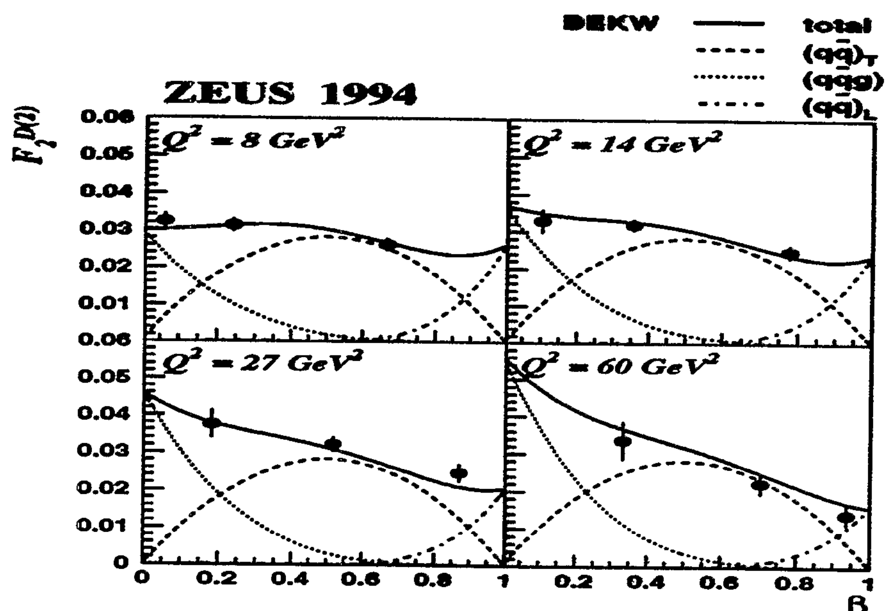

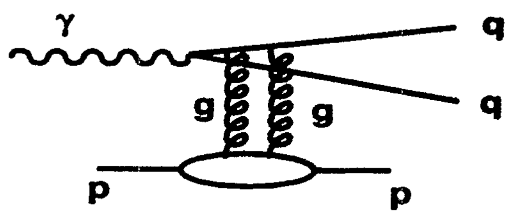

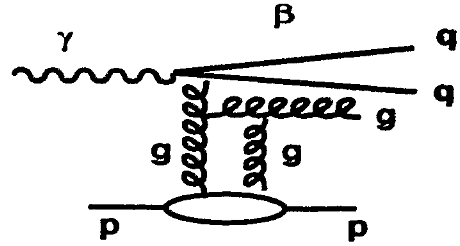

$q\bar{q}g$ contribution dominates at low-β ($\beta = \frac{Q^2}{Q^2+M_X^2}$).

(ZEUS Collab., ICHEP2000 Contributed paper 872)

$5 < Q^2 < 100$ GeV^2
$200 < W < 250$ GeV
$x_{\mathbb{P}} < 0.025$
$23 < M_X < 40$ GeV
$\eta^{\max}_{\text{hadron}} < 3.0$
$N_{\text{jet}} = 3 \ (y_{\text{cut}} = 0.05)$
$-2.3 < \eta^{\text{jet}}_{\text{lab}} < 2.3$
($L = 39\text{pb}^{-1} \rightarrow 678$ evts.)

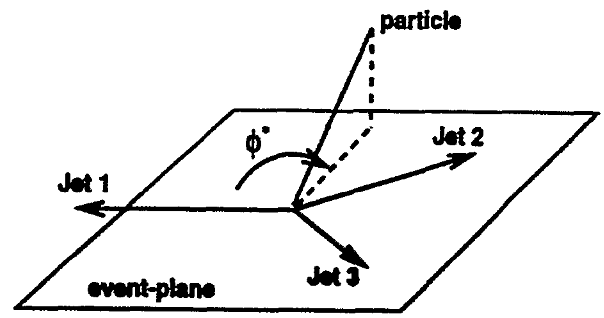

$$x_i = \frac{2 \cdot E_i^{\text{jet}}}{M_X}$$
$$x_1 \geq x_2 \geq x_3$$
$$x_1 + x_2 + x_3 = 2$$

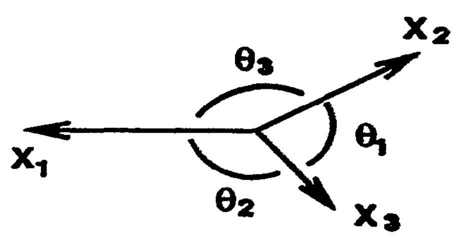

$$x_i \simeq \frac{2 \cdot \sin\theta_i}{\sin\theta_1 + \sin\theta_2 + \sin\theta_3}$$

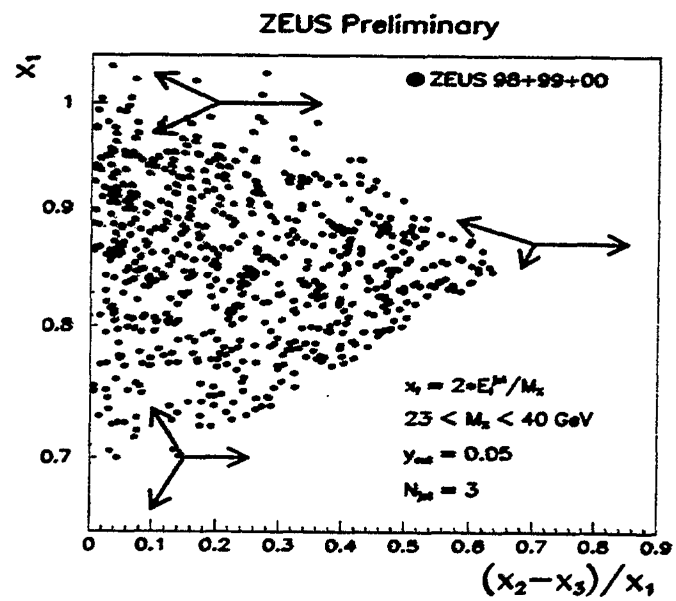

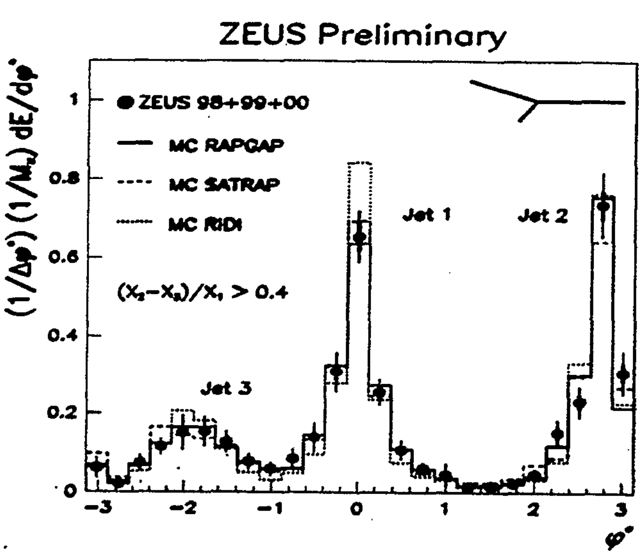

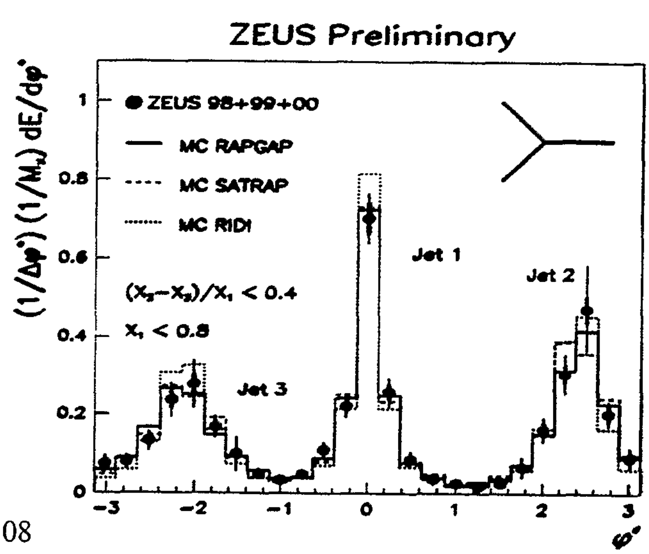

t-slope vs M^2_{VM}

Exponential fall characteristic of diffractive processes

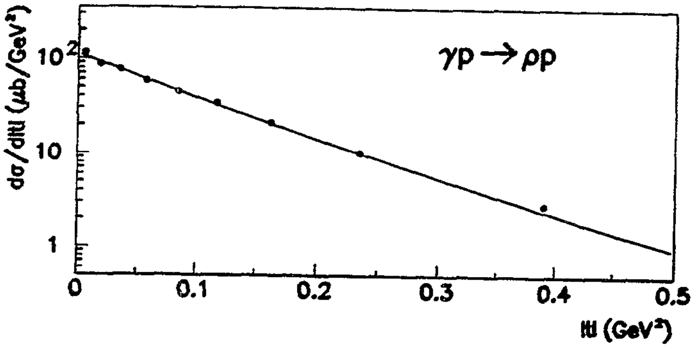

$\frac{d\sigma}{dt} \propto e^{-b|t|}$

ELASTIC

similarity with diffraction of light by a circular aperture $\rightarrow b \propto R^2$

b related to transverse size of the interaction

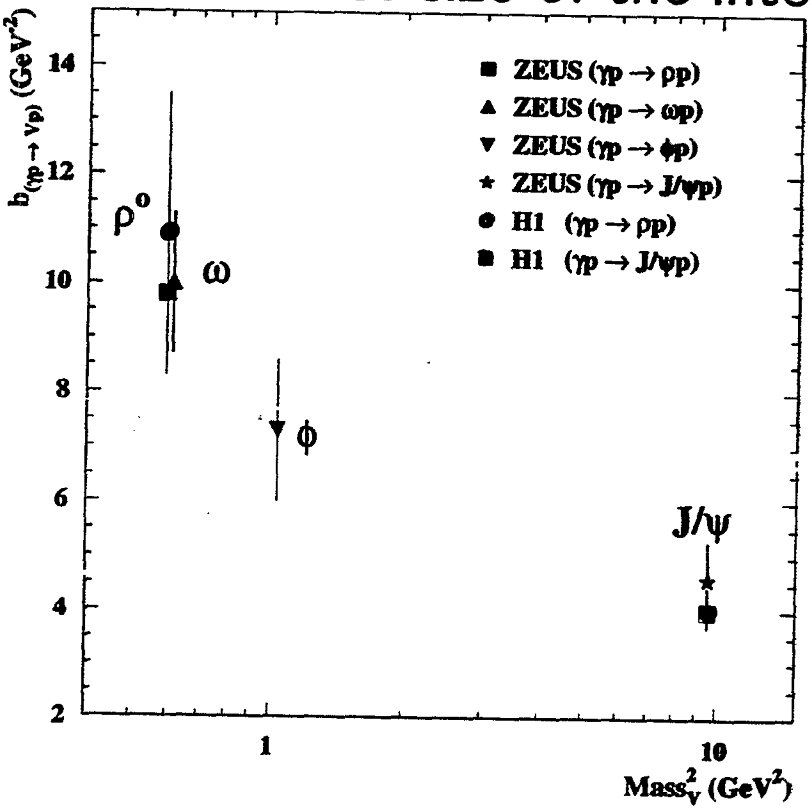

← slope ~4 for J/ψ

- J/ψ radius smaller than ρ, ω and ϕ radius

$b = \frac{R^2}{2}$ $\quad R^2 = R_p^2 + R_V^2$ $\quad$ 5 GeV^{-1} = 1 fm

$\alpha_{I\!P}(t)$ FROM ρ AND J/ψ

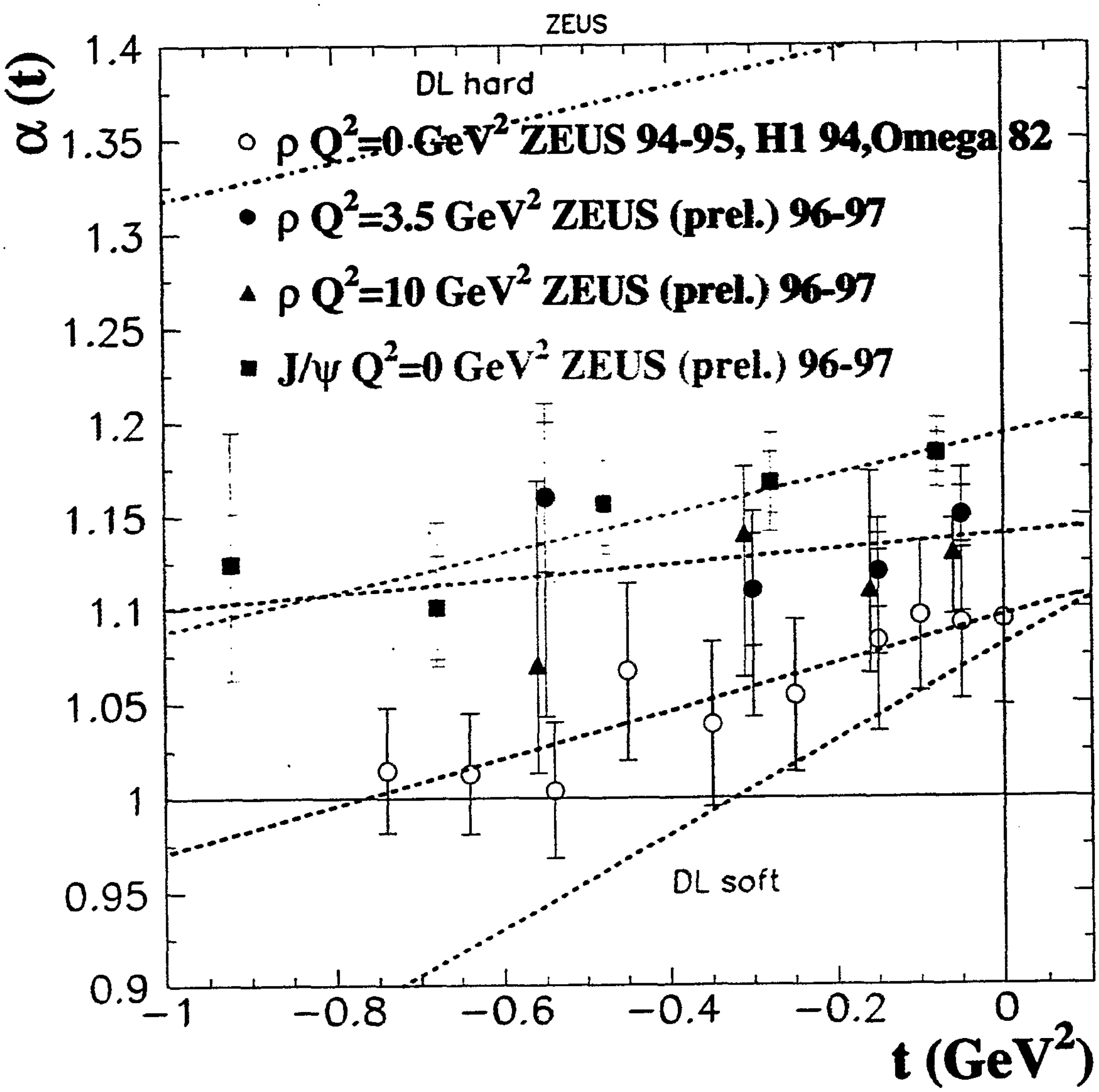

NO UNIVERSAL POMERON.

GB&W Description of $\sigma_{tot}^{\gamma^* p}$

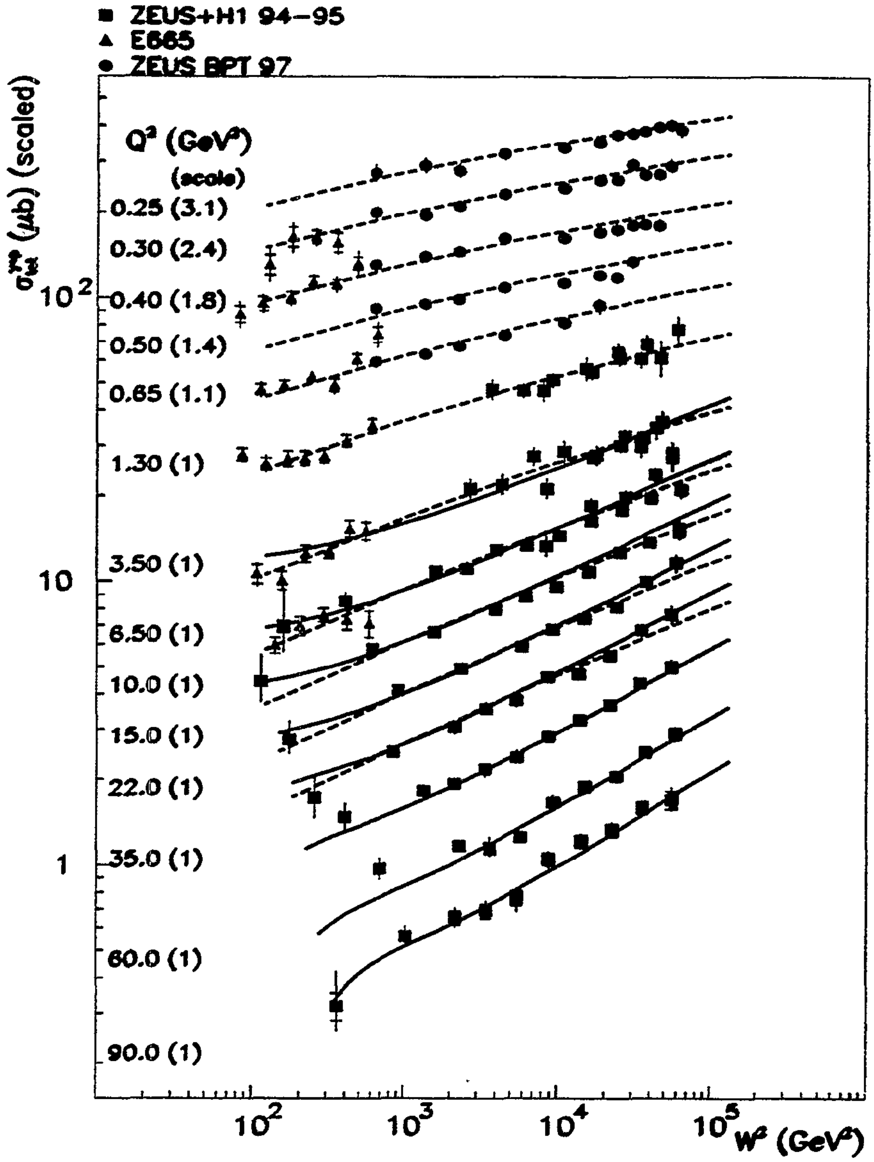

$\sigma_0 = 23.03$ mb

$x_0 = 0.0003$

$\lambda = 0.288$

Dotted line: GB&W model (3 parameter fit) $Q_0 = 1$ GeV

Solid line: MRST NLO QCD fit

$\Rightarrow$ What about $dF_2/dlog(Q^2)$ of NLO DGLAP fits....

BEYOND THE CONVENTIONAL POMERON

Konstantin Goulianos
The Rockefeller University
New York, NY 10021, U.S.A.

High Energy QCD: Beyond the Pomeron
BNL, May 21-25, 2001

ABSTRACT

Diffractive processes at hadron colliders and at HERA exhibit similar but not identical behaviour to that expected for conventional Pomeron exchange. We present the experimental evidence for beyond the standard Pomeron properties of diffraction and review a phenomenological model in which a Pomeron-like behaviour emerges from the quark-gluon sea of the nucleon. Experimental data on soft and hard diffraction are compared with predictions based on this model.

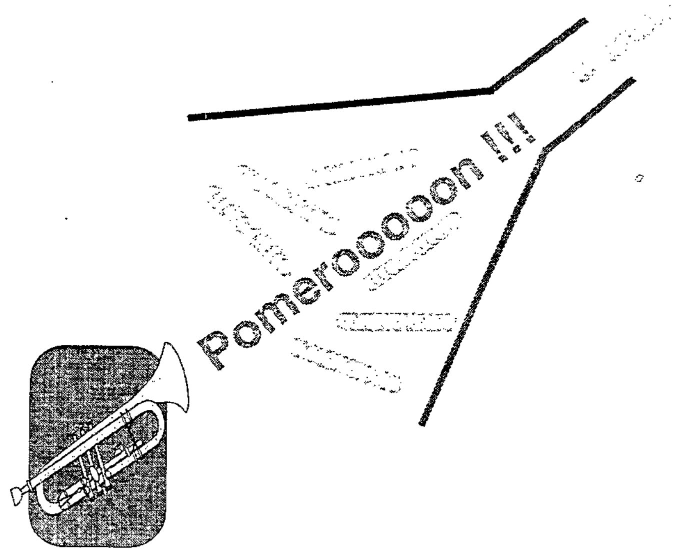

- Introduction
- Elastic and total cross sections
  - Regge approach
  - Parton model approach
- Soft diffraction and multi-gap cross sections
- Hard diffraction

M^2-scaling in diffraction

Single Diffraction

K. Goulianos and J. Montanha PRD **D59**, 114017 (1999)

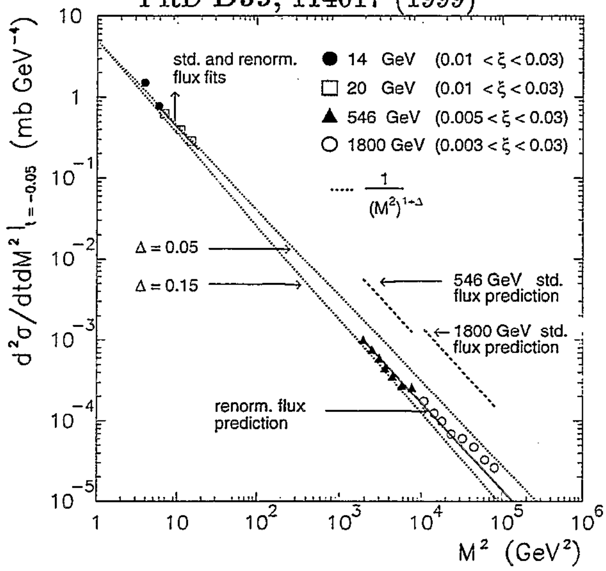

The M^2 dependence of the $\bar{p}p$ single diffraction differential cross section at $t = -0.05$ GeV^2 does not depend on the s-value (M^2-scaling). This is contrary to the Regge theory triple-pomeron prediction of an $s^{2\epsilon}$ dependence.

K. Goulianos, PLB **358**, 379 (1995)

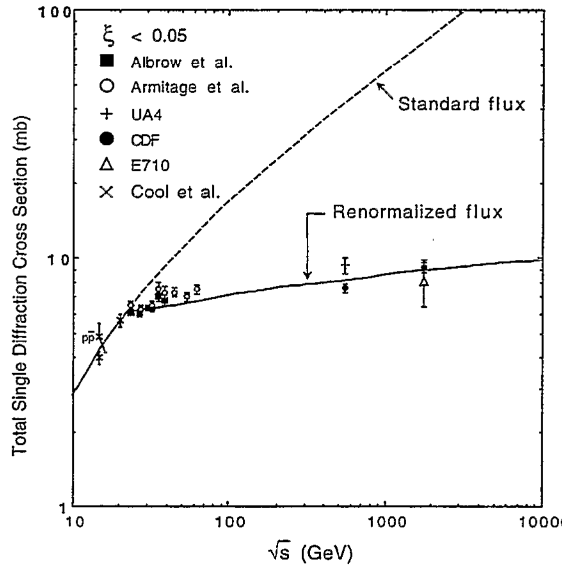

The $\bar{p}p$ total single diffraction cross section has an s-dependence consistent with M^2-scaling, contrary to the Regge theory $s^{2\epsilon}$ behaviour and in agreement with the Pomeron flux renormalization prediction of the above reference.

Double diffraction

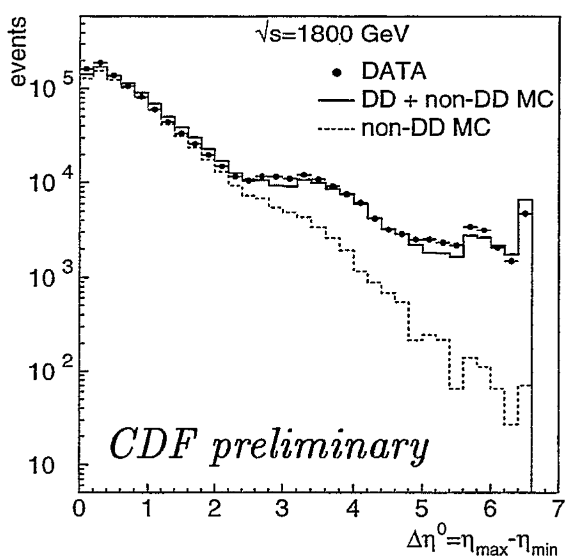

The CDF central rapidity gap data agree in shape with the Monte Carlo prediction for double diffraction dissociation based on Regge theory and factorization.

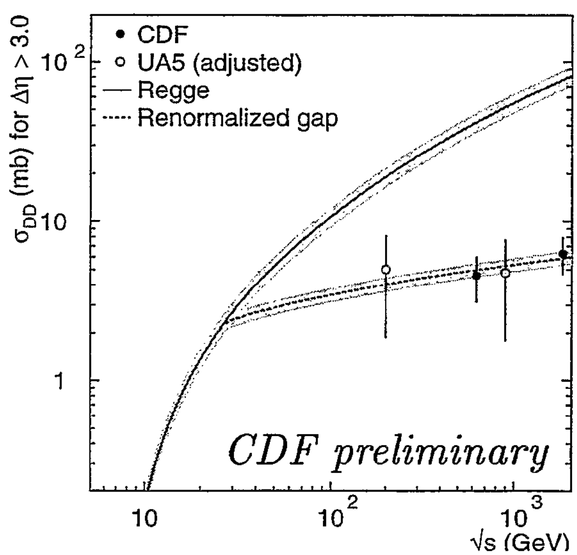

The σ_{DD}^T agrees with the prediction of the *renormalized rapidity gap* model based on M^2-scaling (KG, hep-ph/9806384), contrary to the $s^{2\epsilon}$ expectation from Regge theory.

Multi-gap cross sections

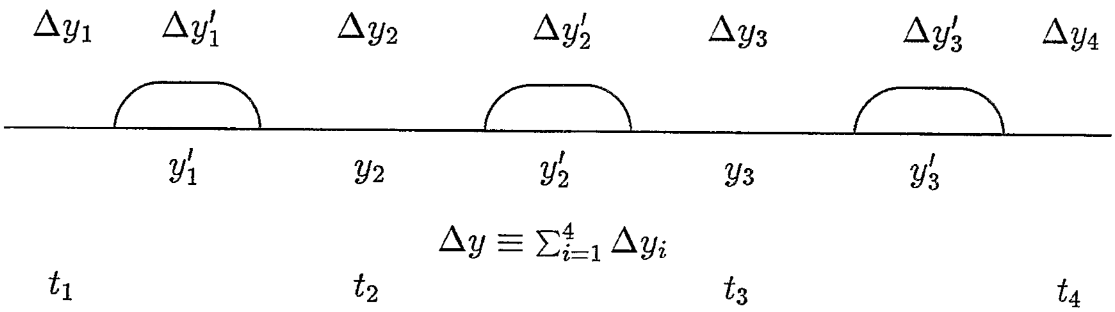

Rules for calculating multi-gap cross-sections

The high energy cross section for a multi-gap process can be calculated from the parton-model scattering amplitude

$$\mathrm{Im}\, \mathrm{f}(t, \Delta y) \sim e^{(\epsilon + \alpha' t)\Delta y}$$

- For the rapidity regions $\Delta y' = \sum_i \Delta y'_i$ where there is particle production, the $t = 0$ parton model amplidude is used and the *sub-energy cross section* is given by $C \cdot e^{\epsilon \Delta y'}$.
- For rapidity gaps, Δy, which can be considered as resulting from elastic scattering between clusters of particles, the square of the full parton-model amplidude is used, $e^{2(\epsilon + \alpha' t_i)\Delta y_i}$, and the form factor $\beta^2(t)$ is included for a surviving (anti)proton.
- The *gap probability* (product of all rapidity gap terms) is normalized to unity.
- A *color factor* κ is included for each gap.

Calculation of the 4-gap differential cross section of the above figure:

- There are 10 independent variables, V_i, shown below the figure.
- $\frac{d^{10}\sigma}{\Pi_{i=1}^{10} dV_i} = P_{gap} \times \sigma(\mathrm{sub-energy})$
- $\sigma(\mathrm{sub-energy}) = \kappa^4 \left[\beta^2(0) \cdot e^{\epsilon \Delta y'}\right] \qquad (\Delta y' = \Sigma_{i=1}^{3} \Delta y'_i)$
- $P_{gap} = N_{gap} \times \Pi_{i=1}^{4} \left[e^{(\epsilon + \alpha' t_i)\Delta y_i}\right]^2 \times [\beta(t_1)\beta(t_4)]^2$

$$P_{gap} = N_{gap} \cdot e^{2\epsilon \Delta y} \cdot f(V_i)|_{i=1}^{10} \qquad (\Delta y = \Sigma_{i=1}^{4} \Delta y_i)$$

- N_{gap} : factor that normalizes P_{gap} over all phase space to unity.

Diffractive DIS

Inclusive DIS $\quad \frac{d^2\sigma}{dx\,dQ^2} \sim \frac{1}{x} \cdot F_2(x, Q^2)$

Diffractive DIS $\quad \frac{d^4\sigma}{dt\,d\xi\,d\beta\,dQ^2} \sim \frac{1}{\beta} \cdot F_2^D(t,\, \xi,\, \beta,\, Q^2)$

$$\boxed{x = \beta\xi}$$

$$F_2^D(t,\, \xi,\, \beta\,, Q^2) = f_c \cdot F_2^{\text{sub-energy}}(\beta,\, Q^2) \cdot P_{gap}(t,\, \xi,\, Q^2)$$

$$\boxed{\Delta y = \ln\frac{1}{\xi} \quad \Rightarrow \quad \frac{d\Delta y}{d\xi} = \frac{1}{\xi}}$$

$$P_{gap} = N_{gap} \cdot \frac{1}{\xi} \cdot \left[e^{[(\epsilon + \alpha' t) + \lambda(Q^2)]\ln\frac{1}{\xi}} \right] \cdot \beta^2(t)$$

$$N_{gap}^{-1}(Q^2,\, \xi_{min}) = \int_{\xi_{min}}^{1} \xi^{-[1+\,\epsilon\,+\,\lambda\,+\,\alpha' t]}\, \beta^2(t)\; dt\, d\xi$$

$$\boxed{\xi_{min} = \frac{x_{min}}{\beta} = \frac{Q^2/s}{\beta} \quad \Rightarrow N_{gap} = f\left(Q^2,\, \frac{Q^2}{s\beta}\right)}$$

Ignoring $t \Rightarrow$ $\qquad N_{gap} = (\epsilon + \lambda) \cdot (Q^2/s\beta)^{\epsilon\,+\,\lambda}$

To guarantee factorization at large Q^2:
$(n = \epsilon + \lambda, \quad C = N_{\text{fact}})$

$$\boxed{F_2^D(\xi,\, \beta,\, Q^2) = C \cdot \frac{n}{\xi^{1+n}} \cdot \left[1 - e^{-\frac{1}{C}(Q^2/s\beta)^n}\right] \cdot \left[f_c \cdot \frac{A_\lambda}{\beta^\lambda}\right]}$$

Comparison with HERA data

Dependence of $\alpha^{I\!P}(0)$ on Q^2:

$\boxed{\alpha^{I\!P}(0) = 1 + \frac{1}{2}\left[\epsilon + \lambda(Q^2)\right]}$ (use $\epsilon = 0.1$ and $\lambda = 0.1 + 0.053\,\ln Q^2$)

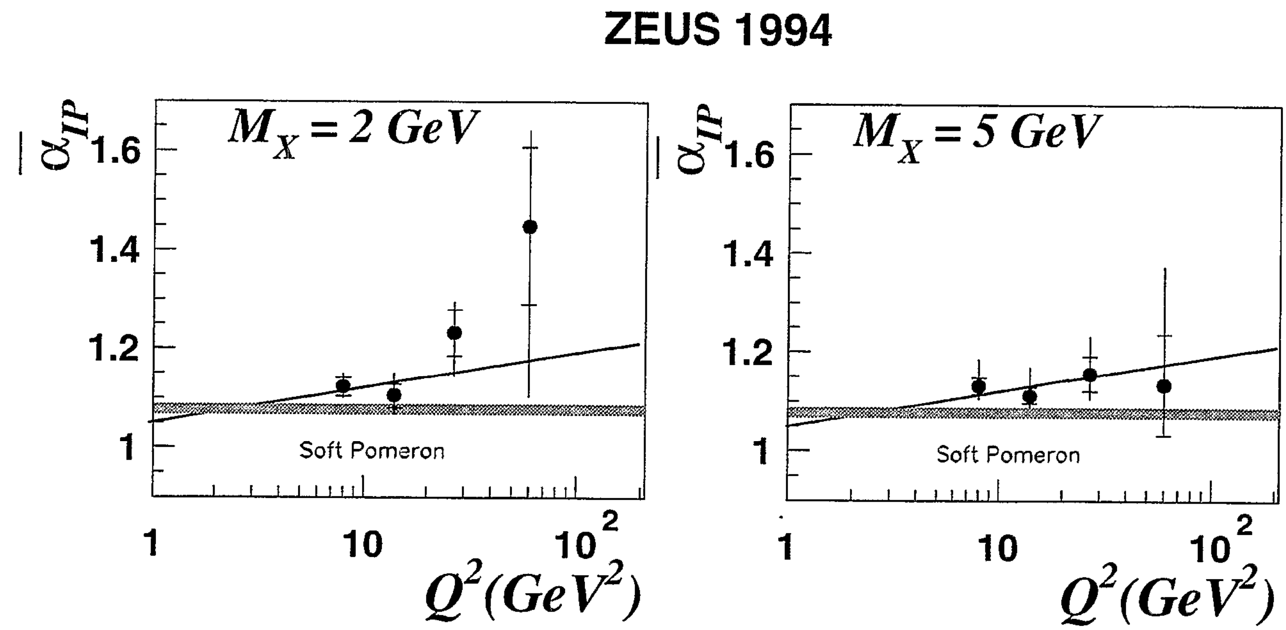

Diffractive structure function prediction (hep-ph/0001092)

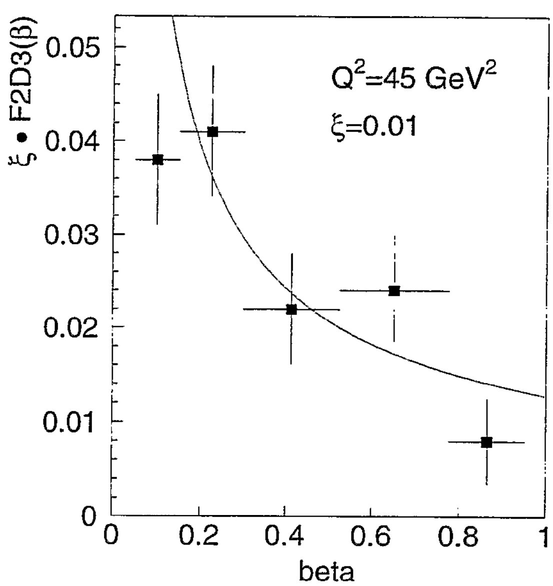

H1 DATA:

$Q^2 = 45$ BeV^2

$F_2(Q^2 = 50,\ x = 0.00133) = 1.46$

$\Rightarrow F_2(x) = 0.2/x^{0.3}$

$\xi \approx 0.01$

$\epsilon = 0.1$

$\lambda = 0.3$

The solid curve in the figure is predicted using the above data/parameters and $f_c = 0.5$.

CONCLUSIONS

- Soft diffraction
  - A parton-model approach to diffraction was presented based on the observed M^2-scaling (s-independence) in single and double diffraction $\bar{p}p$ differential cross sections, $d\sigma/dM^2$.
  - This approach leads to unitarized cross sections without the need to introduce multi-Pomeron exchanges to account for saturation effects (screening, survival-probability ...).
  - Multi-gap differential cross sections are predicted.

- Hard diffraction
  - Diffractive structure function in DIS:

$$F_2^D(\xi, \beta, Q^2) \sim \frac{1}{\beta^\lambda} \cdot \frac{1}{\xi^{1+\epsilon+\lambda}} \times N_{gap}(Q^2, \beta)$$

  - Dependence of Pomeron intercept on Q^2:

$$\alpha(0) = 1 + \frac{1}{2}[\epsilon + \lambda(Q^2)]$$

  - Ratio of diff/non-diff structure functions at the Tevatron:

$$R \sim 1/x^{\epsilon+\lambda}$$

High Energy QCD: Beyond the Pomeron

Brookhaven National Laboratory
21–25 May 2001

Scaling Properties of High-Energy Diffractive Vector-Meson Production at High Momentum Transfer

James A. Crittenden

Deutsches Elektronen-Synchrotron
Notkestrasse 85
D-22603 Hamburg, Germany

May 23, 2001

Abstract

Recent results on the diffractive production of vector mesons in photon-proton reactions at HERA are challenging contemporary understanding of diffractive processes and of hadron structure. Following a brief overview of selected results obtained from the measurement programs of the H1 and ZEUS collaborations during the first eight years of operation, we concentrate on the experimental and phenomenological particulars relating to a recent observation of power-law scaling with momentum transfer in semi-exclusive vector-meson photoproduction. The combination of the observed power and the polarization of the vector meson appear to violate the helicity selection rules of perturbative QCD. This observation fits into a pattern of HERA results pointing to contributions from a point-like transverse-to-transverse vacuum-exchange transition which is difficult to reconcile with QCD.

High Energy QCD Workshop *BNL*

23 May 2001 *Upton, New York*

Scaling Properties of High-Energy Diffractive Vector-Meson Production at High Momentum Transfer

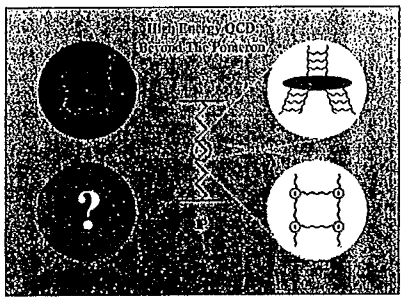

- ☞ Selected Results from HERA
- ☞ Surprise in ρ^0 Photoproduction at High Momentum Transfer

J. A. Crittenden
Deutsches Elektronen-Synchrotron
DESY

General Remarks on Exclusive VM Production at HERA

- ☞ **Investigation of vacuum-exchange processes**

  Vacuum exchange has a complicated, poorly understood structure

- ☞ **Study properties of strong interaction**
  - ⟹ Soft interactions
    - Forward, total cross sections
    - Exponential t-slopes, shrinkage
    - Helicity rules
  - ⟹ Hard interactions
    - Short-distance vacuum exchange
    - Scale definition
    - Sensitive to $|xG(\mu,x)|^2$
    - Helicity rules

  The hard/soft transition can be studied in

  $$Q^2 \qquad M_V^2 \qquad |t|$$

- ☞ **Exclusivity allows study of helicity structure**
  - ⟹ The VM helicity state is directly related to the expected scaling behavior
  - ⟹ The spin-density matrix elements are directly related to meson structure

Quick Review (IV): σ_L/σ_T in Elastic ρ^0 Electroproduction

$$R = \frac{1}{\epsilon}\,\frac{r^{04}_{00} - \Delta^2}{1 - (r^{04}_{00} - \Delta^2)}$$

Δ now known to be small

A. Kreisel/ZEUS at DIS2001

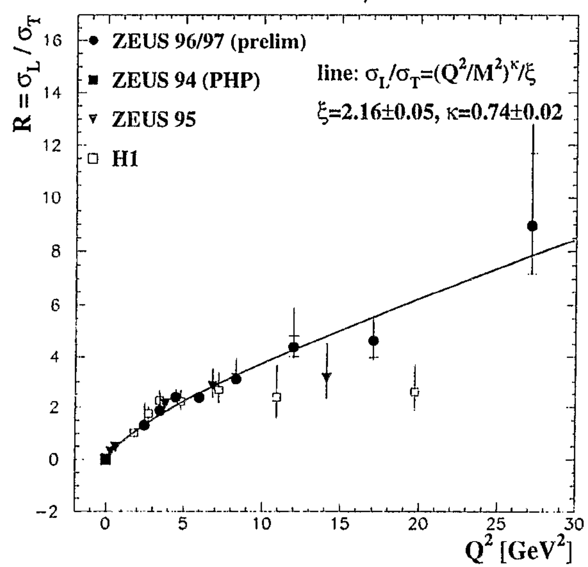

The dominance of σ_L
was an early prediction of pQCD

Quick Review (VI): σ_L/σ_T in Elastic ρ^0 Electroproduction

A. Kreisel at DIS2001

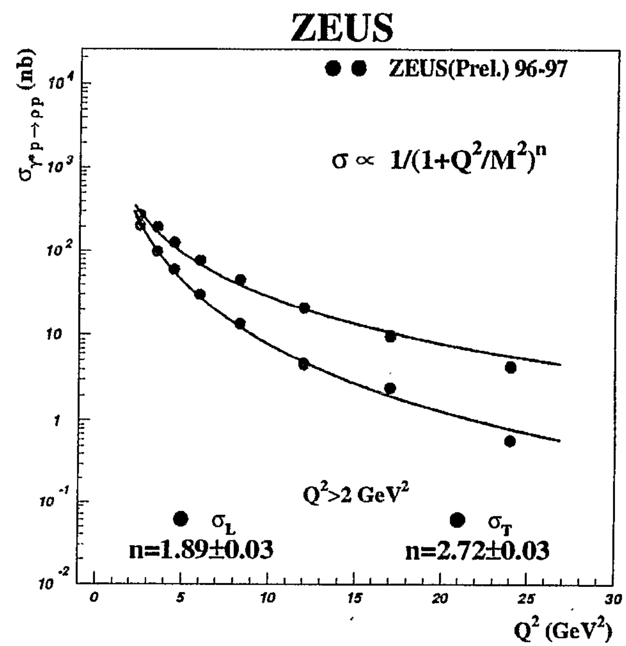

Remarkably hard scaling behavior for σ_T
(The Q^2 dependence is even weaker than Q^{-6})

Main Topic:
VM Photoproduction at High $|t|$

Photoproduction Tagging at $W \simeq$ 100 GeV

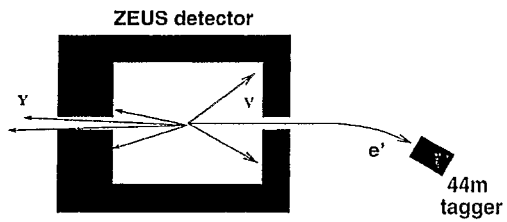

$Q^2 < 0.02$ GeV^2
$23 < E_{e'} < 25$ GeV
($\Rightarrow 80 < W < 120$ GeV)

ZEUS 1996/97 preliminary

Integrated luminosity: 24 pb^{-1}

ρ^0: $\simeq$ 18k
ϕ: $\simeq$ 2k
J/ψ: $\simeq$ 150

Proton-dissociative process dominates at $|t| >$ 1 GeV^2

$$x = \frac{t}{t - M_Y^2}$$

Cross sections $\frac{d\sigma}{dt}$ are integrated over $0.01 < x < 1$

Diffractive ρ^0 Photoproduction (III)

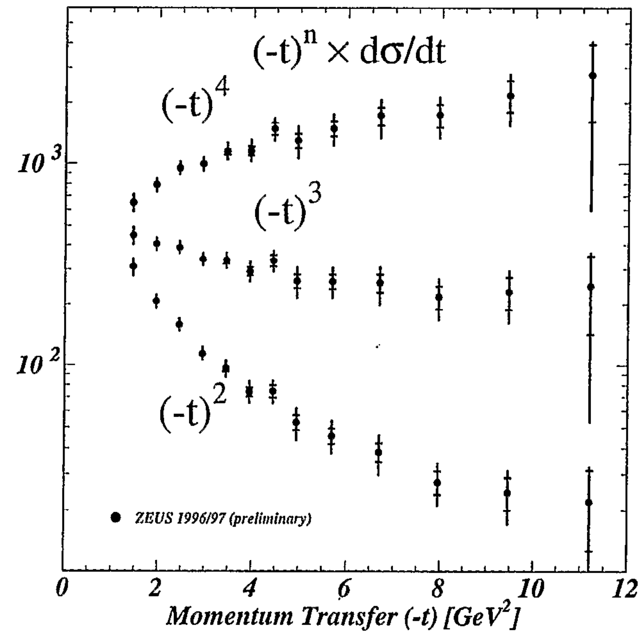

Multiplying with $(-t)^n$

Diffractive ϕ Photoproduction (II)

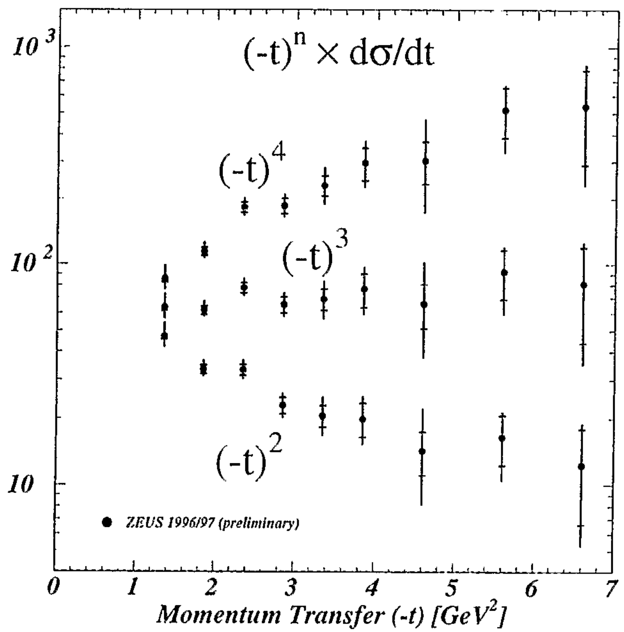

Multiplying with $(-t)^n$

Decay-Angle Analysis (II)

Talk by A. Kowal at DIS2001

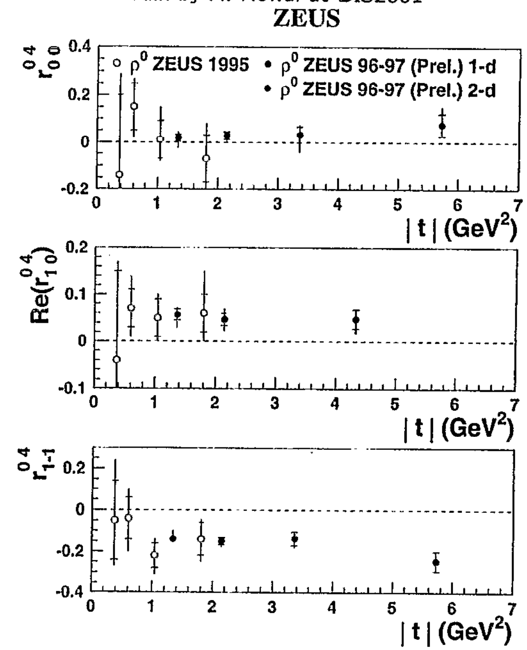

Transverse polarization dominates

Helicity breaking clearly measured at level of few %

(But why no dependence on t?)

Also significant double-flip contribution

See Ivanov et al, Phys. Lett. B478 (2000) 101

Some general remarks
(and some questions)

- These are the first measurements of light-vector-meson photoproduction at values of t comparable to the Q^2 values in DIS which led to the discovery of charged proton constituents in 1967.
- *BUT* this is presumably a strong interaction, rather than electromagnetic.
- We observe an extremely hard t dependence
  $\Rightarrow$ low-order process (*first* order ?)
  $\Rightarrow$ What about the meson form factor ?
- *The QCD helicity selection rules appear to be violated.*
- These values for t exceed the mass scales for ρ^0 and ϕ and exceed Λ^2_{QCD}
  $\Rightarrow$ Asymptotic region
  The t dependence characterizes the interaction.

Perturbative field theory

for vacuum exchange in the strong interaction (?)

What is the exchanged field?

What is the "charge"?
(Strength about 1/100 of confinement)

What is the reacting proton constituent?

Are there point-like interactions of hadronic bound states?

Attempted Synthesis

There appears to be increasing evidence for a point-like T→ T vacuum-exchange transition which is difficult to reconcile with QCD

- A QCD description requires chiral-symmetry breaking, for example, quark-mass effects.
- This requirement results in a t dependence stronger than observed.
- This T→T transition contributes to VM electroproduction well into the Q^2 region where pQCD successfully describes the production of longitudinal vector mesons.
- It is the dominant VM-photoproduction process at high momentum transfer.

The successful field theoretical description of this process will be a prime candidate for a theory which can be used in higher orders to describe diffractive processes at low momentum transfer, elastic and total hadronic cross sections.

Abstract: For Multiplicities,Cross Sections and Diffraction Dissociation

W.D. Walker –Duke University

In figure 1 we see the multiplicity distributions for a range of $\sqrt{s}$ values. The solid curve is the distribution for lower energies (ISR) where KNO multiplicity scaling holds. The quantity x is the charged multiplicity $n/<n_1>$ where $<n_1>$ is the average multiplicity for a single parton-parton collision. KNO scaling works for a part of each of the multiplicity distributions. Figure 2 shows the result of subtracting the solid curve from each of the experimental distributions. The result is a group of curves which peak at a value of $n/<n_1> = 2$. The distributions widen as $\sqrt{s}$ increases.

To begin to understand the position of the energy threshold for double (and triple) parton –parton collisions we use the energy required ,$\sqrt{s}$', for making the multiplicity $<n_1>$ charged particles from e^+-e^- annihilation. This formulation predicts a threshold for two collisions of about $\sqrt{s}$ =100 GeV for p-pbar interactions. The results of the calculations and observations are shown in the Table. The quantity $<n_1>$ is measured and nicely fitted by an expression of the form $<n_1> = A \log(\sqrt{s}) + B$ over the range of $\sqrt{s}$ of 60 to 1800 GeV.. We note that the threshold for 3 collisions should be in the neighborhood of 500 GeV.. We show the decomposition of the multiplicity distribution at 1800 GeV. in Figure 3. We have extrapolated our results to LHC energies. We find that the multiparton collisions account for almost all of the increase in the non-single diffractive cross section, σ_{NSD} ,in the collider energy range. We predict that multi-parton collisions will have a cross section of about an equal magnitude with that for single parton-parton collision at the LHC energy. This is shown in figure 4. Remarkably the cross section for single parton –parton ,σ_1 , seems to be nearly constant as the energy is increased.

Collisions with nuclei will likely obey a different set of rules than single nucleon-nucleon collisions. This makes such studies seem very inviting.

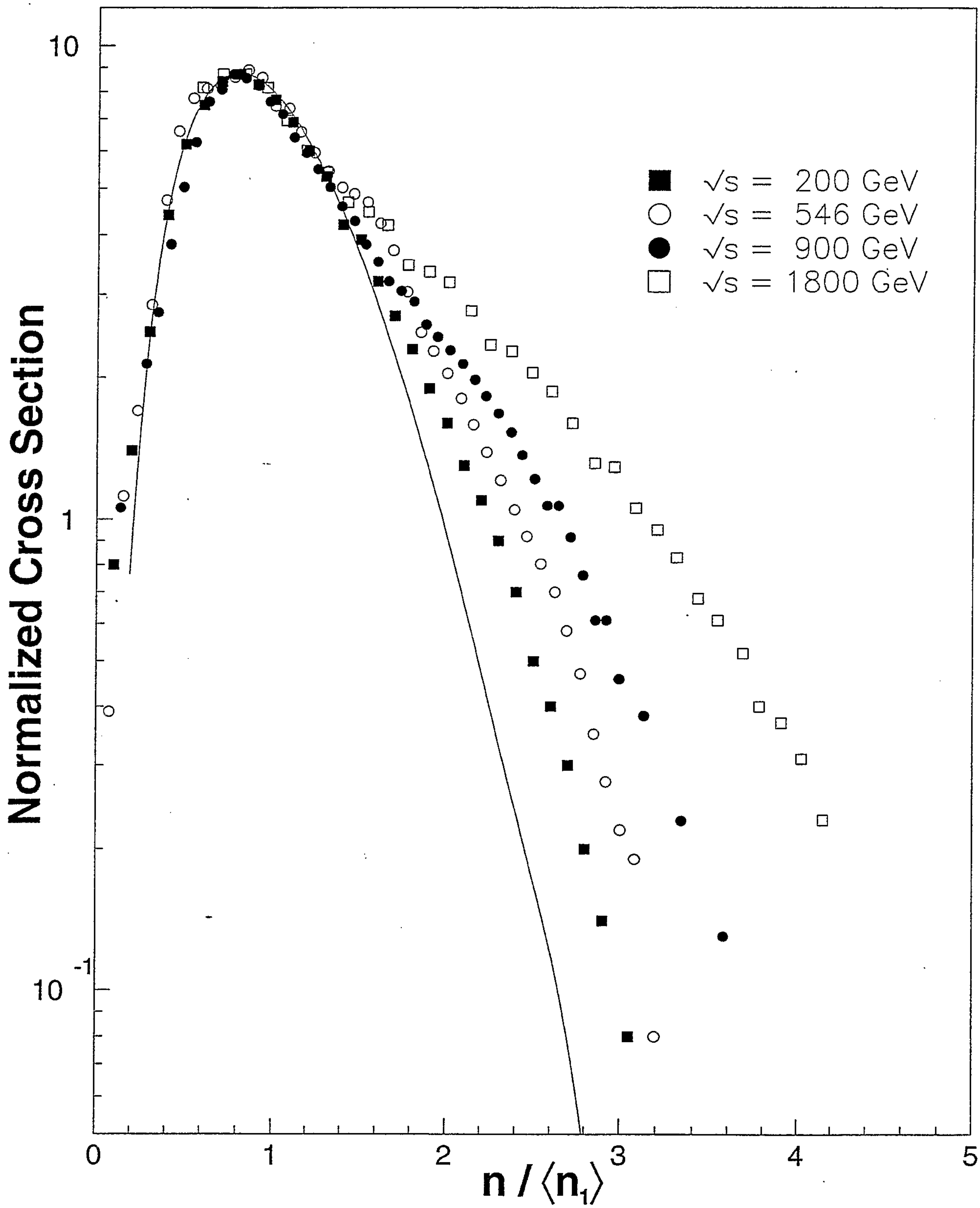

Normalized Cross Section
10
1
10^-1
0
1
2
3
4
5
n / ⟨n1⟩
√s = 200 GeV
√s = 546 GeV
√s = 900 GeV
√s = 1800 GeV

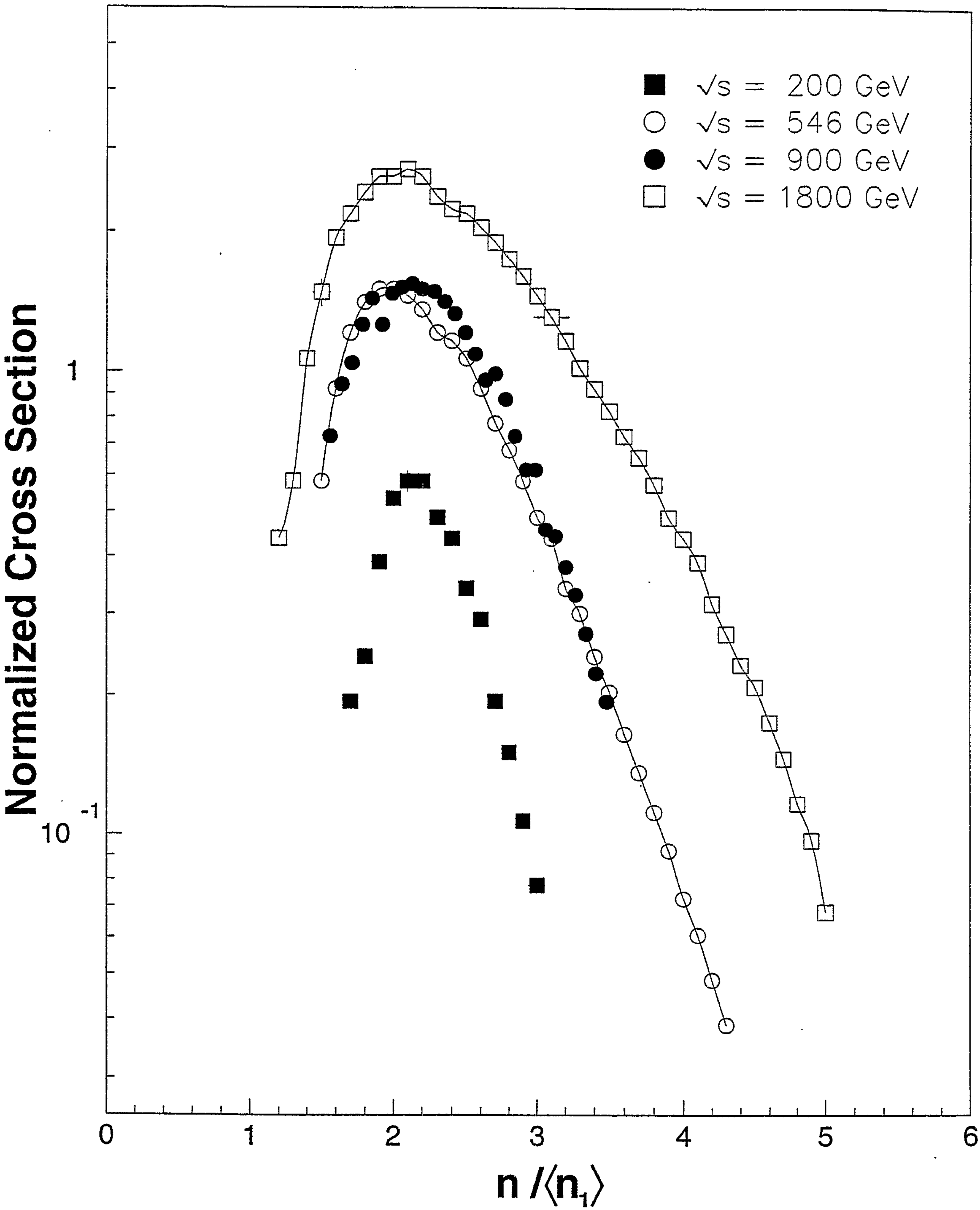
√s = 200 GeV
√s = 546 GeV
√s = 900 GeV
√s = 1800 GeV
Normalized Cross Section
1
10^{-1}
0
1
2
3
4
5
6
$n / \langle n_1 \rangle$

TABLE-COLLISION CHARACTERISTICS

$\sqrt{s}$-GeV	$<n_1>$	$x' = \sqrt{s'}/\sqrt{s}$	σ_{NSD}	σ_1	σ_2	σ_3 (mb)
62	14	.58	30.3	31.0		
200	20.0	.40	35.2	33.5	1.75	
546	25.2	.30	40.2	30.8	9.5	
900	27.6	.24	43.0	31.7	10.2	1.5
1800	31.5	.18	47.0	31.9	12.5	2.7
14000	42.2	.10	$\approx$ 62.0	30.6	17.2	13.9

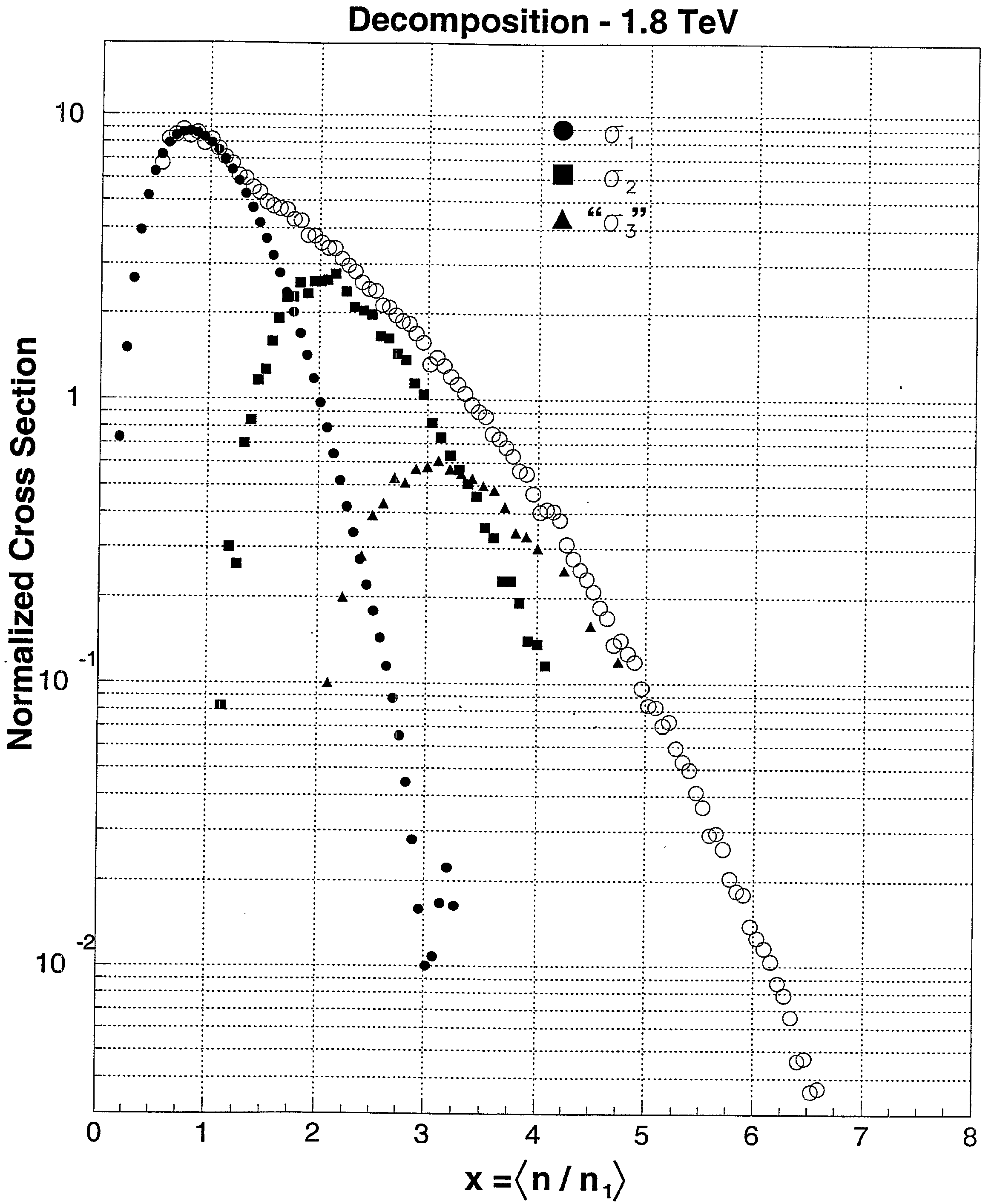

Decomposition - 1.8 TeV
Normalized Cross Section
10
1
10^-1
10^-2
0 1 2 3 4 5 6 7 8
x =⟨n / n_1⟩
σ_1
σ_2
"σ_3"

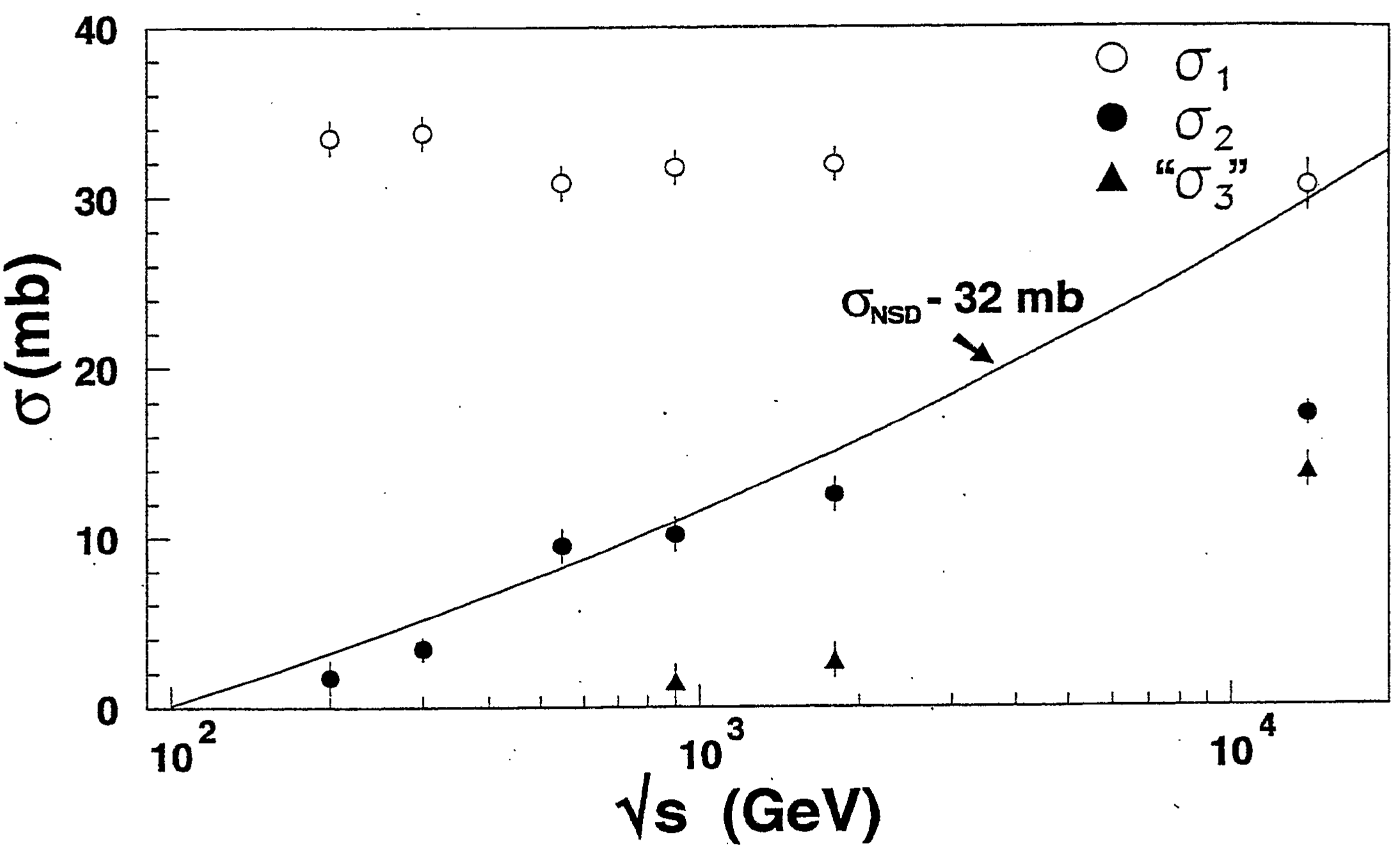

40
30
20
10
0
σ (mb)
σ_1
σ_2
"σ_3"
σ_{NSD} - 32 mb
10^2
10^3
10^4
√s (GeV)

Study of Diffractive Dijet Production at CDF

Kenichi Hatakeyama
Rockefeller University, 1230 York Avenue, New York, NY, 10021
CDF Collaboration

We have studied single diffractive dijet production at $\sqrt{s} = 630$ and 1800 GeV using events triggered on a leading antiproton detected in a Roman Pot spectrometer. In this study, the diffractive structure function of the antiproton is measured and compared between $\sqrt{s} = 630$ and 1800 GeV. We find agreement in the β-dependence of the measured diffractive structure functions (β is the momentum fraction of Pomeron carried by the struck parton), and a ratio in normalization of

$$R[\frac{630}{1800}] = 1.3 \pm 0.2(stat)^{+0.4}_{-0.3}(syst)$$

in the region of $0.1 < \beta < 0.5$, $0.035 < \xi < 0.095$, where ξ is momentum fraction of the $\bar{p}$ carried by the Pomeron, and 4-momentum transfer squared $|t| < 0.2$ GeV^2. This ratio is in general agreement with predictions from the renormalized Pomeron flux model, soft color interaction model, and gap survival model.

We have also studied some characteristics of the diffractive structure function using the higher statistics 1800 GeV data sample. In the region $\beta < 0.5$, $0.035 < \xi < 0.095$ and $|t| < 1$ GeV^2, the measured diffractive structure function can be fitted with the form

$$F_{jj}^{D}(\beta, \xi) = C \cdot \beta^{-n} \cdot \xi^{-m}$$

The fit yields $n = 1.04 \pm 0.01(stat)$ and $m = 0.92 \pm 0.02(stat)$. In the framework of Regge theory, the Pomeron, Reggeon and Pion exchanges have ξ dependences of $\xi^{-(2\alpha(0)-1)} \sim \xi^{-1.2}$, $\sim \xi^{0}$ and $\sim \xi$, respectively. The measured value of $m = 0.92 \pm 0.02(stat)$ indicates that single diffractive dijet production is dominated by Pomeron exchange.

Comparisons are made with results from the UA8 collaboration, which studied single diffractive dijet production and the structure function of the Pomeron in $\bar{p}p$ collisions at $\sqrt{s} = 630$ GeV at the CERN $Sp\bar{p}S$ collider. To compare the CDF 630 GeV data with the UA8 results, the CDF 630 GeV data sample was re-analyzed in a similar way to that used by the UA8 collaboration. The $x(2-jet)$ $(= \beta - x_{bj}(proton))$ distribution for the UA8 data, from which UA8 evaluated the Pomeron structure function, agrees with that for the CDF 630 GeV data reasonably well.

Diffractive Dijets with Leading Antiproton

Physics Motivation:

1. Measure the diffractive structure function $F_{jj}^D(\beta, \xi, Q^2, t)$

$$\left(\begin{array}{c} F_{jj}^D(x, \xi, Q^2, t) = x\left[g^D(x, \xi, Q^2, t) + \frac{4}{9} q^D(x, \xi, Q^2, t)\right] \\ F_{jj}^D(x, \xi, Q^2, t) \longrightarrow F_{jj}^D(\beta, \xi, Q^2, t) \end{array} \right)$$

$$\frac{d^5(p\bar{p} \to pjjX)}{dx_p\, d\beta\, d\xi\, dt\, dp_T^2} = \frac{F_{jj}(x_p, Q^2)}{x_p} \frac{F_{jj}^D(\beta, \xi, Q^2, t)}{\beta} \frac{d\hat{\sigma}_{gg\to gg}}{dp_T^2}$$

2. Test QCD factorization by comparing
   (a) $F_{jj}^D(\beta, \xi, Q^2, t)$ between $\sqrt{s} = 630$ and 1800GeV
   (b) $F_{jj}^D(\beta, \xi, Q^2, t)$ with expectation from the measurements of diffractive DIS at HERA

3. Test Regge factorization

$$F_{jj}^D(\beta, \xi, Q^2, t) \stackrel{?}{=} f_{I\!P/p}(\xi, t)\, F_{jj}^{I\!P}(\beta, Q^2)$$

$$x_{\bar{p}} = p_{g,q}/p_{\bar{p}}, \qquad x_p = p_{g,q}/p_p$$

$$\xi = 1 - x_F = p_{I\!P}/p_{\bar{p}}, \quad \beta = p_{g,q}/p_{I\!P}$$

Diffractive Dijet and Inclusive Events (630 GeV)

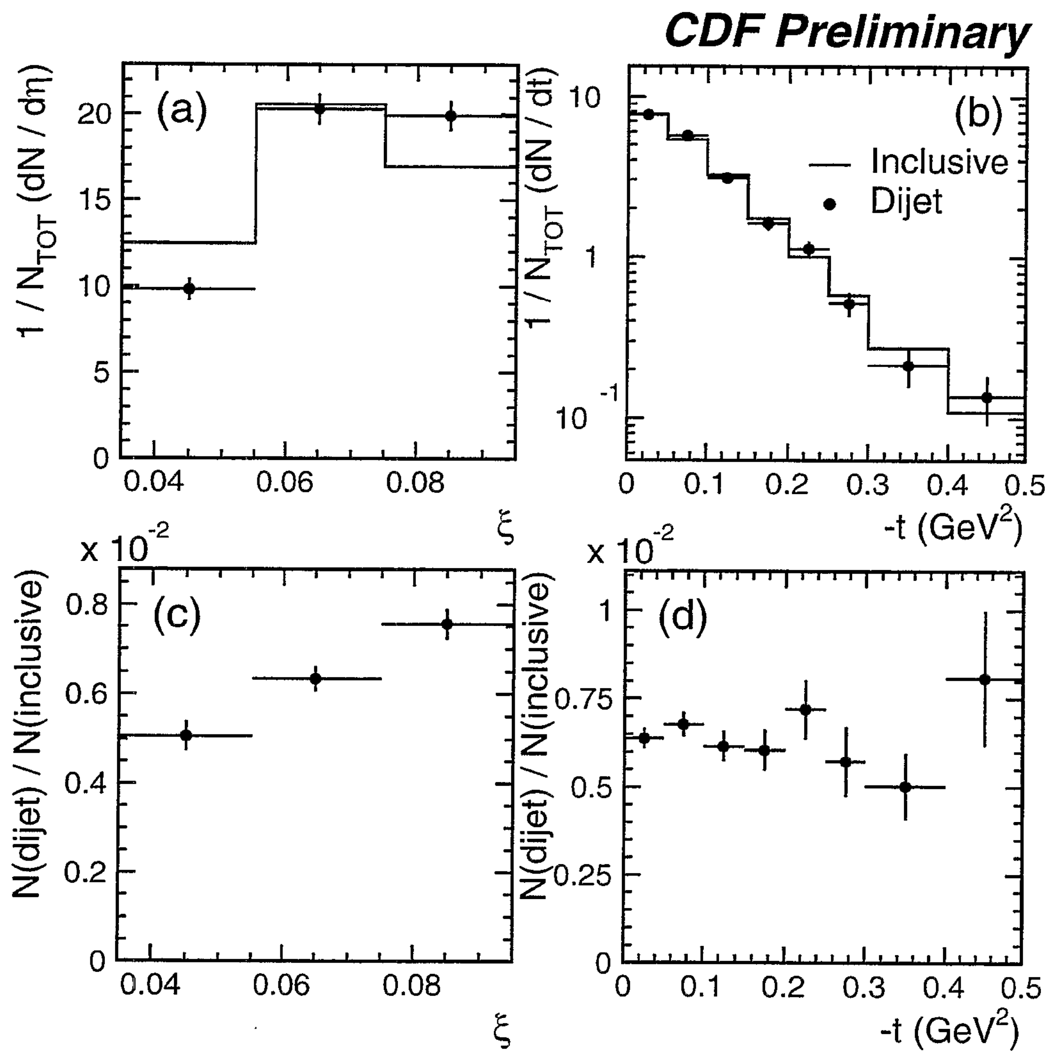

- Diffractive dijet events favor larger ξ values
- The ratio of dijet to inclusive events has a flat t-dependence

Consistent with 1800 GeV results

Diffractive Structure $F_{jj}^D(\beta)$: 630 vs. 1800 GeV

$$F_{jj}^D(x_{\bar{p}}, \xi) = R_{\frac{SD}{ND}}(x_{\bar{p}}, \xi) \times F_{jj}(x_{\bar{p}})$$

$$F_{jj}^D(x_{\bar{p}}, \xi) \longrightarrow F_{jj}^D(\beta, \xi)$$

$$(\beta = x_{\bar{p}}/\xi)$$

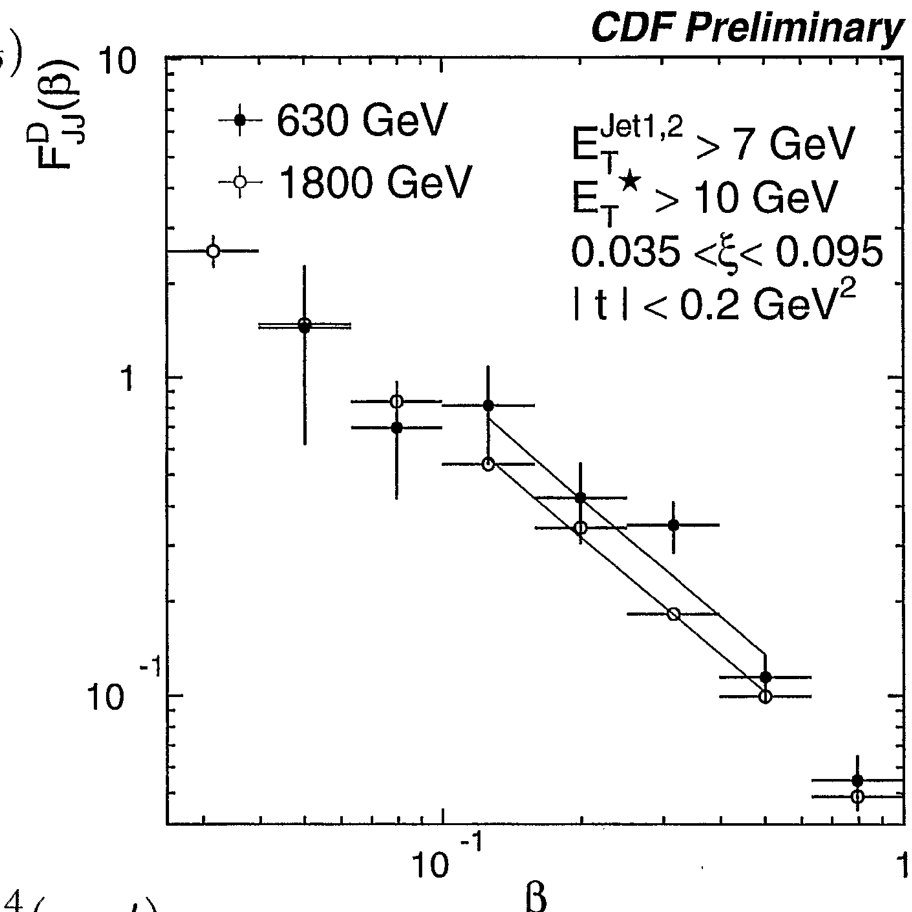

Distributions are fitted to

$$F_{jj}^D(\beta) = B \times (\beta/0.3)^{-n}$$
$$(0.1 < \beta < 0.5)$$

with a common "n" value

$$R_B[\frac{630}{1800}] = 1.3 \pm 0.2(stat)^{+0.4}_{-0.3}(syst)$$

Diffractive Structure $F_{jj}^D(\beta,\xi)$: (1800 GeV)

$$F_{jj}^D(\beta,\xi) = C \times \beta^{-n(\xi)}$$
$$\langle n \rangle = 1.04 \pm 0.01(stat)$$

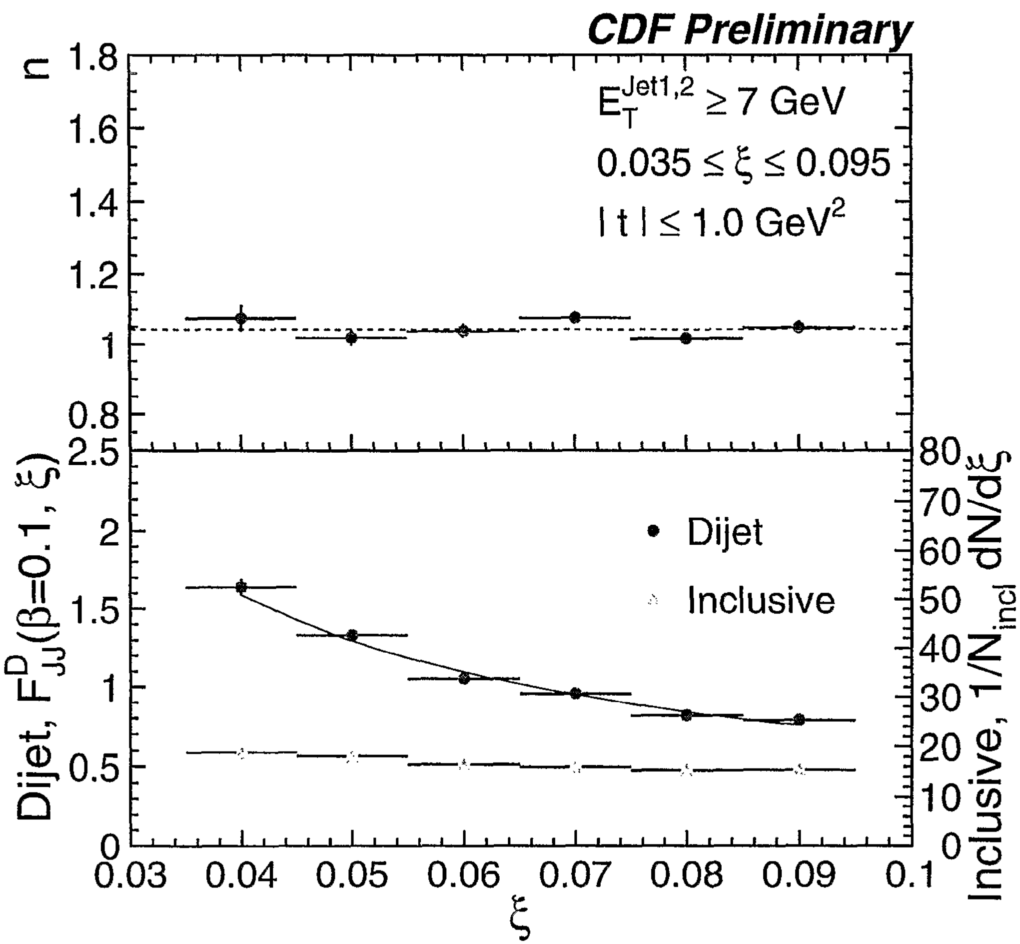

$$F_{jj}^D(\beta,\xi) \propto 1/\xi^m$$
$$m = 0.92 \pm 0.02(stat)$$
$$(\text{at } \beta = 0.1)$$

ξ, β-factorization :

$$F_{jj}^D(\beta,\xi) = C \cdot \frac{1}{\beta^n} \cdot \frac{1}{\xi^m} \qquad (10^{-3}/\xi < \beta < 0.5 \text{ and } 0.035 < \xi < 0.095)$$

Comparison with UA8 (630 GeV)

UA8 has more events at low-ξ than CDF due to different Roman Pot acceptance

$\Rightarrow$ Weight events in CDF data so that the ξ distribution becomes similar to that of UA8

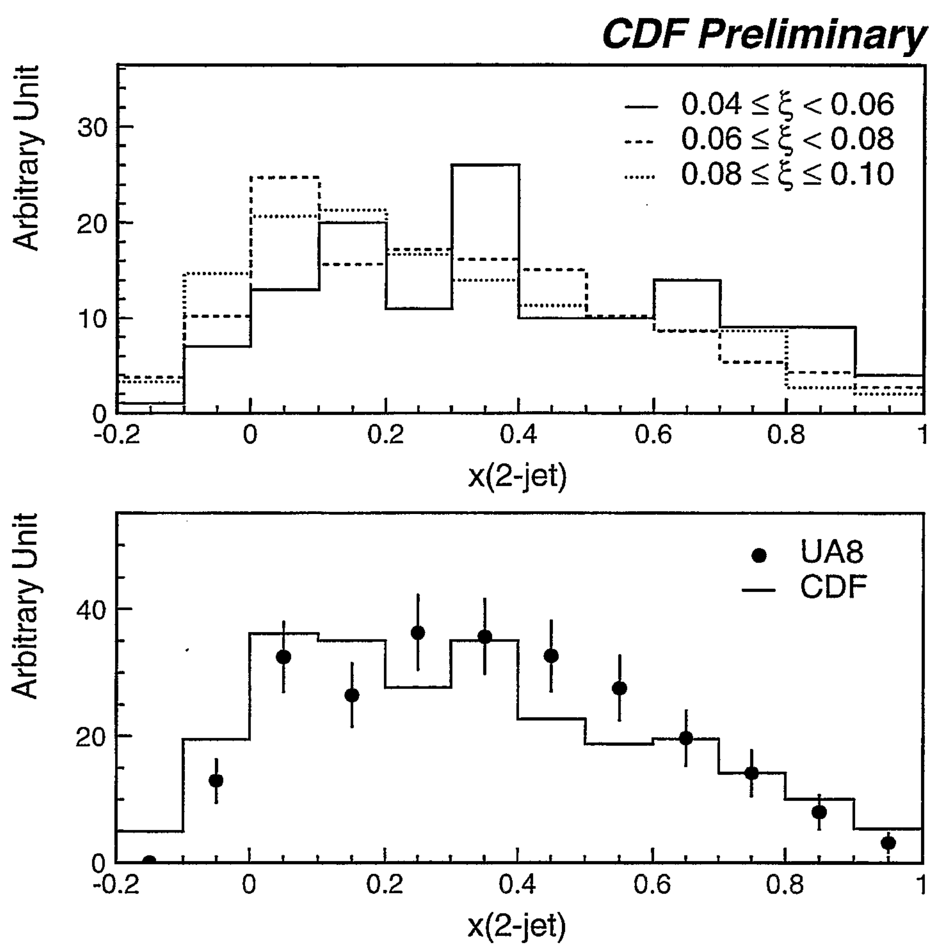

Diffractive J/ψ production at CDF

Andrei Solodsky

Rockefeller University, New York, New York 10021

(for the CDF Collaboration)

Abstract

We report the first observation of diffractive $J/\psi(\rightarrow \mu^+\mu^-)$ production in $\bar{p}p$ collisions at $\sqrt{s}$=1.8 TeV. Diffractive events are identified by their rapidity gap signature. In a sample of events with two muons of transverse momentum $p_T^\mu > 2$ GeV/c within the pseudorapidity region $|\eta|$ <1.0, the ratio of diffractive to total J/ψ production rates is found to be $R_{J/\psi} = [1.45 \pm 0.25]\%$. The ratio $R_{J/\psi}(x)$ is presented as a function of x-Bjorken. By combining it with our previously measured corresponding ratio $R_{jj}(x)$ for diffractive dijet production we extract a value of 0.59 ± 0.15 for the gluon fraction of the (anti)proton diffractive structure function.

Diffractive J/ψ Production in $\bar{p}p$ Collisions

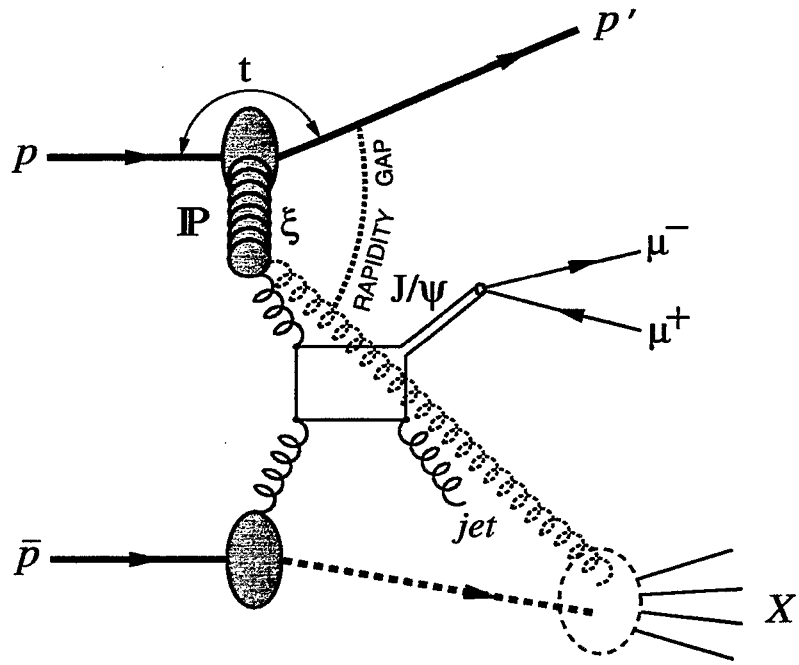

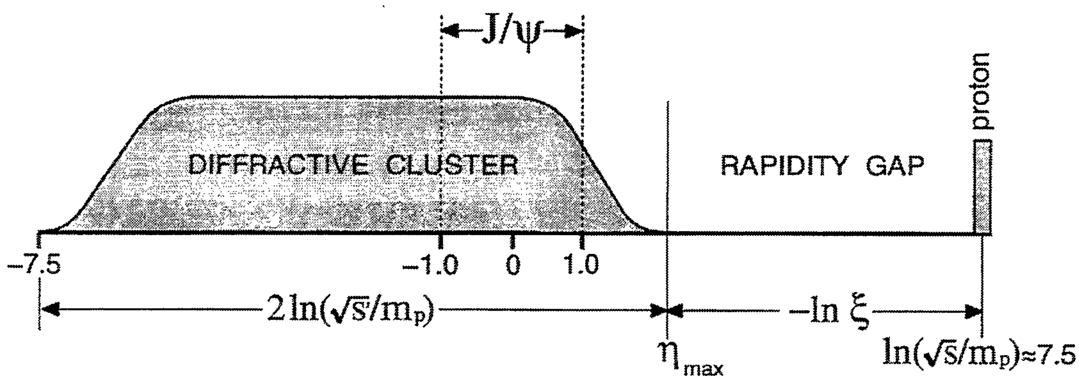

- J/ψ mesons are mostly produced through gg fusion
- *Diffractive* J/ψ production provides measurement of gluonic content of the Pomeron
- Challenging test for the phenomenological models describing J/ψ *anomaly* and diffractive production

Diffractive Event Signal in Dimuon Sample

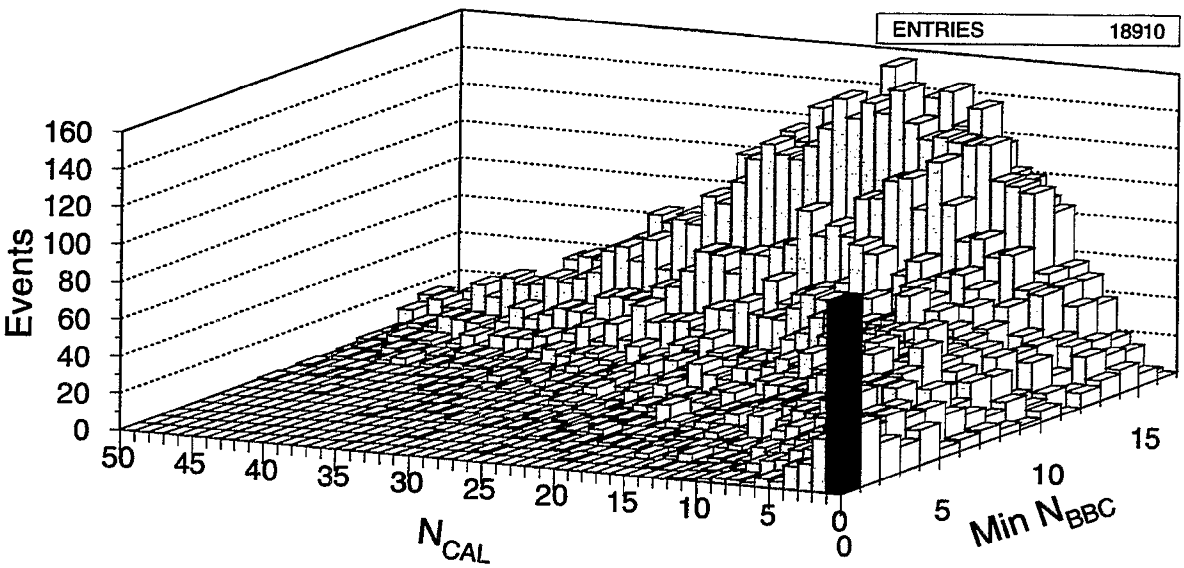

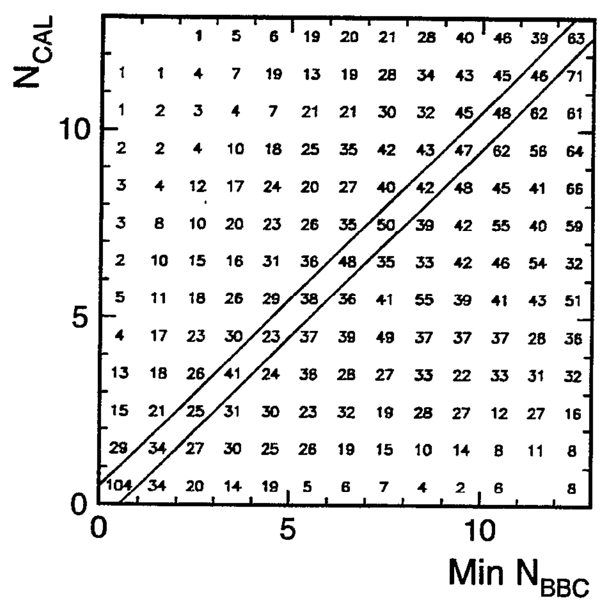

Rapidity gap definition

- No energy above noise in the forward calorimeters
- No hit in the BBC on the *side of calorimeter gap*

Fraction of Diffractive J/ψ Events

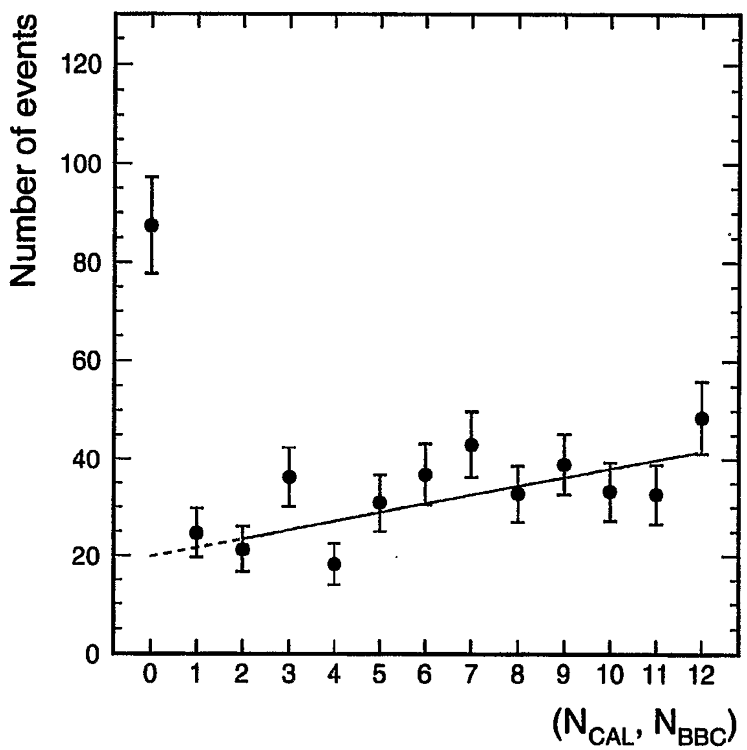

$$R_{J/\psi} \times \mathcal{A}_{\text{gap}} = \frac{N^{\text{SD}}_{J/\psi}}{N^{\text{ND}}_{J/\psi}} \times \frac{\varepsilon^{\text{ND}}_{\text{1vtx}}}{\varepsilon^{\text{SD}}_{\text{1vtx}}} \times \frac{1}{\varepsilon_{\text{Live}}} =$$

$$\frac{67.5 \pm 10.4}{13339 \pm 128} \times \frac{0.57 \pm 0.04}{0.86} \times \frac{1}{0.80 \pm 0.03}$$

$$\boxed{R_{J/\psi} \times \mathcal{A}_{\text{gap}} = (0.42 \pm 0.07)\%}$$

$$N^{\text{SD}}_{(0,0)} = N_{(0,0)} - N^{\text{ND}}_{(0,0)} = (87.4 \pm 9.7) - (19.9 \pm 3.9) = 67.5 \pm 10.4$$

$\mathcal{A}_{\text{gap}}$ is defined as the fraction of single-diffractive interactions having a rapidity gap in the region of $2.4 \leq |\eta| \leq 5.9$.

$R_{J/\psi}\left[\frac{SD}{ND}\right]$ as a Function of Bjorken-X

From the detected jet, we calculate:

$$X_{\mathrm{bj}} = p_{g,q}/p_{p(\bar{p})} = \frac{p_T^{J/\psi} \cdot e^{-\eta_{J/\psi}} + E_T^{jet} \cdot e^{-\eta_{jet}}}{2 \cdot p_0^{p(\bar{p})}}$$

$$\simeq \frac{p_T^{J/\psi}(e^{-\eta_{J/\psi}} + e^{-\eta_{jet}})}{\sqrt{s}}$$

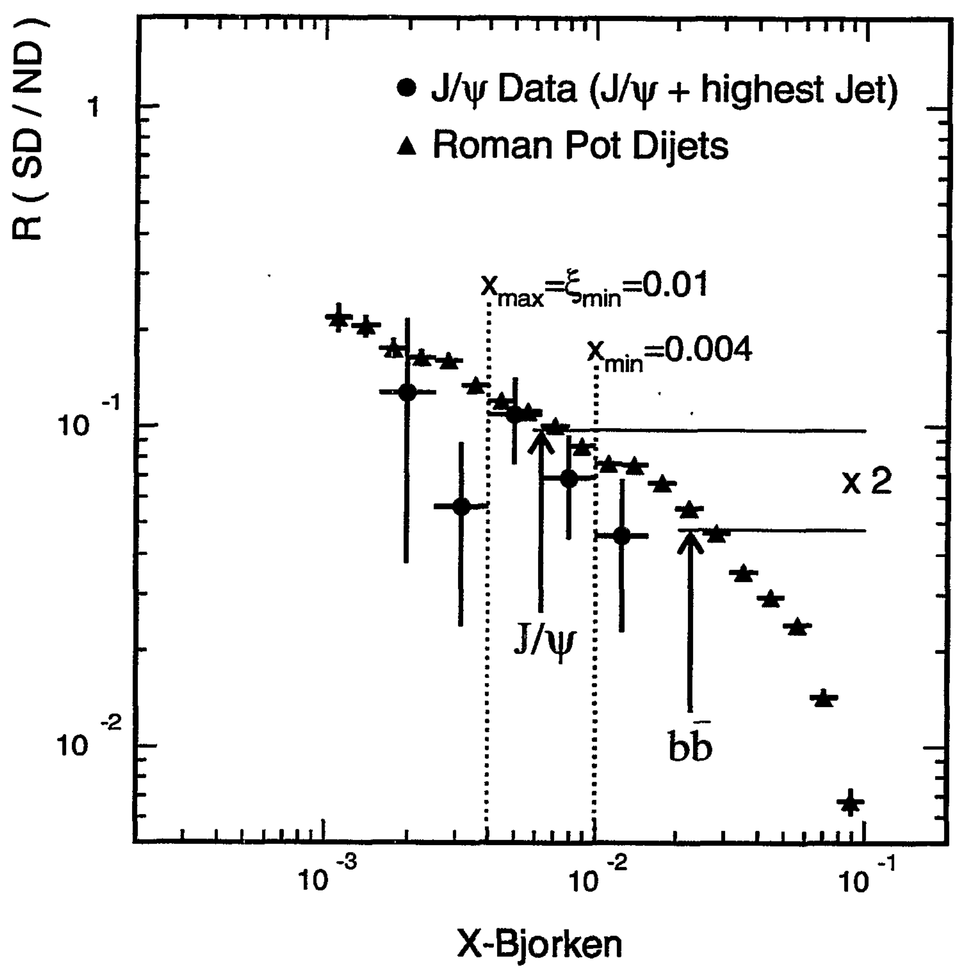

Gluon Content of Pomeron

Ratio of diffr. to non-diffr. dijet production

$$R_{JJ}(x) = \frac{F^D_{JJ}(x)}{F_{JJ}(x)} = \frac{g^D(x)+\frac{4}{9}q^D(x)}{g(x)+\frac{4}{9}q(x)} = \frac{g^D(x)}{g(x)} \times \frac{1+\frac{4}{9}\frac{q^D(x)}{g^D(x)}}{1+\frac{4}{9}\frac{q(x)}{g(x)}}$$

Since

$$R_{J/\psi}(x) = \frac{g^D(x)}{g(x)} \quad \Rightarrow \quad \frac{R_{JJ}(x)}{R_{J/\psi}(x)} = \frac{1+\frac{4}{9}\frac{q^D(x)}{g^D(x)}}{1+\frac{4}{9}\frac{q(x)}{g(x)}}$$

$$\left.\frac{R_{JJ}}{R_{J/\psi}}\right|_{\mathrm{exp}} = 1.17 \pm 0.27(\mathrm{stat}) \quad @\ \bar{x} = 0.0063, \bar{Q} = 6\ \mathrm{GeV}/c$$

From the proton PDF-set GRV94 LO

$$\frac{q(x)}{g(x)} = 0.274 \quad @ \quad x = 0.0063, Q = 6\ \mathrm{GeV}/c$$

- Gluon fraction @ $\bar{x} = 0.0063$ and $\bar{Q} = 6$ GeV$/c$

$$\boxed{f_g^D = 0.59 \pm 0.14(\mathrm{stat}) \pm 0.06(\mathrm{syst})}$$

- From diff. W, $b\bar{b}$ and dijet production

$$\boxed{f_g^D = 0.54^{+0.16}_{-0.14}}$$

MATCHING of SOFT and HARD P O M E R O N S

E. Levin,*

School of Physics, Tel Aviv University, Tel Aviv, 69978, ISRAEL

May 24, 2001

Authors: S. Bondarenko, D. Kharzeev , Yu. Kovchegov, E. Levin and Chung-I Tan.

The main goal: We want to find out how large the contribution of the non-perturbative QCD to the parameters of the phenomenologivcal "soft' Pomeron (Donnachie-Landshoff Pomeron): $\Delta_P = 0.08 \div 0.1$ and $\alpha'_P = 0.25\,GeV^{-2}$.

Key idea: "Soft" Pomeron $\longrightarrow$ nonperturbative QCD but at sufficiently short distances

$$r_\perp(Pomeron) = 1/M_0 \gg r_\perp(separation) \gg 1/\Lambda$$

The results:

- The high energy asymptotic is due to exchange of the resulting Pomeron - Regge pole with the intercept close to 1;
- The pQCD contribution to the resulting Pomeron is essential;
- pQCD leads to
  - Considerable increase of the soft Pomeron intercept: $\Delta_{SH} \approx 3\,\Delta_S$;
  - Decrease of the slope of the soft Pomeron trajectory $\alpha'_{SH} \approx \frac{1}{2}\,\alpha'_S$;
- The result crucially depends on the value of the intercept for the soft Pomeron Δ_S;
- The result is sensitive to our assumption on the values of scales: the nonperturbative scale of the soft Pomeron and the separation scale for the hard (BFKL) Pomeron;

*e-mail: leving@post.tau.ac.il

MATCHING of SOFT and HARD POMERONS

May 30, 2001

Scales of QCD

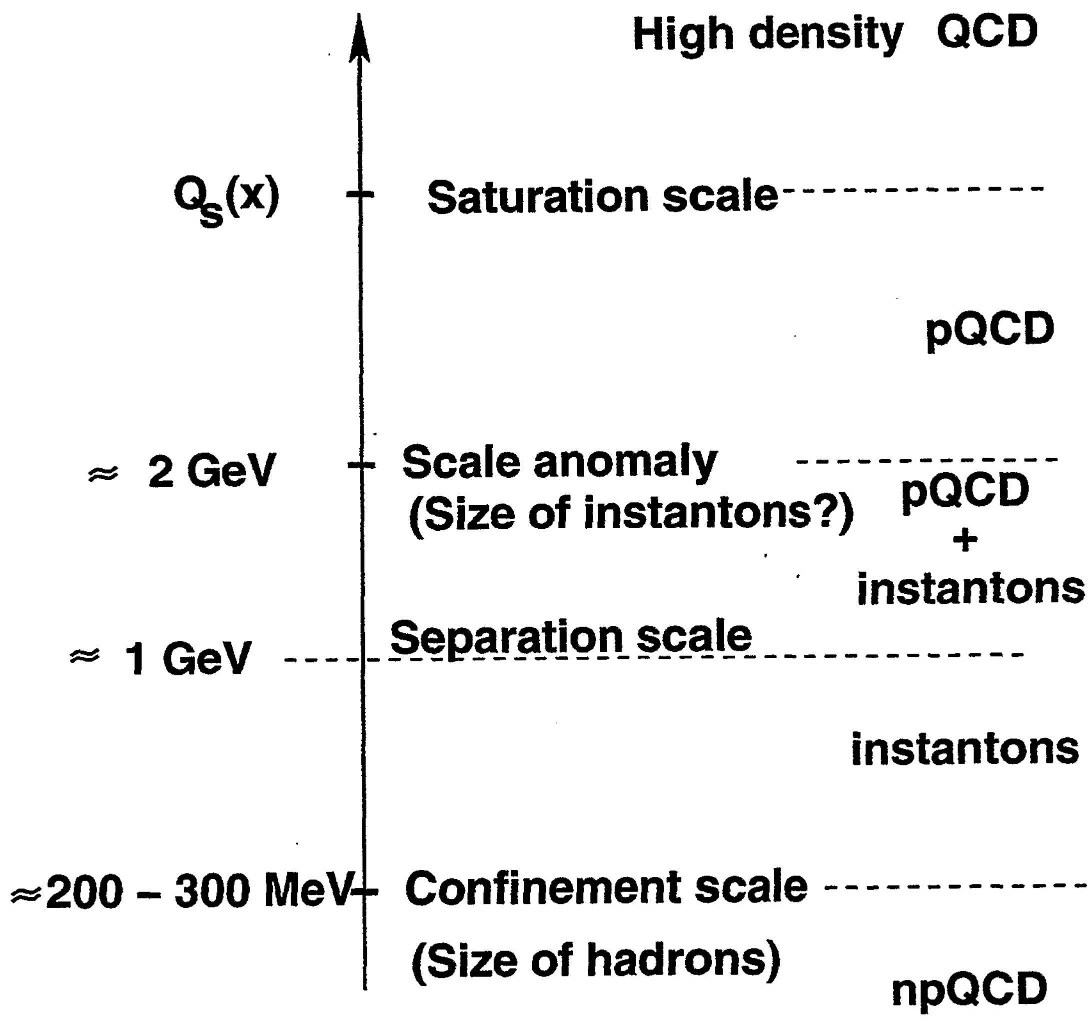

• • Hard Pomeron $\equiv$ BFKL Pomeron in NLO + running α_S • •

- The NLO BFKL kernel: $K_{BFKL}(q^2, q'^2) = \alpha_S(r)$ $K(r - r')$ where $r = ln(q^2/\Lambda^2)$ and $r' = ln(q'^2/\Lambda^2)$

- The Mellin image of $K(r - r')$ $K(f)$ has a form: $K(f) \;=\; \Delta_H(\alpha_S) \;+\; D(\alpha_S)\,(\,f - \frac{1}{2}\,)^2$

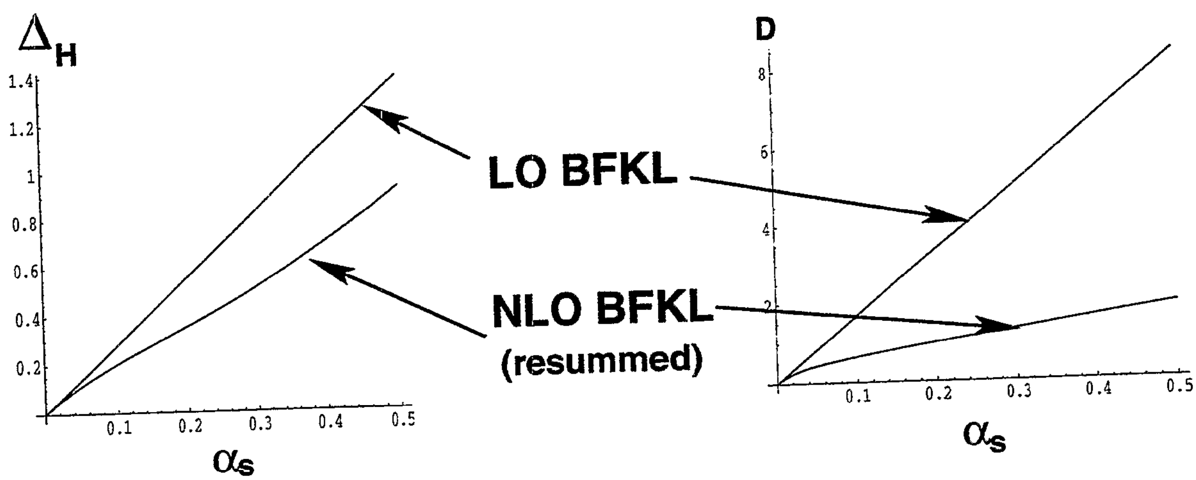

Soft Pomeron

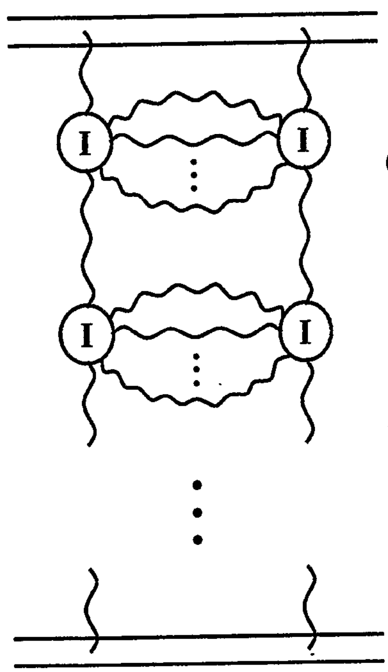

Our approach:

- $K(q^2, q'^2) =$

  $\Delta_S\, \phi(q^2)\, \phi(q'^2)$;

- $\phi(q^2) = e^{-q^2/q_0^2}$;

- $q_0^2 = M_0^2 = 4\ \mathrm{GeV}^2$;

- $K(q^2, q'^2) = \Delta_S \phi(q^2)\, \phi(q'^2) \longrightarrow s^{\Delta_S}$;

- $K(q^2, q'^2) = \Delta_S \phi(q^2)\, \phi(q'^2) \longrightarrow$ **diffusion in impact parameters** (b_t) ;

- $K(q^2, q'^2) = \Delta_S \phi(q^2)\, \phi(q'^2) \longrightarrow R = \alpha'_P \ln s$ where R is the radius of interaction ;

- $K(q^2, q'^2) = \Delta_S \phi(q^2)\, \phi(q'^2) \longrightarrow \alpha'_P \propto 1/q_0^2$;

Soft & Hard Pomerons

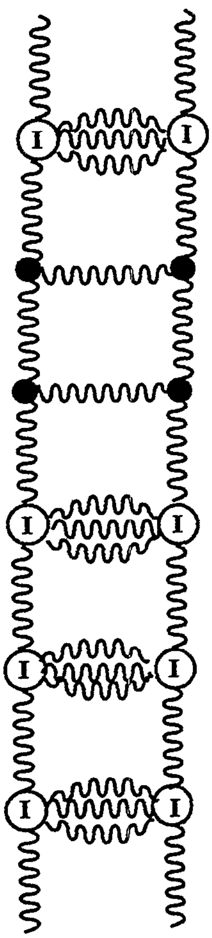

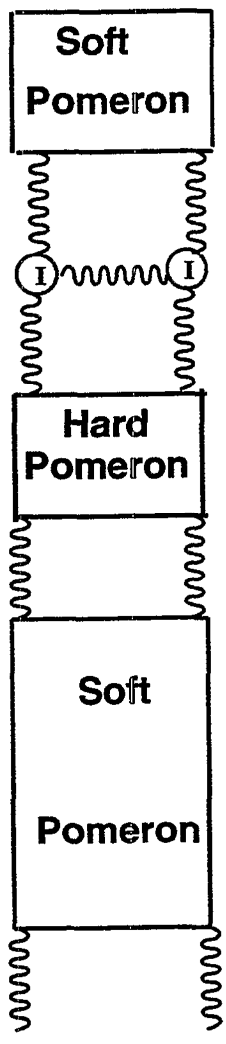

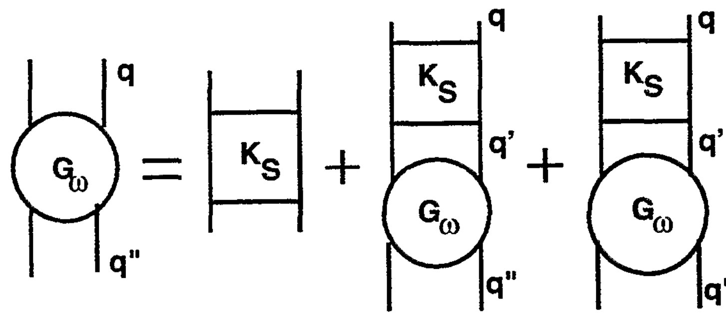

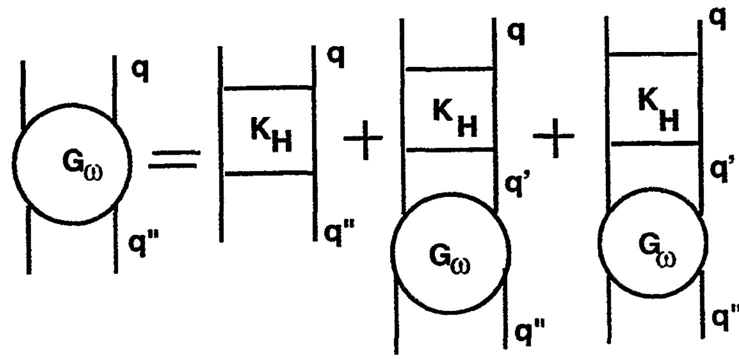

Solution to the two channel problem

$$\Delta_{SH} - \Delta_S = 4\,\Delta_S^2\,\sqrt{r_S/4D\pi\omega}\,\left(\frac{4\omega}{D\,r_H}\right)^{\frac{1}{6}}$$

$F\left(\left(\frac{4\omega}{D\,r_H}\right)^{\frac{1}{6}} \cdot \left(r_S - r_H\frac{\Delta_H}{\omega}\right)\right)$ where $r_S = log(\frac{1}{r^2_{ScaleAnomaly}\Lambda}$

$_H = log(\frac{1}{r^2_{separation}\Lambda^2})$; and $F(z) = \int_0^\infty \frac{dt}{\sqrt{t}}\,\exp(-zt - \frac{t^3}{3})$.

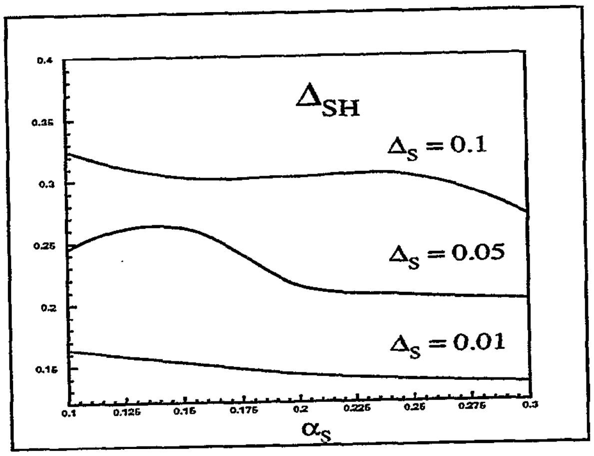

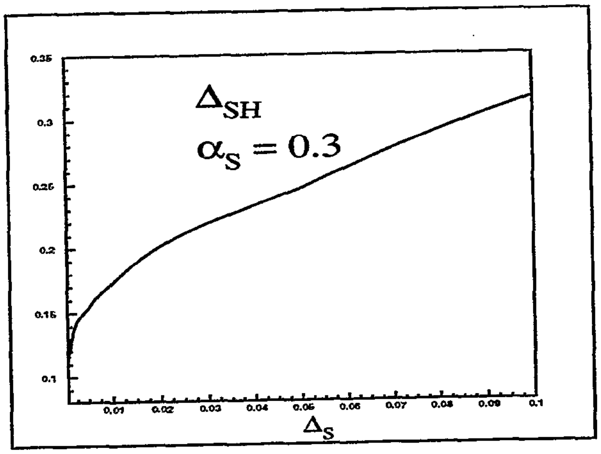

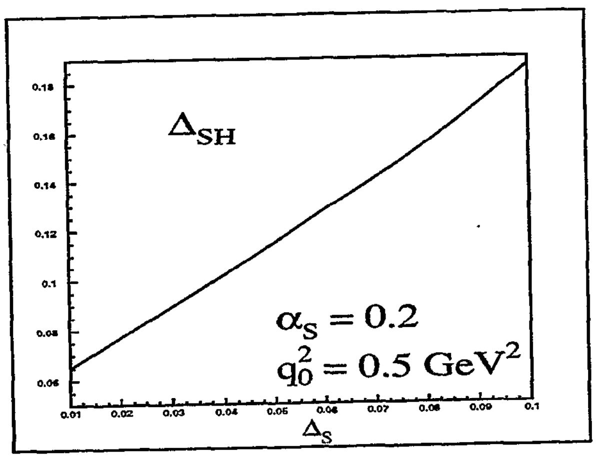

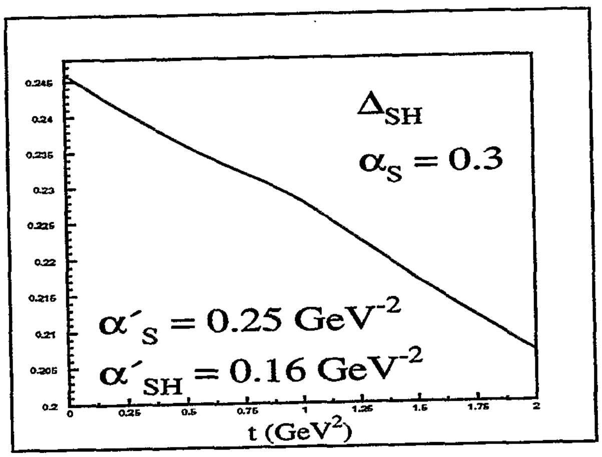

Semihard Component of the Soft $\mathbb{P}$omeron

B. Kopeliovich (MPI Heidelbe

in collaboration with

I. Potashnikova
B. Povh
E. Predazzi

Phys. Rev. Lett. 85(2000)50;
Phys. Rev. D63(2001)05400

Outline

- Large mass diffraction $\Rightarrow$
- Two - scale structure of hadrons $\Rightarrow$
- a specific form of energy dependent $\sigma_{tot}(s) \Rightarrow$
- Phenomenology and elastic data in the impac parameter representation

149

Why large mass diffraction is suppressed?

Why the triple-$\mathbb{P}$omeron coupling is so smal

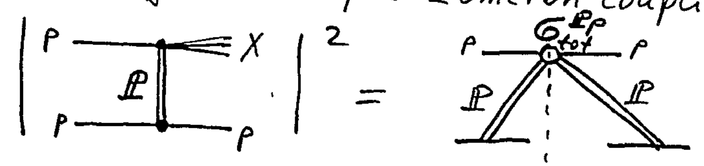

$\sigma^{\mathbb{P}p}_{tot} = ?$ (50 mb ?) $\qquad \sigma^{\mathbb{P}p}_{tot} \simeq 2\,\text{mb}$

$\sigma_{GG} \approx \frac{9}{4}\,\sigma_{q\bar{q}}$

To explain this one has to assume that the $\mathbb{P}$omeron has a small size $r_{\mathbb{P}}$.

Why diffractive gluon bremsstrahlun is suppressed?

Only gluon radiation can provede the large mass behavior $\frac{d\sigma_{dd}}{dM^2} \propto \frac{1}{M^2}$

Excitation of the quark system leads to $\frac{d\sigma}{dM^2} \propto \frac{1}{M^3}$

It is easy to disentangle between these two experimen

Diffractive radiation by a quark

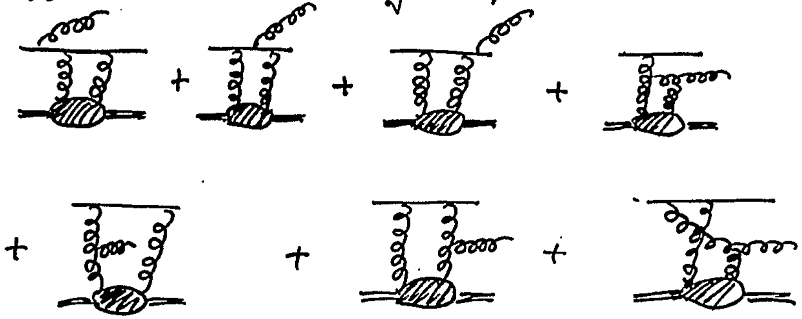

Take a simple form in impact parameter representation at $\alpha_G \ll 1$

$$M^2 \frac{d\sigma(qN \to qGN)}{dM^2 dk_T^2}\Big|_{k_T=0} = \frac{1}{16\pi}\int d^2r_T \left|\Psi_{qG}(\alpha, r_T)\tilde{\sigma}(\rho,\tilde{s})\right|^2$$

B.K.
A. Schäfer
A. Tarasov
Phys. Rev. D62(2000)0541

$\tilde{\sigma}(r_T) = \frac{9}{8}\,\sigma^N_{q\bar{q}}(r_T)$

$\tilde{s} = s\,M_0^2/M^2$

pQCD calculations (with regularized $\alpha_s(Q^2)$ at small Q^2) overestimate the diffractive cross section by an order of magnitude.

$$\sigma(qN \to qGN) \propto \langle r^4_{qG} \rangle$$

In the strong quark-gluon interaction regime

$$\Psi_{qG}(\vec{r}_T, \alpha_G)\Big|_{\alpha_G \ll 1} = -\frac{2i}{\pi}\sqrt{\frac{\alpha_s}{3}}\;\frac{\vec{e}^{\,*}\vec{r}_T}{r_T^2}\;e^{-r_T^2/2r_0^2}$$

The data can be explained if $r_0 = 0.3$ fm

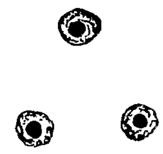

proton

Two sizes in light hadrons:

the quark separation $R_q \gg r_0$

E. Shuryak
V. Braun et al.
A. Di Giacomo et al.

The small size of the gluon clouds makes it diffiqult to shake them off, either diffractively ($\propto r_0^4$) or nondiffractively ($\propto r_0^2$)

What happens if $r_0 \to 0$?

- no gluon radiation is possible, however the inelastic cross section doesn't vanish

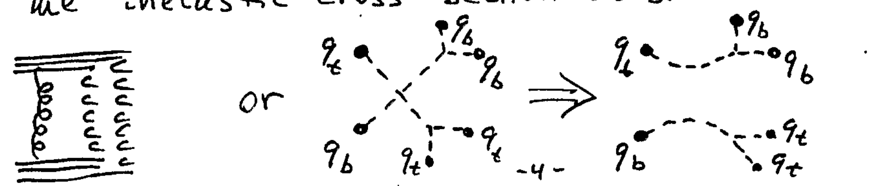

Since gluon radiation is the only source of energy dependence, in this limit of $r_0 \to 0$

$$\sigma_{tot} = \text{const} = \sigma_0$$

if $r_0 \neq 0$, but small

$$\sigma_{tot}(s) = \sigma_0 + r_0^2 f(s) \;\cancel{\Longrightarrow}\; r_0^2 \left(\frac{s}{s_0}\right)^{\varepsilon} \text{ vanishes at } r_0 \to 0$$

$$\Longrightarrow \tilde{\sigma}_0 + r_0^2 \cdot K \cdot \left(\frac{s}{s_0}\right)^{\Delta}$$

$$\Delta = \frac{4\alpha_s}{3\pi} \approx 0.17$$

$$K = 3\frac{9}{4} C \approx 16.2$$

Only one parameter $\tilde{\sigma}_0$ which cannot be evaluated perturbatively.

It needs just one experimental point for σ_{tot} to fix this parameter

Unitarization:

$$\mathrm{Im}\,\Gamma_{P}(b,s) = \frac{1}{D(s)}\left[1 - e^{-D(s)\,\mathrm{Im}\,\gamma_{P}(b,s)}\right]$$

Here

$$\gamma_{P}(b,s) = \sum_{n=0} \gamma_n(b,s)$$

$$D(s) = 1 + \frac{\sigma_{sd}^{pp}(s)}{\sigma_{el}^{pp}(s)}$$

We have only one free parameter $\tilde{\sigma}_0^{pp}$ which we fix adjusting σ_{tot}^{pp} at $\sqrt{s} = 546$ GeV

Then we are in position to predict the energy dependence and the slope of elastic scattering

$$\sigma_{tot}^{pp} = 2\int d^2b\; \mathrm{Im}\,\Gamma(b,s)$$

$$B_{el}^{pp} = \frac{1}{2}\langle b^2\rangle = \frac{1}{\sigma_{tot}}\int d^2b\; b^2\, \mathrm{Im}\,\Gamma(b,s)$$

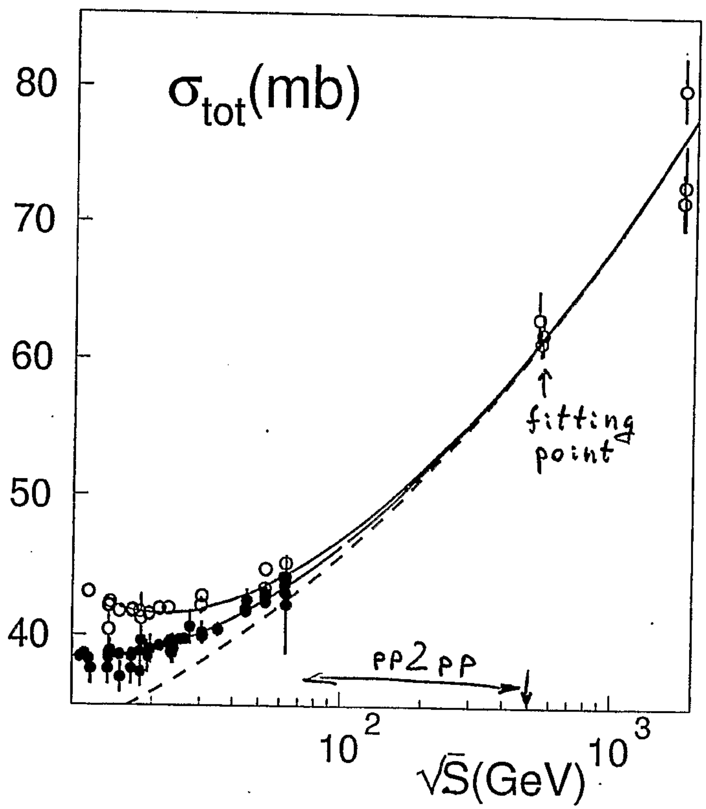

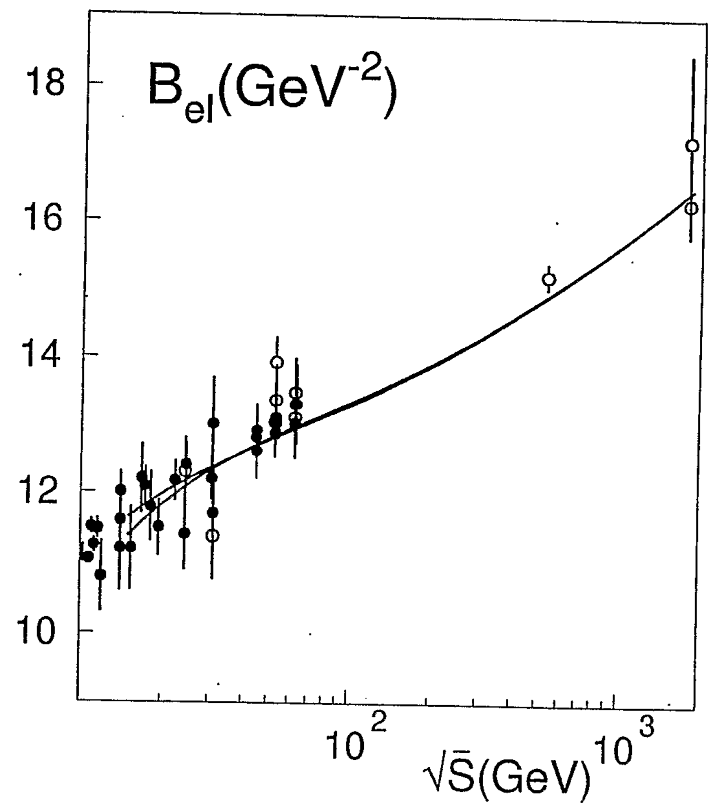

Fully predicted

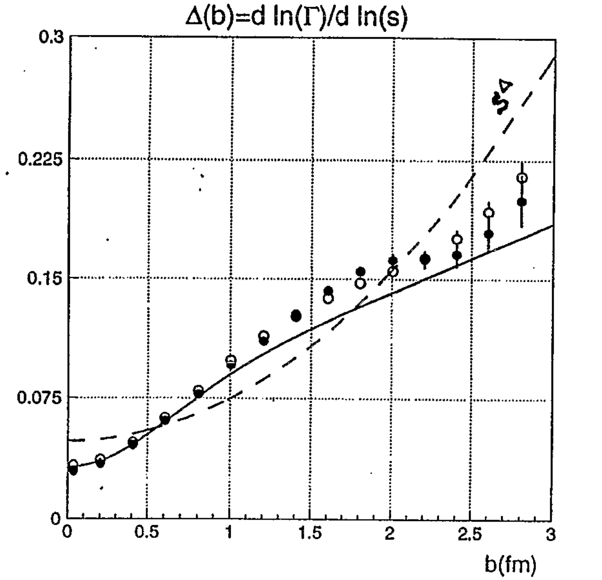

Figure 9: *The exponent $\Delta(b)$ found by the fit to the point in Fig. 8 with power dependence on energy at each value of b. The black and open points correspond to the fits with parameterizations I and II respectively.*

The Pomeron trajectory in the impact parameter

How to get rid of the absorptive/unitarity corrections?

AGK cutting rules for inclusive cross sections
$\Longrightarrow$ Mueller theorem

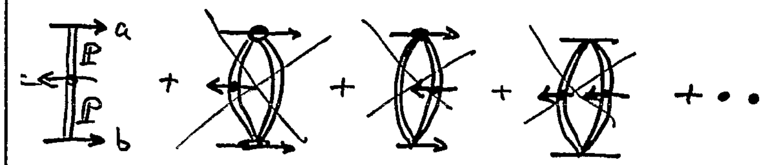

$$-2 \qquad -2 \qquad +2\times 2\cdot\frac{1}{2!}$$

The energy dependence of the inclusive cross section is given by the bare Pomeron, no unitarization is needed.

Fit to available data by

$$\frac{d\sigma(ab\to cX)}{dy} = \sigma_0 + \sigma_1\left(\frac{s}{s_0}\right)^{\Delta}$$

A. Likhoded et al
Phys. Lett. B215(1988)417
Int. J. Mod. Phys. A6(1991)913

- Both terms are demanded by the fit
- $\Delta = 0.17$!

Summary

- High mass diffraction is extremely sensitive to the size of the gluon clouds of valence quarks and fixes it at $r_0 \approx 0.3$ fm
- In the case of $r_0^2 \ll R_h^2$ the cross section consists of two terms
  $$\sigma_{tot}(s) = \sigma_0(R_h) + \sigma_1(s, r_0)$$
  with $\sigma_1(s, r_0) \propto r_0^2$ and $\sigma_0(R_h)$ independent of s,
- There is only one unknown parameter in the model σ_0.
  $\sigma_1(s, r_0) \propto r_0^2 (s/s_0)^{0.17}$ is calculated
- available elastic scattering data translated to the impact parameters are well reproduced
- The forthcoming data from the pp2pp experiment are expected to have a sufficient precision to disentangle between $\sigma_{tot} \propto (s/s_0)^{\Delta}$ and $\sigma_{tot} = \sigma_0 + \sigma_1 (s/s_0)$

The CKMT approach to the Pomeron puzzle*

Elena G. Ferreiro and Carlos Merino

Departamento de Física de Partículas

Universidade de Santiago de Compostela

15706 Santiago de Compostela

Galicia-Spain

The CKMT model for the parametrization of the nucleon structue function F_2 is a model based on Regge theory which phenomenologically takes into account the Regge cuts and the decrease of their contribution with Q^2, and which describes the experimental data on F_2 in the region of low Q^2.

An explicit theoretical model which leads to the above pattern of energy behavior, now confirmed by a simoultaneous description of diffractive production by real and virtual photons, is also presented.

The CKMT model taken as an initial condition for the NLO evolution equations in perturbative QCD, provides a good description of the experimental data of F_2 in the whole available kinematical region of x and Q^2, in particular when these data are presented in the form of the logarithmic slopes.

*High Energy QCD: Beyond the Pomeron Workshop, BNL (NY), May 21-25, 2001.

THE CKMT MODEL PLB 337 (1994) 358

→ WE PROPOSE THE FOLLOWING PARAMETRIZATION OF THE STRUCTURE FUNCTIONS OF THE NUCLEONS AT MODERATE Q^2:

$$\boxed{\begin{aligned} F_2(x,Q^2) &= A\cdot\left(\frac{Q^2}{Q^2+a}\right)^{1+\Delta(Q^2)} \cdot \underbrace{x^{-\Delta(Q^2)}\cdot(1-x)^{n(Q^2)+4}}_{\text{SEA QUARKS}} \\ &+ B\left(\frac{Q^2}{Q^2+b}\right)^{\alpha_R(0)} \cdot \underbrace{x^{1-\alpha_R(0)}\cdot(1-x)^{n(Q^2)}}_{\text{VALENCE QUARKS}} \end{aligned}}$$

WHERE

$$\longrightarrow \Delta(Q^2) = \Delta(0)\left[1+\frac{2\cdot Q^2}{Q^2+d}\right] \longrightarrow \begin{cases} \Delta(0) \simeq 0.07 \div 0.08 \\ \Delta(\infty) \simeq 0.21 \div 0.24 \end{cases}$$

→ THE BEHAVIOUR AT $x \longrightarrow 1$ IS GIVEN BY THE FACTORS $(1-x)$ WITH

$$n(Q^2) = \frac{3}{2}\left[1+\frac{Q^2}{Q^2+c}\right] \longrightarrow \begin{cases} \text{SMALL } Q^2:\ n \sim 1.5 \\ \quad \text{DPM BEHAVIOUR} \\ \text{LARGE } Q^2:\ n \sim 3 \\ \quad \text{DIMENSIONAL COUNTING RULES} \end{cases}$$

→ THE SEPARATE CONTRIBUTION OF THE u AND d VALENCE QUARKS IS GIVEN BY

$$B\cdot(1-x)^{n(Q^2)} = B_u\cdot(1-x)^{n(Q^2)} + B_d\cdot(1-x)^{n(Q^2)+1}$$

WHERE B_u, B_d ARE FIXED BY THE NORMALIZATION CONDITION FOR VALENCE QUARKS.

→ THE SECOND FACTOR IN THE TWO TERMS ACCOUNTS FOR THE CONNECTION WITH REAL PHOTONS.

CKMT → A. CAPELLA, A.B. KAIDALOV, C.M. AND J. TRAN THANH VAN

A.B. KAIDALOV, C. MERINO AND D. PERTERMANN

WE COMPUTE F_2 AND ITS DERIVATIVES

hep-ph/0004237
EUR. PHYS. J. C

$$\frac{dF_2}{d\ln Q^2} \quad \text{AND} \quad \frac{d\ln F_2}{d\ln(1/x)}$$

BY USING THE CKMT MODEL:

- $0 < Q^2 \leq Q_0^2 \quad (\text{e.g., } Q_0^2 = 2.\ \text{GeV}^2)$

  CKMT MODEL WITHOUT PERTURBATIVE EVOLUTION

- $Q_0^2 < Q^2 \leq$ CHARM THRESHOLD

  NLO $(\overline{MS})$ EVOLUTION OF THE F_2 CKMT PARAMETRIZAT. WITH $n_f = 3$.

  $u, d, s \longrightarrow pdf$

- CHARM THRESHOLD $< Q^2 < \infty$

  NLO $(\overline{MS})$ EVOLUTION OF THE F_2 CKMT PARAMETRIZAT. WITH $n_f = 4$.

  $u, d, s, c \longrightarrow pdf$

***DIFFRACTIVE DISSOCIATION**

THE CKMT MODEL USES REGGE FACTORIZATION

PROTON STRUCTURE FUNCTION

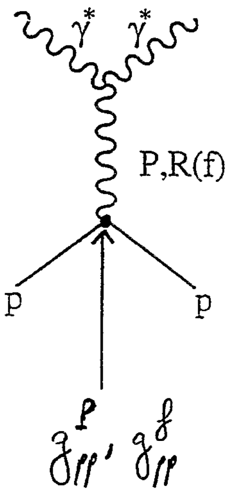

POMERON STRUCTURE FUNCTION

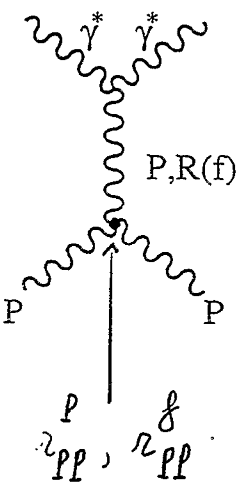

TRIPLE REGGE VERTICES

$$F_2^{P}\left(x, Q^2, x_P, t\right) = \underbrace{\frac{\left[g^{P}_{pp}(t)\right]^2}{16\pi} \cdot x_P^{\,1-2\alpha_P(t)}}_{\text{FLUX FACTOR}} \cdot \underbrace{F_P\left(\beta, Q^2, t\right)}_{\text{POMERON STRUCTURE FUNCTION}}$$

⟶ THE POMERON STRUCTURE FUNCTION DEPENDS ON THE CHOICE OF THE FLUX FACTOR (e.g., DONNACHIE & LANDSHOFF FLUX FACTOR DIFFERS FROM OURS BY $2/\pi$)

$\longrightarrow F_P$ CAN BE RELATED TO THE DEUTERON STRUCTURE FUNCTION $F_2^d = \frac{1}{2}\left(F_2^p + F_2^n\right)$.

IN THE CKMT MODEL: PLB 343 (1995) 403
PRD 53 (1996) 2309

$$\boxed{F_P\left(\beta, Q^2\right) = F_2^d\left(\beta, Q^2; A \rightarrow eA, B \rightarrow fB, n \rightarrow n-2\right)}$$

**

IS A PARAMETRIZATION OF F_P VALID IN THE REGION $1 \leq Q^2 \leq 5\ \mathrm{GeV}^2$

WITH

$$\boxed{e = r_{PP}^{P}(0) \Big/ g_{PP}^{P}(0) \quad \text{AND} \quad f = r_{PP}^{f}(0) \Big/ g_{PP}^{f}(0)}$$

THE t DEPENDENCE OF F_P, WHICH IS EXPECTED TO BE VERY SMALL, IS FACTORED OUT

$\rightarrow$ FROM SOFT DIFFRACTION WITH ABSORPTIVE CORRECTIONS

$$\boxed{e \simeq f \simeq 0.07}$$

THE VALUES OF e AND f HAVE SOME UNCERTAINTIES, THE LARGEST BEING IN THE VALUE OF f.

WE USE THIS PARAMETRIZATION OF $F_P\left(\beta, Q^2\right)$ AS INITIAL CONDITION FOR QCD EVOLUTION.

$\longrightarrow$ NUMERICAL CALCULATIONS HAVE BEEN PERFORMED USING THE QCD EVOLUTION PROGRAM OF DEVOTO ET AL., AURENCHE ET AL. AND ENGEL ET AL.

WE PRESENT THE RESULTS IN AN ONE-LOOP APPROXIMATION BUT WE HAVE CHECKED THAT PRACTICALLY THE SAME RESULTS ARE OBTAINED IN TWO LOOPS.

* EXPLICIT MODEL WITH THE CKMT PATTERN OF ENERGY BEHAVIOR:

A. CAPELLA, E. G. FERREIRO, A. B. KAIDALOV AND C. A. SALGADO
hep-ph / 0006233
PRD 63, 054010 (2001)

QUARK-PARTON PICTURE

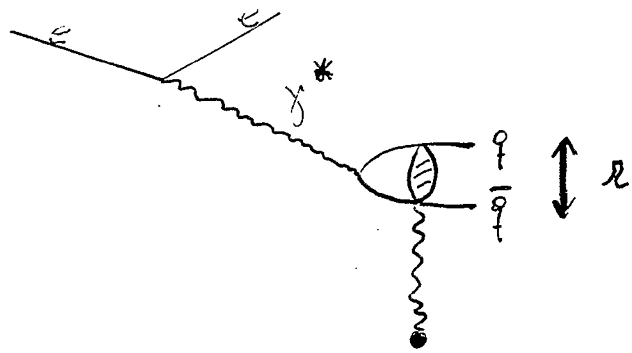

THE VIRTUAL PHOTON γ^* DISSOCIATES INTO A $q\bar{q}$ PAIR OF SIZE r WHICH HAS MULTIPLE INTERACTIONS WITH THE TARGET

• TWO KINDS OF $q\bar{q}$ PAIRS:

• $L \rightarrow$ LARGE SIZE CONFIGURATION

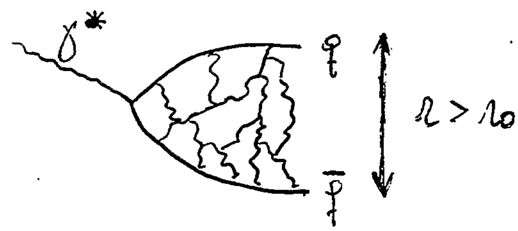

COMPLICATED NON-PERTURBATIVE SYSTEM $\rightarrow$ REGGE PHENOMENOLOGY

• $S \rightarrow$ SMALL SIZE CONFIGURATION

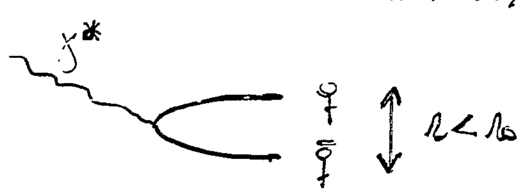

COLOR DIPOLE $\quad \sigma^{(q\bar{q})p} = r^2 \cdot f(s, Q^2) \rightarrow$ PERTURBATIVE QCD APPLICABLE WHEN $r \ll$

$r_0 = 0.2$ fm (FIT IN AGREEMENT WITH THE CORRELATION LENGTH OF NON-PERTURBATIVE INTERACTIONS FROM LATICE CALCULATIONS)

IT USES EIKONAL APPROXIMATION WITH THE STANDARD REGGE FORM FOR THE EIKONALS.

- CORRECT DESCRIPTION OF INELASTIC DIFFRACTION OF BOTH REAL AND VIRTUAL PHOTONS.

Solution of the Baxter equation for the composite states of the Reggeized gluons in QCD

Lipatov L.N.

Annotation

The gluon and quark in QCD are reggeized. Pomeron, Odderon and other colourless reggeons are composite states of the reggeized gluons. The Regge trajectories and couplings for gluons and quarks can be calculated with the use of an effective action. In the generalized leading logarithmic approximation the intercept for the contributions of diagrams with ~~the~~ several reggeized gluons is expressed in terms of the ground state energy for the corresponding Schrödinger equation. In the multi-colour QCD this equation turns out to be completely integrable. The problem is reduced to finding the Baxter function satisfying the Baxter equation. It is shown, that this function is meromorphic and its residues satisfy a recurrent relation. The intercept for the composite state of the reggeized gluons is expressed in terms of

Solution of the Baxter equation for the composite states of the Reggeized gluons in QCD

L. N. Lipatov (St. Petersburg)

Beyond the Pomeron: Reggeized gluons and quarks.

Is it possible to hear the form of a drum? (Kac)
Yes, by the use of the spectral analysis.

Is it possible to establish if the „elementary" particle is elementary or not? (For example – Higgs boson)
Yes, by measuring the Regge trajectory with the corresponding quantum numbers.

Are the gluons and quarks point-like particles?
Not, because they lie on the Regge trajectories.

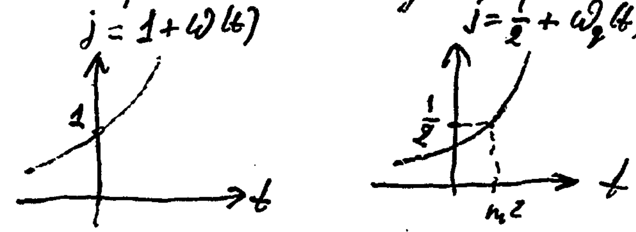

$$\omega(t) = g^2\omega_0(t) + g^4\omega_1 + \dots$$

$$\omega_0(-\vec{q}^{\,2}) = -\frac{N_c}{16\pi^3}\int \frac{d^2k\, \vec{q}^{\,2}}{\vec{k}^2(\vec{q}-\vec{k})^2}$$

ω_0 (BFKL (1975))
ω_1 (Fadin + k^0 (1996))

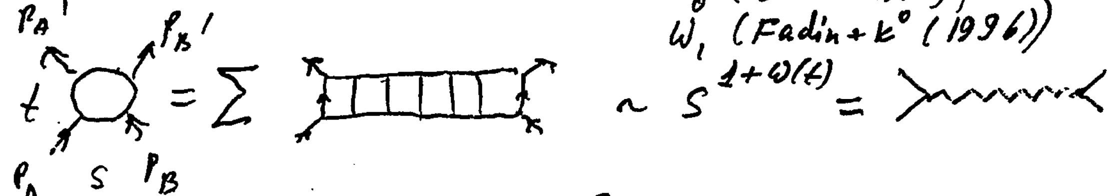

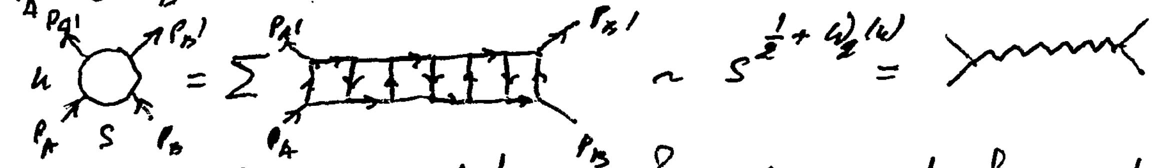

What are their constituents? – Reggeized gluons and quarks

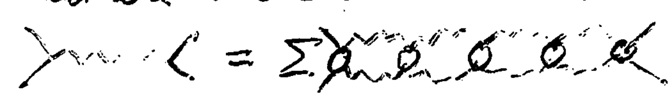

Bootstrap equations.

Integrability of the reggeon interactions for $N_c \to \infty$ (L.L. 1993)

Normalization conditions:

$$\|\Psi\|_1^2 = \int \prod_{k=1}^{n} d^2\rho_k \; \Psi^* \vec{p}_1^{\,2} \vec{p}_2^{\,2} \dots \vec{p}_n^{\,2} \Psi < \infty$$

$$\|\Psi\|_2^2 = \int \prod_{k=1}^{n} \frac{d^2\rho_k}{|\rho_{k,k+1}|^2} |\Psi|^2 < \infty$$

Hermicity properties:

$$h^T = \prod_{k=1}^{n} p_k \; h \left(\prod_{k=1}^{n} p_k\right)^{-1}$$

$$h^T = \left(\prod_{k=1}^{n} \rho_{k,k+1}\right)^{-1} h \prod_{k=1}^{n} \rho_{k,k+1}$$

The integral of motion:

$$[A, h] = 0 \,, \quad A = \prod_{k=1}^{n} \rho_{k,k+1} \prod_{r=1}^{n} p_r$$

Generating function for the integrals of motion:

$$t(u) = tr\left(L_n(u) L_{n-1}(u) \dots L_1(u)\right) = \sum_{r=0}^{n} q_r u^{n-r}$$

transfer matrix

$$q_0 = 2 \,, \quad q_1 = 0 \,, \quad q_2 = \vec{M}^2 \dots, \quad q_n = A$$

$$L_k = \begin{pmatrix} u + \rho_k p_k & -p_k \\ \rho_k^2 p_k & u - \rho_k p_k \end{pmatrix}$$

$$[t(u), t(v)] = 0 \,, \quad [t(u), h] = 0$$

Monodromy matrix $T(u) = L_n(u) L_{n-1}(u) \dots L_1(u) =$

Yang-Baxter equation: 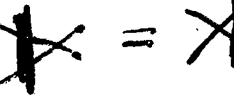. Bethe anzatz

Yang-Baxter equation, Bethe anzatz, Baxter equation

Monodromy matrix is parametrized as follows

$$T(u) = \begin{pmatrix} A(u) & B(u) \\ C(u) & D(u) \end{pmatrix} =$$ 

Yang - Baxter equation:

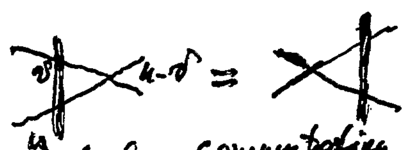

, 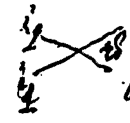

$$= v\,\delta^{i_1'}_{i_1}\delta^{i_2'}_{i_2} + i\,\delta^{i_2'}_{i_1}\delta^{i_1'}_{i_2}$$

means bilinear commutation relations between A, B, C, D

Solution of the Y-B equations = Bethe anzatz.

Faddeev, Korchemsky (1995):

$C(u)\,\Psi_0 = 0$, Ψ_0 - pseudovacuum state in conjugated space

$$L_k(u) = \begin{pmatrix} u + p_k \rho_{k0}, & -p_k \\ p_k \rho_{k0}^2, & u - p_k \rho_{k0} \end{pmatrix}, \quad \Psi_0 = \prod_{k=1}^{n} \rho_{k0}^{-2},$$

because $\begin{pmatrix} * & * \\ 0 & * \end{pmatrix}\begin{pmatrix} * & * \\ 0 & * \end{pmatrix} = \begin{pmatrix} * & * \\ 0 & * \end{pmatrix}$

Algebraic Bethe anzatz:

$$\Psi = B(u_1)\, B(u_2) \dots B(u_k)\, \Psi_0$$

$(A(u) + D(u))\,\Psi = \Lambda(u)\,\Psi$, $\Lambda(u)$ - eigenvalue of $t(u)$

only if $u_1, u_2, \dots u_k$ satisfy the Bethe equations

$$(u_z + i)^n \prod_{t=1}^{k} (u_z + i - u_t) + (u_z - i)^n \prod_{t=1}^{k} (u_z - i - u_t) = 0$$

then $$\Lambda(u) = (u+i)^n \prod_{t=1}^{k} \frac{u + i - u_t}{u - u_t} + (u - i)^n \prod_{t=1}^{k} \frac{u - i - u_t}{u - u_t}$$

Baxter function: $Q(u) = \prod_{t=1}^{k} (u - u_t)$, $m = k$ (nonphys)

Baxter equation:

$$\Lambda(u)\, Q(u) = (u+i)^n\, Q(u+i) + (u-i)^n\, Q(u-i)$$

(Faddeev L., Korchemsky G. (1995))

Analytic properties of the Baxter function
(with H. de Vega)

Baxter equation:

$$V(\lambda)\lambda^n Q(\lambda) = (\lambda+i)^n Q(\lambda+i) - 2\lambda^n Q(\lambda) + (\lambda-i)^n Q(\lambda-i)$$

$$V(\lambda) = \frac{m(1-m)}{\lambda^2} + \frac{q_3}{\lambda^3} + \dots + \frac{q_n}{\lambda^n} \quad , \quad m = \frac{1}{2} + i\nu + \frac{n}{2}$$

Symmetry: $q_k \to (-1)^k q_k \quad , \quad \lambda^n Q(\lambda) \to (-\lambda)^n Q(-\lambda)$

$$\lambda^n Q(\lambda)\Big|_{\lambda\to\infty} \sim c_1 \lambda^m + c_2 \lambda^{1-m}$$

Two solutions with the poles at $\lambda = 0, +i, +2i, \dots$
or at $\lambda = 0, -i, -2i, \dots$

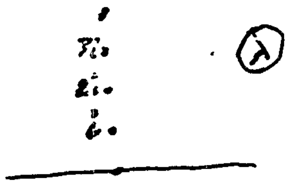

$$Q(\lambda) = \sum_{r=0}^{\infty} \frac{c_r}{\lambda - ir} \quad , \; c_r \text{ satisfy the recurrence relation}$$

The sum is convergent for m near $\frac{1}{2}$.
Zeroes of $Q(\lambda)$ are situated on the imaginary axis between the poles

$$Q(\lambda) = \frac{C}{\lambda} \prod_{r=1}^{\infty} \frac{1 + i\frac{\lambda}{r - \varepsilon_r}}{1 + i\frac{\lambda}{r}}$$

Holomorphic energy:

$$\mathcal{E} = i \lim_{\lambda \to i} \left[\frac{\partial}{\partial\lambda} \ln\left((\lambda - i)\lambda^n Q(\lambda)\right)\right]$$

The poles of $Q(\lambda)$ are a consequence of the complicated analytic properties of $\Psi(\vec{\rho}_1, \vec{\rho}_2 \dots \vec{\rho}_n)$.
In $\Psi(\vec{P}, \vec{\lambda}_1, \vec{\lambda}_2, \dots \vec{\lambda}_{n-1})$ these poles are cancelled providing that $q_3, q_4 \dots q_n$ are quantized.

Pomeron and Odderon in the Baxter - Sklyanin representation

Pomeron wave function in λ - representation

$$\Psi_{m,\tilde{m}}(\vec{P},\vec{\lambda}) = N[Q(\lambda,m)\,Q(\lambda^*,\tilde{m}) + (-1)^n Q(-\lambda,m)\,Q(-\lambda^*,\tilde{m})]$$

$\lambda = \sigma + i\frac{N}{2}$ - quantization of the Baxter function argument

$$Q(\lambda,m) \sim {}_3F_2(-i\lambda+1, 2-m, 1+m; 2,2;1)$$

$$Q(\lambda,m) = \sum_{\ell=0}^{\infty} \frac{\tau_\ell(m)}{\lambda - i\ell} = -\frac{i\pi}{\lambda} - \frac{\sin \pi m}{i\pi} \sum_{\ell=1}^{\infty} \frac{Q(-i\ell,m)}{\lambda - i\ell}$$

$$(\ell+1)^2\,\tau_{\ell+1}(m) + (\ell-1)^2\,\tau_{\ell-1}(m) = [2\ell^2 + m(m-1)]\,\tau_\ell(m)$$

$$\tau_\ell(m) = i\pi m(1-m)\,{}_3F_2(-\ell+1, 2-m, 1+m; 2,2,1)$$

Poles in σ in $\Psi_{m,\tilde{m}}$ are cancelled.

Odderon wave function in the $\vec{\lambda}$ representation:

$$\Psi_{m,\tilde{m}}(\vec{P},\vec{\lambda}_1,\vec{\lambda}_2) = \int d^2t\; e^{i\vec{t}(\vec{\lambda}_1+\vec{\lambda}_2)} \int d^2z\; \Phi_{\vec{\lambda}_1,\vec{\lambda}_2}(\vec{z})\,\Psi_{m,\tilde{m}}(\vec{p}_1,\vec{p}_2,$$

$$\Phi_{\vec{\lambda}_1,\vec{\lambda}_2}(\vec{z}) \sim \chi_{\lambda_1,\lambda_2}(z)\,\chi_{\lambda_1^*\lambda_2^*}(z^*) - \chi_{\lambda_2\lambda_1}(z)\,\chi_{\lambda_2^*\lambda_1^*}(z)$$

$$\chi_{\lambda_1,\lambda_2}(z) \sim z^{-i\frac{\lambda_2-\lambda_1}{2}}\,F(-i\lambda_2, +i\lambda_1; 1-i\lambda_2+i\lambda_1; z)$$

$$t = \ln\frac{p_1(p_1+p_2)}{(p_2+p_3)\,p_3}\,, \quad z = \frac{p_1\,p_3}{(p_2+p_3)(p_1+p_2)}$$

$$\Psi_{m,\tilde{m}}(\vec{p}_1,\vec{p}_2,\vec{p}_3) = \vec{p}_1^{\,2}\,\vec{p}_2^{\,2}\,\vec{p}_3^{\,2} \int d^2\rho_1\,d^2\rho_2\,d^2\rho_3\; e^{i\sum_{k=1}^{3}\vec{p}_k\vec{\rho}_{k0}}\,\Psi_{m,\tilde{m}}(\vec{\rho}_{10},\vec{\rho}_{20},\vec{\rho}_{30})$$

$$\Psi_{m,\tilde{m}}(\vec{\rho}_{10},\vec{\rho}_{20},\vec{\rho}_{30}) = \left(\frac{\rho_{23}}{\rho_{20}\,\rho_{30}}\right)^m \left(\frac{\rho_{23}^*}{\rho_{20}^*\,\rho_{30}^*}\right)^{\tilde{m}} \Psi_{m,\tilde{m}}(\vec{x})\,, \quad x = \frac{\rho_{12}\,\rho_{30}}{\rho_{10}\,\rho_{32}}$$

$\Psi_{m,\tilde{m}}(\vec{x})$ satisfies the differential equations and is known (L.L.; Yanik, Waisik; Braun ...)

Perturbative Radiation in Gap Events

George Sterman
Physics Department, Brookhaven National Laboratory
Upton, NY 11973, U.S.A.
C.N. Yang Institute for Theoretical Physics, SUNY Stony Brook
Stony Brook, NY 11794 – 3840, U.S.A.

Rapidity gap events in the presence of hard scattering are one of the striking features of hadronic final states at HERA and the Tevatron. Although the formation of a gap cannot be a purely perturbative process, it must be consistent with perturbative analysis, where the latter applies. Examples include evolution in diffractive DIS structure functions, and the case considered here, the flow of energy, Q_Ω, into region Ω of rapidity (η) and azimuthal angle (ϕ) between two high-p_T jets. This cross ssection possesses a standard collinear factorization form.

$$\frac{d\sigma_{AB\to J}}{dp_T dQ_\Omega} = f_{a/A} \otimes f_{b/B} \otimes \frac{d\hat{\sigma}_{ab}}{dp_T dQ_\Omega}\,, \tag{1}$$

with corrections of order $\Lambda^2_{\rm QCD}/Q^2_\Omega$, in terms of normal parton distributions f, and hard-scattering functions $d\hat{\sigma}$, where p_T stands for any fixed kinematic variables of the jet(s). The hard-scattering cross section itself may be refactorized into short-distance functions at the scale p_T, and a cross section computed in eikonal approximation, into which all Q_Ω-dependence goes.

$$\frac{d\hat{\sigma}_{ab}}{dp_T dQ_\Omega} = \sum_{IJ} h^*_J(p_T,\mu')h_I(p_t,\mu')\;\sigma^{(\rm eik)}_{JI}(Q_\Omega/\mu')\,. \tag{2}$$

The variable μ' is an arbitrary factorization scale that separates the short-distance functions h and eikonal cross sections $\hat{\sigma}^{(\rm eik)}_{IJ}$, both of which are infrared safe. The indices I and J label the color exchange content of the short-distance functions.

The refactorization of the cross section (2) allows us to quantify the idea of color exchange [1]. As the refactorization scale μ' changes, so does the color exchange. In this sense, Eq. (2) interpolates between "two-gluon exchange" and "soft color" models for gap formation. Radiation into Ω is a result of evolution between the scales p_T to Q_Ω. This evolution is characterized by a set of anomalous dimension matrices, which depend on both p_T and the choice of Ω. In general, reactions involving gluons involve more radiation, and hence a lower gap fraction, that those involving quarks. This is consistent with comparisons of 630 and 1800 GeV data from the Tevatron. An analysis of energy flow, rather than of multiplicity, leads to a constellation of predictions in terms of s, jet p_T and rapidity, as well as Q_Ω [2].

References

[1] G. Oderda and G. Sterman, Phys. Rev. Lett. **81**, 3591 (1998), hep-ph/9806530; G. Oderda, Phys. Rev. D**61**, 014004 (2000), hep-ph/9903240.

[2] C.F. Berger, T. Kucs and G. Sterman, in preparation.

pQCD can help with:

- Evolution - as in F_2^D

- Energy Flow

$$\frac{d\sigma_{AB\to J}}{dp_J\, dQ_\Omega} = f \otimes f' \otimes \frac{d\hat{\sigma}}{dp_J\, dQ_\Omega}$$

energy into region Ω

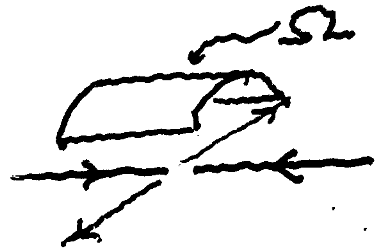

Q_Ω distribution computable via factorization as long as

$Q_\Omega \gg \Lambda_{QCD}$

c.f. Marchesini Webber 88

(brems. vs underlying event)

- Same Applies to Factorized Diffractive Cross Section

- See How Short-time QCD 'ALLOWS' Gaps

○ SKETCH OF METHOD

- Cross section at measured $E_{gap} \gg \Lambda$ is factorizable in standard way:

$$\frac{d\sigma^{AB}}{d\cos\hat{\theta}_J\, dQ_c}(s, E_T, \Delta y) = \sum_{\substack{\text{Partons}\\ i,j}} \phi_{i/A} \otimes \phi_{j/B} \otimes \frac{d\hat{\sigma}_{ij}}{d\cos\hat{\theta}_J\, dQ_c}(\hat{s}, \hat{t}, \Delta y, \alpha_s(-\hat{t})) + \mathcal{O}(\Lambda^2/Q_c^2)$$

PDF's (usual CTEQ, MRS, GRV...)

partonic

- For $Q_c^2 \ll -t$ but still perturbative separate two scales in the partonic cross section:

$$Q_c \frac{d\hat{\sigma}_{ij}}{d\cos\hat{\theta}\, dQ_c} = H^{ij}_{IL}(\hat{s}, \hat{t}, \mu, \alpha_s(\mu^2)) \cdot S_{LI}\left(\frac{Q_c}{\mu}, \Delta y\right) + \mathcal{O}(\alpha_s(t)$$

I, L = singlet, octet...

μ: new factorization scale defines color exchange I, L in hard scattering(s)

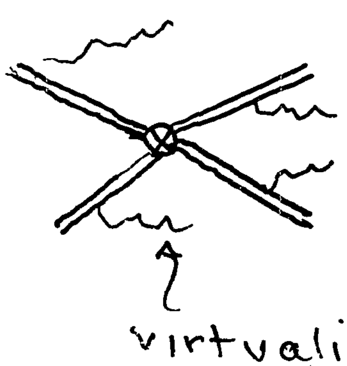

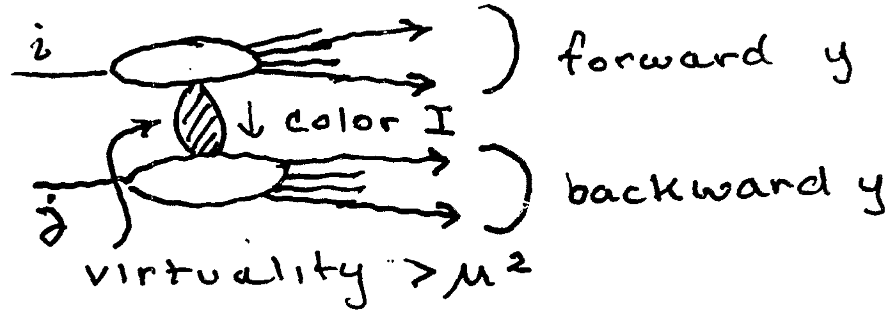

For any Ω: $\quad q\bar{q}$: I, J
= singlet, octet
(t-channel, ...)

$$\mu \frac{d}{d\mu} S_{IJ}^{(Q_c/\mu)} \sim \int_{\substack{\Omega_k \\ k^0=\mu}}$$ 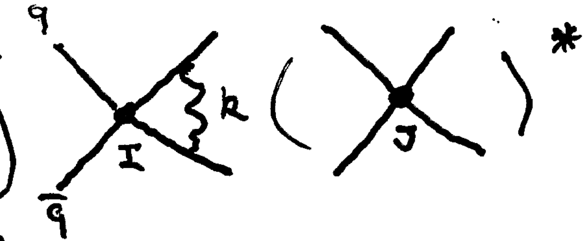

+

$$\int_{\substack{\Omega_k \\ k_0=\mu}}$$ 

as μ increases, these corrections shift from S to H

$$\mu \frac{d}{d\mu} S_{IJ} = -\Gamma^{\dagger}_{IK} S_{KJ} - S_{IK}\Gamma_{KJ}$$

$$\Gamma = \Gamma(\Omega, \theta^*)$$

$$= \Gamma^{(1)}\left(\frac{\alpha_s}{\pi}\right) + \cdots$$

$\alpha \cong \frac{\partial}{\partial \ln \mu} \Big($  $+$ 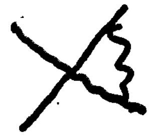 $\Big)^{\text{eik}}_{\Omega}$

$\beta \equiv \frac{\partial}{\partial \ln \mu} \Big($  $+$  $\Big)^{\text{eik}}_{\Omega}$

$\gamma \cong \frac{\partial}{\partial \ln \mu} \Big($ 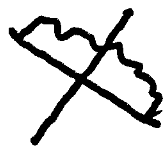 $+$ 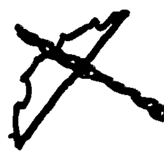 $\Big)^{\text{eik}}_{\Omega}$

$$\Gamma^{\Omega}_{q\bar{q}} = \begin{pmatrix} C_F \beta & \frac{C_F}{2N_c}(\alpha+\gamma) \\ \alpha+\gamma & C_F\alpha - \frac{1}{2N_c}(\alpha+\beta+2\gamma) \end{pmatrix}$$

$$Q_c \frac{d\hat{\sigma}_{ij}}{d\cos\hat{\theta}\, dQ_c} = H^{ij}_{IL}\left(\frac{\hat{t}}{\mu^2}\right) S^{ij}_{LI}\left(\frac{Q_c}{\mu}\right)$$

- Once we know evolution of S and H, we can fix $\mu^2 = -\hat{t}$, and <u>compute</u> $S_{LI}\left(\frac{Q_c}{\mu}\right)$

- Because Γ_{81} $\Gamma_{18} \neq 0$, singlet/octet exchange do <u>not</u> evolve independently (<u>unless</u> $s/t \to \infty$ . . . !) Del Duca Tang

- Linear combinations of 1, 8 exchange do evolve independently

- Eigenvalues of Γ $\Gamma(\Delta y, \Delta \eta)$ determine distribution of engergy flow

- Large eigenvalue → high Egap
  Small eigenvalue → low Egap

- Single-gluon exchange has projection onto 'small' eigenvalue color combination
  ↳ lowest order prediction of gap probability (perturbative)

The HERMES Effect

G.A. Miller

K. Ackerstaff et al Phy Lett B475, 386 (2000)

What is the HERMES Effect?

Our Theory

Coherent Contributions of Nuclear Mesons to Electroproduction–HERMES Effect

Gerald A. Miller, S.J. Brodsky M. Karliner

hep-ph/0002156 PLB 481, 245 (2000)

What is the HERMES Effect? e^-

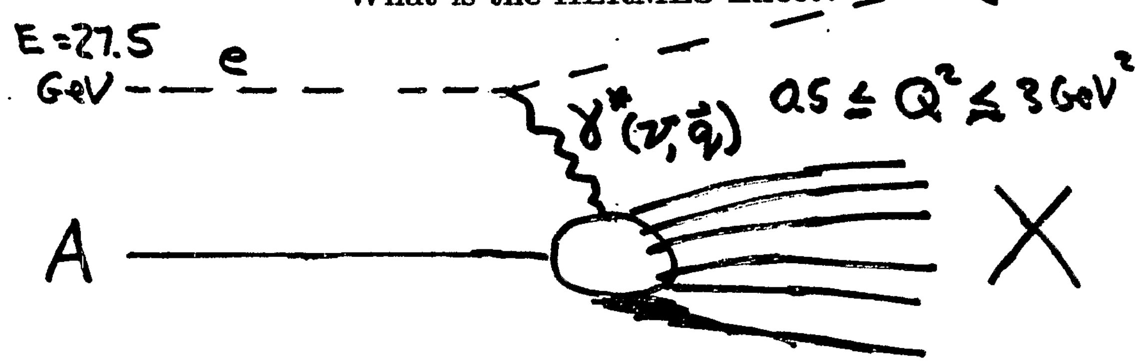

$\sigma \propto \sigma_T + \epsilon\sigma_L \qquad \epsilon \approx \frac{4(1-y)}{4(1-y)+2y^2} \qquad y = \frac{\nu}{E} \qquad R \equiv \frac{\sigma_L}{\sigma_T}$

$$\frac{\sigma_A}{\sigma_D} = \frac{F_2^A}{F_2^D}\,\frac{1+\epsilon R_A}{1+R_A}\,\frac{1+R_D}{1+\epsilon R_D}$$

HERMES extracts $\frac{F_2^A}{F_2^D}$, R_A from x, Q^2, ϵ dependence of $\frac{\sigma_A}{\sigma_D}$

$$\frac{\sigma_L(A)}{\sigma_L(D)} > 1 \qquad \frac{\sigma_T(A)}{\sigma_T(D)} < 1$$

$$\boxed{\frac{R_A}{R_D} \approx 5} \quad x \approx 0.01, \quad Q^2 = 0.5\ \mathrm{GeV}^2$$

Callan-Gross relation severely violated → bosons are the partons!

Mesons in nucleus!

A dependence of $R = \sigma_L/\sigma_T$

NI EF

- Fitted values of R_A/R_D:

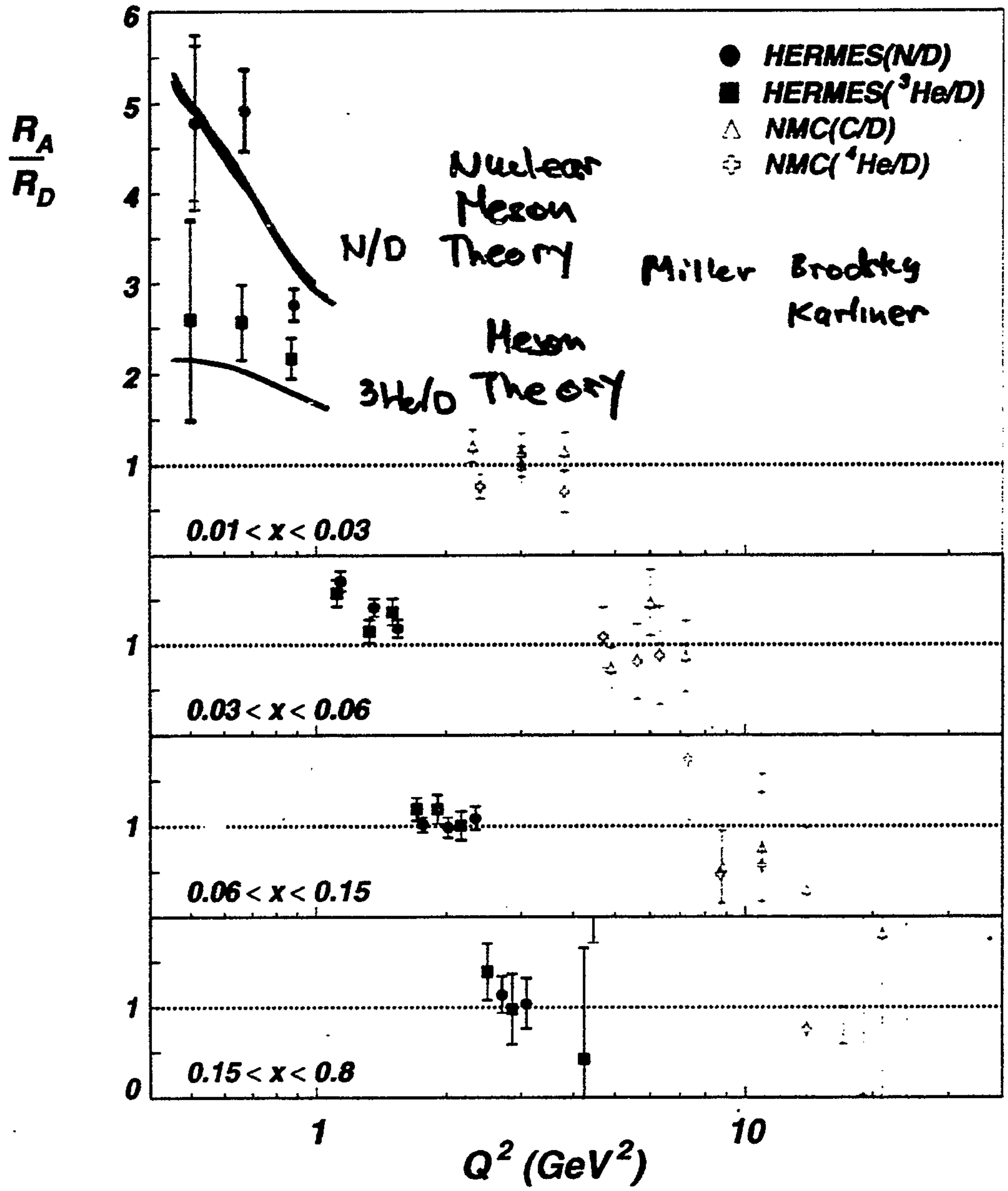

- Conclusion:

$\boxed{R_A > R_D \text{ at } x < 0.06 \text{ and } Q^2 < 1.5\ \mathrm{GeV}^2}$

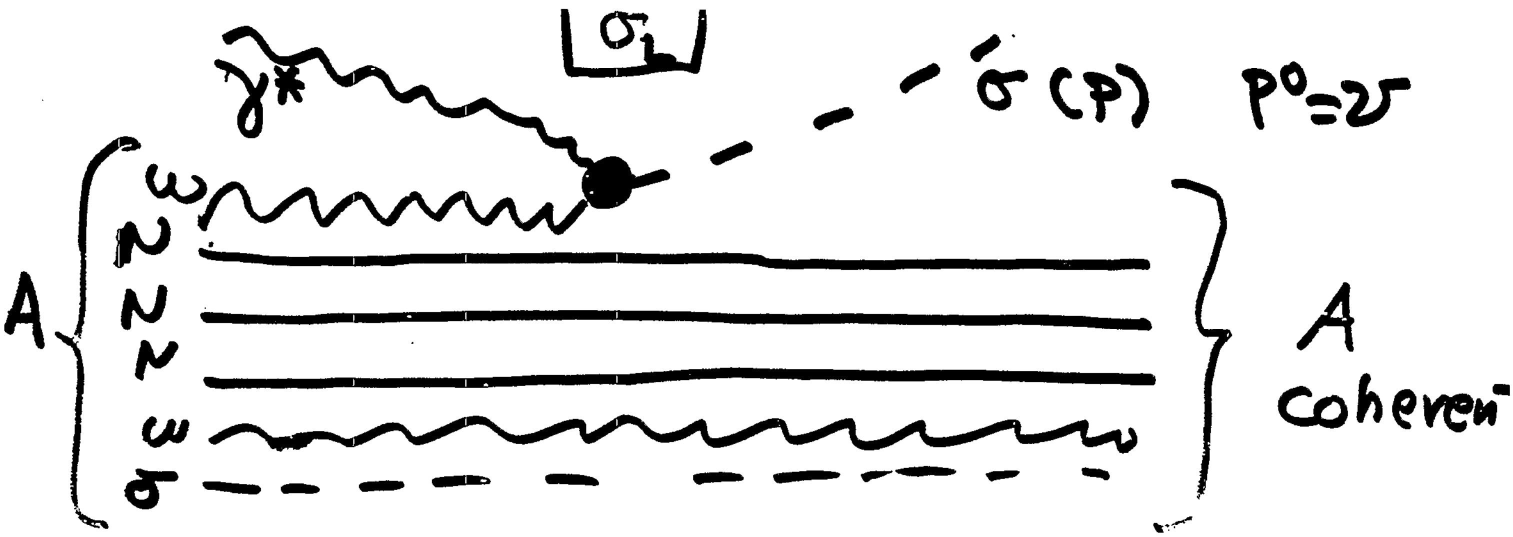

$$\mathcal{L}_I = \frac{ge}{2M_\omega} F^{\mu\nu}(\omega_\nu \partial_\mu \sigma - \omega_\mu \partial_\nu \sigma)$$

$$J^\mu \sim \frac{ge}{m_\omega} p^\mu \, \nu \, \omega^0 \, F_V(Q^2)$$

$\uparrow$ Form factor

$g = ??$

$$BR(\omega \to \pi^+\pi^-\gamma) \leq 3.6 \times 10^{-3} \Rightarrow \frac{g^2 e^2}{4\pi} \leq 2\alpha$$

$\uparrow$ large

$$\frac{\delta W^{00}}{A} \approx \nu^3 (g\omega^0)^2 A^{1/3} F_V^2(Q^2)$$

harmonic oscillator

$$\frac{\sigma_L(A)/A}{\sigma_L(D)/2} = 1 + \frac{Q^4}{\nu(\nu^2+Q^2)} \frac{\delta W^{00}/A}{F_2^D R_D} (1 + R_D)$$

$F_V(Q^2)$ from Ito & Gross or dipole

g < max , ω^0 from Walecka model

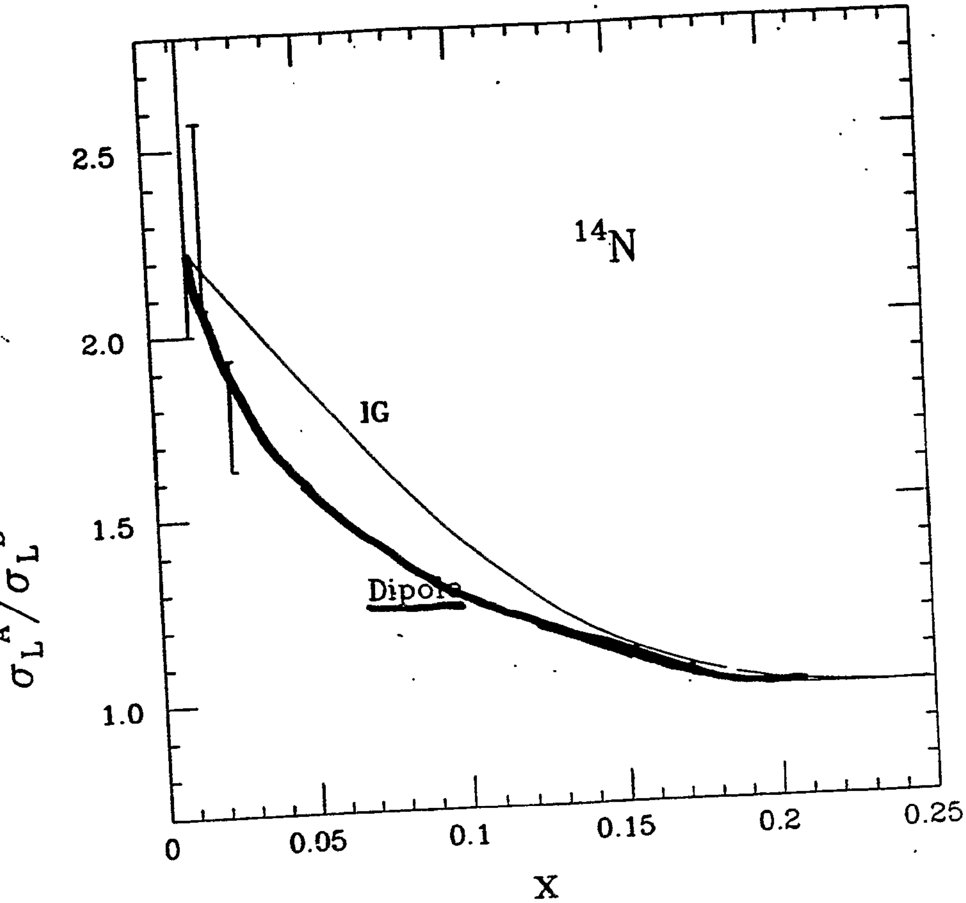

2.5
2.0
1.5
1.0
σ_L^A/σ_L^D
^{14}N
IG
Dipole
0
0.05
0.1
0.15
0.2
0.25
X

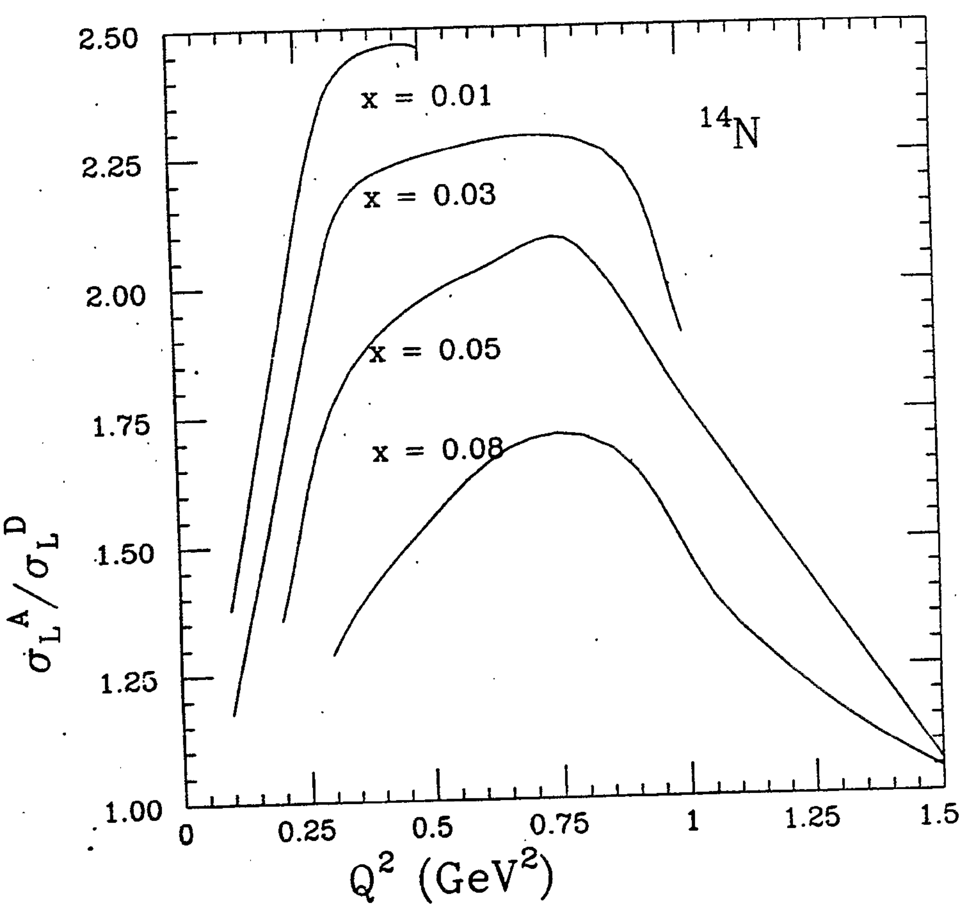

2.50
2.25
2.00
1.75
1.50
1.25
1.00
σ_L^A/σ_L^D
x = 0.01
x = 0.03
x = 0.05
x = 0.08
^{14}N
0
0.25
0.5
0.75
1
1.25
1.5
Q^2 (GeV^2)

$\boxed{\sigma_T}$ $\quad x \sim 0.01 \quad Q^2 \doteq 1\,\mathrm{GeV}^2$

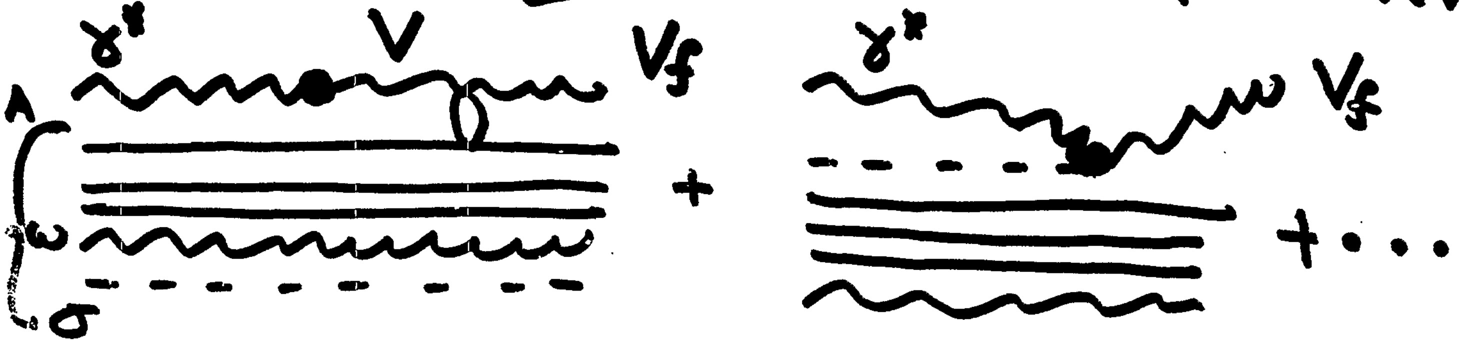

dominant (sea) $\qquad$ interference $\left(\begin{matrix}\text{needed} \\ -\frac{1}{3}\,\text{dom.}\end{matrix}\right)$

$$\mathcal{L}_I = \frac{g_{\gamma V\sigma}}{2m_\sigma} F_{\mu\nu}\left[V^{\mu\nu}\sigma + 1\left(V^\mu\partial^\nu\sigma - V^\nu\partial^\mu\sigma\right)\right]F_1^V$$

Gauge invariant coupling $\alpha\ Q^2$

$g_{\gamma V\sigma}$ - complex, fitted to data
no constraints $\mathcal{O}(\sqrt{\alpha})$

$F_1^V \sim e^{-Q^2R^2/6}$ $\qquad R = 1.0\ \mathrm{fm}$

σ from Walecka model

$$\frac{\sigma_T(A)/A}{\sigma_T(D)/2} = \frac{\left|\mathcal{M}^{\text{sea}}_{\text{dom}}\left[1 - g_{\gamma V\sigma}Q^2 \ldots\right]\right|^2 S(A) + \left|\mathcal{M}^{\text{val}}\right|^2}{\left|\mathcal{M}^{\text{sea}}_{\text{dom}}\right|^2 + \left|\mathcal{M}^{\text{val}}\right|^2}$$

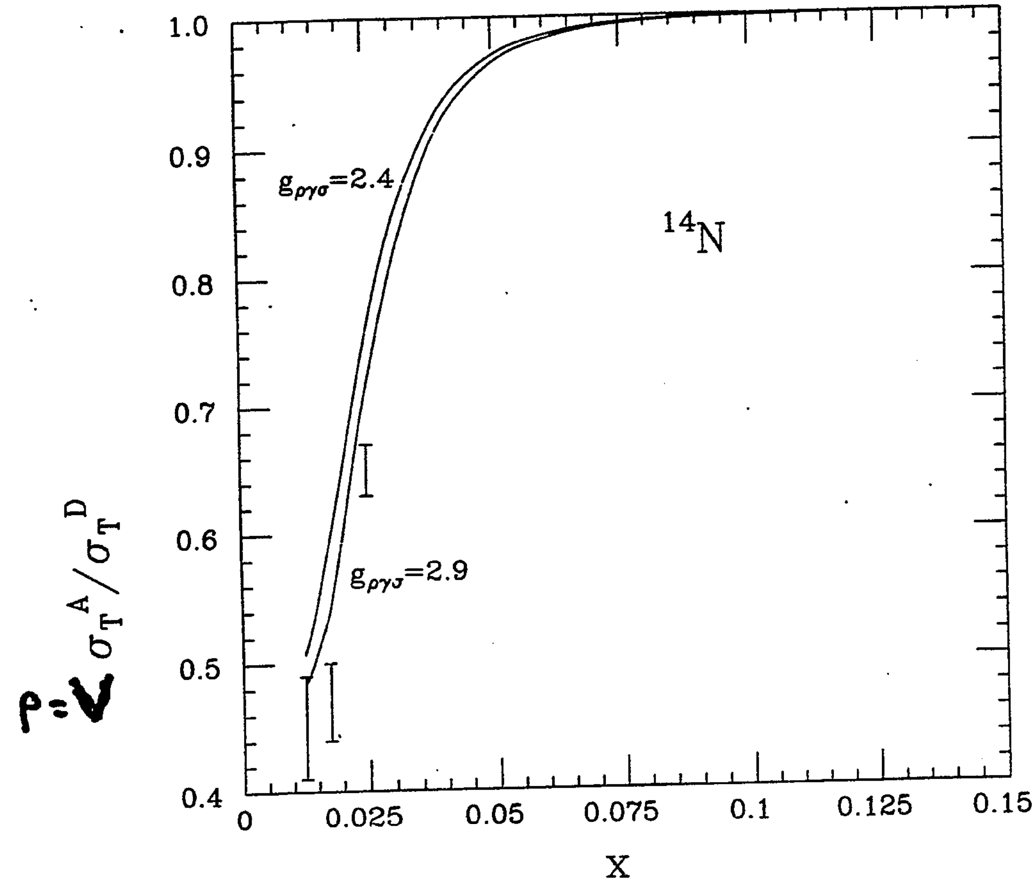

1.0
0.9
0.8
0.7
0.6
0.5
0.4
$g_{\rho\gamma\sigma}$=2.4
$g_{\rho\gamma\sigma}$=2.9
^{14}N
$\rho = \sqrt{\sigma_T{}^A / \sigma_T{}^D}$
0
0.025
0.05
0.075
0.1
0.125
0.15
X

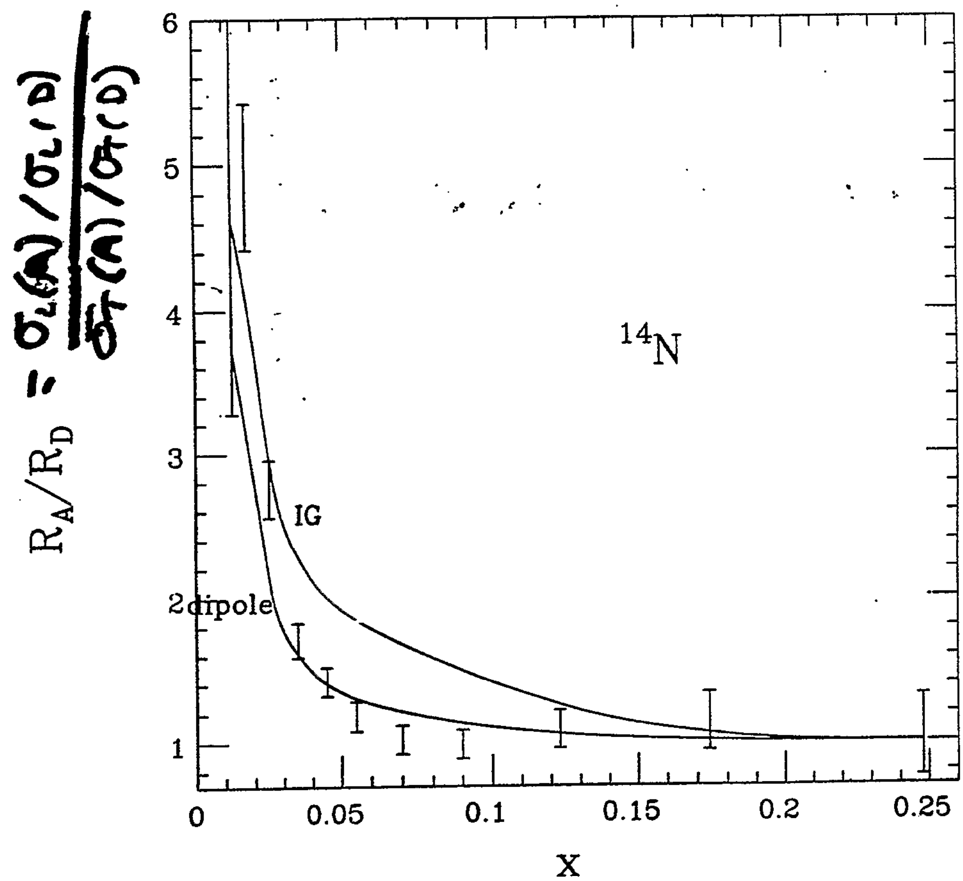

6
5
4
3
2
1
$R_A/R_D = \dfrac{\sigma_L(A)/\sigma_L(D)}{\sigma_T(A)/\sigma_T(D)}$
^{14}N
IG
dipole
0
0.05
0.1
0.15
0.2
0.25
X

Summary -27.5 GeV low Q^2 HERMES

$\sigma_L(A)$ enhanced by nuclear vector mesons

$\sigma_T(A)$ depleted by nuclear scalar mesons

dynamics ≈ consistent with nuclear:
binding, densities, Deep Inel. Scatt (high Q^2) Drell Yan

Verification needed

meson – γ^* interactions (many choices I haven't explored) more expts needed

significant nuclear coherent production of σ mesons $(\pi\pi)\ I=0$ pairs

$\sigma_{T,L}(A)$ depends strongly on x, Q^2, **A**

see π effects at $x \approx 0.1, 0.2$, $Q^2 \approx 0.5\ GeV^2$
enhanced σ_L

Can't rule out HERMES DATA with our theory –

Nuclear mesons may play unanticipated role – fundamental constituents at low Q^2

Unitarity corrections to the BFKL Pomeron

G. Korchemsky (Orsay)

1. Why does the BFKL Pomeron violates the unitarity ?
2. Unitarization procedure in QCD:
   - "weak" unitarization
   - "strong" unitarization
3. Regge effective theory in QCD
4. Comparison with the dipole model

I. Onium - onium scattering at high energy

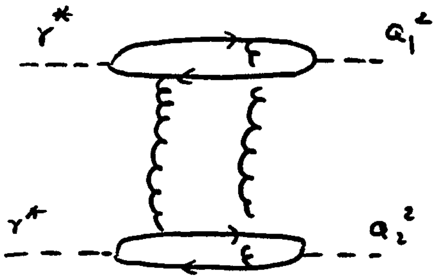

$$Q_1^2 \sim Q_2^2 \ll s = e^Y$$

$$\alpha_s \ln s = \text{fixed}, \qquad \alpha_s = \text{small}$$

Structure of the QCD corrections

$$\sigma(s) = \sigma_{LO}(\alpha_s \ln s) + \alpha_s\, \sigma_{NLO}(\alpha_s \ln s) + \ldots \leq \text{const.} \ln^2 s$$

Leading order = BFKL approximation

$$\sigma_{LO} = \sum_{\text{rungs}}$$

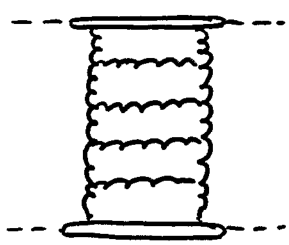

$$= 16\pi R^2 \alpha_s^2 \frac{e^{(\alpha_P - 1)\ln \frac{s}{m^2}}}{\left(\frac{7}{2}\zeta(3)\, \alpha_s N_c \ln \frac{s}{Q^2}\right)^{1/2}}$$

Leading log's comes from planar diagrams only

Large - N_c limit reproduces correctly $\sigma_{LO}(\alpha_s N_c \ln s)$

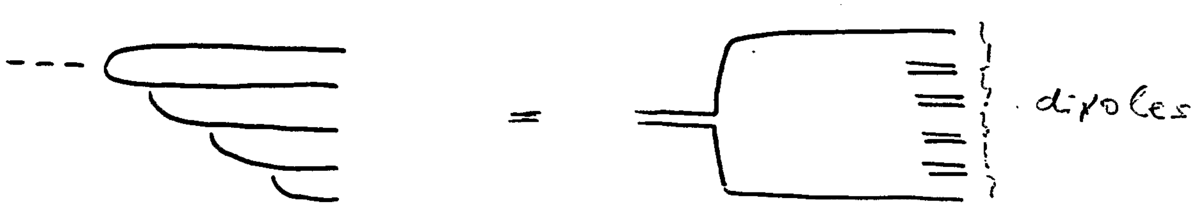

BFKL approximation = Dipole model = σ_{LO}

II. Why the unitarity is broken to the leading order

- Two limits $\alpha_s \to 0$ and $\ln s \to \infty$ do not commute

- Unitarity corrections become important as

$$Y \sim \frac{1}{\alpha_P - 1} \ln \frac{1}{\alpha_s^2} \quad , \quad \sigma_{LO} \sim \alpha_s \, \sigma_{NLO} \qquad \text{Mueller}$$

- Unitarity corrections come from subleading corrections both in α_s and $1/N_c$

? Does the dipole model reproduces correctly the QCD unitarity corrections ? ... not obvious

? How to calculate unitarity corrections in QCD

Feynman-Gribov theorem : " Unitarity constraints allow to reconstruct the loop diagrams out of the Born level graphs"

<u>Unitarity constraint</u> $\quad S S^+ = 1, \quad S = 1 + i T$

$$T - T^+ = i \, T T^+$$

QCD ansatz

$$T_{AB} = \;$$ A 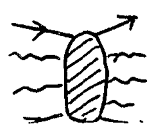 $$= \alpha_s \, T^{(0)} + \alpha_s^2 \, T^{(1)} + \dots$$

Unitarity constraints

$$T^{(0)} = (T^{(0)})^{+}, \qquad T^{(1)} - (T^{(1)})^{+} = i\, T^{(0)} (T^{(0)})^{+}, \ldots$$

- S-matrix in the BFKL approximation

$$T^{(0)} =$$ 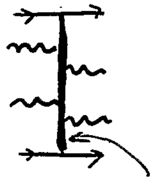 $$, \qquad T^{(1)} = \frac{i}{2} (T^{(0)})^2$$

reggeized gluon + multi-Regge kinematics

$$S_{BFKL} = 1 + i\, \alpha_s T^{(0)} + \frac{1}{2} (i\, \alpha_s T^{(0)})^2 + 0$$

8 ← color charge 8×8

BFKL Pomeron

$$\langle \gamma_A^* \gamma_B^* | S - 1 | \gamma_A^* \gamma_B^* \rangle \ldots \langle \ldots \tfrac{\alpha_s^2}{2} \ldots T^{(0)} | A, B \rangle$$

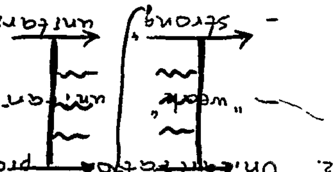

propagation of 2 reggeized gluons

Unitarity is broken:

$$S_{BFKL}\, S^{+}_{BFKL} \neq 1$$

- Unitarization procedure in QCD:

Add the minimal set of corrections to S_{BFKL} to restore unitarity

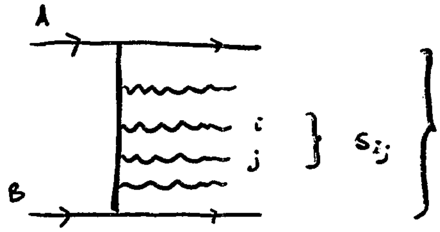

Unitarity constraints:

- "weak": only in the main channels
- "strong": in all energy subchannels s_{ij}

– "Weak" unitarity

$$S_{BFKL} = 1 + i\,(\alpha_s T^{(0)}) + \tfrac{1}{2}(i\alpha_s T^{(0)})^2 \rightarrow S_{weak} = \exp\,(i\alpha_s T^{(0)})$$

Lowest order correction $\sim (T^{(0)})^4$

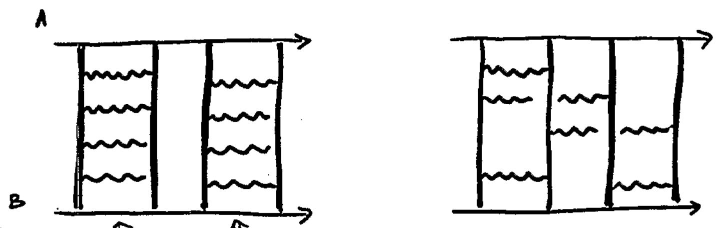

color singlets   irreducible color flow

$$= c_1 \left[\alpha_s^2\, e^{(\alpha_P - 1)Y}\right]^2 + c_2\, \alpha_s^4\, N_c^2\, e^{(\alpha_4 - 1)Y}$$

double BFKL exchange   A new 4-reggeon state

BKP equation

Bartels
Kwiecinski
Praszalowicz

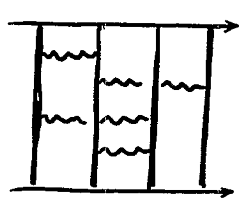 $= \sum$ 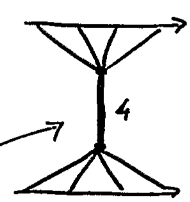 $e^{(\alpha_4 - 1)Y}$

$N = 4$ reggeon compound states

- "Weak" unitarity corrections do not have a natural small parameter

- BFKL states are supplemented by higher ($N_i = 4, 6, \ldots$) reggeon compound states

- N-reggeon states obey "extended" symmetry of integrable Heisenberg magnet

Faddeev
G.K.
Lipatov

BFKL + weak unitarity $= \sum_{N_1 \ldots N_k}$ 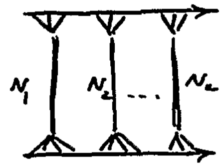

$\equiv$ Quantum Mechanics of $N = 2, 4, \ldots$ reggeon compound states

"strong" unitarity

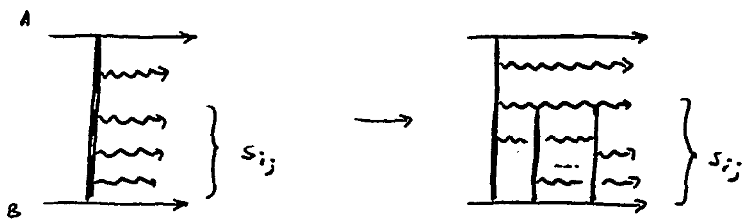

- Number of reggeons is not conserved
- Creation / annihilation of reggeons is allowed

– A new element of the effective theory:

reggeon number changing vertices

$V_{2\to 4}, \quad V_{2\to 6}, \ldots$

Bartels
Wusthoff
Lotter
Ewerz

Explicit form

$V_{2\to4}$ = 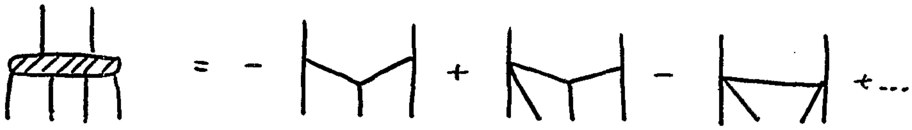

Lowest order correction

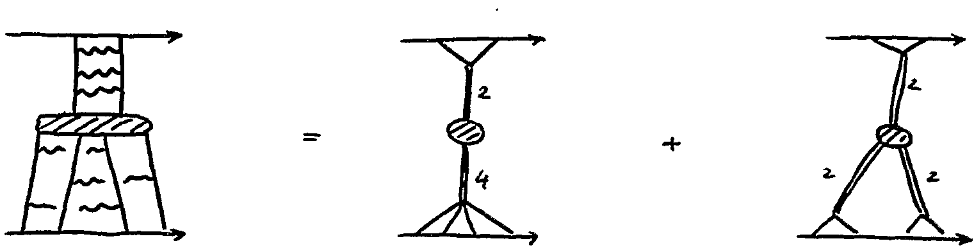

transition between $N=2$ and $N=4$ states

triple BFKL vertex

- Reggeon compound states start to interact
- Interaction is local in "time" Y and is conformal invariant

BFKL approximation $\xrightarrow[\text{unitarity}]{\text{weak}}$ Quantum Mech. of reggeon states $\xrightarrow[\text{unitarity}]{\text{strong}}$ Effective field theory of interacting reggeon states

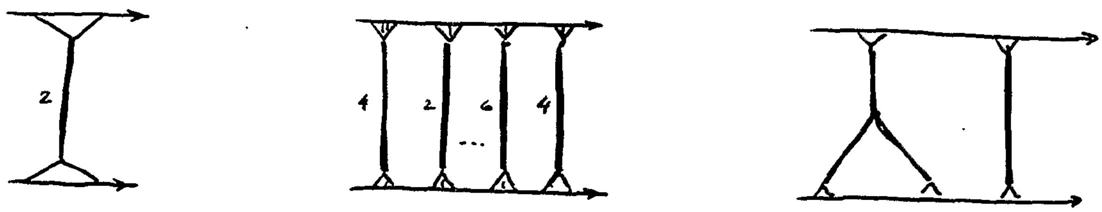

Calculation of ~~of~~ triple BFKL vertex

G. K.

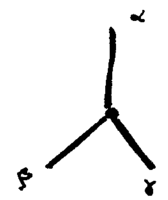

$$\equiv \langle\alpha|\ V_{2\to4}\ |\beta,\gamma\rangle$$

BFKL states

reggeon transition vertex

Feynman diagram representation

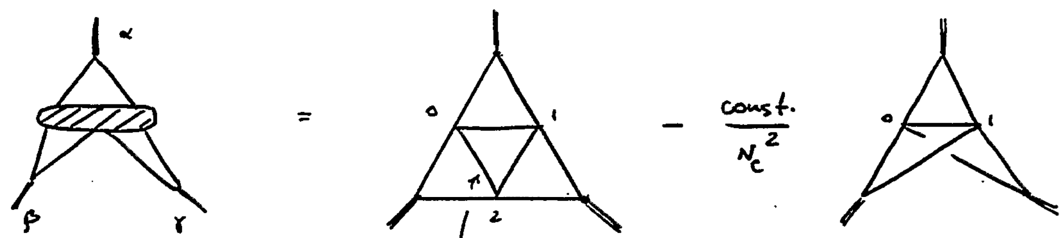

2-dim scalar propagators

- Planar contribution agrees with the dipole model prediction   Mueller, Bialas, Navelet, Peschanski
- Emerging Regge effective theory is different from the dipole model
- Dipole model does not take into account
  - contribution of higher compound reggeon states
  - neglects nonplanar corrections to the effective vertices

  [Beware of the AFS cancellation – planar contribution may be zero after all]

Effective Field Theory for the Small-x Evolution

Ian Balitsky

Old Dominion University
Oceanography and Physics
Hampton Boulevard
Norfolk, VA 23529

and

Jefferson Lab
CEBAF Center - Theory Group
12000 Jefferson Avenue
Newport News, VA 23606

balitsky@jlab.org

Deep inelastic scattering in QCD

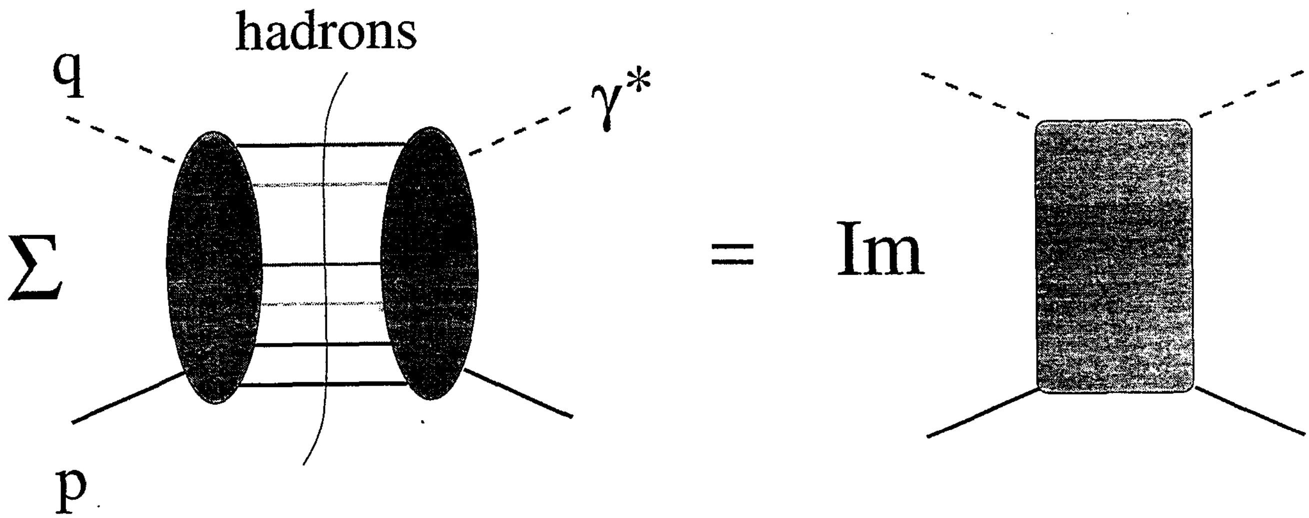

Bjorken limit : $\begin{cases} Q^2 \equiv -q^2 \to \infty \\ x \equiv \frac{Q^2}{2pq} - \text{fixed} \end{cases}$

$$
\begin{aligned}
W_{\mu\nu} &= \left(\frac{q_\mu q_\nu}{q^2} - g_{\mu\nu}\right) F_1(x, Q^2) \\
&+ \frac{1}{pq}\left(p_\mu - q_\mu \frac{pq}{q^2}\right)\left(p_\nu - q_\nu \frac{pq}{q^2}\right) F_2(x, Q^2)
\end{aligned}
$$

Optical theorem

$$W_{\mu\nu} = \frac{1}{\pi} \mathrm{Im} T_{\mu\nu}$$

$$T_{\mu\nu} = i \int d^4 z e^{iqz} \langle p | T\{j_\mu(z) j_\nu(0)\} | p \rangle$$

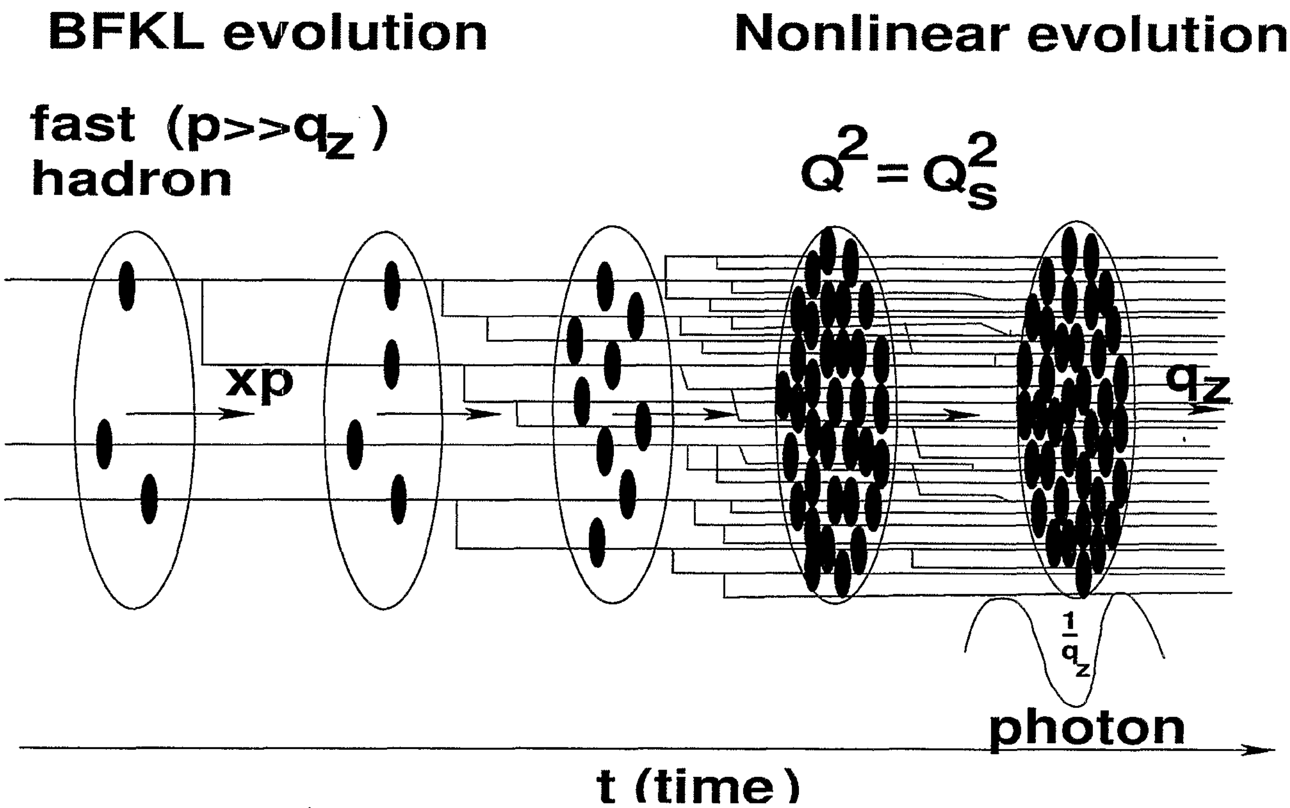

Emission of partons $\sim$ ρ (density)
Annihilation of partons $\sim$ $\frac{\alpha_s}{Q^2}\rho^2$
(the amplitude of the annihilation of two partons in the cascade is $\frac{\alpha_s}{Q^2}$)
$\Rightarrow$
The equilibrium between emission and annihilation (saturation) should be described by simple non-linear equation

$$\frac{d\rho}{d\ln(1/x)} = \frac{N_c\alpha_s}{\pi}\Big(K^{\mathsf{BFKL}}\otimes\rho\ -\ const\times\frac{\alpha_s}{Q^2}\times\rho^2\Big)$$

Small-x DIS from the nucleon

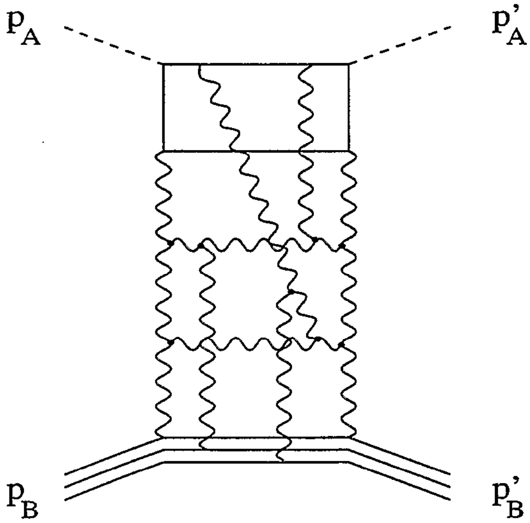

Fast quark moves along the straight line $\Rightarrow$

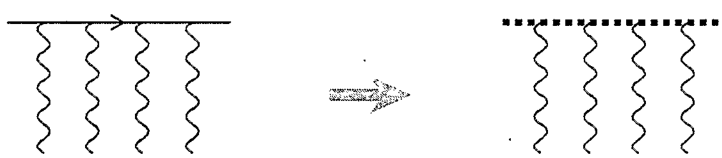

quark propagator reduces to the Wilson line collinear to quark's velocity

$$U(x_\perp, \eta) \equiv [\infty n_\eta + x_\perp, -\infty n_\eta + x_\perp]$$

$$[x, y] \equiv \text{Pexp}\left\{ ig \int_0^1 dv (x-y)^\mu A_\mu(vx + (1-v)y) \right\}$$

Non-linear evolution equation

$$\frac{\partial}{\partial\eta}\mathcal{U}(x_\perp, y_\perp) =$$
$$-\frac{\alpha_s N_c}{4\pi^2}\int dz_\perp \{\mathcal{U}(x_\perp, z_\perp) + \mathcal{U}(z_\perp, y_\perp) - \mathcal{U}(x_\perp, y_\perp)$$
$$+ \mathcal{U}(x, z)\mathcal{U}(z, y)\}\frac{(\vec{x} - \vec{y})^2_\perp}{(\vec{x}_\perp - \vec{z}_\perp)^2(\vec{z}_\perp - \vec{y}_\perp)^2}$$

$$\mathcal{U}(x_\perp, y_\perp) \equiv \frac{1}{N_c}(\mathrm{Tr}\{U(x_\perp)U^\dagger(y_\perp)\} - N_c)$$

LLA for DIS in pQCD $\Rightarrow$ BFKL
LLA for DIS in sQCD $\Rightarrow$ NL eqn
(s for semiclassical)

Example - LLA for the structure functions of large nuclei: $\alpha_s \ln\frac{1}{x} \sim 1$, $\alpha_s^2 A^{1/3} \sim 1$

$\pi \to \partial_\perp^2 \pi \Rightarrow$

$$U^{\eta_A}(x_\perp) \otimes U^{\dagger\eta_A}(y_\perp)$$
$$= \int_{\Omega_{1,2}(\eta_0)=1}^{\pi_{1,2}(\eta_A)=0} D\pi_1(z,\eta)D\pi_2(z,\eta)D\Omega_1(z,\eta)D\Omega_2(z,\eta)$$
$$\times\ \Omega_1^\dagger(x_\perp,\eta_A)U_x^{\eta_0}\Omega_2(x_\perp,\eta_A) \otimes \Omega_2^\dagger(y_\perp,\eta_A)U_y^{\dagger\eta_0}\Omega_1(y_\perp,\eta_A)$$
$$\times\ \exp\Big\{\int_{\eta_0}^{\eta_A} d\eta \int d^2z[\frac{1}{g}\sum_{i=1,2}\vec{\partial}^2\pi_i^a(z,\eta)(\Omega_i^\dagger(z,\eta)\frac{\partial}{\partial\eta}\Omega_i(z,\eta))^a$$
$$-\ \frac{1}{4\pi}\pi_1^a(z,\eta)\vec{\partial}^2(\Omega_1^\dagger(z,\eta)U^{z,\eta_0}\Omega_2(z,\eta))^{ab}\pi_2^b(z,\eta)]\Big\}$$

The action is now local

Perturbation theory

$$\Omega_1(z,\eta) = e^{-ig\phi_1(z,\eta)}, \qquad \Omega_2(z,\eta) = e^{-ig\phi_2(z,\eta)}$$

Propagators:

$$\phi_i^a(x_\perp,\eta)\pi_j^b(y_\perp,\eta') = -i\delta_{ij}\delta^{ab}\theta(\eta-\eta')(\!(x_\perp|\frac{1}{\vec{\partial}_\perp^2}|y_\perp)\!),$$
$$\phi_i^a(x_\perp,\eta)\phi_j^b(y_\perp,\eta') = 0, \quad \pi_i^a(x_\perp,\eta)\pi_j^b(y_\perp,\eta') = 0$$

After integration over canonical momenta π_i

$$U^{\eta_A}(x_\perp) \otimes U^{\dagger\eta_A}(y_\perp)$$
$$= \int_{\Omega_{1,2}(\eta_0)=\mathbb{1}} D\Omega_1(z,\eta) D\Omega_2(z,\eta)\ \Omega_1^\dagger(x_\perp,\eta_A)$$
$$\times\ U^{\eta_0}(x_\perp)\Omega_2(x_\perp,\eta_A) \otimes \Omega_2^\dagger(y_\perp,\eta_A)U^{\dagger\eta_0}(y_\perp)\Omega_1(y_\perp,\eta_A)$$
$$\times\ \exp\Big\{-\frac{1}{\alpha_s}\int_{\eta_0}^{\eta_A} d\eta \int d^2z [\vec{\partial}_\perp^2(\Omega_1^\dagger(z,\eta)U_z^{\eta_0}\Omega_2(z,\eta))]_{ab}^{-1}$$
$$\times\ \vec{\partial}_\perp^2(i\Omega_1^\dagger(z,\eta)\dot{\Omega}_1(z,\eta))^a \vec{\partial}_\perp^2(i\Omega_2^\dagger(z,\eta)\dot{\Omega}_2(z,\eta))^b\Big\},$$

where $\dot{\Omega} \equiv \frac{\partial}{\partial\eta}\Omega$

The action is local (and real). Given the initial conditions

$$\langle p_B|U^{\dagger\eta_0}(zx_1)U^{\dagger\eta_0}(z_2)...U)U^{\dagger\eta_0}(z_n)|p_B\rangle,$$

this functional integral can be calculated.

Summary of the talk *Direct Solutions to Kovchegov Equation*

Leszek Motyka, *Uppsala and Kraków*

The Kovchegov equation describes the evolution of the color dipole density in an onium state and is capable to include multiple scattering of the dipoles off the target. It is compatible with QCD in the leading logarithmic $\log(1/x)$ approximation and large N_c limit. It may be viewed as a minimal extension of the BFKL equation in which the unitarity of the scattering amplitude is preserved. Therefore the properties of the equation and the applications in the high energy phenomenology call for a detailed study. Besides that I want to test wheather the solutions of Kovchegov equation are able to explain the recently reported phenomenon of geometric scaling in $\sigma(\gamma^* p)$.

I focus on the Kovchegov equation for small dipoles and for the cylindrical nucleon, which has a particularly simple form

$$\frac{\partial \hat{N}(\boldsymbol{k},Y)}{\partial Y} = \bar{\alpha}_s \mathcal{K}_{\mathrm{BFKL}} \left(1 + \frac{\partial}{\partial \log k^2}\right) \hat{N}(\boldsymbol{k},Y) - \bar{\alpha}_s [\hat{N}(\boldsymbol{k},Y)]^2 \tag{1}$$

where

$$\mathcal{K}_{\mathrm{BFKL}}(\gamma) = 2\psi(1) - \psi(\gamma) - \psi(1-\gamma), \qquad Y = \log(1/x) \tag{2}$$

Now I substitute

$$n(\boldsymbol{k},Y) = \frac{\hat{N}(\boldsymbol{k},Y)}{k^2} \tag{3}$$

which reduces the equation to the BFKL-like form. This equation was solved numerically by the discretization method with the use of set of orthogonal polynomials. The nonlinear term has is local in $\boldsymbol{k}$ which makes it straightforward to the generalize the standard method used in the linear case. After the discretization one obtains a set of nonlinear differential equations of the first order. The initial condition function is usually assumed to be defined by the Glauber-Mueller Ansatz.

I demonstrate that the unintegrated gluon distribution $f_g(k,Y)$ may be obtained from the solution $\hat{N}(k,Y)$ by the following formula

$$f_g(k^2,Y) = \frac{3S_T}{4\pi^2\alpha_s} k^4 \Delta_k \hat{N}(\boldsymbol{k},Y) \tag{4}$$

with Δ_k used for the 2-dimensional Laplace operator in the $\boldsymbol{k}$ space.

I consider both the fixed and running α_s in the Kovchegov equation. The running coupling (RC) constant case is particularly interesting because the BFKL equation with RC requires an explicit infra-red cut-off (about 1 GeV) due to the Collins-Kwieciński bound for the BFKL pomeron intercept. In the Kovchegov equation the cut-off may be lowered substantially without loosing the stability of the equation. This happens because the growth of the gluon density at low k^2 (and succesively for all k) is tamed by the nonlinear term – the infrared cut-off is now generated by the equation itself. However, the evolution in x is still to rapid and the resulting gluon distributions for low x is by order of magnitude too large in comparison with the existing paramterisations. The potential source of the failure is probably the missing non-leading corrections to the BFKL part of the kernel which would slow down the evolution. The approximate geometric scaling is found to hold for $x < 0.01$.

I also study the Kovchegov equation with α_s fixed to 0.1 in order to guarantee the evolution to be slow. The solving function in the low x region may be approximately expressed as

$$\hat{N}(k,Y) \sim \log(1 + (Q_s/k)^{\beta}) \tag{5}$$

with the saturation scale $Q_s(x)$ growing towards small x as $x^{-0.2}$ and $\beta \sim 1.5$. The solutions is also consistent with the geometric scaling, however it is different from the Glauber-Mueller input and therefore from the corresponding distribution from the Golec-Biernat–Wüsthoff model. The gluon following from the solution agrees reasonably with the accepted parametrisations. The amount of shadowing is investigated by comparing the gluon from the nonlinear and linear equation. It is found, that the shadowing corrections for the gluon are at the level of 30% for $x \simeq 10^{-6}$, 10^{-4} and 10^{-2} for $Q^2 = 100$, 10 and 1 GeV^2 respectively.

As the main conclusion we confirm, that a reasonable phenomenology may be constructed on the basis of the Kovchegov equation with a small coupling constant and that the nonleading corrections should be included for the equation with the running coupling constant.

Solution to Kovchegov equation for fixed $\alpha_s = 0.1$ and $Y = 0, 2, 4, \ldots, 16$

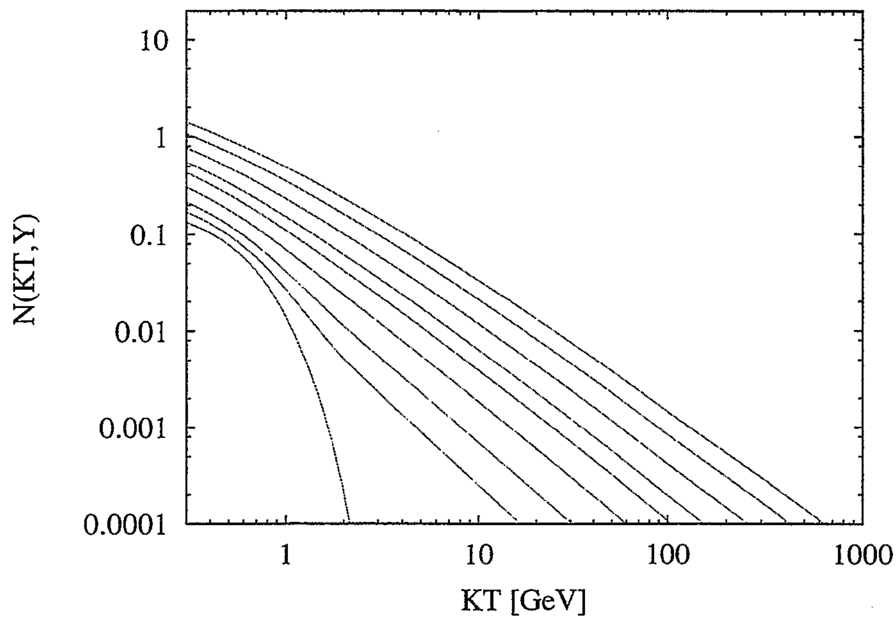

$$N(k, Y) \sim \log(1 + (Q/k_T)^{\beta})$$

$$Q^2 \sim Q_0^2 \exp(\alpha Y)$$

$$\alpha \sim 0.4 \qquad \beta \sim 1.5$$

Test of geometric scaling for fixed $\alpha_s = 0.1$
Scaling variable: $t = k_T \exp(-0.2\,Y)$

All Y, all k_T

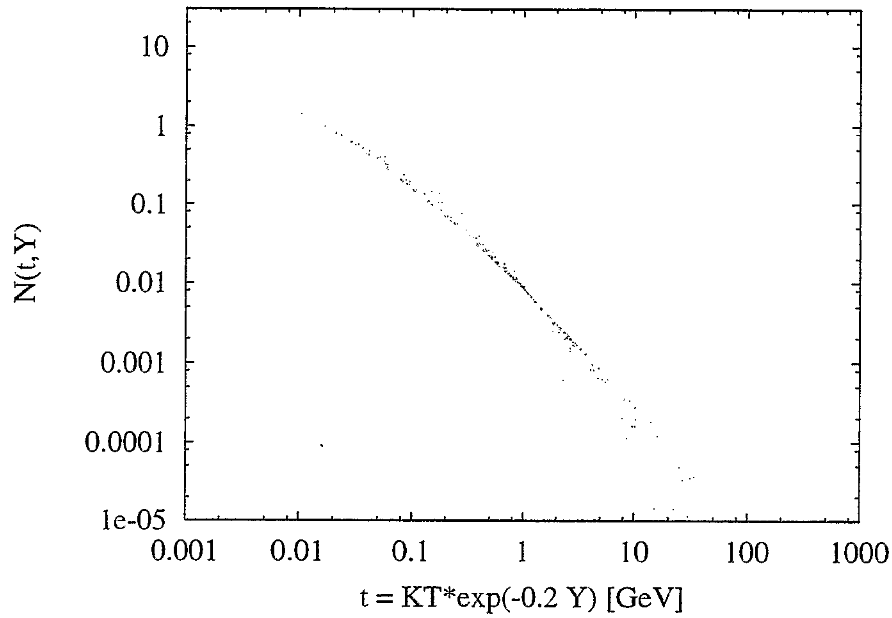

$Y > 4$, all k_T

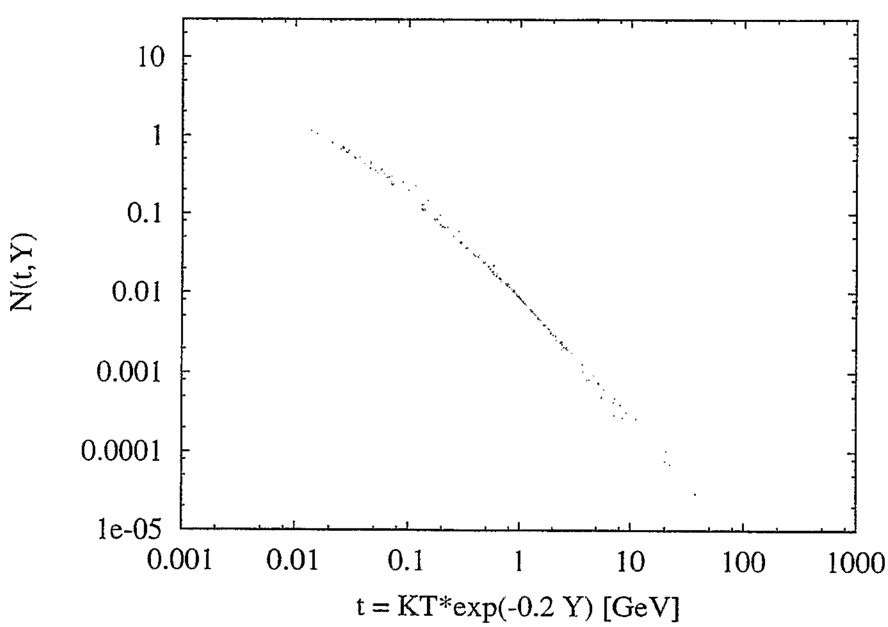

Gluon from Kovchegov equation with $\alpha_s = 0.1$

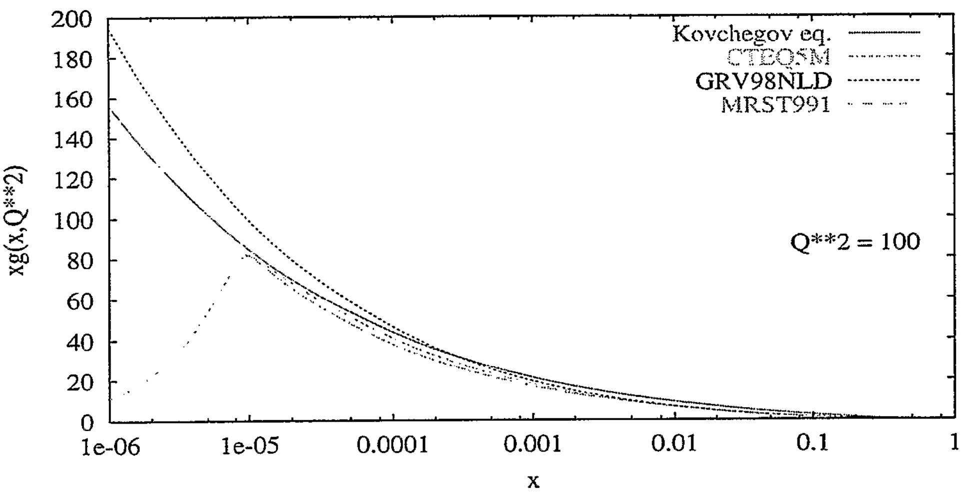

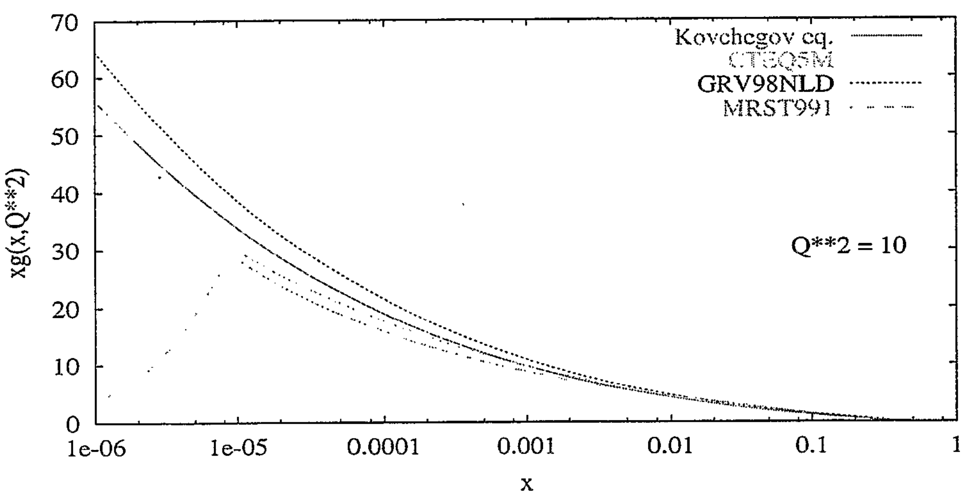

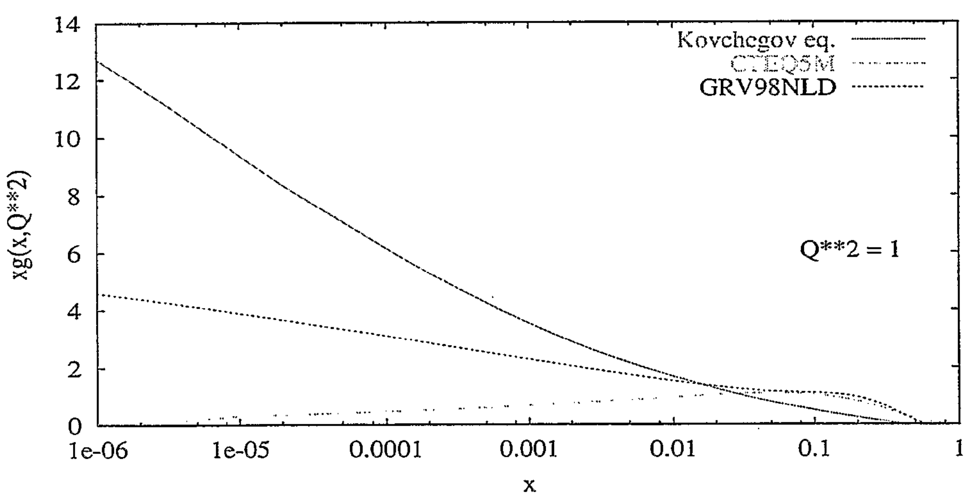

Shadowing from Kovchegov equation with $\alpha_s = 0.1$

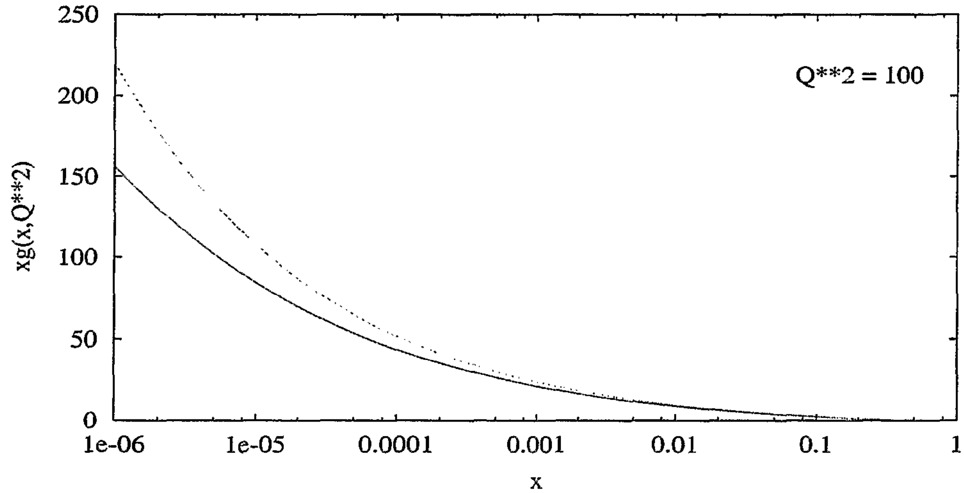

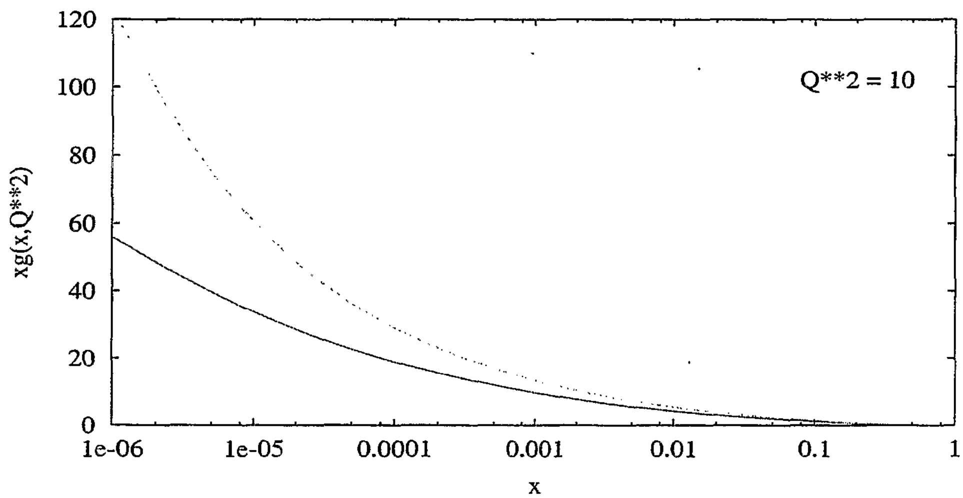

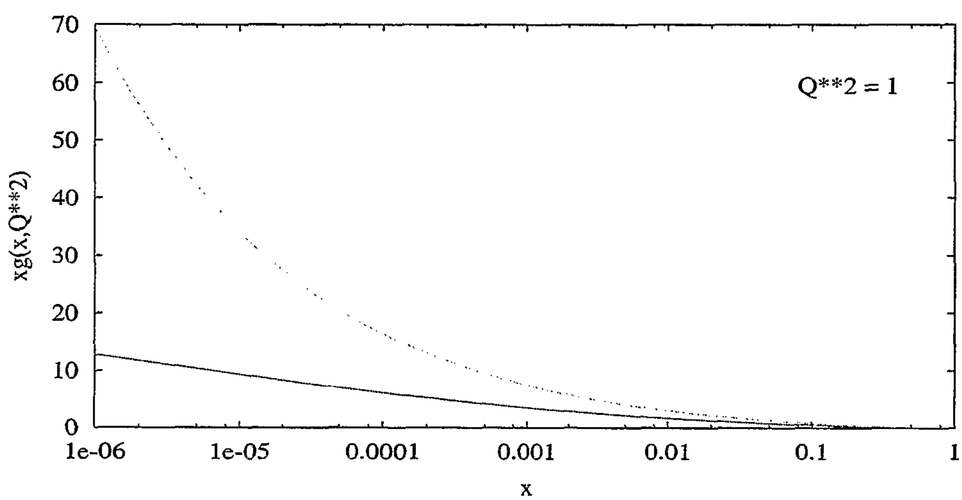

Comparison of solutions with running and fixed α_s at high Y

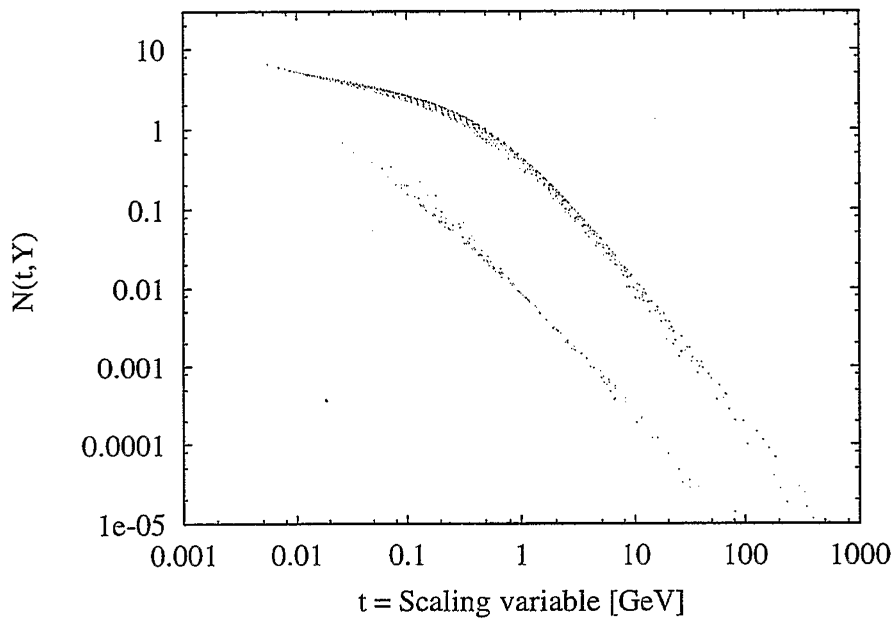

High energy hadron-hadron scattering in a functional integral approach

(O. Nachtmann, Univ. Heidelberg)

Total and differential cross sections for high energy and small momentum transfer elastic hadron-hadron scattering are studied in QCD using a functional integral approach. The hadronic amplitudes are governed by vacuum expectation values of lightlike Wegner-Wilson loops, for which a matrix cumulant expansion is derived. The cumulants are evaluated within the framework of the Minkowskian version of the model of the stochastic vacuum. Using the second cumulant, we calculate elastic differential cross sections for hadron-hadron scattering. The agreement with experimental data is good.

We calculate high-energy photoproduction of the tensor meson $f_2(1270)$ by odderon and photon exchange in the reaction $\gamma + \mathrm{p} \to f_2(1270) + \mathrm{X}$, where X is either the nucleon or the sum of the N(1520) and N(1535) baryon resonances. Odderon exchange dominates except at very small transverse momentum, and we find a cross section of about 20 nb at a centre-of-mass energy of 20 GeV. This result is compared with what is currently known experimentally about f_2 photoproduction. We conclude that odderon exchange is not ruled out by present data. On the contrary, an odderon-induced cross section of the above magnitude may help to explain a puzzling result observed by the E687 experiment.

Some refs. Ann. Phys. 209, 436 (91)
E. Berger, O. N. hep-ph/9808320
E. Berger et al. hep-ph/0001270
H.G. Dosch et al. P.R. D50, 1992 (94)

1 Introduction

- Ideas on non trivial vacuum structure of QCD
  (Savvidy '77, Shifman, Vainshtein, Zakharov 78, Shuryak, Nielsen, Ambjorn, Oleson, ...)
  spaghetti-vacuum, instanton vac. ,...

- Consequences for highenergy scattering?
  (Ellis, Gaillard, Zakrzewski '79,
  Dorià, Frenkel, Taylor '80,
  Reiter, O.N. '84)

  - soft hadronic reactions
  - hard reactions: Drell-Yan process
  - soft photons in hadronic reactions
  - electromagn. formfactors of hadrons at small Q^2

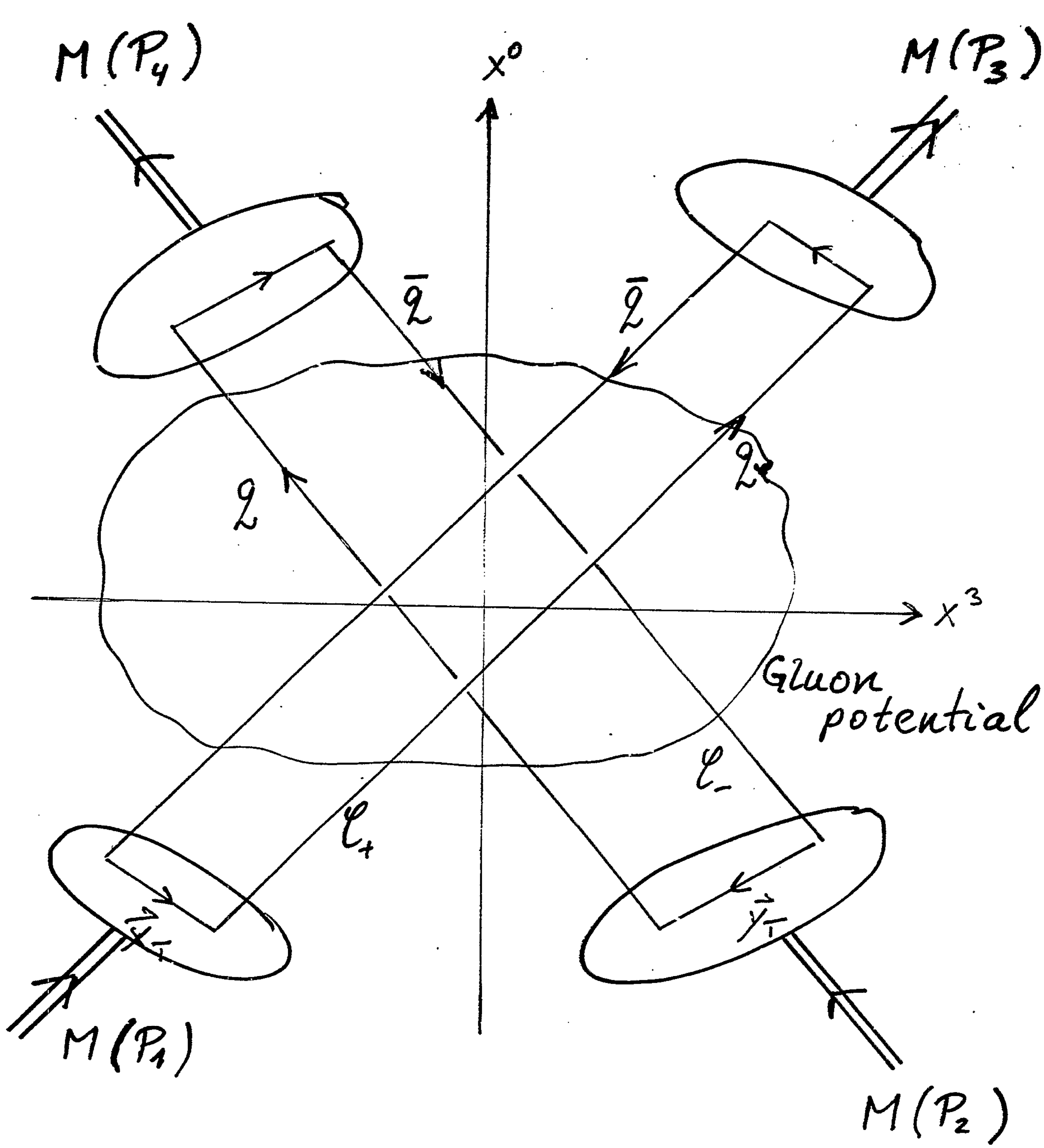

Scatt. ampl. $\propto \quad W(C_+)\, W(C_-) - 1$

$$W(C_\pm) = \mathrm{Tr}\; P\exp\left[-ig \int_{C_\pm} dx^\mu G_\mu(x)\right]$$

$$M_1(P_1) + M_2(P_2) \longrightarrow M_1(P_3) + M_2(P_4)$$

$$\mathcal{T}_{fi} = -2is \int d^2 b_T \, e^{i \vec{q}_T \vec{b}_T}$$

$$\int d^2 x_T \, d^2 y_T \;\; w_1(\vec{x}_T) \;\; w_2(\vec{y}_T)$$

$$\Big\langle W_+\left(\tfrac{1}{2}\vec{b}_T, \vec{x}_T\right) W_-\left(-\tfrac{1}{2}\vec{b}_T, \vec{y}_T\right)$$

$$-1 \Big\rangle_{\text{Gluon average}}$$

- Scattering amplitude

  ~ correlation function of lightlike Wegner Wilson loops

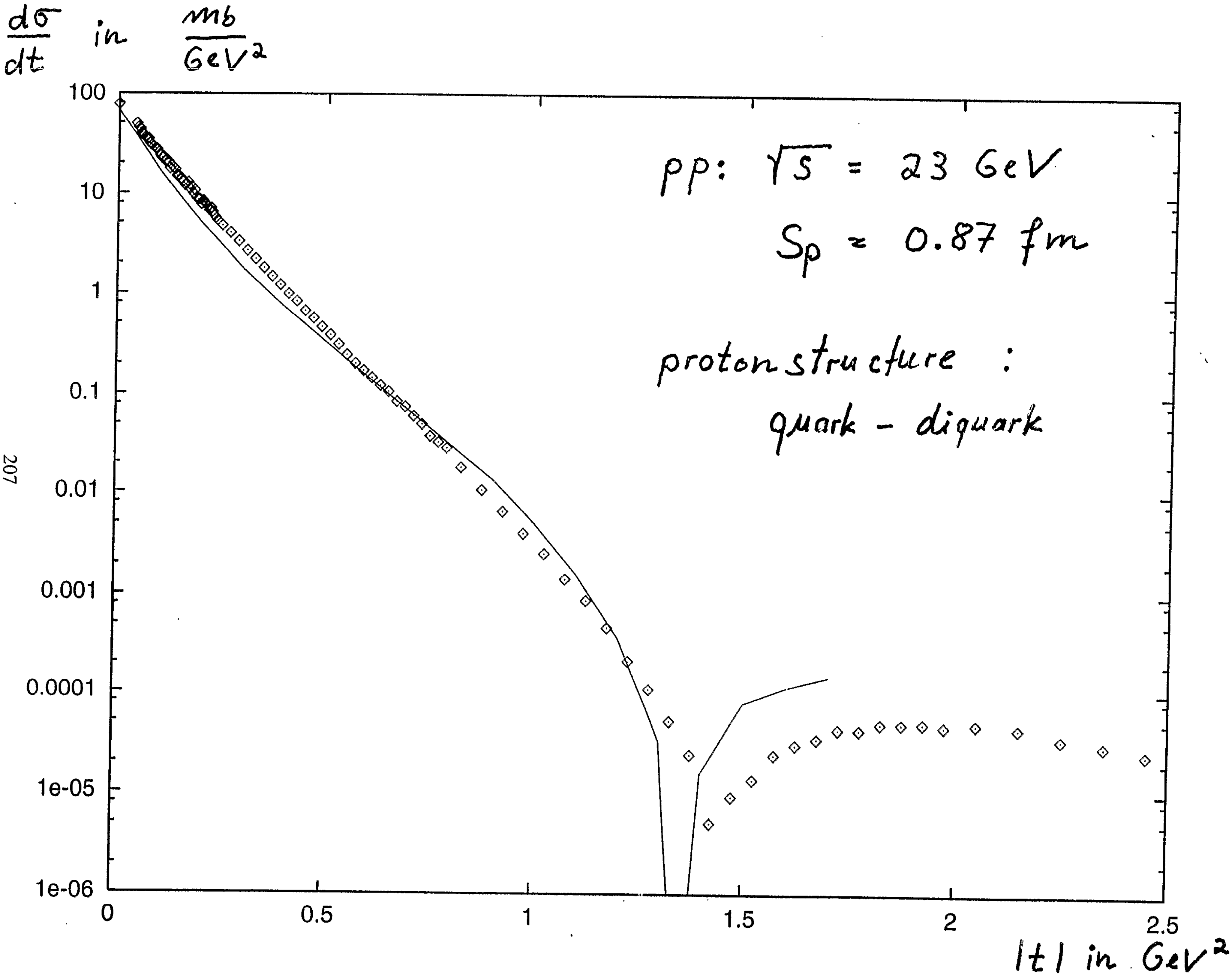

$\frac{d\sigma}{dt}$ in $\frac{mb}{GeV^2}$
100
10
1
0.1
0.01
0.001
0.0001
1e-05
1e-06
0
0.5
1
1.5
2
2.5
$|t|$ in GeV^2
pp: $\sqrt{s}$ = 23 GeV
$S_p \approx 0.87$ fm
protonstructure :
quark - diquark

parameter	lattice calc., quenched	SVM stat. pot.	high energy scattering	
(string tension)$^{1/2}$ $\sqrt{\varrho}$ / MeV	$\underline{420}$	415	435	
gluon cond.)$^{1/4}$ $G_2^{1/4}$ / MeV	486 ± 6	$\underline{486}$	(529)	related to ϱ by SVM
non abelian par. $\varkappa$	0.89 ± 0.02	$\underline{0.89}$	0.74	
correlation length a / fm	0.33 ± 0.01	$\underline{0.33}$	0.32	

$\underline{\qquad}$: input

The Instanton/Sphaleron Mechanism of High Energy Hadronic and Heavy Ion Collisions

Edward V. Shuryak
Department of Physics and Astronomy
State University of New York, Stony Brook, NY 11794-3800

We argue that if the *growing* part of hadron-hadron cross section (described phenomenologically by the $\alpha(0) - 1$ of soft Pomeron) is due to instanton/sphaleron mechanism, as suggested recently. In essence, if the parton collisions happens nearby tunneling event (described semiclassically by instantons) some wee partons can be absorbed by it. The resulting field configuration is close to sphaleron-like spherically symmetric gluomagnetic cluster, which then explodes into several gluons.

New element of the talk is discussion of quark effects. We conjecture that sphaleron decay should go into the same hadronic states as do instanton-induced decays of of $J^P = 0^+, 0^-$ *colorless* objects: (i) the scalar glueball candidate $f_0(1710)$ who decay mostly into η, η and $\bar{K}K$; or (ii) as suggested by Bjorken, $\eta_c \to KK\pi, eta\pi\pi, eta'\pi\pi$. Common signature of these final states is unusually large fraction of "delayed pions" coming from η, eta', K_S decays. This correlates well with experimentally observed but unexplained *decrease* of HBT correlation parameter λ from its usual value ≈ 0.5 to ≈ 0.2 in high multiplicity events.

Instanton mechanism should be even more important for high energy heavy ion collisions in the RHIC energy domain, where it is no longer a rare process, due to very large number of parton-parton collisions. We predict production of of the order of a hundred produced sphalerons per unit rapidity. Unlike perturbative gluons (or mini-jets), these *classically unstable* objects promptly decay into several gluons, quarks and antiquarks, leading to very rapid entropy generation. This may help to explain why the QGP seem to be produced at RHIC so early. We further argue that this mechanism cannot be important at higher energies (LHC), where the relevent scale is expected to go above 1 GeV and the perturbative description should apply.

Instanton/sphaleron mechanism of high energy hadronic and heavy ion collisi

E.V.Shuryak
SUNY Stony Brook

- – Introduction: the "substructure scale"
- – Instanton liquid, properties, counting rules
- – Elastic scattering
- – Inelastic scattering: multi-gluon production, unitarization
- – Evaluating Soft Pomeron parameters, Δ, α'
- X – The Sphaleron and its decay
- – Instanton/sphaleron mechanism for heavy ion collisions at RHIC
- Sphaleron + (fermions from 't Hooft vertex)
  ⇒ What are hadronic final states?
  ⇒ Do they have special features?
  ⇒ Can those be found experimentally

Qualitative Pictures

anti-instanton

instanton

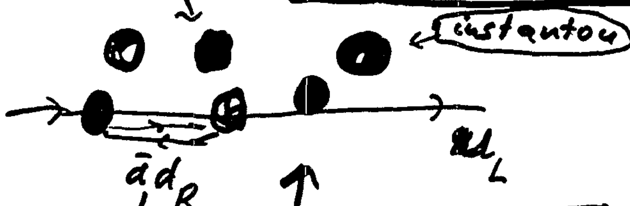

One quark in the instanton vacuum...

Quark moves through the instanton vacuum. (Note: Sea quarks are opposite in flavor and chirality!) and becomes a constituent quark, $m_{eff} \simeq 400$ MeV

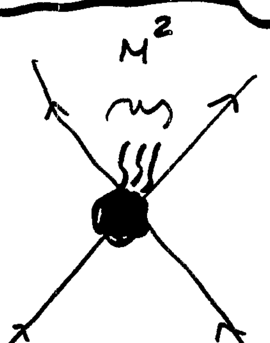

Two quarks collide near the instanton...

If 2 partons collide $\Rightarrow$ Instantons transform some of their field into a different form which is emitted

sphaleron

contin...

Low energy

Optimal energy

High Energy

At zero energy instanton cannot produce!
$E^2 = -B^2,\ E^2+B^2=0$

?

"Unitarization"

$$\kappa_0 B \kappa_0 \qquad \kappa_0 B \kappa_0 B \kappa_0 B \kappa_0$$

(a la Shifman, Maggiore...)

$$\frac{\kappa_0 B(M)}{1+\kappa_0^2 B^2(M)}$$

contains multi... phase... and ... with ...

• What the instanton-induced clusters should look like? (in NN, not AA.

hadrons

g, q in Q

I

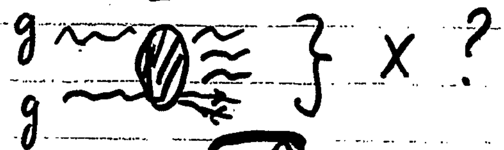

• $\boxed{J^P} = 0^+,\ 0^-$ but not 2^+

$(G^2_{\mu\nu}), (G\tilde{G})$

large for instanton

$(G_{\alpha\beta}G_{\beta\gamma} - \frac{1}{4} g_{\alpha\beta} G^2)$

→ 0 for instanton fie

• $\boxed{\text{Color}}$ $8 \otimes 8$, even if multi-gluon processes resu (NSZ)

actually both gluons ∈ to one SU(2)

$3 \otimes 3 = 1 + 3 + 5$

$\boxed{J=0}$ 1 2

• For color singlet we have phenom. info:

$\boxed{0^+}$ $J/\psi \to \gamma + (g\,g)$

$(G^2_{\mu\nu})$

↓ scalar glueball

• Prominent resonance (Mark III) with very strong coupling to (GG)

• $f_0(1710)$

↓

$\eta\eta$ large

KK large

$\pi\pi$ seen but small

• Was discussed by itself: ES 2000, Kharzeev, Levin 2000

Contribute to $\Delta(0) \approx 0.05$ or so!

$\boxed{0^-}$ $J/\psi \to \gamma + (gg)$

$(G\tilde{G})$

↳ η', or η, or η_c

Nobody ha seen the PS glueball

$\boxed{\eta_c}$ is especially interesting

2.9 GeV

J.Bjorken, hep-ph/00

• All multiparticle modes, except the following 3:

• $KK\pi$

• $\eta'\pi\pi$

• $\eta\pi\pi$

each ≈ 5% | no $\pi\pi\pi$

$(\bar{u}u)(\bar{d}d)(\bar{s}s)$

↑ ↑ ↑

Fits to 't Hooft Lagrangian

?

- Is there any special signature of instanton-induced clusters? (Distinct from mini-jets!)
- If so, can it be observed?

Yes
- Presence of $\bar{s}s$ and strong dominance of PS mesons leads to $\bar{K}K$, or η', η
- All of them lead to <u>delayed pions</u>

$K_s K_s \to 4\pi \qquad \eta \to 3\pi \qquad \eta' \to \pi\pi\eta \to 5\pi$

unable to participate in HBT correlations with <u>promptly produced</u> pions! Prob(delayed π) $\simeq 0$

<u>For comparison:</u> In the usual string breaking those are also produced, but <u>much</u> less prominently

$\boxed{\text{Prob}(\text{delayed } \pi) \simeq 0.3} \Longleftrightarrow \boxed{\lambda_{HBT} = (1-0.3)^2 \simeq 0.5\,!}$

b.d.w. Significantly from $\omega \to 3\pi$

Indeed observed in the usual pp, heavy ions, e^+e^-. Always the same!

So, let us look at λ_{HBT} as <u>multiplicity goes up</u>

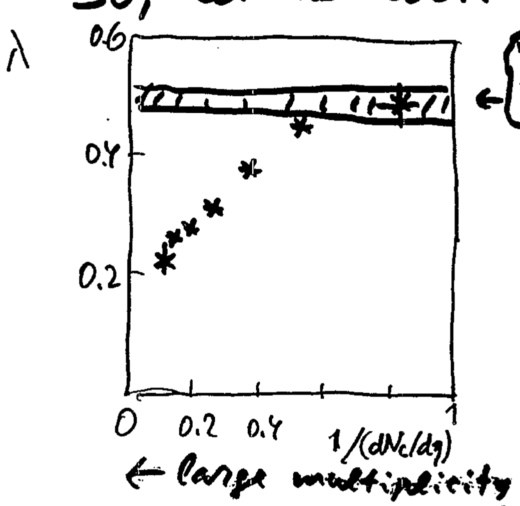

From Buschbeck et al hep-ex/0003029

?

Huge effect has been seen already!

(no other explanation???)

$\lambda = 0.2$ means Prob(delayed π) = 0.55

Phenomenological Summary

Mini-jets vs Instanton-induced Clusters

• In hh'

→ Both can explain growth of $\sigma(s)$, multiplicity rise ...

CORRELATION

→ Mini-jets can be looked for as clusters in (θ, φ) statistically ...

→ Instanton-induced clusters, $M = 2.5$-3 GeV, isotropic $\Delta y \sim 1$, but $\Delta\varphi = 2\pi$

HBT

→ Mini-jets are expected to fragment as string fragm.
  → Standard $\lambda \approx 0.5$ and standard η/π, η'/π, K

→ Enhanced η', η, K, λ_{HBT} decreases, as observed!

• In AuAu etc

→ Both can explain multiplicity growth, and why there appears new component at RHIC $\sim N_{coll}(b)$ (instead of $\sim N_{part}(b)$)

→ Minijets with a cutoff from pp fit (HIJING) lead to $\frac{dN}{dy} \sim 200$ <u>minijets</u> (central AuAu at RHIC)
It is <u>not enough</u> for <u>collective effects</u> and <u>jet quench.</u>

?

→ Instanton-induced reactions (into QGP, no hadrons, with similar cross section

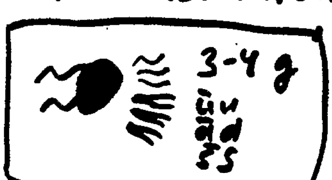

leads to: <u>much higher entropy</u>!

and may solve <u>quark production</u> problem

Classical Gluon Production in Hadronic Collisions

Gregory W. Carter [1]

Department of Physics and Astronomy, SUNY Stony Brook, NY 11794-3800.

Abstract

The instanton liquid model of the QCD vacuum has been rather successful in describing low-energy phenomenology. Recent work suggests these localized, classical solutions of the gauge field play a role in the semi-hard processes relevant to hadron-hadron and heavy ion collisions. Specifically, the high-energy growth in inelastic partonic cross sections might be due to partons probing instantons. Excited by the energetic partons, an instanton may be transformed from a Euclidean vacuum tunneling event into a color magnetic configuration which sits atop the barrier – a *sphaleron* – and decays into perturbative gluons.

We have derived and solved the field equations for the intial sphaleron state and, drawing from work done on electroweak sphaleron decays, estimate its decay will produce roughly 6 gluons after a time of 1.5 fm/c.

[1]Based on work done in collaboration with E. V. Shuryak.

THE INITIAL STATE

A STATIC, UNSTABLE CLASSICAL SOLUTION:

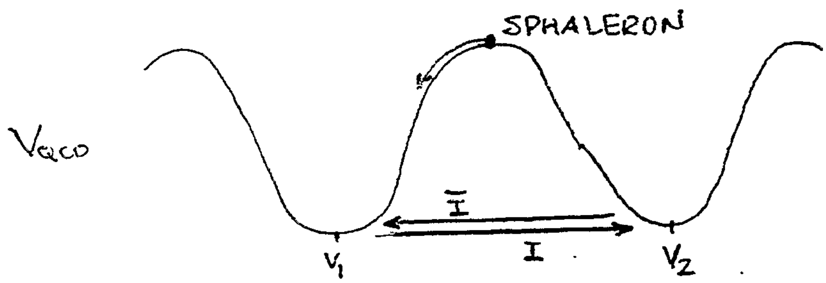

AS THE SPHALERON ROLLS DOWN THE HILL TO V_1, IT DECAYS INTO GLUONS.

TOPOLOGICAL CHARGE:

$$Q_{inst} = \pm 1$$

$$Q_{SPH} = \pm \frac{1}{2}$$

THE STATIC, CLASSICAL SOLUTION:

USING WITTEN'S NOTATION PRL 38 (1977) 121.

$$A_0^a = \frac{x^a}{r} A_0$$

$$A_j^a = \frac{1+\varphi_2}{r^2} \epsilon_{jak} x_k + \frac{\varphi_1}{r^3}(\delta_{ja} r^2 - x_a x_j) + A_1 \frac{x_a x_j}{r^2}$$

ONE HAS

$$S = -\frac{1}{4}\int d^4x\, F^2$$

$$= -8\pi \int_{-\infty}^{\infty} dt \int_0^{\infty} dr \left[\frac{1}{8} r^2 F_{\mu\nu}^2 + \frac{1}{2}(D_\mu \varphi_i)^2 + \frac{1}{4r^2}(1-\varphi_1^2-\varphi_2^2)^2 \right]$$

$$\mu,\nu = 0,1 \quad i=1,2 \quad D_\mu \varphi_i = \partial_\mu \varphi_i + \epsilon_{ij} A_\mu \varphi_j$$

$$F_{\mu\nu} = \partial_\mu A_\nu - \partial_\nu A_\mu$$

SIMILAR TO 2-D ABELIAN HIGGS.

FOR A COLOR MAGNETIC SOLUTION, WE CONSIDER

$$A_0 = A_1 = \varphi_1 = 0, \quad \partial_0 \varphi_2 = 0$$

AND SOLVE FOR φ_2 IN 1+1 D.

TIME EVOLUTION

OUR SOLUTION RESEMBLES THAT OF KLINKHAMER + MANTON PRD 30 (1984) 2212 FOR ELECTROWEAK PHYSICS.

DECAY WAS STUDIED BY ZADROZNY PLB [illegible] (1992) [illegible] AND HELLMUND + KRIPFGANZ NPB 373 (1991) 749.

THE SPHALERON EXPANDS AS A SHELL; FREE FIELD BEHAVIOR IS EVENTUALLY OBSERVED $\Rightarrow$ $W^{\pm}$, Z, AND HIGGS BOSONS.

COMPARING OUR RESULT WITH THE ELECTROWEAK, WE CAN ESTIMATE N_{gluons}

ENERGY (CALCULATED NUMERICALLY)

$$E_{EW} \simeq 108\, M_W \qquad E_{QCD} \simeq 63\, \frac{m}{g^2}$$

PARTICLE NUMBERS

$$N_{EW} \simeq 51 \approx \frac{1}{2} \frac{E_W}{M_W}$$

SO $\quad N_{GLUONS} \approx \dfrac{1}{2} \dfrac{E_{QCD}}{m}$

$$\boxed{N_{GLUONS} \approx 5-6}$$

DECAY TIME

$$\tau_{EW} \approx 4.5\, M_W^{-1}$$

SO $\quad \tau_{QCD} \approx 4.5\, m^{-1}$

$$\boxed{\tau_{QCD} \approx 1.5\ \mathrm{fm}/c}$$

NOW WE SPECULATE:

HOW MANY IN A-A COLLISIONS?

$$\frac{dN_{PROMPT}}{dy} \simeq 200$$

SHURYAK'S MAXIMAL ESTIMATE FOR CENTRAL COLLISIONS AT RHIC hep-ph/[illegible]

TOTAL GLUON PRODUCTION:

$$\frac{dN_{GLUONS}}{dy} \approx 1000.$$

THIS, AN ESTIMATE OF THE MAXIMUM PRODUCTION FROM THE SPHALERON MECHANISM, IS IN LINE WITH THE RHIC DATA.

THUS OUR ESTIMATES SUGGEST THAT THE DECAY OF TOPOLOGICAL OBJECTS IN QCD MIGHT PLAY A ROLE IN GLUON PRODUCTION IN HIGH-ENERGY COLLISIONS.

Saturation 101 (Discussion: Thursday, 5/24/01)

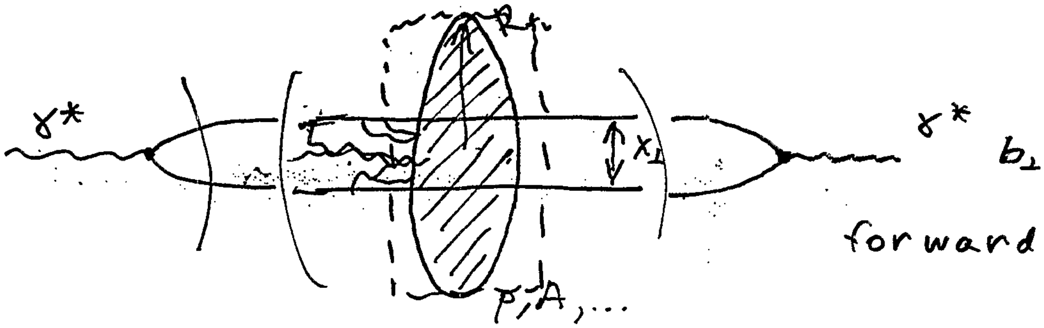

forward amplitude

$$\sigma^{\gamma^* p} \propto \int d^2x_\perp \, dz \; \Phi^{\gamma^* \to q\bar{q}}(x_\perp, z) \cdot \hat{\sigma}^{q\bar{q}p}(x_\perp, W^2)$$

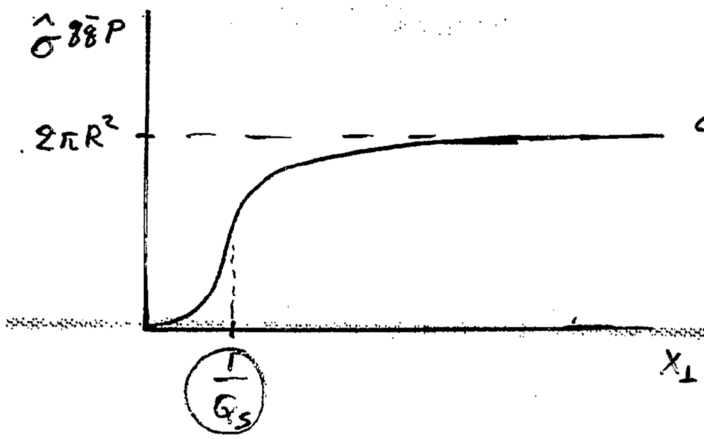

← black disk, can not be exceeded

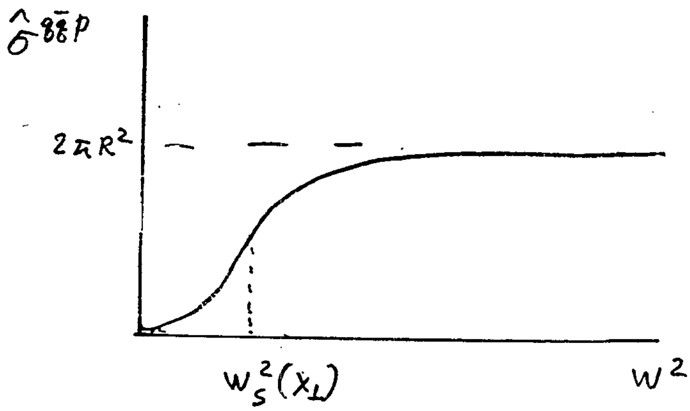

At very high W^2 the cross sections saturate.

The transition is described by "saturation scale" Q_s.

$$Q_s^2(W^2, A) \sim (W^2)^{(\alpha_P - 1)} A^{1/3} \gg \Lambda^2_{QCD}$$

Saturation 102

What does this mean for gluon distributions?

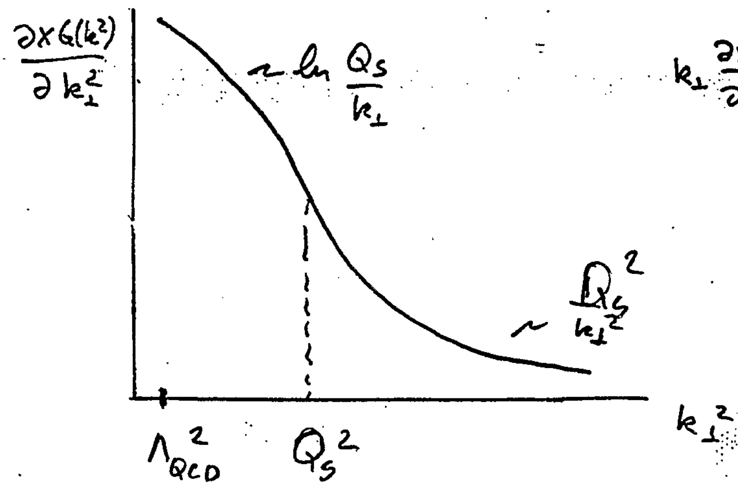

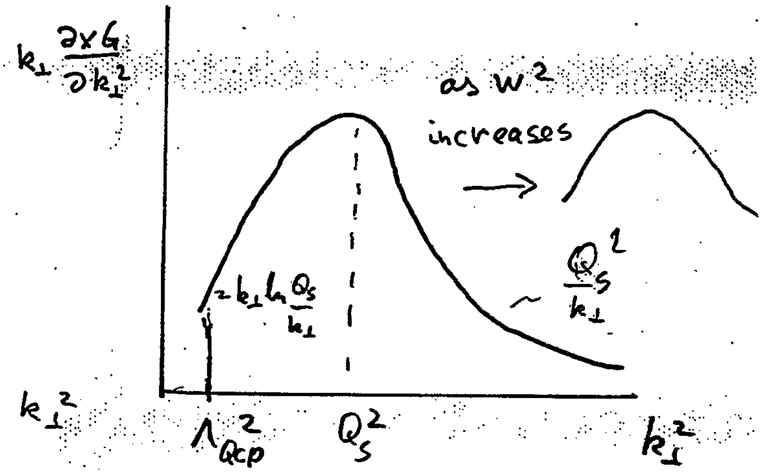

$\Rightarrow$ Most gluons have $k_\perp \sim Q_s \gg \Lambda_{QCD}$ thus the gluon distribution is insensitive to non-perturbative region, and $\alpha_s(k_\perp \sim Q_s) \ll 1$ allowing us to calculate things analytically from first principles QCD!

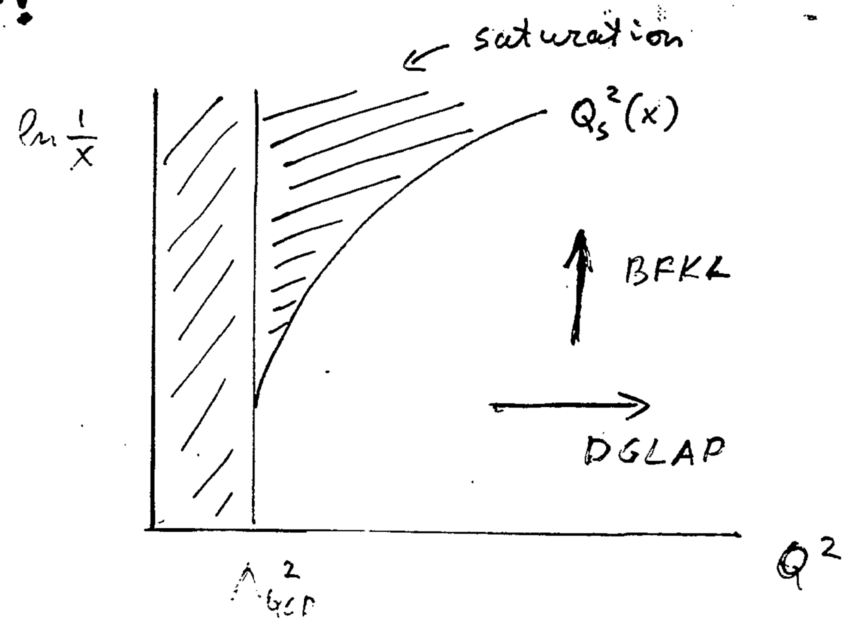

Experimental signals of (no) saturation at HERA.

(et al)

$\Rightarrow$ all small-x and small-Q^2 data could be described by saturation models (as well as by DGLAP and/or Pomerons). The difference is that unlike DGLAP-based approach saturation does not assume much about non-perturbative region and unlike Pomerons/Reggeons is QCD-based.

① DGLAP-based fits work, but usually have

$x\,G(x,\ Q^2 \sim 1\,\text{GeV}^2) \lesssim 0.$ $\quad (Q_s = Q_s(W^2)\ ?$

Is this good / consistent / reasonable ?

② Saturation predicts $F_2 \sim Q^2 R^2 \ln \frac{1}{x}$ $\quad \begin{pmatrix} \text{small } x \\ \text{small } Q^2 \end{pmatrix}$

(i) with diffusion $F_2 \sim (R + a \ln \frac{1}{x})^2 \ln \frac{1}{x} \sim \ln^3 \frac{1}{x}$

(other models? hard to distinguis ... ?)

D. Haidt
has a parametr.
maybe not unique (?)

(ii) $F_2 \sim Q^2$, $\frac{\partial F_2}{\partial \ln Q^2} \sim Q^2$ (small Q^2)

$Q^2 < Q_s^2$

gauge invariance?

vector mesons? $\sim W^{2(\alpha_P - 1)}$

in saturation the region $Q^2 < Q_s^2 \sim A^{1/3}$ unlike ?

need an eA collider?

(3) Diffraction : $\left.\frac{\sigma_D}{\sigma_{tot}}\right|_{\text{fixed } Q^2} \sim \text{const}\,(W^2)$

Saturation: $\sigma_D \underset{Q^2\to\infty}{\sim} \int_{1/Q^2}^{1/Q_s^2} \frac{dx_\perp^2}{x_\perp^4}\left(x_\perp^2\, xG\right)^2 \sim \frac{(xG)^2}{Q_s^2} \sim xG$

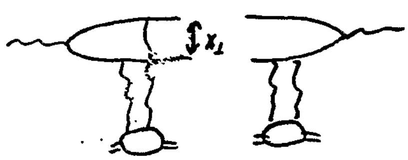

as $Q_s^2 \sim xG$

since $\sigma_{tot} \sim xG \ln\frac{Q^2}{Q_s^2} \Rightarrow \boxed{\frac{\sigma_D}{\sigma_{tot}} = \frac{1}{2\ln\frac{Q^2}{Q_s^2}}}$

Simple explanation of GBW fit.

(4)

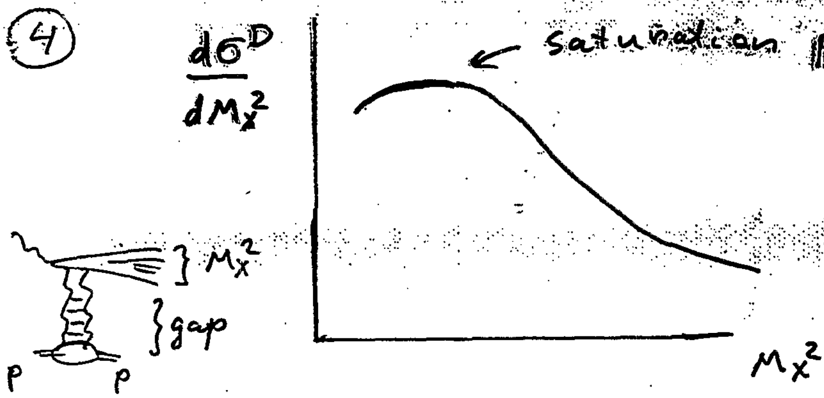

saturation predicts leveling off or even a turnover at high W^2 at lower (but still large) M_X^2

(5)

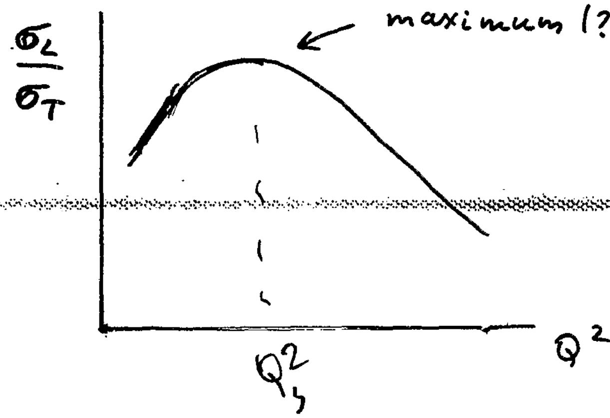

maximum (?) ≈ saturation prediction

(6) Saturation $\Longleftrightarrow$ strong gluonic fields $A_\mu \sim \frac{1}{g}$

$\rightarrow$ strangeness enhancement in both pA and AA

even in pp! (with large multiplicity $\Rightarrow$ extreme conditions) NA49 NA50

$\longrightarrow$ J/ψ production / suppression $m_c \sim 1.5$ GeV $m_{J/\psi} \sim 3$ GeV

$Q_s^2 \sim 2$ GeV^2

7 Scaling $\sigma = \sigma\left(\frac{Q}{Q_S(W^2)}\right)$

(Motyka's talk)

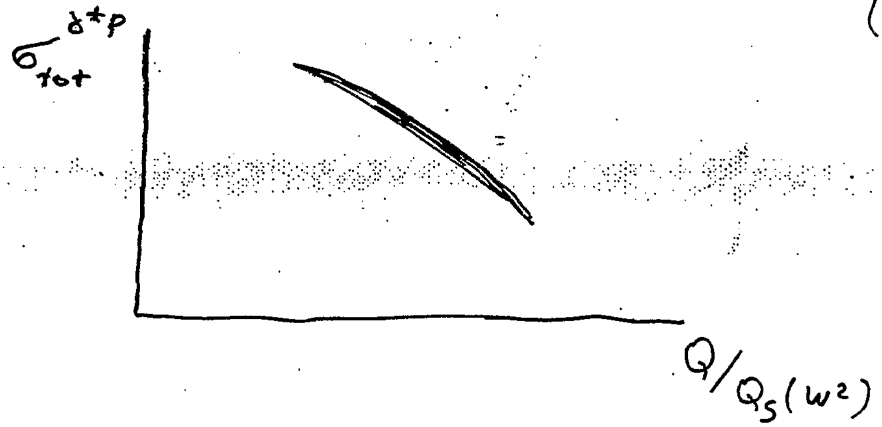

8 Slope of vector meson production
Shrinkage of diffractive peak
α' does not vanish at large Q^2.

Summary of the Discussion on Pomeron Physics Program at RHIC

Summary by Wlodek Guryn, BNL

(Discussion leader Dima Kharzeev, BNL)

The general questions for the discussion were:

1. What (if any) are the <u>fundamental physics questions</u> that make diffractive interactions at high energies worth studying?

2. What (if any) are the measurements that can be done at RHIC to address these questions?

3. How (if at all) will the measurements with $p^{\uparrow}p^{\uparrow}$, pA, AA advance the field?

At present the diffraction studies at RHIC are focused around pp2pp experiment. Some of the questions are addressed in the approved physics program of the pp2pp experiment. Some, like central glueball production, could be addressed by combining the Roman pots of the pp2pp experiment with the existing HI RHIC detectors. A dedicated study of this was strongly endorsed by the workshop participants.

In the following are specific questions and the summary of the discussion.

1. What is the high energy asymptotics of strong interactions: does it satisfy Froisssart-Martin bound, which requires that $\sigma_{tot} < \pi/m_{\pi}^2 \log^2 s$?

The most popular fit to the present data shows that σ_{tot} grows like s^{Δ}, violating Froissart-Martin bound. One of the reasons why the simple parametrization $\sigma_{tot} \sim s^{\Delta}$ is successful describing data is poor accuracy of high-energy points. It is important to point out that even though there are higher energy data available from Tevatron at $\sqrt{s} = 1800$ GeV, the two existing data points differ significantly enough so that the ambiguity in terms of asymptotic behavior of total cross sections persists. In short there is a great need for accurate pp data from RHIC. Given that maximum $\sqrt{s} = 500$ GeV at RHIC, which is in the range where one expects that σ_{tot} (pp) is measurably different from σ_{tot} (pp), a very precise measurement of both σ_{tot}(pp) and ρ parameter may reveal that a different functional form is needed for the fit, which could ultimately satisfy Froissart-Martin bound.

2. What is the difference between high-energy interactions of particles and antiparticles? The Pomeranchuk theorem predicts that asymptotically, with increasing energy the total cross sections for particle-particle and particle-antiparticle converge to be the same. Odderen question?

As mentioned earlier RHIC energy range in where a sizable difference between pp and pp interaction exists. So it is the best place to study those differences, which are expected to show in the shape if differential cross section, especially in the dip region where the contribution of the Odderon exchange, the C odd partner of the Pomeron, is expected to show up. In addition cross sections for meson (photon) and nucleon – nucleus scattering can be studied as important part of the program of hadron-hadron interactions.

3. How does the range of strong interaction depend on energy? What is the size of the gluon cloud around the nucleon? How does it show in the slope of the Pomeron trajectory?

This question is studied at RHIC by measuring the energy dependence of σ_{tot} (pp), $d\sigma_{el}/dt$, σ_{diff}, $d^2\sigma_{diff}/dt\, d\xi$, ρ. Also in the polarized proton elastic scattering the hadronic spin-flip will be measured by measuring analyzing power $A_N(t)$ in the Coulomb Nuclear Interference (CNI) region.

4. What is the high parton density, high color strength asymptotic behavior of strong interactions?

These questions can be addressed by studying diffraction in pp, pA ($p^{\uparrow}A$?), AA, γA, "Meson"A collisions. This area of research is unique to RHIC because of its energy range and ability of using variety of colliding beams. However a detector in addition to Roman pots of pp2pp experiment to detect production of J/Ψ, η_c and other open charm particles would be needed. Also inclusive cc production with polarized proton beams could provide answers to the question.

5. Is the proton polarization transferred to the "wee" coherent gluon field?

The following measurements, which can be done uniquely at RHIC, will address the above question.

- Spin asymmetries in pp elastic scattering.
- Azimuthal correlations in $p^{\uparrow} p^{\uparrow} \rightarrow pp + X$, where $X=\Lambda\Lambda$, a self analyzing channel or investigating spectroscopy of X, in particular where X is a glueball.

6. What traces the baryon number (B) in high-energy interactions?

Few mechanisms of baryon number (B) transfer over large rapidity interval compete. The B of the projectile can be transferred to the central rapidity region either by a diquark, a valance quark or even by gluons. Available data for pp collisions from the ISR at CERN are limited by $\sqrt{s}$= 62.8 GeV. New data at much higher energies are desperately needed to clarify relative role of different mechanisms. Good understanding of this dynamics is vital to our understanding of baryon stopping mechanism in heavy ion collisions.

Following is a table summarizing the discussion:

Physics Question	Can RHIC answer this question?	Comment
1. What is the high-energy asymptotics of strong interactions: does it satisfy Froisssart bound requiring that $\sigma_{tot}<\pi/m_{\pi}^2\log^2 s$? How about the unitarity of the total cross-sections?	Maybe	Given Tevatron data, surprise is possible. pp2pp experimnet
2. What is the difference between high-energy interactions of particles and antiparticles?	Yes	pp2pp experiment
3. How does the range of strong interaction depend on energy? What is the size of the gluon cloud around the nucleon? (How does it show in the slope of Pomeron trajectory?)	Yes	pp2pp experiment
4. What is the high parton density, high color strength asymptotic behavior of strong interactions?	Yes, Unique	Requires "Central" Detector and Roman pots
5. Is the proton polarization transferred to the "wee" coherent gluon field?	Yes, Unique	Requires "Central" Detector and Roman pots
6. What traces the baryon number in high-energy interactions?	Yes	Requires Central Detector

HIGH ENERGY QCD BEYOND THE POMERON
WORKSHOP SUMMARY

George Sterman

THE POMERON

(Through the mists of time)

- Heuristics of the Pomeranchuk Theorem

Elastic Scattering

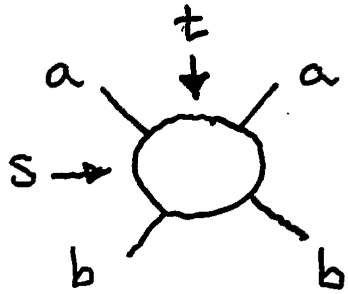

$f_{ab}(s,t)$

- Dispersion

$$f_{ab}(s,0) \sim \int \frac{ds'}{2\pi i} \frac{\operatorname{Im} f_{ab}(s,0)}{s-s'}$$

- Crossing

$f_{ab}(s,0) - f_{\bar{a}b}(s,0)$ bounded

- Optical Theorem

$$\sigma^{ab}_{tot}(s) \sim \operatorname{Im} f_{ab}(s,0)$$

$$\Rightarrow \quad \sigma^{ab}_{tot}(s) - \sigma^{\bar{a}b}_{tot}(s) \xrightarrow[s\to\infty]{} 0$$

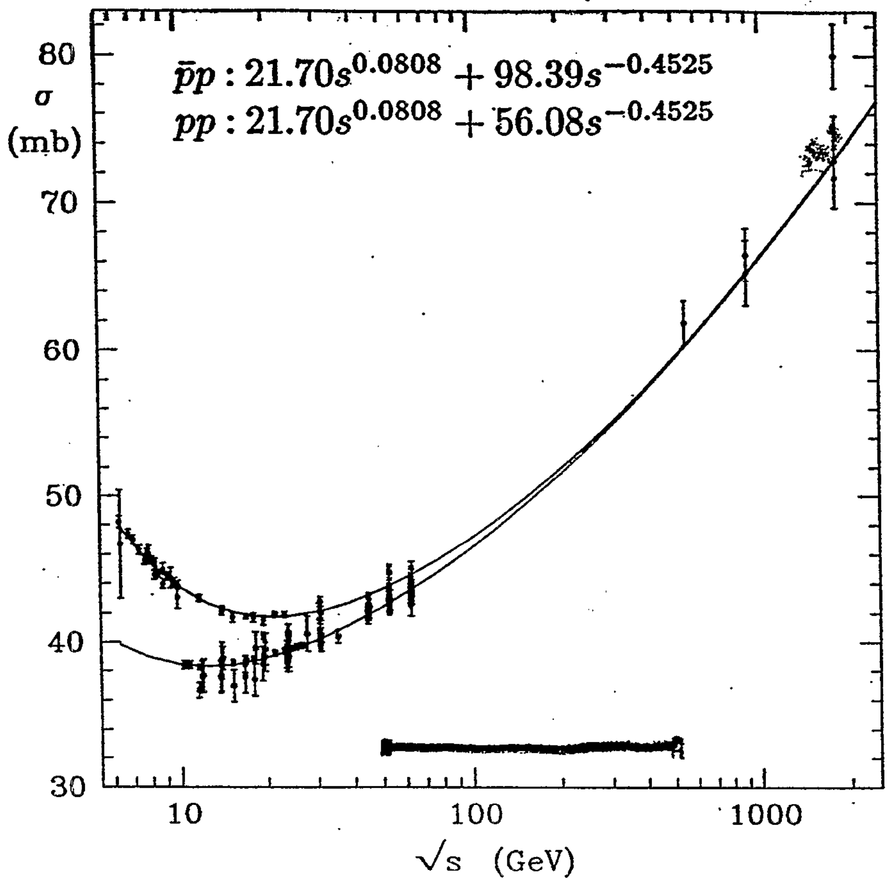

$\bar{p}p : 21.70s^{0.0808} + 98.39s^{-0.4525}$
$pp : 21.70s^{0.0808} + 56.08s^{-0.4525}$
σ
(mb)
80
70
60
50
40
30
10
100
1000
$\sqrt{s}$ (GeV)

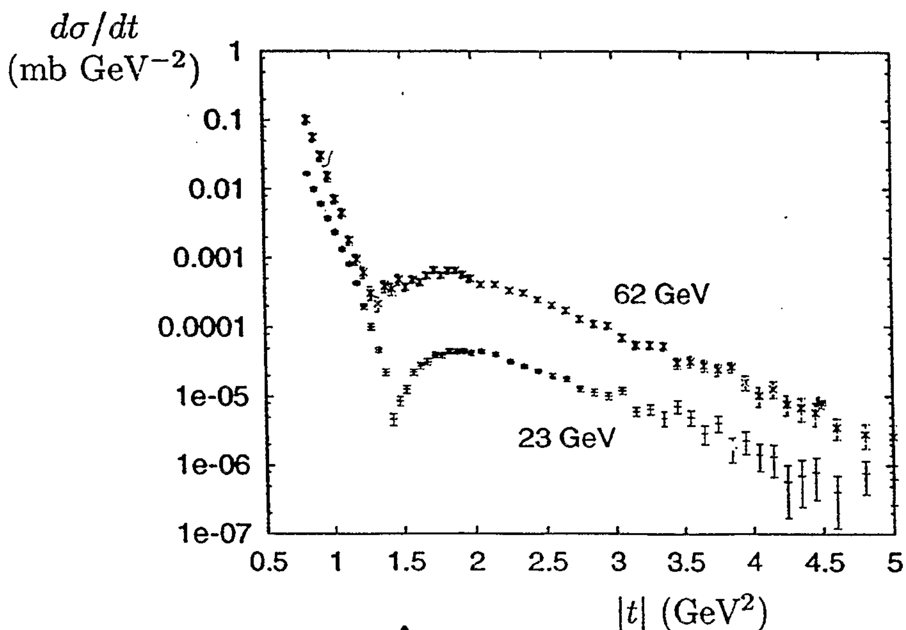

$d\sigma/dt$
(mb GeV^{-2})
1
0.1
0.01
0.001
0.0001
1e-05
1e-06
1e-07
0.5
1
1.5
2
2.5
3
3.5
4
4.5
5
62 GeV
23 GeV
$|t|$ (GeV^2)

SPIN AND S-DEPENDENCE

Tree exchange for particle spin σ

$f_{ab}(s,t) =$ 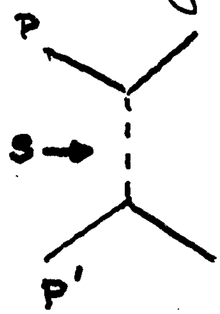

$$\sim \frac{1}{t} p_{\mu_1} \cdots p_{\mu_\sigma} \varepsilon^{\mu_1 \ldots \mu_\sigma}_{\nu_1 \ldots \nu_\sigma} p'^{\nu_1} \ldots p'^{\nu_\sigma}$$

$$\sim \frac{s^\sigma}{t}$$

Regge Generalization

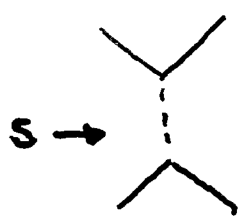

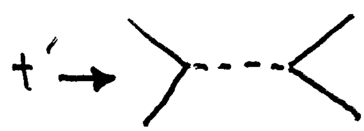

$$\frac{1}{t} s^{\alpha(t)-1} \qquad \frac{1}{t' - t_N}$$

$$\alpha(t_N) = N$$

'Reggeon'

(Linear) Trajectory

$$\alpha(t) = \alpha(0) + bt$$

Reggeons from Field Theory

Basic process (scalars)

$$\int \frac{dk^+}{2k^+} d^2k'_\perp \left| \right.$$ 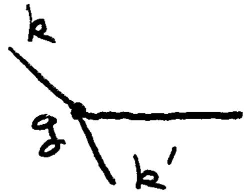

$$\left. \right|^2 \delta\left((k-k')^2\right)$$

$$\sim \underset{\substack{\uparrow \\ \dim m^2}}{g^2} \ln \frac{k^+_{max}}{k^+_{min}} \underbrace{\int \frac{d^2k'_\perp}{(k'^2_\perp + m^2)^2}}_{\alpha(0) \sim \frac{1}{m^2}}$$

Ladders

$$s \rightarrow \left| \right.$$ 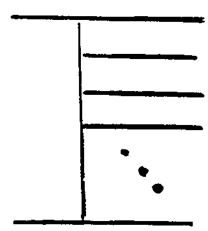 $$\left. \right|^2 \equiv$$ 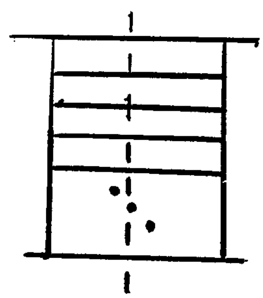 $$= \frac{\alpha^n(0)}{n!} \ln^n \frac{s}{m}$$

$$\swarrow$$

$$s^{\alpha(0)}$$

QCD

$$\int dk \left| \right.$$ 

$$\left. \right|^2 \sim \underset{\substack{\uparrow \\ \dim[1]}}{g_s^2} \ln \frac{k^+_{i+2}}{k^+_i} \underset{\substack{\uparrow \\ \text{dimensionless}}}{\int \frac{dk^2_{i\perp}}{k^2_{i\perp}}}$$

ENTER: THE REAL WORLD

Experiment

$$\sigma_{pp} \sim \sigma_{p\bar{p}} \sim s^{0.08+\alpha' t} + \# s^{-1/2} + \cdots$$

$\alpha' \sim 0.25 \text{ GeV}^2$

Donnachie
Landshoff

Hypothesis

This behavior due to the exchange of the 'Pomeron' ($\mathbb{P}$)

$\mathbb{P}$: $\sigma_{pp} \sim \sigma_{p\bar{p}} \to$ 'vacuum' quantum nos

$\mathbb{P}$: reggeon with $\alpha(0) \sim 1$

$\mathbb{P}$: 'pure' carrier of strong interactions

$\mathbb{P}$: No quantum numbers... Is it dull?

Not at all...

REGGE INFERENCE

See this: ⟹ Means this

$S^{\alpha_{\mathbb{P}}(t)-1}$ 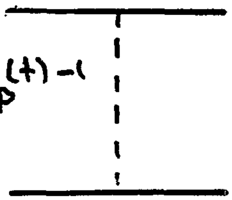 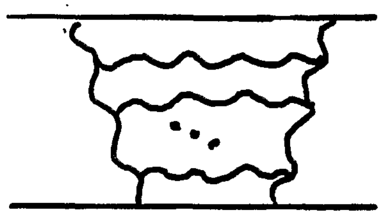

And this ← Encodes this

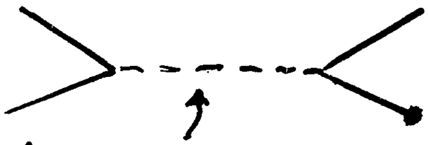 ← 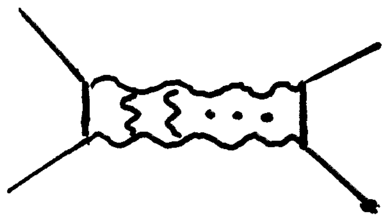

(2^{++} glueball?)

$\alpha_{\mathbb{P}}(?) = 2$

AND

Im 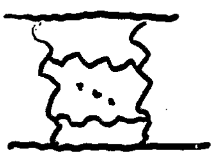 $= \sum_n \Big|$ 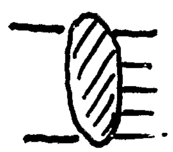 $\Big|^2_{n = p, \bar{p}, \pi, K, \Lambda \ldots}$

By carrying no label, $\mathbb{P}$ encodes all of the strong interactions ...

... including confinement

THE POMERON PROGRAM IN A NUTSHELL

Approach $\mathbb{P}$ from...

- Outside 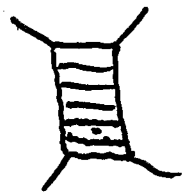 Elastic (polarized, unpolarized)

- Inside  Total (polarized, unpolarized)

- Inside and Out 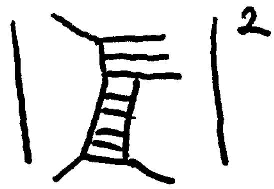 Diffractive (pol., unpol.; single, double; hard, soft)

- Inside-Out 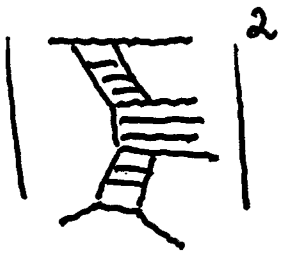 Double-$\mathbb{P}$ (pol., unpol.; hard, soft)

POMERON N.B.'s

- $\alpha > 0 \Rightarrow$ violation of unitarity (eventually)
  is our $\mathbb{P}$ the 'real' $\mathbb{P}$?

- diffractive σ: only 'part' of $\mathbb{P}$ at diffractive end
  may affect α, α'

- γ^* and other off-shell particles
  how to relate to $\mathbb{P}$ of 'normal' hadrons?

Each issue a center of theoretical debate, experimental tests...

- Is $\mathbb{P}$ 'wrong end of the stick': just 'shadow of everything that can happen'?

SEEKING OUT THE POMERON

- Rapidity

$$y = \frac{1}{2} \ln \frac{E + P_3}{E - P_3} \quad \left(\underset{m/E \to 0}{\sim} \eta = \ln \cot \frac{\theta}{2} \right)$$

$a + b \to a + b$ (forward scattering)

$P_b = - P_a$

$$Y = y_a - y_b \simeq 2 y_a = \ln \frac{s}{m^2}$$

(maximum y)

$$s^\alpha = \cancel{e^{\alpha Y}} \; e^{\alpha Y}$$

- Any large Y-interval $\to$

no particles but momentum transfer: diffraction; '$\mathbb{P}$' physics

Rapidity Gap 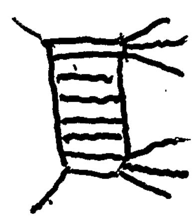

- Gap events have twice the power!

$\frac{d\sigma}{dM^2} \sim \Big|$ 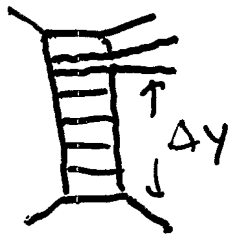

$\Big|^2 \sim e^{2(\alpha-1)\Delta y}$

(very cooperative)

- Role of high-multiplicity events:

  $2\langle n\rangle, 3\langle n\rangle \ldots$

William Walker
Yuri Dokshitzer

- THE SOFT-HARD DICHOTEMY

(more general than '2-IP model' Landshoff Donnachie)

$$s^{\alpha(0)+\alpha' t}$$

- hadron-hadron data: $\alpha(0) \cong 0.08$ $\quad$ 'SOFT IP'

  $\alpha' \cong 0.25\ \mathrm{GeV}^{-2}$

- gluon ladders (BFKL IP)

  $\alpha(0) = \frac{4N_c}{\pi} \ln 2 \cdot \alpha_s$ 'large'

  $\sim 3\alpha_s$ $\quad$ 'HARD IP'

  α' 'small'

Expectation: Replace 1 or both hadrons by short-distance scattering but keep ΔY

$\hookrightarrow \begin{cases} \text{larger } \alpha \\ \text{smaller } \alpha' \end{cases}$

ELASTIC and TOTAL CROSS SECTIONS

$\sigma^{tot}_{p\bar{p}}$ (Tevatron) measured to much higher energy than pp (cf $\mathbb{P}$-theorem)

↳ pp2pp at RHIC Stephen Bueltmann

- elastic → indep. det. of Re, Im f_{pp}

$$\mathrm{Re}\, f_{pp} - \mathrm{Re}\, f_{p\bar{p}} \underset{s \to \infty}{\not\to} 0 \quad (\text{`}\mathbb{P}\text{allowed'})$$

'odderon'
(not yet seen)

Nachtman: Other tests/signals

- polarization: open terrétory

Single Transverse Spin Asymmetry A_N

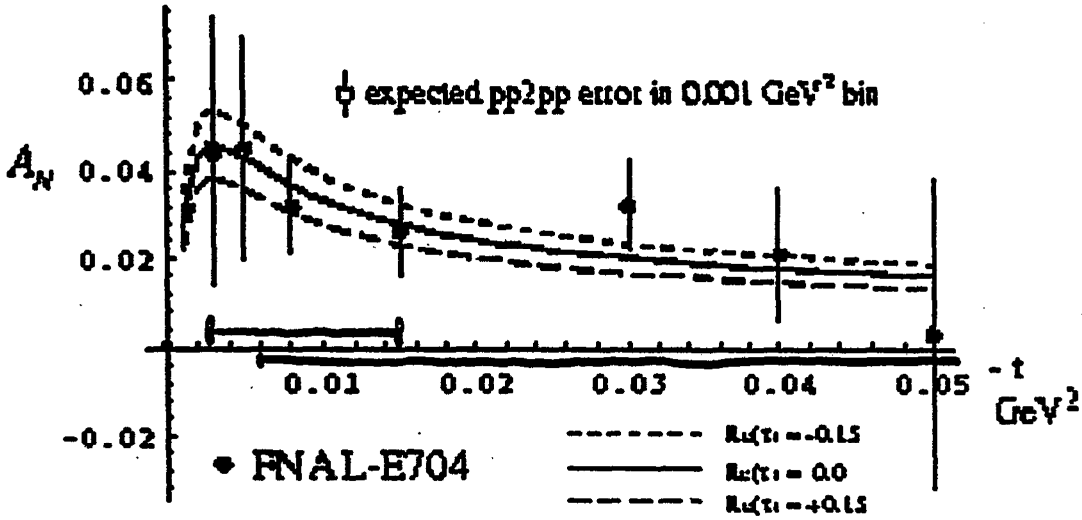

$\sqrt{s} = 200$ GeV
$\sqrt{s} = 500$ GeV

THE SPIN DEPENDENCE OF HIGH-ENERGY PROTON SCATTERING.
N.H. Buttimore, B.Z. Kopeliovich, E. Leader, J. Soffer, T.L. Trueman
Phys.Rev.D59:114010,1999

$$A_N(t) = \frac{1}{P\cos\phi} \frac{N_\uparrow(t) - N(t)_\downarrow}{N_\uparrow(t) + N_\downarrow(t)}$$

with ϕ the azimuthal angle
and P the proton polarization

SMALL-x DIS; SATURATION

$F_2 \sim \Big|$ 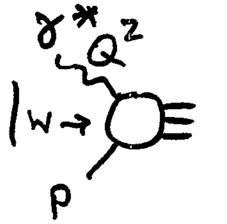

$\Big|^2 \sim \mathrm{Im}\Big($ 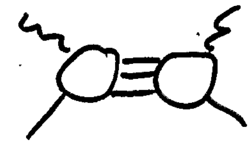 $\Big)$

$$W^2 \sim \frac{Q^2}{x}(1-x) \leftrightarrow s$$

$$\ln\frac{1}{x} \sim \ln s = \ln W^2$$

$F_2 \sim$ 

$\Delta Y \sim \ln\frac{1}{x}$

large Q^2: $\mathbb{P}$ 'squeezed at one end

how does this affect $\alpha_{DIS}(W^2)$?

STUDY $\quad x\,G(x,Q) \underset{x\to 0}{\sim} F_2(x,Q)$

$$f_{g/p}(x) \Rightarrow \frac{1}{x^{\lambda(Q)}}$$

• Why is F_2 so convenient?

$\frac{1}{x^{\lambda(Q)}}$: vary x, Q in one expt. in large range

$\lambda \sim 0.2-0.4$ 'Hard $\mathbb{P}$'

For $x \lesssim 10^{-4-5}$ begin to knock on door of unitarity, through

• saturation of gluon density.

$Q_S(x)$: saturation scale

$$\left(\frac{x G(x, Q_S)}{R_H^2}\right) \frac{1}{Q_S^2} = 1$$

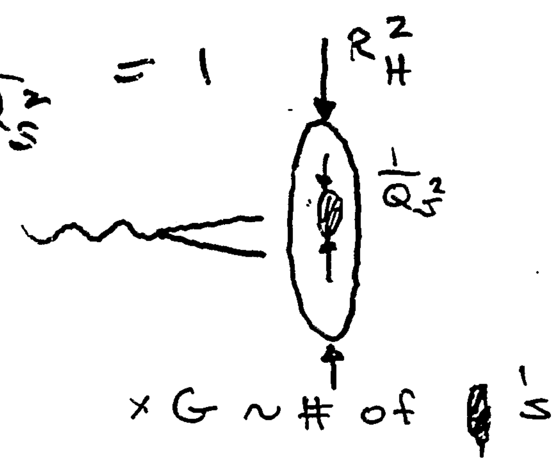

At $Q_S \rightarrow$ turnover to NP

Hard $\mathbb{P} \rightarrow$ Soft $\mathbb{P}$

eA Seen... but no clear x-dependence (?)
(HERMES) Jerry Miller: VM's as parton low Q^2

HARD DIFFRACTION(S)

- A remarkable discovery → (ies)
  80's ... 90's
  UA8 . . . D0, CDF, ZEUS, H1

- DIS, Photoproduction
  ~10% of events!

John Dainton
Frank-Peter Schilling
Malcom Derrick
James Crittendon

- 'Inclusive'

$\gamma, \gamma^*(Q^2)$

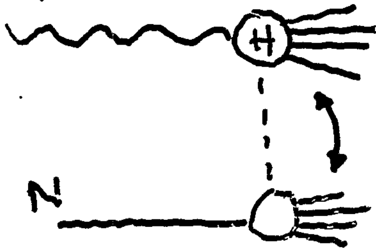

low or high M_X^2 (Jet(s), $b\bar{b}$ . . .)

gap ΔY → $e^{2(\alpha-1)\Delta Y}$ ↳ Q^2 . . .

N

low M^2

(Soper, Berera
(J. Collins)

Factorization:
- gap formation soft physics
- incoherent from hard scatteri[ng]
  ('universal')

$$d\sigma^D_{\gamma p} = \sum_{a=q,g} f^{diff}_{q/p} \otimes d\hat{\sigma}_{\gamma q}$$

$$\mu \frac{d}{d\mu} f^{diff}_{a/p}(x, Q) = P_{ab}(\alpha_s, x) \otimes f_b^{diff}(x; Q)$$

evol^n, universality → many predictions { dijets, $c\bar{c}$, $b\bar{b}$ . . .

QCD Factorization @ Work

Predict diffr. dijet cross sections with PDF's obtained from inclusive $F_2^{D(3)}$ measurement:

[resolved γ^* component included]

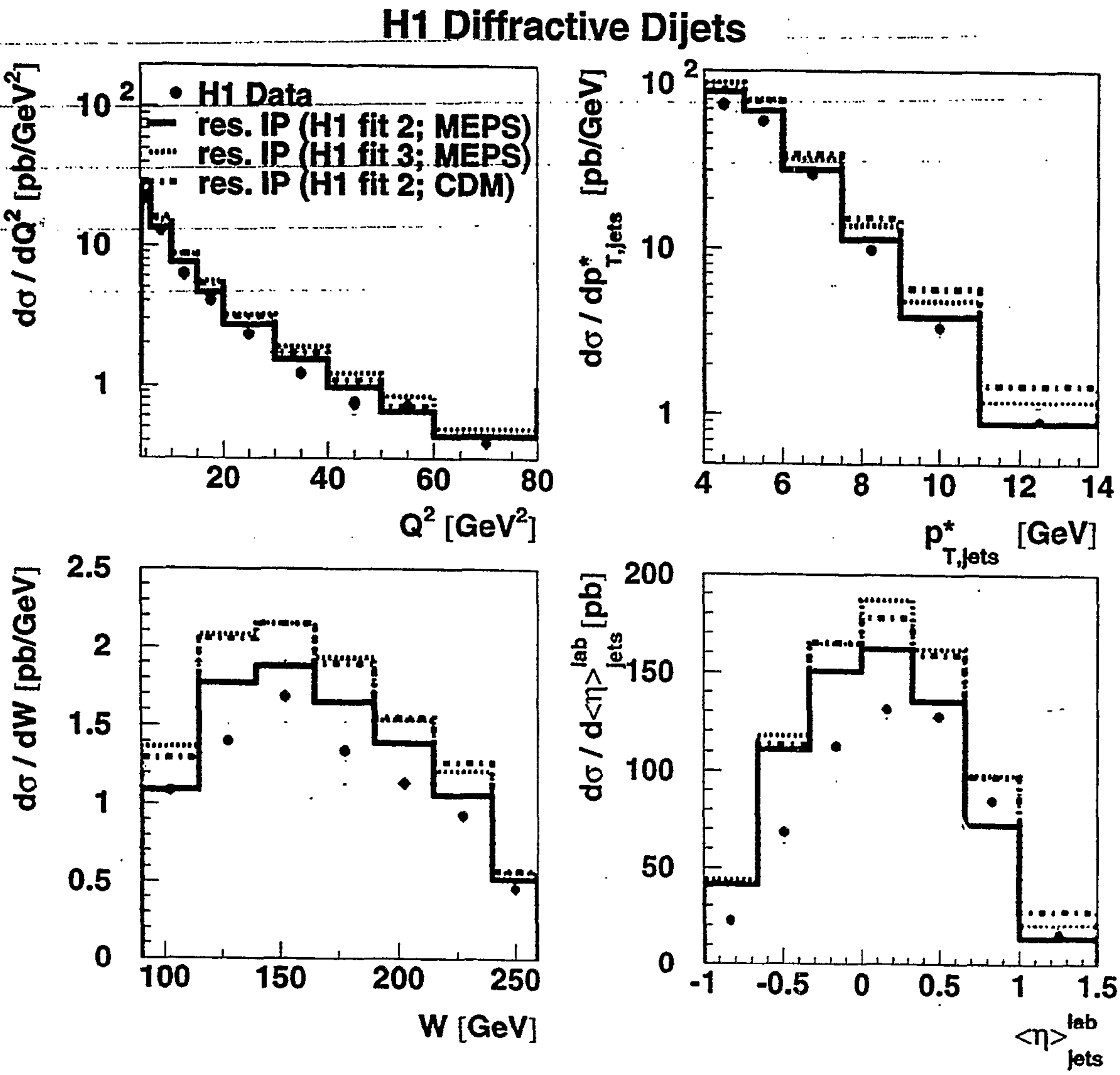

⇒ Consistent with QCD factorization in diffr. DIS !

(Ingelman, Schlein

Pomeron distributions

$$f^{\text{diffrac.}}_{q/p}(x, \Delta y) = f_{q/\mathbb{P}}(\beta) \otimes f_{\mathbb{P}/B}(\underset{\xi}{x_{\mathbb{P}}})$$

+ Reggeons...

$$x = \beta x_{\mathbb{P}}$$

H1's choice...

- Exclusive Vector Meson

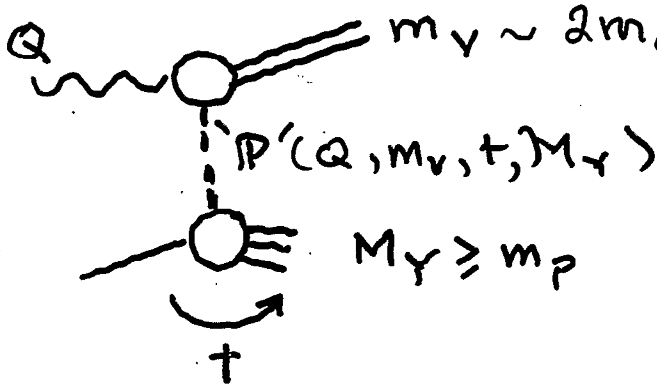

$m_V \sim 2m_q$; $q =$ u d — ρ, ω
s — ϕ
c — J/ψ
b — Υ

$M_Y \geq m_p$

general trend:
more localized '$\mathbb{P}$' → harder '$\mathbb{P}$'
Q, M_V, t (α up, α' down)

- Relation to $f_{G/p}$ for $M_Y = m_p$, $t \to 0$

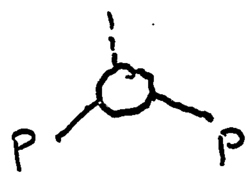

$\sim x\,G(x)$; small $x \sim 10^{-3}$

- t-dependence, polarization 'anomaly' in exclusive ρ production at high t
  why is $\sigma_T > \sigma_L$?

Fit of ρ^0 Lineshape

ZEUS $\gamma p \dashrightarrow (\rho^0 + \pi^+\pi^-)p$

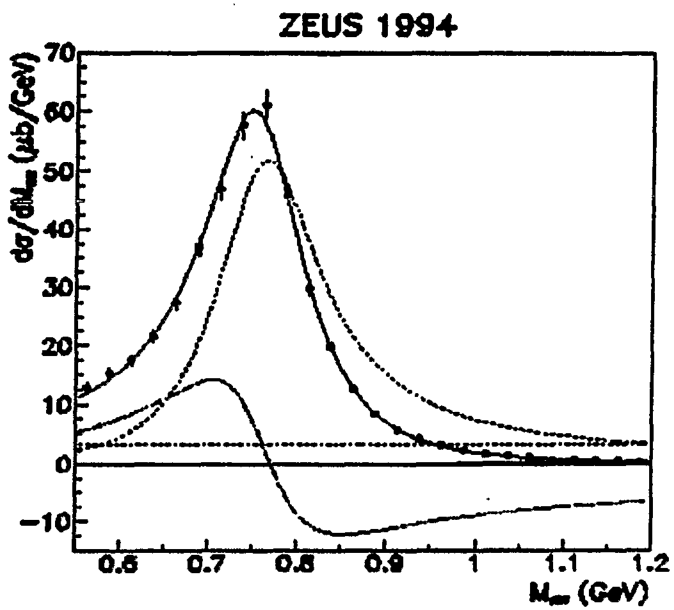

STAR $\gamma Au \dashrightarrow (\rho^0 + \pi^+\pi^-)Au$

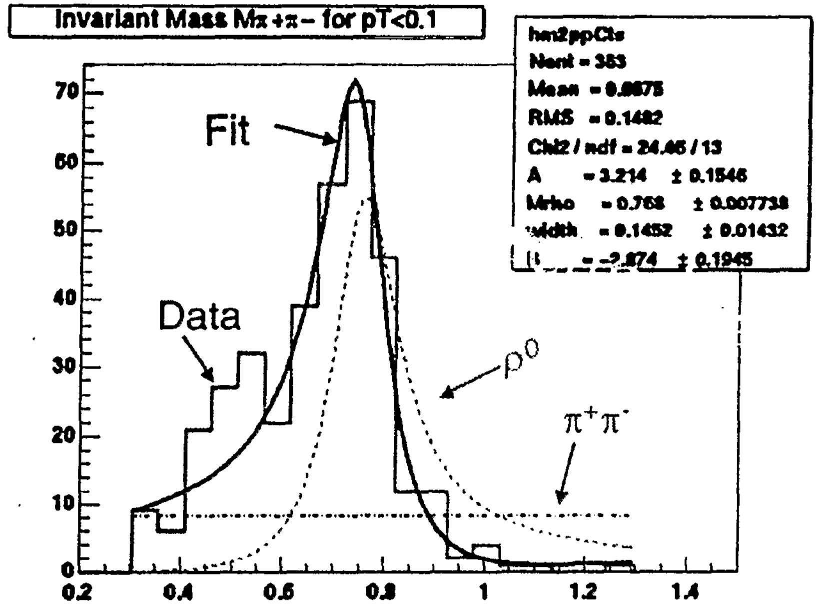

$$\frac{d\sigma}{dM_{\pi\pi}} = \left| A \frac{\sqrt{M_{\pi\pi} M_\rho \Gamma_\rho}}{M_{\pi\pi}^2 - M_\rho^2 + i M_\rho \Gamma_\rho} + B \right|^2 + f_{PS}$$

Set =0 for STAR

Fit all data to $\rho^0 + \pi^+\pi^-$
interference is significant
$\pi^+\pi^-$ fraction is high (background?)

Photon-$\mathbb{P}$ at RHIC

Joakim Nystrand
Falk Meissner

$$\gamma Au \to (\rho^0, \pi^+\pi^-) Au$$

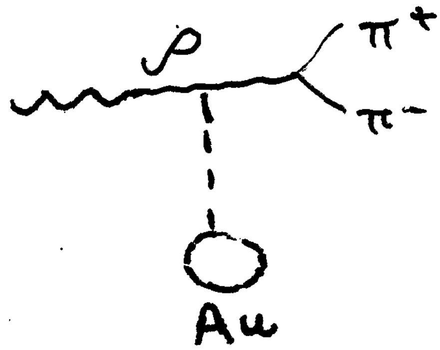

- Hadron-hadron

Samim Erhan
Andrew Brandt
Anwar Bhatti
Konstantin Goulianc

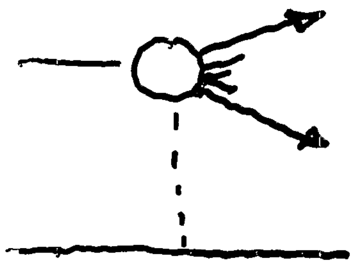

single-diffractiv

Kenichi Hatakagaw
Andrei Solodsky

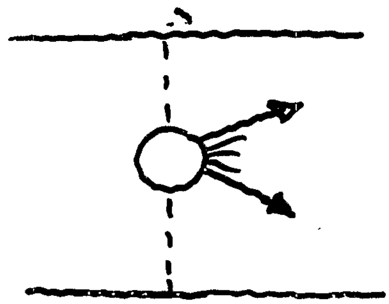

double pomeron

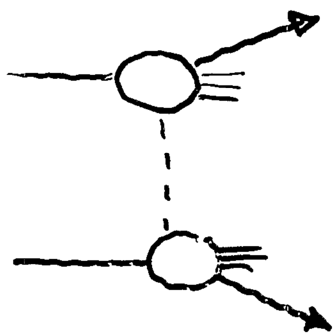

single-gap dijet

$$\sigma^{diff}_{p\bar{p}} = f^{diff}_{p} \otimes f^{diff}_{\bar{p}} \otimes \hat{\sigma}$$

- $f^{diff}_{a/p}$ from DIS → too large by 5-10

σ^{diff}_{AB} does not enjoy collinear factorization (Collins Frankfurt Strikman...)

gap formation of 2 (protons, $p\bar{p}$...

<u>not</u> incoherent

- Rapidity Gaps in pQCD

→ not natural for 1-gluon exchange

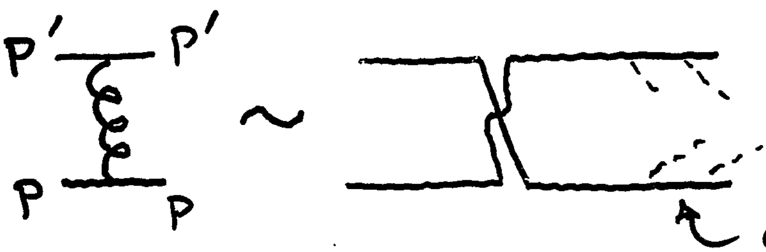

$t = 0$

even at $t = 0$
quark need new Coulomb field!
- Radiates
- Fills Gap

$-t \gg \Lambda^2_{QCD}$ → two gluon color singlet exchange

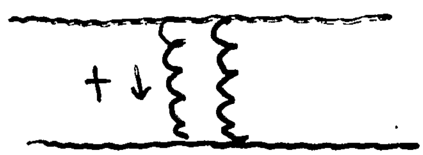

no problem

$-t \gg \Lambda^2_{QCD}$ → 'soft color' picture

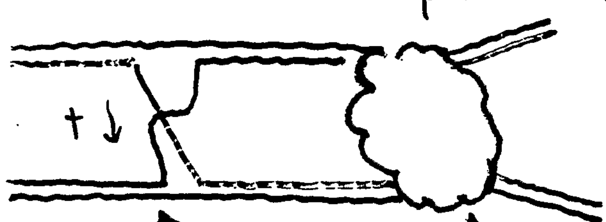

kinematics

statistical color equilibration

- pQCD in H-H Diffraction

  - Jets look like jets in inclusive events + initiated by 'normal' collinear partons

  - Parton distributions in x should not interfere with gap (re) formation (of outgoing $p, \bar{p} \ldots N^* \ldots$)
    - ↳ fits to diffractive PDFs 'make sense' but will not be same as in DIS, & may not factor between $p, \bar{p}$ (overall constant?)

  - Perturbative treatment of soft radiation into dijet gaps: find evolution in color exchange. Replaces 2gluon/soft color dichotomy

G.S.

THEORETICAL APPROACHES

- Modelling the Pomeron

Peter Landshoff
Sandy Donnachie
Carlos Merino
Jacques Soffer

2-IP model

$$F_2(x,Q^2) = f_1(Q^2)\,x^{-\epsilon_1} + f_0(Q^2)\,x^{-\epsilon_0}$$

$$\epsilon_1 = 0.08$$
$$\epsilon_0 = 0.4$$

fit to DIS, VM and γp data
Genya Levin: Matching with Evoln.
CKMT: include evoln. in fit to PDFs.

Also: fit to hadronic data Soffer

Dipole-based models

calculable

$$\sigma(\gamma p) \sim \int d^2 r_\perp\, dz\, |\psi(z, r_\perp)|^2\, \sigma_D(z, r$$

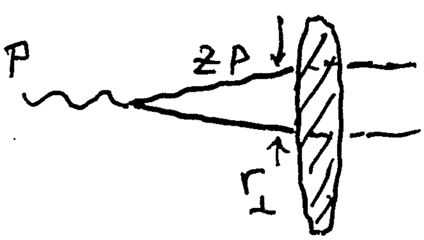

r^2 + NP

$$\sigma_0\left(1 - e^{-r^2/4R_s^2}\right)$$

(Golec-B. Wusthoff)

(→ Saturation)

Boris Kopelevich: semi-hard component,

$$\rightarrow \sigma \sim \sigma_0 + s^{\Delta}$$

- NONPERTURBATIVE APPROACHES I: QCD VACUUM

Instanton-mediated elastic

↓

Sphaleron-inelastic

AA @ (RHIC)

Ismail Zahed
Edward Shuryak
Gregory Carter

Instanton-ladders

Yuri Kovchegov

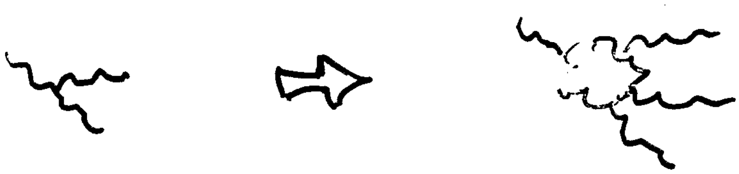

Stochastic Vacuum

Otto Nachtmann

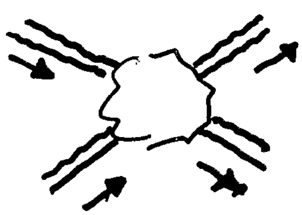

NP II : PARTONS → REGGEONS

Lev Lipatov

Gregory Korchemsky

Generalizes BFKL Ladder

Reggeized gluon ($s^{\alpha_G(t)}$)
a new player in effective
field theory

Connection to exactly
soluble models!

$$\partial_Y \Psi = H_{eff} \Psi$$

eigenstates: pomeron, odderon.

true behavior: an infinite
series

NP III: RESUMMED DIPOLE CROSS SECTIONS

another BFKL generalization

Robi Peshanski
Ian Balitsky
Leszak Motyka
Genya Levin

Balitsky-Kovchegov Eq.

$n(\underline{k}, Y)$ ← densit

$$\frac{\partial n}{\partial Y} = \alpha_s \underset{\substack{\uparrow \\ \text{BFKL pomeron}}}{K \otimes} n - \alpha_s \underset{\substack{\uparrow \\ \text{'rescatteri} \\ \text{overlap!}}}{\frac{n^2(\underline{k}, Y)}{\underline{k}^2}}$$

A theory of saturation...

NP IV: STRING-BASED POMERONS

'Duality' (a rule to calculate)
QCD ($g_s \to \infty$, $N_c \to \infty$)! from
classical supergravity in
>4 dimensional curved space

Tan! glueball trajectory
Janik: Wilson lines

Chung-I Tan
Romuald Jai

CONCLUSION:

TRANSCENDING THE POMERON

The Pomeron is:

- An organizing theme
- An intellectual guide
- A range with many peaks
- (Foothills have been climbed)
- A doorway to a unified dynamics of QCD

HIGH ENERGY QCD: BEYOND THE POMERON
A RIKEN BNL Research Center and BNL Nuclear Theory Group Workshop
May 21 – 25, 2001

REGISTERED PARTICIPANTS

Name	Mailing Address	E-Mail Address
Ian Balitsky	Theory Group Jefferson Laboratory 12000 Jefferson Avenue Newport News, VA 23606 USA	balitsky@jlab.org
Tony Baltz	Physics Department – Building 510A Brookhaven National Laboratory Upton, NY 11973 USA	baltz@bnl.gov
Andrei Belitsky	C.N. Yang Institute for Theoretical Physics State University of New York Stony Brook, NY 11794 USA	belitsky@insti.physics.sunysb.edu
Anwar Bhatti	High Energy Physics Laboratory Rockefeller University – Box 188 1230 York Avenue New York, NY 10021 USA	bhatti@physics.rockefeller.edu
Dietrich Bodeker	RIKEN BNL Research Center Physics Department – Building 510A Brookhaven National Laboratory Upton, NY 11973 USA	bodeker@bnl.gov
Andrew Brandt	University of Texas PO Box 19059 Arlington, TX 76019 USA	brandta@uta.edu
Stephen Bueltmann	Physics Department – Building 510D Brookhaven National Laboratory Upton, NY 11973 USA	bueltmann@bnl.gov
Kyrill Bugaev	Institute for Theoretical Physics University of Frankfurt Robert-Mayer-Str-10 60054 Frankfurt GERMANY	bugaev@th.physik.uni-frankfurt.de
Gregory Carter	Department of Physics and Astronomy State University of New York Stony Brook, NY 11794 USA	carter@tonic.physics.sunysb.edu
James Crittenden	DESY Notkestrasse 85 22607 Hamburg GERMANY	James.Crittenden@desy.de
John Dainton	Department of Physics Oliver Lodge Laboratory University of Liverpool Oxford Street Liverpool L69 7ZE UNITED KINGDOM	dainton@mail.desy.de

Malcolm Derrick	High Energy Physics Argonne National Laboratory Argonne, IL 60439 USA	mxd@hep.anl.gov
Yuri Dokshitzer	LPT Bat 210 Universite Paris Sud 91405 Orsay FRANCE	yuri@th.u-psud.fr
Sandy Donnachie	Department of Physics and Astronomy University of Manchester Manchester M13 9PL ENGLAND	ad@a35.ph.man.ac.uk
Samim Erhan	EP Division CERN CH 1211 Geneva 23 SWITZERLAND	Samim.Erhan@cern.ch
Ron Gill	Physics Department – Building 510A Brookhaven National Laboratory Upton, NY 11973 USA	rongill@bnl.gov
Konstantin Goulianos	Rockefeller University 1230 York Avenue New York, NY 10021 USA	dino@physics.rockefeller.edu
Sourendu Gupta	Physics Department – Building 510A Brookhaven National Laboratory Upton, NY 11973 USA	sgupta@quark.phy.bnl.gov
Wlodek Guryn	Physics Department – Building 510C Brookhaven National Laboratory Upton, NY 11973 USA	guryn@bnl.gov
Kenichi Hatakeyama	Rockefeller University Box 188 1230 York Avenue New York, NY 10021 USA	hatake@physics.rockefeller.edu
Kazunori Itakura	RIKEN BNL Research Center Physics Department – Building 510A Brookhaven National Laboratory Upton, NY 11973 USA	Itakura@bnl.gov
Jamal Jalilian-Marian	Physics Department – Building 510A Brookhaven National Laboratory Upton, NY 11973 USA	jamal@bnl.gov
Romuald Janik	Institute of Physics Jagellonian University ul. Reymonta 4 30-059 Krakow POLAND	ufrjanik@theta.uoks.uj.edu.pl
Judith Katzy	10 Park Woods Lane Kings Park, NY 11754 USA	katzy@bnl.gov
Dima Kharzeev	Physics Department – Building 510A Brookhaven National Laboratory Upton, NY 11973 USA	Kharzeev@bnl.gov
Boris Kopeliovich	Max-Planck-Institut fuer Kernphysik Postfach 103980 69029 Heidelberg GERMANY	boris.kopeliovich@mpi-hd.mpg.de
Gregory Korchemsky	LPT Universite Paris XI Bat 210 91405 Orsay Cedex FRANCE	korchems@th.u-psud.fr

Yuri Kovchegov	Department of Physics Box 351560 University of Washington Seattle, WA 98195-1560 USA	yuri@phys.washington.edu
Alexander Kovner	Theory Division CERN CH-1211 Geneva 23 SWITZERLAND	Alexander.Kovner@cern.ch
Tibor Kucs	C.N. Yang Institute for Theoretical Physics State University of New York Stony Brook, NY 11794 USA	tkkucs@grad.physics.sunysb.edu
Peter Landshoff	DAMTP, CMS Wilberforce Road Cambridge CB3 0WA UNITED KINGDOM	pvl@damtp.cam.ac.uk
Eugene Levin	HEP Department School of Physics Tel Aviv University Ramat Aviv, 69978 ISRAEL	leving@post.tau.ac.il
Lev Lipatov	Theory Department Petersburg Nuclear Physics Institute Orlova Roscha Gatchina, 188300 St. Petersburg RUSSIA	lipatov@thd.pnpi.spb.ru
Ronald Longacre	Physics Department – Building 510A Brookhaven National Laboratory Upton, NY 11973 USA	longacre@bnl.gov
Larry McLerran	Physics Department – Building 510A Brookhaven National Laboratory Upton, NY 11973 USA	McLerran@bnl.gov
Falk Meissner	Lawrence Berkeley National Laboratory MS 70-319 1 Cyclotron Road Berkeley, CA 94720 USA	FMeissner@lbl.gov
Carlos Merino	Dpto. Fisica de Particulas Facultade de Fisica Campus Universitario s/n 15706 Santiago de Compostela SPAIN	Merino@fpaxp1.usc.es
Christina Mesropian	Rockefeller University Box 188 1230 York Avenue New York, NY 10021 USA	chris@physics.rockefeller.edu
Gerald Miller	Department of Physics University of Washington Box 351560 Seattle, WA 98195-1560 USA	miller@phys.washington.edu
Leszek Motyka	High Energy Physics Department of Radiation Sciences Uppsala University – Box 535 S-75121 Uppsala SWEDEN	motyka@tsl.uu.se
Otto Nachtmann	Institute for Theoretical Physics University of Heidelberg Philosophenweg 16 D-69120 GERMANY	O.Nachtmann@thphys.uni-heidelberg.de

Joakim Nystrand	Department of Physics Division of Cosmic and Subatomic Physics Box 118 SE-221 00 Lund SWEDEN	Joakim.Nystrand@kosufy.lu.se
Sandra Padula	Nuclear Theory Group Physics Department – Building 510A Brookhaven National Laboratory Upton, NY 11973 USA	padula@quark.phy.bnl.gov
Robi Peschanski	SPhT, Orme des Merisiers CEN-Saclay F-91191 Gif-sur-Yvette FRANCE	pesch@spht.saclay.cea.fr
Naohito Saito	RIKEN BNL Research Center Physics Department – Building 510A Brookhaven National Laboratory Upton, NY 11973 USA	saito@bnl.gov
Frank-Peter Schilling	DESY H1 Collaboration (1c/353) Notkestr. 85 D-22607 Hamburg GERMANY	fpschill@mail.desy.de
Edward Shuryak	Department of Physics and Astronomy State University of New York Stony Brook, NY 11794 USA	shuryak@dau.physics.sunysb.edu
Jack Smith	C. N. Yang Institute for Theoretical Physics State University of New York Stony Brook, NY 11794 USA	smith@insti.physics.sunysb.edu
Jacques Soffer	Centre de Physique Theorique CNRS Luminy Case 907 13288 Marseille Cedex 09, FRANCE	soffer@cpt.univ-mrs.fr
Andrei Solodsky	Rockefeller University 1230 York Avenue, #368 New York, NY 10021 USA	solodsky@rock16.rockefeller.edu
George Sterman	Physics Department – Building 510A Brookhaven National Laboratory Upton, NY 11973 USA	sterman@quark.phy.bnl.gov
Chung-I Tan	Physics Department Brown University Providence, RI 02912 USA	tan@het.brown.edu
Larry Trueman	Physics Department – Building 510A Brookhaven National Laboratory Upton, NY 11973 USA	trueman@bnl.gov
Raju Venugopalan	Physics Department – Building 510A Brookhaven National Laboratory Upton, NY 11973 USA	raju@bnl.gov
William Walker	Physics Department Box 90305 Duke University Durham, NC 27708-0305 USA	walker@phy.duke.edu
Ismail Zahed	Physics Department State University of New York Stony Brook, NY 11794 USA	zahed@zahed.physics.sunysb.edu

High Energy QCD: Beyond the Pomeron
Physics Department, Brookhaven National Laboratory
May 21-25, 2001

Agenda

Monday, May 21 ---- Small Seminar Room

8:30 - 9:00 Registration

Opening Session

Chair: Larry McLerran

9:00 - 9:15	Wlodek Guryn	Welcome from the Organizers
9:15 - 9:50	John Dainton	High Energy QCD Overtakes the Pomeron?
9:50 - 10:30	Yuri Dokshitzer	High Energy Physics: Besides the Pomeron
10:30 - 11:00	*Coffee Break*	

Chair: Larry Trueman

11:00 - 11:40	Peter Landshoff	Two Pomerons
11:40 - 12:20	Robi Peschanski	Hard Diffraction and the Nature of the QCD Pomeron
12:20 - 2:00	*Lunch*	

Non-Perturbative Approaches to Pomerons I

Chair: Boris Kopeliovich

2:00 - 2:30	Sandy Donnachie	Disentangling Pomeron Dynamics from Vertex Function Effects
2:30 - 3:00	Yuri Kovchegov	QCD Instantons and the Soft Pomeron
3:00 - 3:30	*Coffee Break*	

Chair: Jerry Miller

3:30 - 4:00	Chung-I Tan	Pomeron Intercept at Strong Coupling
4:00 - 4:30	Jacques Soffer	Universal Pomeron from High Energy Relativistic Quantum Field Theory
4:30 - 5:30	Formation of Discussion and Working Groups	
5:30 -	*Welcoming Reception, Large Seminar Room Lounge, Physics Department*	
5:30 - 5:40	Tom Kirk	Welcome from BNL

Tuesday, May 22 ---- Large Seminar Room

RHIC Experiments

Chair: Peter Landshoff

9:00 - 9:30	Joakim Nystrand	Coherence in Nuclear Interactions at RHIC
9:30 - 10:00	Falk Meissner	Photon Pomeron Interactions at RHIC
10:00 - 10:30	Stephen Bueltman	pp2pp experiment at RHIC
10:30 - 11:00	*Coffee Break*	

Collider Experiments I

Chair: John Dainton

11:00 - 11:30	Andrew Brandt	D0 Hard Diffraction in Run I and Prospects in Run II
11:30 - 12:00	Anwar Bhatti	Diffractive Results from CDF
12:00 - 12:30	Samim Erhan	The Effective Pomeron Trajectory and Double-Pomeron-Exchange in UA8
12:30 - 2:00	*Lunch*	

Non-Perturbative Approaches to Pomerons II

Chair: Konstantin Goulianos

2:00 - 2:30	Ismail Zahed	Non-Perturbative QCD and High-Energy Scattering
2:30 - 3:00	Romuald Janik	String Fluctuations, AdS/CFT and the Soft Pomeron
3:00 - 3:30	*Coffee Break*	
3:30 - 6:30	Discussion	

Wednesday, May 23 ---- Small Seminar Room

Collider Experiments II

Chair: Sandy Donnachie

9:00 - 9:30	Frank-Peter Schilling	Hard Diffraction: Results from H1 at HERA
9:30 - 10:00	Malcolm Derrick	Pomeron Physics Studied with the ZEUS Detector
10:00 - 10:30	Konstantin Goulianos	Beyond the Conventional Pomeron
10:30 - 11:00	*Coffee Break*	

Wednesday, May 23 ---- Small Seminar Room, continued

Chair: Yuri Kovchegov

11:00 - 11:30	James Crittenden	Scaling Properties of High-Energy Diffractive Vector-Meson Production at High Momentum Transfer
11:30 - 12:00	William Walker	Analysis of Hadron Multiplicities and Diffraction Dissociation
12:00 - 12:15	Kenichi Hatakeyama	Study of Diffractive Dijet Production at CDF
12:15 - 12:30	Andrei Solodsky	Diffractive J/Psi Production at CDF
12:30 - 2:00	*Lunch*	

Non-Perturbative Approaches to Pomerons III

Chair: Dmitri Kharzeev

2:00 - 2:30	Eugene Levin	Matching of Soft and Hard Pomerons
2:30 - 3:00	Boris Kopeliovich	Semihard Components of the Soft Pomeron
3:00 - 3:30	Carlos Merino	The CKMT Approach to the Pomeron Puzzle
3:30 - 4:00	*Coffee Break*	
4:00 - 6:00	Discussion	

Thursday, May 24 ---- Large Seminar Room

Perturbative and Non-Perturbative QCD I

Chair: Otto Nachtmann

9:00 - 9:30	Lev Lipatov	Solution of the Baxter Equation for the Composite States of the Reggeized Gluons in QCD
9:30 - 10:00	George Sterman	Perturbative and Non-Perturbative Radiation
10:00 - 10:30	Gerald Miller	The HERMES Effect
10:30 - 11:00	*Coffee Break*	

Chair: Eugene Levin

11:00 - 11:30	Gregory Korchemsky	Unitarity Corrections to the BFKL Pomeron
11:30 - 12:00	Ian Balitsky	Effective Field Theory for the Small-x Evolution
12:00 - 12:30	Leszek Motyka	Direct Solutions to Kovchegov Equation
12:30 - 2:00	*Lunch*	
2:00 - 3:30	Discussion	
3:30 - 4:00	*Coffee Break*	
4:00 - 5:30	Discussion	
7:00 -	*Workshop Dinner*	

Friday, May 25 ---- Large Seminar Room

Perturbative and Non-Perturbative QCD II

Chair: Raju Venugopalan

9:00 - 9:30	Otto Nachtmann	High Energy Hadron-Hadron Scattering in a Functional Integral Approach
9:30 - 10:00	Edward Shuryak	Instanton/Sphaleron Mechanism in Hadronic Nuclear Collisions
10:00 - 10:30	Gregory Carter	Classical Gluon Production in Hadronic Collisions
10:30 - 11:00	*Coffee Break*	
11:00 - 12:30	Discussion	
12:30 - 2:00	*Lunch*	

Chair: Yuri Dokshitzer

2:00 - 3:00	George Sterman	Summary
3:00 -	Conference Adjourns	

Photographs

from

Workshop Dinner

~ ~ ~

May 24, 2001

Painters' Restaurant
416 South Country Road
Brookhaven Hamlet, NY 11719


Bulletin


SABRETT

Additional RIKEN BNL Research Center Proceedings:

Volume 34 – High Energy QCD: Beyond the Pomeron – BNL-
Volume 33 – Spin Physics at RHIC in Year-1 and Beyond – BNL-52635
Volume 32 – RHIC Spin Physics V – BNL-52628
Volume 31 – RHIC Spin Physics III & IV Polarized Partons at High Q^2 Region – BNL-52617
Volume 30 – RBRC Scientific Review Committee Meeting – BNL-52603
Volume 29 – Future Transversity Measurements – BNL-52612
Volume 28 – Equilibrium & Non-Equilibrium Aspects of Hot, Dense QCD – BNL-52613
Volume 27 – Predictions and Uncertainties for RHIC Spin Physics & Event Generator for RHIC Spin Physics III – Towards Precision Spin Physics at RHIC – BNL-52596
Volume 26 – Circum-Pan-Pacific RIKEN Symposium on High Energy Spin Physics – BNL-52588
Volume 25 – RHIC Spin – BNL-52581
Volume 24 – Physics Society of Japan Biannual Meeting Symposium on QCD Physics at RIKEN BNL Research Center – BNL-52578
Volume 23 – Coulomb and Pion-Asymmetry Polarimetry and Hadronic Spin Dependence at RHIC Energies – BNL-52589
Volume 22 – OSCAR II: Predictions for RHIC – BNL-52591
Volume 21 – RBRC Scientific Review Committee Meeting – BNL-52568
Volume 20 – Gauge-Invariant Variables in Gauge Theories – BNL-52590
Volume 19 – Numerical Algorithms at Non-Zero Chemical Potential – BNL-52573
Volume 18 – Event Generator for RHIC Spin Physics – BNL-52571
Volume 17 – Hard Parton Physics in High-Energy Nuclear Collisions – BNL-52574
Volume 16 – RIKEN Winter School - Structure of Hadrons - Introduction to QCD Hard Processes – BNL-52569
Volume 15 – QCD Phase Transitions – BNL-52561
Volume 14 – Quantum Fields In and Out of Equilibrium – BNL-52560
Volume 13 – Physics of the 1 Teraflop RIKEN-BNL-Columbia QCD Project First Anniversary Celebration – BNL-66299
Volume 12 – Quarkonium Production in Relativistic Nuclear Collisions – BNL-52559
Volume 11 – Event Generator for RHIC Spin Physics – BNL-66116
Volume 10 – Physics of Polarimetry at RHIC – BNL-65926
Volume 9 – High Density Matter in AGS, SPS and RHIC Collisions – BNL-65762
Volume 8 – Fermion Frontiers in Vector Lattice Gauge Theories – BNL-65634
Volume 7 – RHIC Spin Physics – BNL-65615
Volume 6 – Quarks and Gluons in the Nucleon – BNL-65234
Volume 5 – Color Superconductivity, Instantons and Parity (Non?)-Conservation at High Baryon Density – BNL-65105

Additional RIKEN BNL Research Center Proceedings:

Volume 4 – Inauguration Ceremony, September 22 and Non -Equilibrium Many Body Dynamics – BNL-64912

Volume 3 – Hadron Spin-Flip at RHIC Energies – BNL-64724

Volume 2 – Perturbative QCD as a Probe of Hadron Structure – BNL-64723

Volume 1 – Open Standards for Cascade Models for RHIC – BNL-64722

For information please contact:

Ms. Pamela Esposito
RIKEN BNL Research Center
Building 510A
Brookhaven National Laboratory
Upton, NY 11973-5000 USA

Phone: (631) 344-3097
Fax: (631) 344-4067
E-Mail: pesposit@bnl.gov

Homepage: http://quark.phy.bnl.gov/www/riken.html
http://penguin.phy.bnl.gov/www/riken.html

RIKEN BNL RESEARCH CENTER

High Energy QCD: Beyond the Pomeron

May 21 - 25, 2001

Li Keran

Nuclei as heavy as bulls
Through collision
Generate new states of matter.
T.D. Lee

Speakers:

I. Balitsky	A. Bhatti	A. Brandt	S. Bueltman	G. Carter
J. Crittenden	J. Dainton	M. Derrick	Y. Dokshitzer	S. Donnachie
S. Erhan	K. Goulianos	K. Hatakeyama	R. Janik	B. Kopeliovich
G. Korchemsky	Y. Kovchegov	P. Landshoff	E. Levin	L. Lipatov
F. Meissner	C. Merino	G. Miller	L. Motyka	O. Nachmann
J. Nystrand	R. Peschanski	F.-P. Schilling	E. Shuryak	J. Soffer
A. Solodsky	G. Sterman	C.-I. Tan	W. Walker	I. Zahed

Organizers: John Dainton, Wlodek Guryn, Dmitri Kharzeev, and Yuri Kovchegov